CHARACTERIZATION OF CALCIUM REGULATED ADENYLYL CYCLASES

by

Trevor Burgess Doyle

A Dissertation

Submitted to the Faculty of Purdue University

In Partial Fulfillment of the Requirements for the degree of

Doctor of Philosophy

Department of Medicinal Chemistry and Molecular Pharmacology

West Lafayette, Indiana

December 2018

THE PURDUE UNIVERSITY GRADUATE SCHOOL
STATEMENT OF COMMITTEE APPROVAL

Dr. Val Watts, Chair
Department of Medicinal Chemistry and Molecular Pharmacology
Dr. Richard van Rijn
Department of Medicinal Chemistry and Molecular Pharmacology
Dr. Chang-Deng Hu
Department of Medicinal Chemistry and Molecular Pharmacology
Dr. Angeline Lyon
Department of Chemistry

Approved by:

Dr. Zhong-Yin Zhang
Head of the Graduate Program

“Adenylyl cyclase is a hateful enzyme”

- Alfred Gilman

ACKNOWLEDGMENTS

I wish to thank my mentor, Dr. Val Watts for his continued support and effort to help me grow as an independent scientist. I would also like to thank the members of my thesis advisory committee, Dr. Richard van Rijn, Dr. Chang-Deng Hu, and Dr. Angeline Lyon for their continued encouragement and support.

I would like to thank the past and current members of the Watts laboratory, Dr. Jason Conley, Dr. Tarsis Brust, Dr. Monica Soto-Velasquez, Dr. Karin Ejendal, and Dr. Mike Hayes for their friendship and support. I would also like to thank Dr. Christopher Rochet, Dr. Matthew Tantama, Dr. Eric Barker, and Dr. Gregory Hockerman for their collaborations, assistance, and kindness.

I would also like to thank my previous mentors Dr. David Sibley, Dr. R Benjamin Free, and Dr. Christopher Lowry for their patience, inspiration, and investment in my scientific career.

Finally, I wish to thank my darling wife Meridith for her continued encouragement, love, and support during graduate school.

TABLE OF CONTENTS

LIST OF TABLES

LIST OF FIGURES

ABSTRACT

Author: Doyle, Trevor, B. PhD
Institution: Purdue University
Degree Received: December 2018
Title: Characterization of Calcium Regulated Adenylyl Cyclases.
Committee Chair: Val Watts

Adenylyl cyclases are key points for the concurrent integration of diverse signaling pathways. Controlling production of the second messenger cAMP, adenylyl cyclases provide an important mechanism for the regulation of physiological functions by amplifying signaling events to stimulate downstream effectors. While different isoforms of adenylyl cyclase exhibit distinct patterns of expression and regulation, of particular interest are two groups of Ca^{2+} regulated isoforms that are highly expressed in the central nervous system. Adenylyl cyclase type 5 (AC5) is a Ca^{2+} inhibited isoform that is highly expressed in the striatum, and whose activity is involved in the regulation of movement, pain, and metabolism. Adenylyl cyclase type 8 (AC8) is stimulated by Ca^{2+} in a calmodulin dependent manner, and appears to be involved with long-term memory, anxiety, and reward pathways. Studying the signaling characteristics of these adenylyl cyclase isoforms is necessary for improving our scientific understanding of biological pathways, as well identifying therapeutic targets that can be exploited for treatment of disease. In this work, we investigated changes in the protein interaction network of AC5 following prolonged $G\alpha_{i/o}$-mediated inhibition that results in heterologous sensitization. The diversity of signaling pathways and multitude of protein interactions that have been implicated in the development of the heterologous sensitization response prompted the development of a novel screening strategy to capture and identify AC5-protein interactions which occur following prolonged $G\alpha_{i/o}$-mediated inhibition. We utilized bimolecular fluorescence complementation (BiFC) in conjunction with fluorescence activated cell sorting (FACS) and Next Generation sequencing to capture, identify, and characterize novel AC5 interacting partners. We further studied the effects of increased AC5 activity by functionally characterizing a series of gain-of-function mutations that have been identified in patients diagnosed with Familial Dyskinesia and Facial Myokymia (FDFM). Our results demonstrate that the AC5 mutants exhibit enhanced activity to $G\alpha_s$-mediated stimulation and reduced inhibition by $G\alpha_{i/o}$-coupled receptors. We further suggest that this dysregulation of

AC5 in striatal medium spiny neurons likely results in an imbalance in the direct and indirect striatal signaling pathways that coordinate the initiation and maintenance of movement. Genetic models of AC8 regulation have implicated its activity in signaling pathways that may regulate comorbid long-term anxiety and ethanol consumption. Therefore, we developed and conducted a high-throughput screen and validation paradigm of small molecules for the discovery of AC8 selective inhibitors. The screening effort identified two lead compounds that demonstrate enhanced efficacy and selectivity over AC1 compared to currently available adenylyl cyclase inhibitors.

CHAPTER 1. INTRODUCTION

1.1 G protein-coupled receptors (GPCRs)

1.1.1 G protein signaling overview

G protein-coupled receptors (GPCRs) are the largest and most diverse family of membrane-bound receptors identified in humans (Lefkowitz, 2004). GPCRs are composed of a single polypeptide folded into seven transmembrane helices which span the entire width of the membrane, with loops connecting helices at intracellular and extracellular junctions to form a globular helical bundle embedded in the cell plasma membrane (Cherezov et al., 2007). GPCRs are tasked with transmitting signals from the extracellular environment into amplified intracellular signaling events (Lagerstrom & Schioth, 2008). On the cell surface, these receptors interact with a variety of extracellular proteins, biogenic amines, polypeptide hormones, ions, photons, small molecules, and neurotransmitters (Fredriksson, Lagerstrom, Lundin, & Schioth, 2003; Gilman, 1987). The interaction of the receptor with a recognizable ligand induces a change in conformation that physically transmits the extracellular binding event into the cell, triggering an activation of the associated Gα and Gβγ proteins that leads to diverse signaling events through a range of effectors (Fig. 1.1) (Lefkowitz, 2004; Rasmussen et al., 2011).

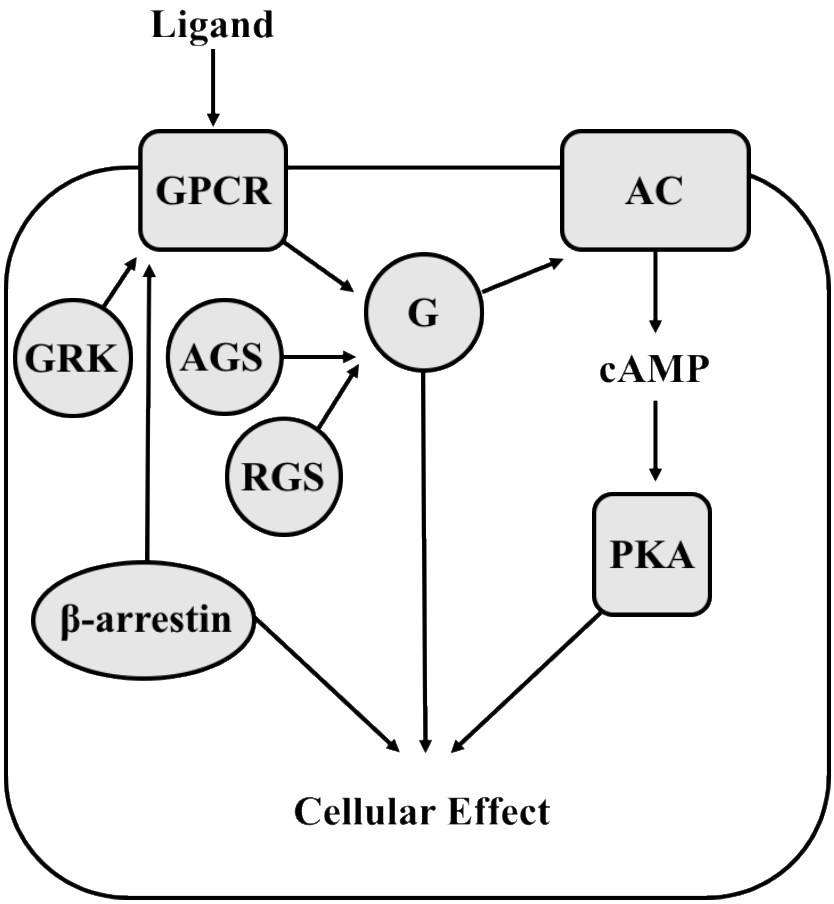

Figure 1.1: GPCR signaling overview.

Ligand activation of the G protein-coupled receptor (GPCR) results in heterotrimeric G protein activation (G), which can lead to signaling events through Gα and Gβγ dependent mechanisms. G protein subunits can bind and regulate adenylyl cyclase (AC) activity, subsequently regulating downstream effectors such as cAMP dependent protein kinase (PKA). Activators of G protein signaling (AGS) and regulators of G protein signaling (RGS) proteins can inhibit or promote GTP hydrolysis, respectively, thus modulating the G protein signaling cascade. G protein receptor kinases (GRKs) phosphorylate the active receptor, resulting in β-arrestin recruitment that can promote receptor desensitization as well as unique signaling events.

1.1.2 Families of GPCRS

G protein-coupled receptors (GPCRs) are the largest class of membrane proteins in the human genome, and various systems have been developed to subdivide and further classify the GPCR family (Alexander et al., 2017). Structural features of the membrane spanning motifs, as well as the biological and physiological functions of the receptor, have been used in previous classification methods to subdivide the GPCR superfamily (Attwood & Findlay, 1994; Kolakowski, 1994). Presently, the International Union of Basic and Clinical Pharmacology guideline for vertebrate receptor nomenclature and classification is based upon a 2003 phylogenic analysis of GPCR sequences in the human genome that establishes five classes (Alexander et al., 2017; Fredriksson et al., 2003). The five classes of vertebrate GPCRs are Rhodopsin-like (Class A), Secretin receptor family (Class B), Metabotropic Glutamate (Class C), Adhesion, and Frizzled (Fredriksson et al., 2003).

The rhodopsin-like (Class A) family of GPCRs contains the largest number of receptors, and interacts with a tremendous variety of small molecules, neurotransmitters, peptides, hormones, visual pigments, and photons (Alexander et al., 2017). The rhodopsin-like family of receptors encompasses most classical examples of GPCRs, including the dopamine, opioid, and adrenergic receptors and will be the main focus of the research discussed hereafter. Class A GPCRs share several interesting characteristics, including the NSxxNPxxY motif that connects the transmembrane helix 7 (TMVII) to the cytoplasmic helix 8, and is believed to play a central role in the conformational change that leads to a rearrangement and stabilization of the activated state of the receptor (Alexander et al., 2017; Rosenbaum, Rasmussen, & Kobilka, 2009). Another conserved characteristic of the rhodopsin-like class is the DRY (Asp-Arg-Tyr) motif at the cytosolic interface between transmembrane helix 3 (TMIII) and the intracellular loop 2 (IL2) (Wess, 1998). Mutations to the DRY motif have been shown to confer enhanced binding affinity for agonist ligands despite disrupting G protein signaling (Alewijnse et al., 2000; Samama, Cotecchia, Costa, & Lefkowitz, 1993). These results support a role for the DRY motif in G protein coordination, as well as the isomerization and stabilization of receptors between the active and inactive conformations (Flanagan, 2005).

The secretin family (Class B GPCRs) of receptors are characterized by an extracellular hormone-binding domain and are stimulated by peptide hormones through paracrine signaling

(Lagerstrom & Schioth, 2008). Nearly all receptors in this class have a series of conserved cysteine residues in the N-terminal tail that form a system of three cysteine bridges (Fredriksson et al., 2003). These bridges are believed to support a well-defined and stable conformation of the N-terminus, which plays a significant role in ligand binding (Grauschopf et al., 2000). Cysteine resides located in the extracellular loops 2 (EL2) and 4 (EL4) form an additional bridge that, together with transmembrane helix 6 (TM6) and the N-terminus, is thought to define the binding pocket (Grace et al., 2004). Ligand binding is believed to bridge the N-terminal segment with the pocket defined by extracellular loops and transmembrane segments to stabilize the active conformation of the receptor to promote signaling events (Lagerstrom & Schioth, 2008).

The metabotropic glutamate family (Class C GPCRs) includes eight glutamate receptors, as well as two GABA receptors, and several taste and calcium receptors (Fredriksson et al., 2003). While the metabotropic glutamate receptors are best known for their role in modulating excitatory synapses in the central nervous system, most members of the glutamate receptor family bind their respective ligand glutamate with a similar mechanism despite differences in receptor function (Fredriksson et al., 2003; Lagerstrom & Schioth, 2008). The extracellular N-terminal region of the glutamate receptor is folded into two distinct lobes, with a tertiary structure that is stabilized by disulphide bridges and resembles an open “Venus fly trap” (Lagerstrom & Schioth, 2008). Ligand binding to an orthosteric site within the two lobes promotes a change in the arrangement of the two lobes into a closed conformation (Kunishima et al., 2000). This movement on the extracellular surface is thought to affect the separation and conformation of the transmembrane, as well as the intracellular regions, to stabilize an active receptor conformation and stimulate signaling (Kunishima et al., 2000).

The adhesion receptor family is characterized by an exceedingly long N-terminal region, which contains several functional domains with adhesion-like motifs as well as glycosylation sites (Fredriksson et al., 2003; Paavola & Hall, 2012). The binding of ligands, such as large glycoproteins, to the adhesion domain on the N-terminal tail facilitates cell adhesion (Fredriksson et al., 2003; Vallon & Essler, 2006). An additional trait shared by members of the adhesion receptor family is a N-terminal GPCR proteolytic site motif that is thought to undergo self-proteolysis (Paavola & Hall, 2012). Curiously, mutant receptors with truncated N-termini exhibit constitutive activation with enhanced coupling of G proteins and stimulation of downstream signaling pathways (Okajima, Kudo, & Yokota, 2010; Paavola & Hall, 2012). These results suggest that

differential ligand binding to adhesion GPCRs can affect two distinct responses. The binding of a ligand that prevents the proteolysis of the N-terminal tail may facilitate adhesion; conversely, a ligand that promotes the removal of the N-terminus stimulates receptor coupling to G proteins and activation of G protein mediated signaling (Paavola & Hall, 2012).

The final subcategory of the GPCR superfamily contains the frizzled receptors, which can be subdivided into two distinct clusters, the frizzled and the taste2 receptors. Very little is known about taste2 receptors other than their expression in the palate and tongue epithelial tissues, and these receptors are thought to function as bitter taste receptors (Fredriksson et al., 2003). Frizzled receptors are the principle target for the Wnt family of lipoglycoprotein signaling molecules and participate in the regulation of cellular differentiation, polarity, proliferation, and cell fate during early embryonic development (Fredriksson et al., 2003; Koval & Katanaev, 2012). Because of their role in cellular differentiation and proliferation, the dysfunction of frizzled receptor signaling pathways are strongly implicated physical and mental developmental disorders, as well as various cancers, and are therefore rapidly becoming an area of significant interest (Koval & Katanaev, 2012; Kramer, 2016).

1.1.3 Structure of GPCRS

With the wealth of information available today, the concept of specific receptors that bind ligands to initiate biological effects is often taken for granted. The work of Paul Ehrlich and John Langley in the early 20th century established the foundation of receptor theory which would continue to be built upon for the next half century (Lefkowitz, 2004). The evolution of novel techniques such as radioligand binding in the 1970s led to dramatic changes in the scientific understanding of GPCR coupling to G proteins and spurred the development of a more complex model of receptor affinity that defined both low and high affinity states depending on G protein coupling (De Lean, Stadel, & Lefkowitz, 1980). The early 1980s brought advances in receptor purification and cloning techniques that led to the first GPCR structural clues of the bovine rhodopsin, followed shortly by the isolation and sequencing of the gene encoding human rhodopsin (Hargrave et al., 1983; Nathans & Hogness, 1984). Two years later, the cloning of the β-adrenergic receptor astounded the scientific community by revealing structural and functional similarities with the rhodopsin GPCR, and these unexpected results introduced the hypothesis that the seven transmembrane structure may be a hallmark of a larger class of receptors (Dixon et al., 1986; Lefkowitz, 2004).

The August 2000 issue of Science contained the first high resolution (2.8Å) X-ray crystal structure of a GPCR, heralding in a new millennium of scientific discovery with a great milestone (Palczewski et al., 2000). The crystal structure of rhodopsin revealed the first 3-dimensional experimental evidence of the highly organized geometry of the seven transmembrane helices, as well as the three intracellular and extracellular loop domains in the ground state (Palczewski et al., 2000). The structure also identified the two-strand beta sheet conformation of the extracellular loop 2 (EL2) that is positioned at the opening of the ligand-binding pocket and serves as a lid to contain the ligand during activation. The position of the beta sheet is stabilized by hydrophobic interactions, as well as the conserved disulphide bond between cysteine resides, which connect the extracellular portion of transmembrane helix 3 (TM3) with the beta sheet. This interaction is thought to participate in the recognition of small molecule ligands and maintain the position of the beta sheet during receptor activation (Costanzi, Siegel, Tikhonova, & Jacobson, 2009; Palczewski et al., 2000; Zhou, Melcher, & Xu, 2012). Another important feature of the structure is an ionic salt bridge that forms between transmembrane helix 3 (TM3) and transmembrane helix 6 (TM6) that is necessary to maintain the inactive conformation and prevent G protein binding (Costanzi et al., 2009; Palczewski et al., 2000). The crystal structure of rhodopsin also exposed the geography of side chains within the binding pocket that surrounds the 11-cis-retinal chromophore. Together, this information links the orientation of the transmembrane helices and loops with the ground state of the receptor, providing insight into the structural changes that take place during activation (Costanzi et al., 2009; Palczewski et al., 2000). Additional insights into the structural changes that occur following GPCR activation became possible with the crystallization of opsin. The structure revealed that the helical core made up by transmembrane helices 1-4 (TM1-TM4) remains relatively stable upon activation; however, large conformation changes were observed from helices 5—7 (TM5-TM7) (Scheerer et al., 2008; Zhou et al., 2012). The elongation of transmembrane helix 5 (TM5) and the tilting of transmembrane helix 6 (TM6) breaks the ionic bond that stabilizes the inactive receptor, and exposes contacts along the inner surfaces of these helices to uncover an interface for G protein binding (Scheerer et al., 2008; Zhou et al., 2012).

The β_2 adrenergic receptor (β_2AR) initially emerged as the predominant model system to characterize GPCR pharmacology and signaling pathways, and the crystallization of agonist bound β_2AR in its active state coupled to $G\alpha_s$ represented a substantial leap forward in the scientific understanding of GPCR activation across the membrane. Consistent with the conformational

changes observed in the rhodopsin/opsin structures, the largest structural changes in β_2AR activation mechanism include a large 14Å outward bending of the cytoplasmic portion of transmembrane helix 6 (TM6) and a two helical turn extension of transmembrane helix 5 (TM5) that enables the G protein heterotrimer to bind the receptor (Chung et al., 2011; Rasmussen et al., 2011). The Gα subunit consists of two domains with a nucleotide-binding domain located between them, the Ras-like domain that has endogenous GTPase activity and the α helical domain (Chung et al., 2011; Rasmussen et al., 2011). The Ras-like domain forms an interaction with the recently exposed GPCR cytosolic interface, and the formation of this G protein-receptor complex leads to the release of GDP from the nucleotide-binding pocket of the Gα subunit (Chung et al., 2011; Duc, Kim, & Chung, 2015; Rasmussen et al., 2011). Subsequently, the Gα subunit binds GTP, which initiates the dissociation of Gα and Gβγ subunits from their position at the receptor to stimulate their respective signaling pathways (Fig. 1.2) (Chung et al., 2011; Duc et al., 2015). This signaling event can be terminated by the GTPase activity of the Gα subunit or by regulators of G protein signaling (RGS) proteins (Duc et al., 2015).

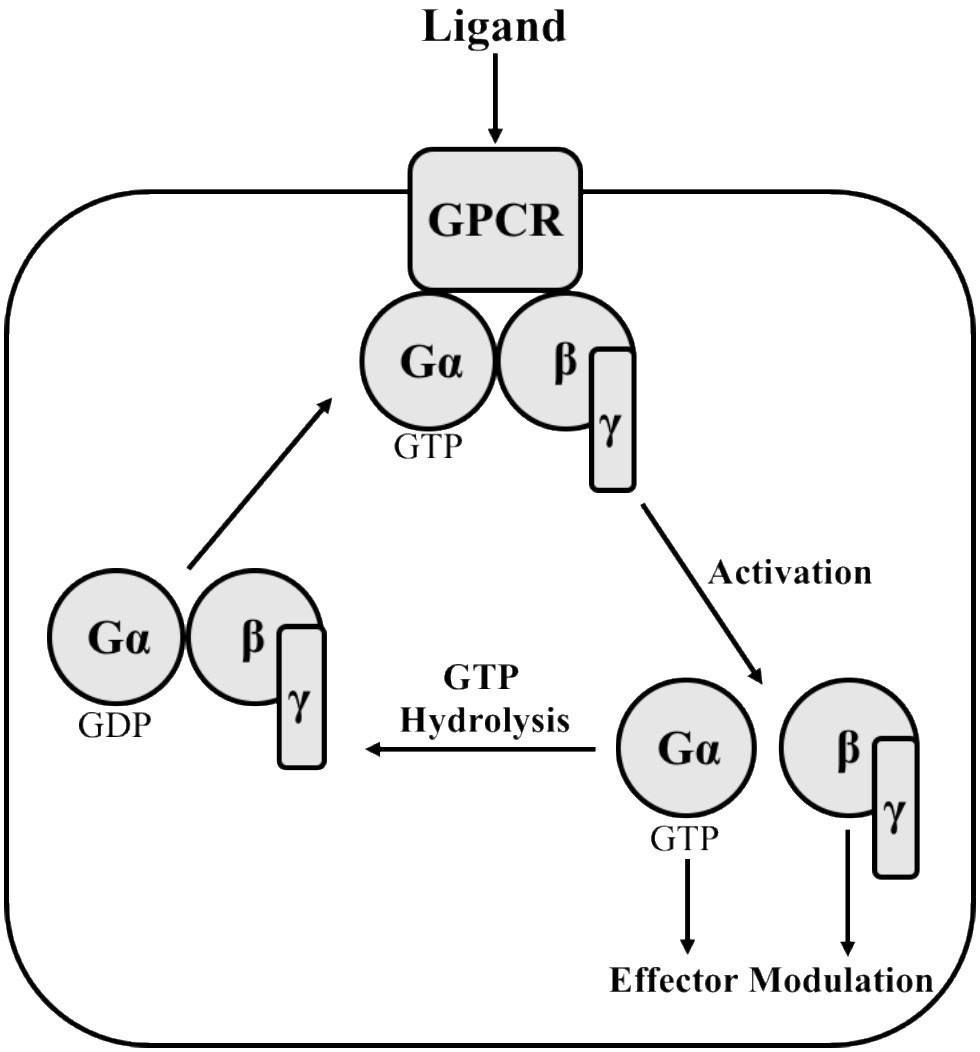

Figure 1.2: Heterotrimeric G protein activation cycle.

Ligand binding activates the G protein-coupled receptor (GPCR), inducing a conformational change that transmits the extracellular signal intracellularly. The structural change of the receptor promotes the exchange of bound GDP for GTP on the Gα subunit, the rate limiting step for G protein activation. The GTP binding induces a conformational change, promoting the dissociation of the heterotrimeric G protein to effect downstream targets. The inherent GTPase activity of Gα subunits hydrolyzes GTP, terminating the signal.

1.1.4 Mechanism of GPCR signaling /Activation cycle/Bias signaling

1.1.4.1 Gα subunits

There are 16 Gα subunits that are typically grouped into four main categories: $G\alpha_s$ ($G\alpha_s$, $G\alpha_{olf}$), $G\alpha_i$ ($G\alpha_t$, $G\alpha_{i1}$, $G\alpha_{i2}$, $G\alpha_{i3}$, $G\alpha_{o1}$, $G\alpha_{o2}$, $G\alpha_\zeta$), $G\alpha_{q/11}$ ($G\alpha_q$, $G\alpha_{11}$, $G\alpha_{14}$, $G\alpha_{15}$, $G\alpha_{16}$), and $G\alpha_{12}$ ($G\alpha_{12}$, $G\alpha_{13}$) (Table 1.1) (L. Birnbaumer, 2007; Moreira, 2014). The stimulatory G alpha subunits ($G\alpha_s$, $G\alpha_{olf}$) are critical components of the classical signal transduction pathway, linking receptor activation with the stimulation of adenylyl cyclase and production of the second messenger cAMP. All human isoforms of adenylyl cyclase are stimulated by $G\alpha_s$, where stimulation increases the rate of production of cAMP from ATP (Dessauer, Tesmer, Sprang, & Gilman, 1998). Crystallographic studies indicate that $G\alpha_s$ subunits bind directly to adenylyl cyclase through interactions within the groove of the α2 helix and α3-β4 loops of the C2a domain to stimulate activity (Dessauer et al., 1998; Moreira, 2014; Tesmer, Sunahara, Gilman, & Sprang, 1997). While $G\alpha_s$ and $G\alpha_{olf}$ are highly homologous and exhibit similar stimulatory effects on adenylyl cyclase, their differential expression patterns influence GPCR signaling pathways (Herve, 2011). For example, the predominant stimulatory G protein in the brain is $G\alpha_s$; however, within striatal medium spiny neurons (MSN), $G\alpha_{olf}$ replaces $G\alpha_s$ and is critical for D_1 dopamine receptor signaling (Herve, 2011).

In contrast, the inhibitory Gα subunits ($G\alpha_t$, $G\alpha_{i1}$, $G\alpha_{i2}$, $G\alpha_{i3}$, $G\alpha_{o1}$, $G\alpha_{o2}$, $G\alpha_\zeta$) directly inhibit adenylyl cyclase activity to downregulate cAMP production. While all adenylyl cyclase isoforms are stimulated by $G\alpha_s$, only types 1, 5, and 6 are inhibited by $G\alpha_i$, and $G\alpha_\zeta$, with $G\alpha_o$ inhibiting type 1 alone (Dessauer et al., 1998; Taussig, Iniguez-Lluhi, & Gilman, 1993; Taussig, Tang, Hepler, & Gilman, 1994). A crystal structure of the complex between inhibitory Gα subunits and adenylyl cyclase has not yet been determined; however, mutational studies suggest that these subunits bind to the region between the α2-α3 helices of the C_{1a} domain of adenylyl cyclase, a site directly opposite of the $G\alpha_s$ binding surface (Dessauer et al., 1998; Tesmer & Sprang, 1998). The binding of inhibitory Gα subunits is believed to prevent the formation of the catalytic site around the substrate ATP (Tesmer & Sprang, 1998).

Table 1.1 Classes of Gα subunits and their general signaling effect.

Group	Isoforms	Signaling effects
$G\alpha_s$	$G\alpha_s$, $G\alpha_{olf}$	Adenylyl cyclase activation
$G\alpha_{i/o}$	$G\alpha_{i1}$, $G\alpha_{i2}$, $G\alpha_{i3}$, $G\alpha_o$, $G\alpha_z$, $G\alpha_t$	Adenylyl cyclase inhibition
$G\alpha_{q/11}$	$G\alpha_q$, $G\alpha_{11}$, $G\alpha_{14}$, $G\alpha_{16}$	Activation of PLC
$G\alpha_{12/13}$	$G\alpha_{12}$, $G\alpha_{13}$	Activation of RhoGEF

The $G\alpha_{q/11}$ family of G proteins is particularly significant because of the broad range of cellular properties mediated by these effectors. Activation of $G\alpha_{q/11}$-coupled GPCRs stimulates phospholipase C (PLC) activity, which in turn hydrolyzes membrane bound phosphatidylinositol-4,5-biphosphate (PIP_2) into two components: diacylglycerol (DAG) and inositol 1,4,5 triphosphate (IP_3) (Kamato et al., 2017). Diacylglycerol stimulates protein kinase C (PKC) activity to phosphorylate target proteins, while IP_3 promotes Ca^{2+} release from intracellular stores (Kamato et al., 2017). While $G\alpha_q$ and $G\alpha_{11}$ share 88% sequence homology and show similar tissue expression patterns, their tertiary structures exhibit discernible differences suggesting that the two isoforms may have distinct functional roles, though presently none have been identified (Kamato et al., 2017).

Members of the $G\alpha_{12/13}$ family of G proteins couple receptors to Rho guanine-nucleotide exchange factors (RhoGEF) that promote RhoA activation, which mediates changes in morphology, cell migration, adhesion, and contraction (Buhl, Johnson, Dhanasekaran, & Johnson, 1995; Worzfeld, Wettschureck, & Offermanns, 2008). Most receptors that couple to $G\alpha_{12/13}$ subunits also couple $G\alpha_{q/11}$, suggesting that $G\alpha_{12/13}$ mediated signaling events may occur in parallel with $G\alpha_{q/11}$ mediated processes (Y. Q. Li et al., 2016; Worzfeld et al., 2008). Interest in $G\alpha_{12/13}$ mediated processes has grown considerably as many of the downstream signaling pathways regulate cell migration and adhesion, critical factors in the metastasis of cancers (Kelly et al., 2006; Y. Q. Li et al., 2016). *In vivo* studies of $G\alpha_{12/13}$ inhibition have shown no effect on tumor growth but exhibited reduced metastatic spread, suggesting a possible role for $G\alpha_{12/13}$ modulators in future cancer treatments (Kelly et al., 2006; Y. Q. Li et al., 2016).

Lipid modifications to Gα subunits are common post-translational changes, typically consisting of the addition of a myristol and/or palmitoyl group near their N-terminus (Lutz Birnbaumer, 2010; Casey, 1995). Palmitoylation of Gα subunits involve the addition of a 16-carbon saturated fatty acyl group to a N-terminal cysteine residue via thioester linkage (Casey, 1995). This modification facilitates anchoring the subunit to the plasma membrane (Lutz Birnbaumer, 2010). Inhibitory $G\alpha_{i/o}$ subunits are also myristolated at N-terminal glycine residues through an amide linkage of a saturated 14-carbon chain (Casey, 1995). Myristolation of $G\alpha_{i/o}$ subunits increases their affinity for the Gβγ heterodimer (Lutz Birnbaumer, 2010). Mutation of $G\alpha_{i/o}$ N-terminal glycine residues prevents myristolation and renders the subunits ineffective as inhibitors of adenylyl cyclase (Lutz Birnbaumer, 2010).

Bacterial ADP-ribosylating toxins are family of lethal protein complex toxins that include pertussis toxin (PTX) and cholera toxin (CTX) (Mangmool & Kurose, 2011; J. Sanchez & Holmgren, 2011). These two cytotoxic agents cause severe diseases through the covalent modification of Gα subunits. PTX is the toxin produced by the bacterium *Bordetella pertussis* responsible for whooping cough (Mangmool & Kurose, 2011). The PTX protein complex catalyzes the ADP-ribosylation of the inhibitory Gα subunits $G\alpha_{i}$, $G\alpha_{o}$ and $G\alpha_{t}$ (except $G\alpha_{\zeta}$), locking the Gα subunit into the inactive GDP bound state (Mangmool & Kurose, 2011). This covalent modification blocks the Gα subunit from interacting with their receptor and prevents the inhibition of adenylyl cyclase, resulting in an enhanced accumulation of cAMP (Mangmool & Kurose, 2011). In contrast, cholera toxin from *Vibrio cholerae* targets the stimulatory Gα subunits $G\alpha_{s}$ and $G\alpha_{olf}$ for ADP-ribosylation (J. Sanchez & Holmgren, 2011). After the covalent modification, the stimulatory Gα subunit remains in the activated GTP-bound state, resulting in enhanced adenylyl cyclase activity and increased cAMP production (J. Sanchez & Holmgren, 2011).

1.1.4.2 Gβγ subunits

Humans express five distinct Gβ subunits ($G\beta_{1\text{-}5}$), and 12 Gγ proteins ($G\gamma_{1\text{-}5,7\text{-}13}$) (Khan et al., 2013). The Gβ subunit consists of twisted antiparallel β-sheets, packed together in a circular formation like the blades of a fan propeller (Murzin, 1992). Crystallographic studies of the Gβγ heterodimer indicate that the Gβ protein contains seven structurally similar WD motif repeats. These motifs are approximately 40 amino acids in length and are typically terminated by a tryptophan (W) – asparagine (D) dipeptide, thus giving rise to the WD motif name (Sondek, Bohm, Lambright, Hamm, & Sigler, 1996). Each of the seven WD motifs contains conserved residues that stabilize a mutual set of interactions with the neighboring blade of the β-propeller, providing strength to the tertiary protein structure (Murzin, 1992; Sondek et al., 1996). The Gβ subunit is cupped and partially encompassed by α-helical Gγ, which forms extensive hydrophobic interactions along Gβ (Lambright et al., 1996; Sondek et al., 1996). The N-terminal helix of Gγ forms a coiled-coil with the N-terminal helix of Gβ, further stabilizing the pair (Lambright et al., 1996; Sondek et al., 1996). In fact, Gβ and Gγ are so tightly associated, expressing them independently results in an unstable Gβ subunit and unfolded Gγ protein (Higgins & Casey, 1994).

The inactive GDP-bound form of Gα has been shown to bind the Gβγ subunit at two distinct regions. The interface of Gα adjacent to the switch I and II regions binds at the top of the β-propeller, while the N-terminal helical tail of Gα forms interactions across the side of the β-propeller (Lambright, Noel, Hamm, & Sigler, 1994; Lambright et al., 1996). During activation of Gα, the exchange of GDP for GTP promotes the formation of new interactions between the γ-phosphate of GTP and glycine 199 of Gα (Lambright et al., 1994; Lambright et al., 1996). While the conformational change is relatively small, these new interactions disrupt the hydrogen bonding between glycine 199 of Gα and asparagine 119 of Gβ, contributing to the release of Gα from Gβγ (Lambright et al., 1994; Lambright et al., 1996).

Lipid modification, as with Gα subunits, is a common post-translational processing step for Gβγ subunits. The Gβγ heterodimer is anchored to the plasma membrane through the addition of a 15-20 carbon polyisoprene group to Gγ via thioester linkage to a C-terminal cysteine within a CAAX motif (Lutz Birnbaumer, 2010). The post-translational prenylation of Gγ also involves the removal of the last 3 residues and methylation of the new C-terminus (Lutz Birnbaumer, 2010). While prenylation is not essential for the association of Gγ with Gβ, it is required for the association of the Gβγ heterodimer with GDP bound Gα subunits, as well as regulation of effector enzymes such as adenylyl cyclase (Lutz Birnbaumer, 2010).

Initially believed to negatively regulate Gα subunits during GPCR signaling, the Gβγ dimer was first found to have an independent role when purified Gβγ subunits were shown to activate the cardiac muscarinic-gated Kir3 inward-rectifying potassium channel (Khan et al., 2013; Logothetis, Kurachi, Galper, Neer, & Clapham, 1987). Since that initial discovery, the roles of Gβγ dimers have grown substantially. Gβγ binding sites have since been identified on multiple types of voltage-dependent calcium channels. Here, they exert an inhibitory action on the channel, thereby potentially allowing for crosstalk or fine-tuning of intracellular calcium signaling (Evans & Zamponi, 2006; Khan et al., 2013). Adenylyl cyclases are also modulated by Gβγ subunits, stimulating type II cyclases (AC2, AC4, AC7) while inhibiting other isoforms (AC1, AC5, AC6). The mechanism of Gβγ stimulation of AC activity is through a direct interaction with a unique PFAHL motif that is present on the C1 catalytic domain of type II adenylyl cyclases, but absent in other isoforms (Weitmann, Schultz, & Kleuss, 2001). The inhibitory mechanism of Gβγ is less well understood and may be dependent on the subtypes of Gβ and Gγ present in the subunit (Bayewitch et al., 1998). Furthermore, phospholipase C activation is another example of Gβγ-

mediated regulation of signaling effectors which results in the cleavage of PIP_2 into diacylglycerol and inositol 1,4,5-triphosphate (IP_3) (Bunney & Katan, 2011; Khan et al., 2013). These signaling molecules have wide reaching effects, including the mobilization of intracellular calcium stores and activation of protein kinase C (PKC). Finally, GPCRs are capable of initiating the mitogen-activated protein kinase (MAPK) cascade via Gβγ stimulation of PLCβ as well as the recruitment of receptor tyrosine kinases (RTK) (Bunney & Katan, 2011; Khan et al., 2013). Several novel non-canonical actions of Gβγ subunits are being characterized, including their role in cell division and cytoskeleton assembly, endosomal signaling, mitochondrial functioning, as well as the regulation of transcriptional activity in the nucleus (Khan et al., 2013). Our understanding of both the canonical and non-canonical roles of Gβγ subunits in diverse intracellular process highlights the fact that the specific contents of distinct Gβγ subunits, made up from 5 Gβ and 12 Gγ isoforms, underlies the distinct roles of these subunits (Khan et al., 2013; Khan, Sung, & Hebert, 2016). Better characterization of effects of individual isoforms is necessary to understand the specific roles of distinct Gβγ subunits, and restraint should be taken to prevent overgeneralizing the effects of one particular Gβγ heterodimer (Khan et al., 2016).

1.1.4.3 β-arrestins

Agonist stimulation of G protein-coupled receptors results in conformational changes that expose the cytosolic binding domains for heterotrimeric G proteins. Following the exchange of GDP for GTP and activation of Gα subunits, the heterotrimer dissociates and the Gα and Gβγ subunits activate their various effectors (Shenoy & Lefkowitz, 2011). The agonist occupied GPCR then becomes a target for phosphorylation by G protein receptor kinases (GRKs) (Shenoy & Lefkowitz, 2011). Receptors are phosphorylated at multiple intracellular sites without a particular consensus phosphorylation sequence, suggesting that the specific site of phosphorylation is less important than the bulk negative charge on the intracellular face of the receptor (Tobin, 2008). This newly established receptor modification acts to recruit arrestins, a family of proteins appropriately named for their ability to "arrest" temporal GPCR signaling by stimulating receptor endocytosis.

Four mammalian arrestins can be divided into two categories, visual and non-visual (Kang, Tian, & Benovic, 2013). The two non-visual arrestins, arrestin 2 (β-arrestin 1) and arrestin 3 (β-arrestin 2) are ubiquitously expressed and share 78% amino acid sequence homology (J. S. Smith & Rajagopal, 2016). The general arrestin structure is composed of two 7-stranded parallel beta

sheets, termed the N-terminal and C-terminal domains, which are connected by a 10-residue hinge region (Celver, Vishnivetskiy, Chavkin, & Gurevich, 2002; Zhan, Gimenez, Gurevich, & Spiller, 2011). A highly conserved polar core of charged residues forms a series of buried salt bridges to stabilize the tertiary structure and maintain a basal inactive conformation (Celver et al., 2002; Zhan et al., 2011). This unusual network of charged residues, as well as a portion of the C-terminal tail, has been identified as the critical component of the arrestin phosphate-sensing domain (Celver et al., 2002; Zhan et al., 2011). Mutational studies have shown that perturbations to these regions create constitutively active mutants that promote receptor desensitization regardless of the receptor's phosphorylation state (Celver et al., 2002).

The endocytosis of activated GPCRs serves as a mechanism to regulate the duration and magnitude of the signaling event by preventing re-association with heterotrimeric G proteins and controlling receptor expression on the cell surface (Moore, Milano, & Benovic, 2007; Shenoy & Lefkowitz, 2011; Sondek et al., 1996). The most common method of receptor endocytosis is through a clathrin-dependent mechanism in which receptors are moved to clathrin-coated pits in a dynamin-dependent manner (Goodman et al., 1996; Moore et al., 2007; Sondek et al., 1996). The receptor does not bind clathrin directly, but rather the arrestin acts as an adapter protein, facilitating the interaction through a series of complementary residues on the C-terminal tail (Goodman et al., 1996; Tian, Kang, & Benovic, 2014). Additional interactions within clathrin-coated pits are formed between the arrestin and the adapter protein AP2, which facilitates the internalization of the receptor into early endosomes (Moore et al., 2007; Tian et al., 2014). This multi-protein complex of interacting partners is internalized and subsequently sorted into recycling endosomes that traffic the internalized receptors back to the cell surface, or late endosomes that facilitate lysosomal degradation of the receptor (Moore et al., 2007).

In addition to acting as a scaffolding protein, previous research has suggested that arrestins are capable of initiating unique signaling patterns that are spatially and temporally distinct from G protein-mediated signaling (Shenoy & Lefkowitz, 2011; H. Wei et al., 2003). In particular, the arrestin dependent activation of ERK1/2 has been proposed to be a distinct mechanism to G-protein mediated activation and has been the subject of substantial research (H. Wei et al., 2003). Recent advances in CRISPER/Cas9 technology has allowed for the development of a HEK293 cell line that was genetically devoid of $G\alpha_s$, $G\alpha_q$, and $G\alpha_{12/13}$ expression, and in combination with PTX-mediated inhibition of $G\alpha_{i/o}$, this model provides a blank slate to study the effects of receptor

activation on arrestin signaling (Grundmann et al., 2018). The results of this study indicate that arrestin recruitment in the absence of functional G protein signaling regulates GPCR surface expression levels but has no effect on the activation of ERK1/2 (Grundmann et al., 2018). This data suggests that signaling processes previously attributed to arrestin dependent pathways are in fact the result of G protein mediated signaling (Grundmann et al., 2018). While these results await replication, this conflict clearly highlights the need to reconsider the methods used to establish and validate basic principles of GPCR signal transduction.

1.1.5 Modulators of G protein signaling

The regulation of heterotrimeric G protein-mediated signaling is critically important for the functional control of many biological processes. In addition to the modulation of G protein-coupled receptor activity, G protein signaling can be activated or repressed through mechanisms independent of receptor activity (Blumer, Smrcka, & Lanier, 2007). Activators of G protein signaling (AGS) or regulators of G protein signaling (RGS) are classes of small accessory proteins that influence G protein signaling and downstream effector activation through diverse mechanisms including regulating the rate of GTP hydrolysis, modifying the availability of Gα or Gβγ subunits, or otherwise affecting subunit stability (Blumer et al., 2007).

1.1.5.1 Activators of G protein signaling

Activators of G protein signaling (AGS) proteins are generally divided into three classes: guanine nucleotide exchange factors (GEF), nucleotide dissociation inhibitors, and modifiers of Gβγ interaction. Though mechanistically the three classes of AGS are distinct in their function, they all serve to stimulate or enhance Gα activity. Guanine nucleotide exchange factors (Group I AGS Proteins) stimulate the release of bound GDP and promote the binding of GTP for Gα and/or Gαβγ, thereby activating the G protein independently of receptor stimulation (Blumer & Lanier, 2014). Specific Gα subunits are selectively activated by particular GEFs, thereby promoting stimulation of specific Gα-mediated signaling pathways rather than broad-spectrum activation (Blumer & Lanier, 2014). Guanine nucleotide exchange factors therefore are involved in diverse physiological processes, including cell growth and cancer proliferation, angiogenesis, and neurotransmitter signaling (Blumer & Lanier, 2014).

Nucleotide dissociation inhibitors (Group II AGS Proteins) contain one to four G protein regulatory (GPR) motifs that preferentially bind inactive $G\alpha_{i/o}$-GDP to form a GPR-$G\alpha_{i/o}$ complex in an apparent contrast to their classification (Blumer & Lanier, 2014; De Vries et al., 2000). Evidence suggests that this GPF-$G\alpha_{i/o}$ complex may participate in unique signaling pathways, or be further targeted by guanine nucleotide exchange factors to promote G protein activation (Blumer & Lanier, 2014; Blumer, Oner, & Lanier, 2012). By preventing the inactive GDP bound $G\alpha_{i/o}$ from returning to the receptor, nucleotide dissociation inhibitors effectively prolong Gβγ-mediated signaling pathways (Blumer et al., 2012; De Vries et al., 2000). Research has implicated nucleotide dissociation inhibitors in processes such as cell division, protein trafficking, cytoskeleton rearrangement, and cell polarity; however, greater effort is necessary to fully understand the role of these proteins in cellular processes (Blumer et al., 2012).

Modifiers of Gβγ interaction (Group III AGS Proteins) are a diverse set of proteins, and their roles in G protein mediated signaling events are not well defined. It is generally believed that proteins in this group interact with the Gαβγ complex independent of nucleotide exchange and promote the disassociation of Gα and Gβγ, thus allowing for Gβγ to engage with its particular effectors to stimulate Gβγ-mediated signaling (Blumer & Lanier, 2014). Evidence suggests that the Group III AGS protein AGS8 binds to a unique site on $G\beta_1\gamma_2$ to promote interaction and activation of phospholipase C (Yuan, Sato, Lanier, & Smrcka, 2007). Further analysis indicates that the AGS-Gβγ interaction takes place at a site distinct from the Gα binding site, thus directing Gβγ signaling through alternate mechanism independent of Gα or receptor activation (Blumer & Lanier, 2014; Yuan et al., 2007).

1.1.5.2 Regulators of G protein signaling

In opposition of AGS proteins, regulators of G protein signaling (RGS) reduce the duration of G protein signaling by enhancing the endogenous GTPase activity of Gα proteins or by modulating the interactions of Gα with effector proteins to promote GTP turnover. All RGS proteins share a conserved sequence of approximately130 residues (defined as the RGS domain) that binds GTP-bound Gα subunits and accelerates the rate of GTP hydrolysis to promote early termination of the G protein signaling cycle (Tesmer, 2009). Multiple crystal structures have exposed structural information regarding the RGS domain as well as its interaction with Gα subunits. The canonical RGS domain consists of a bundle of nine α-helices that roughly adopt a two-lobed conformation,

termed the bundle subdomain and terminal subdomain (Tesmer, 2009). The crystal structure of the RGS4-$G\alpha_{i/1}$ complex has indicated that the RGS domain contacts the Gα subunit at the three switch regions, and these areas known to undergo conformational change following the binding of GTP (Tesmer, 2009). Two main interactions are formed between RGS4 and $G\alpha_{i/1}$ that regulate the GTP accelerating activity, specifically a binding pocket established by three loops from helices α3-α4, α5-α6, and α7-α8 which accommodates the side chains of the switch I region, as well as a semi-conserved arginine residue in the α5-α6 loop that packs against the switch I and switch II regions and to directly contacts residues involved in the catalysis of GTP (Tesmer, 2009).

Research has now identified 30 known RGS-domain containing proteins in the human genome, and these proteins can be divided into four categories based upon sequence homology (Sjogren, Blazer, & Neubig, 2010; Tesmer, 2009). The R4 family of RGS proteins is the largest, and its members contain short N- and C-terminal extensions of the RGS domain but otherwise have little significant structural variability. The R4 family exhibits broad specificity for G proteins, and has been shown to bind and function as GTP accelerating proteins (GAPs) for all $G\alpha_q$ and $G\alpha_{i/o}$ subunits (Sjogren et al., 2010; N. Watson, Linder, Druey, Kehrl, & Blumer, 1996). The R7 family is structurally larger than the R4 and includes various domains in addition to the RGS domain. Members of the R7 family exhibit selectivity for $G\alpha_{i/o}$ and do not interact with $G\alpha_q$ subunits (Hooks et al., 2003; Sjogren et al., 2010). The R12 family of RGS proteins is more structurally diverse with some members containing small N- and C-termini similar to the R4 family, while others are structurally larger proteins and contain various domains such as those facilitating protein-protein interaction, as well as GoLoco motifs that exhibit GDI activity toward $G\alpha_{i1}$ $G\alpha_{i2}$, and $G\alpha_{i3}$(Siderovski & Willard, 2005; Sjogren et al., 2010). Finally, the RZ family of RGS proteins is the least characterized, but has been shown to be the only RGS family that has selective GAP activity on $G\alpha_z$, a member of the $G\alpha_{i/o}$ family that is pertussis toxin (PTX) insensitive (Ajit et al., 2007; Sjogren et al., 2010).

1.1.6 Therapeutic relevance

Members of the GPCR superfamily are diverse in their structure and function, as well as in their expression across different tissues and organ systems. These characteristics make GPCRs and their associated signal transduction pathways important targets for manipulating a variety of physiological functions. Presently, 108 G protein-coupled receptors are targeted by a

disproportionate amount (34%) of FDA approved drugs, and GPCR-targeting drugs account for over 180 billion US dollars annually in global sales (Hauser et al., 2018).

GPCRs are clearly a viable and productive target for pharmaceutical development, and future developments in technology and genetics will continue to encourage their growth as druggable targets. Moreover, while over 800 GPCRs have been identified in humans, the endogenous ligands of more than 140 GPCRs remain undefined, leaving the physiological function of these orphan receptors unknown (Fredriksson et al., 2003; Mombaerts, 2004). Expanded efforts to deorphanize GPCRs through advances in molecular biology and screening technology have resulted in the characterization of endogenous ligands for these previously unclassified receptors (X. L. Tang, Wang, Li, Luo, & Liu, 2012). These continued efforts may likely yield attractive new drug targets in the near future.

Furthermore, the crystallization of receptors bound to endogenous ligands or small molecules provides a wealth of information on the 3-dimensional structure of the receptor, as well as the specific residues defining the ligand-binding site (Cherezov et al., 2007). While compound screening and structure-activity relationship analysis are well-defined and successful methods for the development of more potent and efficacious compounds, it is believed that high-resolution structural information of the target is necessary to develop ligands with sub-nanomolar potency (Lefkowitz, 2004). As the number of high-resolution structures continues to grow, these findings will provide an ever increasingly detailed molecular guide for designing new small molecule therapeutics.

In addition to the novel insights screening and structural studies have lent to the GPCR field, the natural genetic variation that occurs across individual human genomes has been identified as a cause of differential responses to medications, defined as pharmacogenomics. Because GPCRs are a substantial target of small molecule therapeutics, polymorphisms that occur within the receptors have important clinical and therapeutic implications (Lefkowitz, 2004). Such mutations can modify the risk of a medication or the progression of a disease. With incredible advancements in genetics over the past decade, the advent of personalized medicine has allowed an individual's unique gene expression to help guide pharmacological treatment for an optimal outcome (Hauser et al., 2018).

1.2 Adenylyl cyclases

1.2.1 Adenylyl cyclase structure

As described earlier, adenylyl cyclases play a pivotal role in GPCR signal transduction. There are nine membrane-bound adenylyl cyclase isoforms (ACs 1-9) that share a common tertiary protein structure that consists of a cytoplasmic N-terminal domain of variable length, two six-transmembrane domains (TM1, TM2), and two well-conserved cytosolic domains (C_1, C_2) (Dessauer et al., 2017). The two transmembrane spanning domains are organized clusters of α-helices, separated by the C_1 cytosolic domain, and followed by the large C-terminal C_2 domain. The cytosolic domains can be further subdivided into catalytic (C_{1a} and C_{1b}) and regulatory (C_{1b} and C_{2b}) subdomains and together make up the catalytic core (Fig. 1.3) (Hurley, 1999).

A majority of our knowledge regarding the adenylyl cyclase catalytic core is based upon the X-ray structural analysis of recombinant C_{1a} and C_{2a} from canine AC5 and rat AC2 respectively ($5C_1$-$2C_2$) bound in complex with bovine $G\alpha_s$ (Tesmer & Sprang, 1998; Tesmer et al., 1997). Expression of the two catalytic subunits results in the formation of a circular heterodimer, with the active site formed at the interface by residues from both the C_{1a} and C_2 domains (Tesmer & Sprang, 1998; Tesmer et al., 1997). The position of ATP in the active site was solved by crystalizing the $5C_1$-$2C_2$ construct bound to the P-site inhibitor 2'd3'AMP•PP_i, then modeling ATP to occupy the active site in a closed conformation (Tesmer & Sprang, 1998; Tesmer et al., 1997). This model shows that the purine ring of ATP binds within a hydrophobic pocket at the interface between the C_{1a} and C_{2a} domains, and two Mg^{2+} ions and three basic residues (Arg-484, Arg-1029, and Lys-1065) bind the ribose and triphosphate tail of ATP (Tesmer & Sprang, 1998; Tesmer et al., 1997). The magnesium ions are stabilized by two conserved aspartic acids (Asp-440, Asp-396), and the carbonyl oxygen of Iso-397 (Tesmer & Sprang, 1998; Tesmer et al., 1997). The specificity of the ATP binding site is regulated by Lys-938 and Asp-1018 of the C_2 domain, which directly interact with the nitrogen atoms N-1 and N-6 of the adenine ring, mutation of these residues disrupts the ATP specificity and creates a non-specific nucleotidyl cyclase (Sunahara et al., 1998).

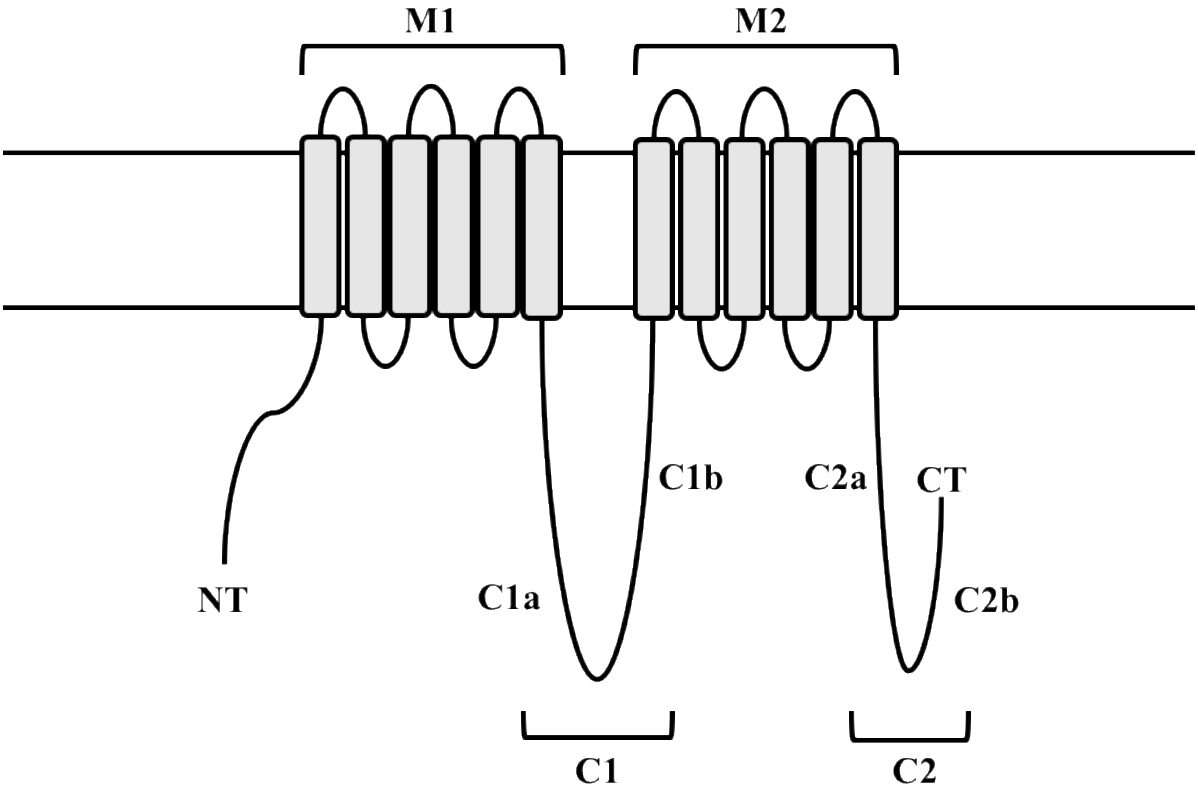

Figure 1.3: Topology of membrane-bound adenylyl cyclase.

Membrane-bound adenylyl cyclases share a similar structural arrangement, consisting of an N-terminal tail (NT), two membrane clusters (M1 and M2) each composed of six transmembrane spanning alpha helices, a large cytoplasmic domain (C1), and a large C-terminal cytoplasmic domain (C2).

1.2.2 Catalytic mechanism

Adenylyl cyclase converts the substrate ATP to 3', 5'-cAMP with an inversion of stereochemistry at the α-phosphate (Eckstein, Romaniuk, Heideman, & Storm, 1981; Tesmer & Sprang, 1998). While the association of the C_{1a} and C_{2a} subunits is required for basal catalytic activity, the presence of an activator such as $G\alpha_s$ or the allosteric small molecule activator forskolin dramatically increases the affinity of the two subunits (Tesmer & Sprang, 1998). Based on the $5C_1$-$2C_2$ crystal structure, $G\alpha_s$ has been shown to interact primarily to the cleft between the α1-α2 and α3-β4 loops of the C_{2a} domain, but also interacts with several hydrophobic residues near the N-terminus of C_{1a} (Tesmer & Sprang, 1998; Tesmer et al., 1997). The binding of $G\alpha_s$ to the catalytic domains has been proposed to expand the cleft between the α1-α2 and α3-β4 loops, causing the α1-α2 loop to sterically force the C_{1a} domain to rotate 10° with respect to C_{2a} (Tesmer & Sprang, 1998; Tesmer et al., 1997). The resulting change in conformation properly orients the catalytic residues to convert ATP to cAMP. Interestingly, this change in conformation increases the catalytic velocity of the reaction, without dramatically changing the K_m for ATP (Tesmer & Sprang, 1998; Whisnant, Gilman, & Dessauer, 1996). Forskolin binds to a region within the C_{1a}-C_{2a} interface that is adjacent to the $G\alpha_s$ binding site, and is believed to induce a conformational change similar to that described for $G\alpha_s$ (Hurley, 1999; Tesmer & Sprang, 1998).

The inhibitory $G\alpha_{i/o}$ subunits have been shown to act as non-competitive inhibitors of $G\alpha_s$ mediated stimulation of AC5/AC6 (Tesmer & Sprang, 1998). The sequence and structural homology between $G\alpha_{i/o}$ and $G\alpha_s$ suggest these subunits may interact with the adenylyl cyclase catalytic domains in a similar manner (Hurley, 1999). The pseudosymmetrical cleft between the α1-α2 and α3-β4 loops of the C_{1a} domain have been shown to collapse upon the active site following ATP binding, and it is hypothesized that $G\alpha_{i/o}$ binds this region and prevents the collapse of the catalytic residues around the substrate (Dessauer et al., 1998; Tesmer & Sprang, 1998). Site-directed mutagenesis to the α1-α2 and α3-β4 loops of the C_{1a} domain has been shown to significantly increase or decrease the potency of myristolated-$G\alpha_s$ to inhibit adenylyl cyclase activity (Dessauer et al., 1998). These results further support a mechanism by which $G\alpha_{i/o}$ inhibits catalytic activity by interaction with the C_{1a} domain.

Protein interactions with non-catalytic regions of adenylyl cyclase also exhibit modulatory effects. The effects of Gβγ subunits on adenylyl cyclase are isoform dependent - inhibiting AC1 while conditionally activating AC2 and AC4 with $G\alpha_s$, and having no discernible effect on other

isoforms (Tesmer & Sprang, 1998). A peptide derivative of the α3 helix of the C_{2a} domain has been shown to mitigate the effects of Gβγ by binding and sequestering the subunit; however, because of the lack proper characterization of this peptide, it remains unknown if this segment of α3 accurately represents the Gβγ binding site (J. Chen et al., 1995). Calcium-bound calmodulin stimulates isoforms AC1 and AC8 and has been shown to interact with both the N and C-terminal regions (Hurley, 1999; Masada, Schaks, Jackson, Sinz, & Cooper, 2012). While Ca^{2+}/calmodulin binds AC1 via a calmodulin-binding domain in the C_{1b} region, the interaction at AC8 takes place at both the N-terminal and C_{2b} domains (Masada et al., 2012). The stimulation of AC1 and AC8 by Ca^{2+}/calmodulin appears to be through distinct mechanisms, where binding to the C_{1b} region of AC1 results in the relief from an autoinhibited state, Ca^{2+}/calmodulin binding to AC8 seems to have some degree of redundancy between the N-terminal and the C_{2b} domain (Masada et al., 2012).

1.2.3 Regulatory properties of adenylyl cyclase isoforms

1.2.3.1 Group 1 ACs

While all membrane localized adenylyl cyclases are stimulated by $G\alpha_s$, the various adenylyl cyclase isoforms differ in their specific activation and inhibitory characteristics (summarized in Table 1.2). Group 1 adenylyl cyclases are represented by AC1, AC3, and AC8 and have been shown to be stimulated by Ca^{2+}/calmodulin. Calcium-bound calmodulin stimulates AC1 and AC8 through direct interaction with the catalytic domain; however, the kinetics of these two isoforms differ significantly in response to cytosolic Ca^{2+}. AC3 appears to be conditionally stimulated by Ca^{2+}/calmodulin when the enzyme has been activated by $G\alpha_s$ or the small molecule forskolin, suggesting a possible mechanism by which calmodulin interaction can enhance or amplify AC3 signaling (Choi, Xia, & Storm, 1992). Although AC1 is approximately 3.5x more sensitive to Ca^{2+} than AC8, AC1 responds more slowly and produces cAMP at a steadily increasing rate, whereas AC8 stimulation produces cAMP in rapid oscillations in response to Ca^{2+}entry (Masada et al., 2012). Presently, it is hypothesized that the distinct localization of the calmodulin binding domains between the two cyclases may underlie the differential regulation and different kinetics observed in these two isoforms. AC1 binds Ca^{2+}/calmodulin in the C_{1b} region of the catalytic domain, and it is hypothesized to activate the cyclase through the release of an autoinhibited state. Mutagenesis to the residues arginine-503 and lysine-504 within the C_{1b} domain of AC1 were shown to significantly decrease the sensitivity to calmodulin, indicating that these residues may help

coordinate interactions with calmodulin or play a role in regulating the autoinhibited state of AC1 (Z. Wu, Wong, & Storms, 1993). In contrast, research has identified two Ca^{2+}/calmodulin binding sites on AC8. The N-terminal site is structurally similar to calmodulin-binding domains, which are defined by patterns of hydrophobic, basic, and aromatic amino acids that tend to form an amphipathic α-helix (Gu & Cooper, 1999). The other binding site is located in the C_{2b} domain, and although it resembles a Ca^{2+} independent IQ-motif, mutagenesis and functional studies have confirmed the site is the Ca^{2+}-dependent calmodulin-binding site that is primarily responsible for the Ca^{2+}/calmodulin stimulation of AC8 (Gu & Cooper, 1999).

Calmodulin is a small protein that is comprised of globular N- and C-terminal heads (N-lobe and C-lobe) that each bind two Ca^{2+} ions and are connected by a long, flexible α-helical linker region (Masada et al., 2012). Both the N-lobe and C-lobe have differing affinities for Ca^{2+} and can interact with protein targets independently or in a unified manner (Masada, Ciruela, Macdougall, & Cooper, 2009). Studies have shown that Ca^{2+} binding to both lobes of calmodulin is required for interaction with AC1 (Masada et al., 2009). In contrast, the N-terminus of AC8 can interact with partially filled calmodulin (Masada et al., 2009). The C-lobe bound to two Ca^{2+} ions was sufficient to promote interaction with AC8 N-terminal fragments; however, the interaction was enhanced when calmodulin was fully bound with four Ca^{2+}ions (Masada et al., 2012). Interestingly, the C_{2b} region of AC8 exhibited greater interaction with a calmodulin mutant only capable of binding two Ca^{2+} ions at the N-lobe, compared with wild-type calmodulin that could bind two Ca^{2+} ions at the N-lobe and 2 at the C-lobe (Masada et al., 2012). Together these results suggest that a partially filled calmodulin may be sufficient to stimulate AC8, which may underlie the more rapid activation of AC8 activity in response to calcium influx. Whereas the slower activation of AC1 activity may be the result of dependence on fully bound calmodulin.

In addition to their regulation by Ca^{2+}/calmodulin, Group 1 adenylyl cyclases also exhibit differential inhibition in response to both $G\alpha_i$ and Gβγ subunits, as well as phosphorylation by protein kinases. The Ca^{2+}-mediated stimulation of AC1 using the ionophore A23187 could be robustly inhibited by the activation of the $G\alpha_i$-coupled somatostatin and D_2 dopamine receptors (Nielsen, Chan, Poser, & Storm, 1996). In contrast, A23187 stimulated AC8 activity was not inhibited by stimulation of either the somatostatin or D_2 receptor (Nielsen et al., 1996). All Group 1 adenylyl cyclases have been shown to be directly inhibited by Gβγ subunits; however, different combinations of Gβ and Gγ isoforms exhibited variable efficacy and efficiency, suggesting that

receptor coupling and Gβγ expression patterns likely influence the significance of their inhibitory role (Diel, Beyermann, Llorens, Wittig, & Kleuss, 2008; Steiner, Saya, Schallmach, Simonds, & Vogel, 2006; W. J. Tang & Gilman, 1991). Both AC1 and AC3 are directly inhibited by calmodulin-dependent kinase (CaMK), highlighting a mechanism of calcium-mediated feedback inhibition. AC1 is inhibited by CaMKIV specific phosphorylation, while AC3 is sensitive to CaMKII (Wayman, Wei, Wong, & Storm, 1996; J. Wei, Wayman, & Storm, 1996). Additionally, both AC1 and AC3 are stimulated by phorbol ester activation of PKC, indicating that phosphorylation can have both inhibitory and stimulatory effects for these two isoforms (Jacobowitz, Chen, Premont, & Iyengar, 1993). AC8 does not appear to be sensitive to CaMK or PKC mediated phosphorylation (Jacobowitz et al., 1993).

Table 1.2: Regulatory properties of the membrane bound adenylyl cyclase isoforms.
↑=stimulation, ↓=inhibition

Group	Isoforms	$G\alpha_s$	$G\alpha_{i/o}$	$G\beta\gamma$	Ca^{2+}	Forskolin
1	AC1, AC3, AC8	↑	↓	↓	↑	↑
2	AC2, AC4, AC7	↑		↑		↑
3	AC5, AC6	↑	↓		↓	↑
4	AC9	↑			↓	

1.2.3.2 Group 2 ACs

Group 2 adenylyl cyclases are represented by AC2, AC4, and AC7. These isoforms share an insensitivity to Ca^{2+} and $G\alpha_{i/o}$-mediated inhibition, in addition to differential regulation by PKC (W. J. Tang & Gilman, 1991; Taussig et al., 1993; Taussig et al., 1994). AC2 and AC7 are directly phosphorylated and activated via phorbol ester (PMA) stimulated PKC, although the isoforms exhibit different effects in response to PKC-mediated activation (Jacobowitz & Iyengar, 1994; P. A. Watson, Krupinski, Kempinski, & Frankenfield, 1994). AC7 rapidly increases cAMP production and reaches a maximum four minutes after stimulation, while AC2 appears to respond more slowly, reaching maximal cAMP accumulation after 20 minutes (Jacobowitz & Iyengar, 1994; P. A. Watson et al., 1994; Soto-Velasquez et al., 2018). Studies examining the PKC phosphorylation sites on AC2 have identified serine 490 and serine 543 in the C_{1b} domain as required residues for PKC-mediated stimulation (Shen, Wachten, Halls, Everett, & Cooper, 2012). Mutation of these residues to alanine produced a phosphorylation deficient mutant insensitive to PMA, while phosphomimtetic (S490/543D) mutant produced activity similar to PKC-stimulated AC2 (Shen et al., 2012). While similar mapping studies have not yet been conducted regarding AC7, the homology between the isoforms indicates the C_{1b} domain plays a significant regulatory role in PKC-mediated stimulation. In contrast, AC4 exhibits no significant increase above basal activity following PMA-mediated PKC activation; however, a significant reduction in $G\alpha_s$-mediated AC4 activity was observed following PKCα activation (Zimmermann & Taussig, 1996).

Additionally, Group 2 adenylyl cyclases are known to be conditionally regulated by Gβγ subunits, in which the stimulatory effects of the heterodimer are most pronounced in the presence of $G\alpha_s$ of forskolin (B. N. Gao & Gilman, 1991; W. J. Tang & Gilman, 1991; Zimmermann & Taussig, 1996). Multiple Gβγ interaction sites within the C_{1a}, C_{1b}, and C2 domains have been identified for AC2 (Boran, Chen, & Iyengar, 2011; Diel et al., 2008). Studies have focused on the PFAHL motif present in the C_{1b} domain as the stimulatory region critical for Gβγ-mediated activation of AC2 (Boran et al., 2011; Diel et al., 2008; Shen et al., 2012). Together, these results suggest that the binding of $G\alpha_s$ to the catalytic domain results in a conformational change that exposes a Gβγ binding site, where interaction with the heterodimer further increases the rate of cAMP production. While this working hypothesis fits the existing data, further structural information is necessary to support an interaction with a hidden catalytic domain interface.

1.2.3.3 Group 3 ACs

The group 3 members AC5 and AC6 are characterized by an increased sensitivity to free Ca^{2+}, where they exhibit inhibition by sub-micromolar concentrations. While all membrane bound adenylyl cyclases exhibit inhibition by free Ca^{2+} at high (10-100μM), AC5 and AC6 exhibit a unique biphasic response to Ca^{2+}, signifying the presence of two binding sites of high and low affinity (Cooper, 2003). Kinetic analyses indicate that sub-micromolar concentrations of Ca^{2+} inhibit cyclase activity through non-competitive inhibition of Mg^{2+} activation, suggesting an allosteric mechanism (B. Hu, Nakata, Gu, De Beer, & Cooper, 2002; Mou, Masada, Cooper, & Sprang, 2009). However, supramicromolar concentrations of Ca^{2+} directly compete with Mg^{2+} binding sites (B. Hu et al., 2002; Mou et al., 2009). By soaking $5C_1$-$2C_2$ protein crystals with varying concentrations of Ca^{2+}, crystallographic studies have given insight into the structural basis for inhibition by calcium (Mou et al., 2009). The non-competitive inhibition attributed to binding of the high affinity site is believed to be the result of Ca^{2+} stabilizing the substrate-enzyme complex in an open conformation (Mou et al., 2009). Crystal structures of the calcium soaked catalytic subunits showed Ca^{2+} coordinated with the β and γ phosphates of ATP, and as a result are not available to engage with Mg^{2+} at metal site B to form the AMP•PPi transition state (Mou et al., 2009). At 100μM concentration, Ca^{2+} was shown to bind both A and B sites (Mou et al., 2009). The physiological impact of these results is significant, as it indicates that AC5 and AC6 are key intersections for integration of not only G protein-mediated signaling, but also for hormonal and electrochemical events that terminate in intracellular calcium release.

While all membrane bound adenylyl cyclases are activated by $G\alpha_s$ stimulation, isoforms differ substantially in their response to $G\alpha_{i/o}$-mediated inhibition. AC5 and AC6 are the most sensitive isoforms to inhibition by $G\alpha_{i/o}$ subunits (Taussig et al., 1993; Taussig et al., 1994). *In vitro,* Group 3 cyclases exhibit strong non-competitive inhibition by $G\alpha_{i1,2,3}$ subunits, but initially appeared insensitive to $G\alpha_o$ (Taussig et al., 1993; Taussig et al., 1994). Studies using a cell model that expressed a PTX-insensitive $G\alpha_o$ construct demonstrated that opioid receptors could still inhibit adenylyl cyclase activity after the inactivation of $G\alpha_i$ proteins with PTX (Clark, Harrison, Zhong, Neubig, & Traynor, 2003). Furthermore, in striatal tissue, antibodies against $G\alpha_o$ were shown to decrease subunit expression and decrease opioid receptor-mediated inhibition of adenylyl cyclase activity (B. D. Carter & Medzihradsky, 1993). These results indicate that while $G\alpha_o$ is

insufficient to inhibit AC5 and AC6 *in vitro*, it can inhibit cyclase activity in recombinant cell lines and tissues expressing these isoforms (Beazely & Watts, 2006).

Gβγ has been shown to bind multiple sites on AC5 and AC6, including the N-terminus as well as the C1 and C2 catalytic domains to enhance $G\alpha_s$ stimulated cAMP production (Brand, Sadana, Malik, Smrcka, & Dessauer, 2015; X. Gao, Sadana, Dessauer, & Patel, 2007; Sadana, Dascal, & Dessauer, 2009). Gβγ binding to the N-terminus of AC5 and AC6 has been previously observed either as an independent heterodimer or in complex with $G\alpha_s$ (Sadana et al., 2009). Because the N-termini of AC5 and AC6 vary in their length and sequence, the regulatory function of Gβγ is also variable. Site directed mutagenesis of the Gβγ heterodimer has indicated that the site required for stimulation of AC5 is different from the surface that interacts with the N-terminus (Brand et al., 2015). Mutation of residues Trp-99, Met-101, Asp-186, and Asn-230 within the WD40 repeat "blades" of the Gβ subunit reduced the ability of Gβγ to enhance $G\alpha_s$-mediated AC5 stimulation, however these mutations did not disrupt interaction with the N-terminus (Brand et al., 2015). In contrast to AC5, the same Gβ mutations reduced both binding and stimulation of AC6 indicating that Gβγ participates in different interactions between the two closely related isoforms (Brand et al., 2015). The catalytic domains of AC5 and AC6 exhibit high sequence homology, and both isoforms have been shown to bind Gβγ subunits and increase $G\alpha_s$ stimulated cyclase activity (Beazely & Watts, 2006; Brand et al., 2015; X. Gao et al., 2007). However, the catalytic domains have been shown to exhibit differential interaction based on the Gβ subtype present in the heterodimer. For example, $G\beta_1$ will bind the C1 and C2 domains of AC5 but not AC6, demonstrating that Gβγ regulation of adenylyl cyclase isoforms may be subtype dependent (X. Gao et al., 2007).

In addition to modulation by calcium and heterotrimeric G proteins, Group 3 adenylyl cyclases are also regulated by protein kinases. PKA-mediated phosphorylation of AC5 and AC6 decreases both forskolin and $G\alpha_s$ stimulated cAMP production through feedback inhibition (Bauman et al., 2006; Beazely & Watts, 2006; Iwami et al., 1995). Previous studies have shown that this inhibition results from the phosphorylation of a single residue, Ser-674 in AC6, and the corresponding serine residue in AC5 (Beazely & Watts, 2006; Y. Chen et al., 1997; Iwami et al., 1995). These results suggest that PKA targets the consensus sequence Asp-Leu-Glu-Lys-Lys-Tyr-Ser-Lys/Arg at the junction of the $C1_b$ domain and transmembrane helix 7 (Bauman et al., 2006; Beazely & Watts, 2006). Mutation of Ser-674 to alanine prevents PKA phosphorylation and

inhibition of AC6 activity (Y. Chen et al., 1997). Mutation of the corresponding serine in AC5 has also been shown to mediate PKA-dependent inhibition (Bauman et al., 2006; Beazely & Watts, 2006; Iwami et al., 1995).

Phosphorylation of AC5 and AC6 by protein kinase C (PKC) is more complex as PKC phosphorylation potentiates AC5 activity while inhibiting AC6 in some models. Studies using purified protein have shown that two PKC isoforms, PKCα and the atypical PKCζ, directly phosphorylate AC5 (J. Kawabe et al., 1994). PKCζ-mediated phosphorylation results in a 20-fold increase in AC5 catalytic activity, while co-treatment with forskolin synergistically enhances activity 100-fold (J. Kawabe et al., 1994). Phorbol ester stimulated PKCα is markedly less potent, enhancing activity 30% above basal (J. Kawabe et al., 1994). In stably transfected HEK293 cells, PMA has been shown to enhance forskolin-stimulated AC5 activity in a dose-dependent manner (Ji Kawabe et al., 1996). Treatment of the cells with insulin also increased cAMP accumulation, which could be further potentiated by co-transfection of PKCζ but not PKCα (Ji Kawabe et al., 1996). These results indicate that the regulation of AC5 activity can be modulated by PKC isoforms, but through different extracellular stimuli. PKCα is considered a classical PKC isoform and contains Ca^{2+} binding domains, and is activated in a calcium-dependent manner, while PKCζ is not affected by calcium (Ji Kawabe et al., 1996; J. Kawabe et al., 1994). Because sub-micromolar levels of free calcium inhibit AC5, it may be more difficult to gauge the extent of competing PKCα activation and Ca^{2+} mediated inhibition on the regulation of enzymatic activity.

In contrast to AC5, the activation of PKC has shown mixed results. PKC phosphorylation of Ser-10 in the N-terminus of AC6 has been previously shown to reduce the maximal activity; however, an N-terminal truncation of residues 1-86 revealed that AC6 could still be phosphorylated (T. H. Lin et al., 2002). Further analysis revealed that four residues may be targeted for phosphorylation: Ser-10 in the N-terminus, Ser-568 and Ser-674 in the C1 domain, and Thr-931 in the C2 domain (T. H. Lin et al., 2002). Mutation of these residues to non-phosphorylatable alanine exhibited mixed results, with Ser-568 and Thr-931 producing the largest change in activity for single residue mutation (T. H. Lin et al., 2002). Mutation of all the identified serine residues was necessary to abolish PKC-mediated phosphorylation; however, this did not reduce the activity of AC6 beyond mutation of Ser-568 alone (T. H. Lin et al., 2002). These results are difficult to interpret however, due to the use of PKC purified from rat brain with no clear isoform specificity. Subsequent studies conducted in intact cells, rather than purified protein, showed the opposite

result - that PMA could enhance forskolin or isoproterenol-mediated cAMP accumulation (Beazely, Alan, & Watts, 2005). These results appeared consistent across three different cell lines stably expressing endogenous and recombinant AC6, HEK293, Cath a. differentiated, and Chinese hamster ovary cell lines (Beazely et al., 2005). It is clear from the conflicting results of multiple studies that further analysis of PKC isoforms and their effect on both AC6 activity and phosphorylation state is required to draw any meaningful conclusions regarding their interactions.

1.2.3.4 Group 4 ACs

AC9 is the single member of Group 4 and is uniquely defined as the only member insensitive to stimulation by the small molecule forskolin. Mutational analysis of the catalytic domains indicates that Tyr-1082 is the residue responsible for the distinct forskolin insensitivity of AC9, and that a Tyr-1082-Leu mutation is capable of restoring forskolin-mediated AC9 stimulation (Yan, Huang, Andrews, & Tang, 1998). As with other membrane bound isoforms, AC9 is activated in a $G\alpha_s$-dependent manner, but also exhibits regulation by both Ca^{2+} and $G\alpha_{i/o}$ subunits (Cumbay & Watts, 2004; Paterson, Smith, Harmar, & Antoni, 1995; Premont et al., 1996).

Early studies suggest that the Ca^{2+}-mediated inhibition of basal AC9 activity occurs through the calcium stimulated serine/threonine phosphatase calcineurin (Paterson et al., 1995). Interestingly, studies have also indicated that $G\alpha_s$ stimulated AC9 activity can be attenuated through PMA-mediated stimulation of PKC in an isoform dependent manner (Cumbay & Watts, 2004). Furthermore, $G\alpha_q$-mediated activation of the Ca^{2+}/calmodulin/CaMKII pathway has been shown to potentiate $G\alpha_s$ stimulation of AC9 activity (Cumbay & Watts, 2005). The multifaceted regulation of AC9 by calcium-regulated protein kinases and phosphatases overtly appear contradictory. However, these regulatory mechanisms may preferentially control basal or stimulated states of the enzyme, or may respond to different levels of intracellular calcium. Further research is needed to better characterize these competing pathways in more physiologically relevant cell models in order to be able to draw any conclusions on the calcium-mediated regulation of AC9.

Initial studies indicated that isoproterenol-stimulated AC9 activity was insensitive to inhibition by the $G\alpha_{i/o}$–coupled somatostatin receptor (Hacker et al., 1998). Follow-up studies have shown that the level of $G\alpha_{i/o}$–mediated inhibition achieved by transfection of the somatostatin receptor is markedly lower than that observed with the D_{2L} dopamine receptor (Nielsen et al.,

1996). In models expressing both AC9 and the D_{2L} dopamine receptor, robust $G\alpha_{i/o}$–mediated inhibition was observed, and occurred in a PTX-dependent manner (Cumbay & Watts, 2004). Interestingly, sequestration of Gβγ subunits promoted the potentiation of $G\alpha_s$-stimulated cAMP accumulation, suggesting that AC9 may be sensitive to inhibition by the Gβγ heterodimer (Cumbay & Watts, 2005).

1.2.4 Physiological distribution and relevance

1.2.4.1 PNS/CNS distribution of adenylyl cyclase isoforms

A complete characterization of adenylyl cyclase isoform distribution across cell and tissue types has been hampered by the heterogeneous expression of adenylyl cyclases at relatively low levels, as well as the high homology and common regulatory properties between isoforms (Antoni, Wiegand, Black, & Simpson, 2006; Gottle et al., 2009; Sadana et al., 2009). These factors create an environment in which it becomes difficult to exploit sequence and structural differences between isoforms using traditional scientific tools such as antibodies or isoform selective chemical probes. Presently, a majority of published studies have relied on mRNA quantification methods to gain an understanding of the expression patterns of adenylyl cyclases (Table 1.3) (Defer, Best-Belpomme, & Hanoune, 2000; Sanabra & Mengod, 2011). Despite the variety of tools available to examine mRNA expression, the methods are plagued by the poor correlation between mRNA and protein (Schwanhausser et al., 2011). These points emphasize the need for restraint in using mRNA as the sole technique or as a substitute for measuring protein expression when making conclusions about relative expression of adenylyl cyclases. The accurate characterization of adenylyl cyclase distribution across tissues is essential to understanding signaling pathways in disease states and identifying valid, druggable targets.

Table 1.3: Physiological distribution patterns of membrane bound adenylyl cyclases.

Isoform	Human mRNA Tissue Distribution	Rodent CNS Tissue Distribution
AC1	Leukocytes, heart, skeletal muscle, kidney, pancreas, spleen, testis, ovary	Hippocampus, cerebellum, cortex, thalamus
AC2	Skeletal muscle, testis, heart, prostate, ovary, colon	Limbic, widespread
AC3	Placenta, testis, ovary, colon, lung, spleen, thymus	Widespread
AC4	Testis, heart, prostate, ovary, small intestine, colon	Not detected
AC5	Heart, kidney, prostate, testis, ovary, small intestine, colon	Caudate putamen, olfactory subercle
AC6	Heart, kidney, prostate, testis, ovary, small intestine, colon	Widespread
AC7	Leukocytes, placenta, lung, spleen, thymus, heart, liver, ovary, colon	Thalamus, hypothalamus
AC8	Testis	Hippocampus, cerebellum, cortex, thalamus
AC9	Heart, placenta, lung, liver, skeletal muscle, kidney, pancreas, testis, ovary, leukocytes	Cortex, hippocampus

The identification and characterization of adenylyl cyclase isoforms in cardiac tissues is necessary for a complete understanding of the pathophysiology and etiology of heart failure. Heart failure is a disease that currently affects over 5 million adults in the United States, and is expected to grow by 3 million new cases before 2030 (Penny, Henry, Watkins, Patel, & Hammond, 2018). Cardiac-specific adenylyl cyclases have become prominent new targets in the development of therapies for reduced ejection fraction heart failure (Penny et al., 2018). Cardiac fibroblasts make up the largest cell population of the heart and are responsible for the synthesis and deposition of collagen and extracellular matrix necessary for structural framework (Souders, Bowers, & Baudino, 2009). These cells play a critical role in maintaining normal cardiac function, as well as tissue remodeling during pathological conditions such as chronic hypertension or myocardial infarction (Souders et al., 2009). The mRNA for all nine membrane-bound adenylyl cyclase isoforms has been identified at varying levels in cultured adult rat cardiac fibroblasts (Ostrom et al., 2003). Follow-up experiments examining protein expression via immunoblot analysis identified the presence of select adenylyl cyclase isoforms in either caveolin-enriched or deficient fractions (Ostrom et al., 2003). These results indicated that AC3, AC5, and/or AC6 were present in the caveolin-enriched membrane fractions, while AC2, AC4, and AC7 were unique to the caveolin-deficient fractions (Ostrom et al., 2003). No immunoreactivity was observed for AC8 or AC9 in rat cardiac fibroblasts (Ostrom et al., 2003). An evaluation of the human cardiovascular system indicated that AC4, AC6, and AC7 were expressed in all tissues examined (right atrial appendage, left ventricle, left internal mammary artery, coronary arteries, saphenous veins, and lymphocytes), while AC5 was found to be expressed exclusively in the right atrial appendage, left ventricle, and the left internal mammary arteries (T. Wang & Brown, 2004). Further analysis of tissues using *in situ* hybridization confirmed the presence of AC4, AC5, AC6, and AC7 in human atrial tissue (T. Wang & Brown, 2004). No distinction between cardiac fibroblasts and cardiomyocytes was presented in this study (T. Wang & Brown, 2004). Despite the variable AC isoform expression patterns that have been observed by quantifying mRNA in cardiac tissues, AC5 and AC6 have emerged as central targets to study cardiac pathophysiology.

In the central nervous system, the characterization of adenylyl cyclase isoforms offers the potential to target specific types on neurons based on expression patterns. AC5 is the principal adenylyl cyclase isoform expressed in striatal medium spiny neurons and accounts for approximately 80% of cAMP generated in these cells (Glatt & Snyder, 1993; K. W. Lee et al.,

2002). Known to facilitate stimulatory signaling pathways with D_1 dopamine receptors and A_{2A} adenosine receptors, as well as inhibitory pathways with the D_2 dopamine and M_2 muscarinic receptors, AC5 is a critical point of signal integration in the striatum (Corvol, Studler, Schonn, Girault, & Herve, 2001; Herve, 2011). Disruption of AC5 results in both impairment of receptor signaling, as well as amplified downstream effects that usually manifest as behavioral dyskinesia or ataxia (K. W. Lee et al., 2002; Park et al., 2014). AC5 expression in the dorsal root ganglion of the spinal cord has recently been implicated in nociceptor hyperactivity following spinal cord injury (Bavencoffe et al., 2016). While behavioral deficits in nociception and pain in AC5 knockout animals have previously been reported, these results were assumed to reflect disrupted central nervous system signaling rather than an effect originating from nociceptive neurons (Bavencoffe et al., 2016; Kim et al., 2007).

Within the central nervous system, AC8 *in situ* hybridization reveals distinct patterns of expression in the mouse brain. Neonatal mice express AC8 mRNA in the spinal cord, cortex, cerebellum, olfactory bulbs, amygdala, basal ganglia, CA1 region of the hippocampus, and hypothalamus (Conti et al., 2007; Nicol, Muzerelle, Bachy, Ravary, & Gaspar, 2005). As the animals mature into adulthood, AC8 expression is maintained within the cortex, cerebellum, olfactory bulbs, habenula, CA1 region of the hippocampus, hypothalamus, hypothalamic supraoptic and paraventricular nuclei, and thalamus (Conti et al., 2007; Sanabra & Mengod, 2011; H. Wang & Storm, 2003). Synaptosome analysis of the adult brain indicated AC8 is enriched in the presynaptic active zone and extrasynaptic fractions of these areas (Conti et al., 2007). A lack of AC1 expression in the hypothalamus indicates that AC8 is the only Ca^{2+}/calmodulin stimulated isoform in this region (Conti et al., 2007; Schaefer et al., 2000). Consistent with these results, AC8 knockout animals exhibit altered stress responses (Conti et al., 2007; Schaefer et al., 2000).

In contrast, AC8 expression in the periphery appears to be quite limited. Several studies have identified moderate to high expression of AC8 in rat lung epithelium, pancreas, and testes using methods to examine mRNA as well as protein expression (Clement, Glorian, Raymondjean, Andreani, & Limon, 2006; Defer et al., 2000; Jourdan et al., 2001; Willoughby & Cooper, 2007). Additionally, AC8 mRNA is expressed in rat vascular smooth muscle cells, and has been shown to mediate the transition to a proliferative phenotype during inflammation (Clement et al., 2006; Defer et al., 2000; Jourdan et al., 2001). Studies with human tissues illustrate that cyclase expression is difficult to compare consistently across animal models. Although AC8 mRNA was

identified in elevated levels in rat lung epithelium and vascular smooth muscle cells, it was not initially identified in human pulmonary tissues (D. Xu, Isaacs, Hall, & Emala, 2001). This discrepancy was resolved through more detailed analysis, which later discovered that only intimal vascular smooth muscle cells highly express AC8, while very few cells were found to express AC8 in the medial tissue layer (Gueguen et al., 2010).

1.2.4.2 Transgenic animal models

A large degree of our understanding of the specific roles of individual adenylyl cyclase isoforms comes from gene knockout and transgenic mice. The role of AC5 in cardiac pathophysiology has been a subject of intense investigation, and the development of both AC5 cardiac knockout as well as overexpression mouse models have been valuable tools to further explore the effects of this specific adenylyl cyclase isoform. Two independent labs have generated cardiac $AC5^{-/-}$ mouse lines which exhibit reductions in basal and isoproterenol or forskolin-stimulated adenylyl cyclase activity in isolated primary cells, as well as reduced left ventricle contractile responsiveness to β-AR stimulation (consistent with a reduction in cAMP production in cardiac myocytes) (Iwamoto et al., 2003; Okumura et al., 2003; T. Tang et al., 2006). The model developed by Tang et al. reports significant reductions in $G\alpha_s$ protein expression, in addition to decreased potency of β-AR mediated stimulation, although no difference in the maximal efficacy (Guellich, Mehel, & Fischmeister, 2014; T. Tang et al., 2006). In contrast, a study by Okumura et al. indicated there was a substantial decrease in $G\alpha_i$ mediated regulation in $AC5^{-/-}$mice, possibly accounting for the paradoxical increase in resting heart rates observed in this model (Okumura et al., 2003). Additionally, the animals from the Okumura study were reported to exhibit Parkinsonian-like motor deficits, consistent with disruption of dopaminergic signaling in the striatum. However, quite paradoxically, these mice were later reported to have glowing health benefits, including extended lifespan, better exercise endurance, enhanced antioxidant capacity, and resistance to age-related cardiac dysfunction (L. Lai et al., 2013; Okumura et al., 2003; D. E. Vatner et al., 2015; Yan et al., 2007).

Additionally, three independent labs have developed transgenic mouse models with cardiac specific overexpression of AC5 (Esposito et al., 2008; L. Lai et al., 2013; Tepe et al., 1999). The AC5 transgenic mice in the Hanoune model exhibited a 2-fold increase in cAMP production with no effect on cardiac performance, heart rate, or average blood pressure (Esposito et al., 2008).

However, these animals did exhibit an enhanced exercise capacity and significantly greater long-distance run compared to wild-type animals (Esposito et al., 2008). The Liggett animal model exhibited a similar 2-fold increase in basal cAMP production, although it was associated with increased PKA activity, PLB phosphorylation, heart rate, and fractional shortening compared with wild-type mice (Tepe et al., 1999). The Vatner model exhibited a 13-fold increase in cAMP production, and was associated with elevated PKA activity, PLB phosphorylation, and left ventricle function (L. Lai et al., 2013).

In comparison to the potential cardioprotective effects, AC5 deletion has significant consequences for central nervous system functioning. AC5 is highly enriched in the striatum, accounting for approximately 80% of cAMP production, and is essential for planning and executing voluntary movements (as well as some cognitive functions) (Kim et al., 2006; Sadana & Dessauer, 2009). AC5 knockout mice have been shown to exhibit Parkinson's-like motor dysfunction characterized by abnormal coordination and bradykinesia as examined by rotarod and pole testing (Iwamoto et al., 2003). These behavioral deficits were accompanied by significant reductions in D_1 and D_2 dopamine receptor-mediated signaling to adenylyl cyclase in the striatum of AC5 knockout animals; however, these effects could be partially rescued by D_1 and D_2 receptor specific agonists (Iwamoto et al., 2003).

Conversely, the long-term treatment of Parkinson's patients with increasing doses of the dopamine precursor L-DOPA results in the development of debilitating involuntary movements as an unfortunate side effect (Picconi et al., 2003). Adenylyl cyclase activity in the striatum is known to play a central role in the development of L-DOPA induced dyskinesia, although the exact mechanism remains unknown (Picconi et al., 2003). In models of L-DOPA induced dyskinesia, AC5 knockout mice appear profoundly resistant to develop this side effect after short or long-term L-DOPA treatment (Park et al., 2014). Furthermore, similar behavioral results could be achieved with a lentiviral shRNA AC5 knockdown specifically targeted to the dorsal striatum, and were also accompanied by decreased phosphorylation of PKA substrates and FosB expression (Park et al., 2014). These results indicate that a delicate balance of dopaminergic signaling via AC5 is necessary in the striatum to maintain normal motor control, and significant increases or decreases in this pathway result in motor dysfunction.

The calcium/calmodulin-stimulated adenylyl cyclases AC1 and AC8 have many overlapping functions and expression patterns; therefore, the development of AC8 knockout

animals was an important tool to identify the isoform specific roles of each cyclase. AC8 is highly expressed in the adult central nervous system, and knockout mice exhibit reductions in calcium-stimulated adenylyl cyclase activity in the hippocampus, thalamus, hypothalamus, and brainstem (Defer et al., 2000; Schaefer et al., 2000; H. Wang et al., 2003). Hippocampal CA1 long-term depression has been previously shown to be reliant upon NMDA receptor and PKA activity (Qi et al., 1996). The Ca^{2+}/calmodulin-stimulated AC8 has been identified as the link from calcium influx through NMDA receptor activation to the production of cAMP necessary for PKA activation, where activation further promotes the phosphorylation and removal of NMDA receptors from the cell surface (Schaefer et al., 2000). Hippocampal slices isolated from AC8 knockout mice fail to show CA1 long-term depression following low-frequency stimulation, as well as reduced CREB activation and biomarkers of anxiety in response to stress (Schaefer et al., 2000). The provocation of long-lasting anxiety in mice through repeated exposure to the elevated plus-maze could be eliminated through genetic deletion of AC8, but not AC1 (Bernabucci & Zhuo, 2016), further emphasizing the role of AC8 in anxiety-like behavior. AC8 knockout mice also exhibit impaired hippocampus-dependent episodic memory that prevents the acquisition of new spatial information (M. Zhang et al., 2008). Furthermore, because AC1/AC8 double knockout mice display normal hippocampal long-term potentiation and long-term memory, these results suggest that AC8 is an essential component of a distinct set of processes that govern long-term depression and the formation of short-term memory (Sadana & Dessauer, 2009).

1.2.4.3 Adenylyl cyclase mutations and disease states

Whole exome sequencing has recently identified a number of AC5 gain-of-function mutations in patients suffering from childhood onset involuntary paroxysmal choreiform and dystonic movement disorders (D. H. Chen et al., 2015; Y. Z. Chen et al., 2014). These patients clinically exhibit symptoms including hypotonia, motor milestone delay, fluctuating dyskinesias, dystonia, and myoclonys which can be exacerbated before sleep (D. H. Chen et al., 2015; Waalkens et al., 2018). While the total number of individuals affected appears to be limited to specific family lineages in an autosomal dominant manner, the impact on the quality of life for affected individuals is quite severe. Multiple mutations have been identified in the C_{1a}, C_{1b}, and C_{2a} domains, however none of the identified mutations are located in areas of the active site or in areas that have been previously identified to interact with $G\alpha_s$ subunits (D. H. Chen et al., 2015). Rather, the majority

of the mutations appear to occur at the interface between the adenylyl cyclase alpha helical membrane spanning domains and the cytosolic catalytic subunits (D. H. Chen et al., 2015). Interestingly, the mutations do not appear to have an effect on the efficacy of the small molecule forskolin (Y. Z. Chen et al., 2014). The enhanced gain-of-function of these AC5 mutations is apparent only following stimulation of a $G\alpha_s$ /$G\alpha_{olf}$ – coupled receptor (Y. Z. Chen et al., 2014). The direct mechanism linking increased cAMP production to enhanced neuronal excitability has yet to be established; however, there is substantial evidence in the literature suggesting that cAMP effectors such as PKA can influence ion channel conductance.

AC3 gain-of-function mutations have also been identified in populations of mice subjected to high fat diet, and these mutations appear to be protective against obesity (Pitman et al., 2014). In contrast, genome wide screening of human patients has associated AC3 single nucleotide polymorphisms with enhanced height-adjusted BMI (Stergiakouli et al., 2014). Mice containing the M279I mutation exhibited significantly lower body weights, fat mass, and insulin production compared to their wild-type siblings (Pitman et al., 2014). These results may be due in part to the fact that the AC3 mutant mice are more active and expend more energy compared to wild-type controls (Pitman et al., 2014). Unlike the AC5 gain-of-function mutations, the M279I mutation in AC3 makes the enzyme more responsive to stimulation by forskolin (Pitman et al., 2014). It appears that no experiments examining $G\alpha_s$ - mediated stimulation of $AC3^{M279I}$ have been published presently, and whether the enhanced activity is the result of a shift in potency to forskolin of $G\alpha_s$ remains unknown. Furthermore, changes in the expression of AC3, as well has single nucleotide polymorphisms, have been identified in patient populations effected by colon cancer (Mariman et al., 2016; Warrington et al., 2015; H. Wu et al., 2017).

1.2.5 Scaffolding and signaling of adenylyl cyclases

1.2.5.1 Cellular localization and compartmentalization

It is widely believed that adenylyl cyclases are parts of dynamic complexes of interacting partners which localize signaling machinery to specifically control intracellular processes, both spatially and temporally (Cooper & Tabbasum, 2014; Ostrom, Bogard, Gros, & Feldman, 2012). However, confirming and further studying the specific cellular localization and compartmentalization of adenylyl cyclase signaling has been severely hampered both by the reliance on over-expression systems as a means to amplify signal, as well as a general lack of new scientific technology capable

of measuring endogenous adenylyl cyclase activity. Despite these shortcomings, different adenylyl cyclase isoforms have been shown to localize in specific cellular compartments where signaling from a subset of GPCRs forms distinct complexes with specific downstream effects.

While GPCRs can be found in diverse plasma membrane domains, indicating an increased mobility at the membrane, adenylyl cyclases appear to be more strictly localized. In fact, an early distinction between AC isoforms was determined by their preference to localize in caveolin or lipid rich "raft" microdomains, or in non-raft domains. AC3, AC5, AC6, and AC8 have all been shown to preferentially associate in lipid/caveolin rich regions, while AC1, AC2, AC4, AC7, and AC9 are found in non-raft domains (Dessauer et al., 2017; Johnstone, Agarwal, Harvey, & Ostrom, 2018). The localization preference of adenylyl cyclase isoforms appears to be consistent across species and cell types (Ostrom & Insel, 2004).

AC5 and AC6 are the two predominant isoforms expressed in human cardiac tissue, and while highly homologous, these two isoforms play divergent roles in the cardiac function and dysfunction (Dessauer et al., 2017; Timofeyev et al., 2013). For example, the subcellular compartmentalization of both adenylyl cyclase and β-adrenergic receptor signaling promotes diverse biological functions to be regulated simultaneously by a small amount of signaling proteins (Timofeyev et al., 2013). Within the heart, AC5 appears to be preferentially expressed in T-tubules, whereas AC6 is found in sarcolemmal membranes (Timofeyev et al., 2013). While both β_1 and β_2 adrenergic receptors (AR) are expressed in T-tubules, only the β_1-AR (not the β_2-AR) couples effectively to AC5 (Johnstone et al., 2018; Timofeyev et al., 2013). The selectivity of this signaling pathway in a specific cellular compartment is purportedly because of the interaction of the N-terminal helical tail of AC5 with the lipid caveolin-3 (Johnstone et al., 2018; Timofeyev et al., 2013).

The generation and amplification of a specific intracellular signal has little importance if the 2nd messenger freely diffuses throughout the cell. Adenylyl cyclase-generated cAMP signals are constrained by numerous of factors within the cell. A variety of data indicates that the movement of small molecules such as cAMP occurs at rates slower than free diffusion (Johnstone et al., 2018). Intracellular diffusion is affected by the viscosity of the cytoplasm, binding interactions that occur with both mobile and static partners, and collisional interactions that occur as a result of the molecular organization within a specific cell type (Johnstone et al., 2018; Richards et al., 2016). The compartmentalization of signaling cascades is often directly regulated by the

compartmentalization of the cell itself. For example, the diffusion coefficient of EGFP was found to be 3-fold slower than diffusion in the cytoplasm of simple HEK 293 cells compared to an aqueous solution (Agarwal, Clancy, & Harvey, 2016). Furthermore, the diffusion coefficient of EFGP was 15-fold slower in the highly complex and compartmentalized cardiac myocytes (Agarwal et al., 2016; Richards et al., 2016). These results indicate that direct barriers often play a significant, but under-recognized role, in intracellular diffusion.

1.2.5.2 A-kinase anchoring proteins

Within particular intracellular compartments, the specific expression of adenylyl cyclase and phosphodiesterase (PDE) isoforms plays important roles in the maintenance and degradation of cAMP signaling pools; however, both of these components are further organized by A-kinase anchoring proteins (AKAPs) (Kapiloff & Chandrasekhar, 2011). AKAPs are classically known for their PKA binding motif, thus highlighting their role in organizing key components of cAMP signaling to specific points within the cell (Dessauer et al., 2017; Kapiloff & Chandrasekhar, 2011). AKAP isoforms have been shown to interact with protein kinases such as PKA and PKC, phosphatases, phosphodiesterases, as well as adenylyl cyclases themselves (Dessauer et al., 2017; Kapiloff & Chandrasekhar, 2011). Presently, the specific AC-AKAP interactions that have been characterized are AKAP9 interaction with AC1, AC2, AC3, and AC9 (Piggott, Bauman, Scott, & Dessauer, 2008). mAKAP exhibits interactions with AC2 and AC5, while AKAP79/150 interacts with AC2, AC3, AC5, AC6, AC8, and AC9 (Delint-Ramirez, Willoughby, Hammond, Ayling, & Cooper, 2011; Efendiev et al., 2010; Kapiloff et al., 2009; Shen & Cooper, 2013). Presently, more than 50 AKAPs and splice variants have been identified (Kapiloff & Chandrasekhar, 2011). Unique AKAP-AC interactions are far from being fully characterized, and as more is understood about these scaffolding proteins and their interacting partners, we will be able to more fully understand the spatial and temporal regulation of intracellular signal transduction.

Not only do AKAPs specifically bind adenylyl cyclases at the membrane, but their interaction can directly affect adenylyl cyclase activity. In a study by Efendiev et al., membranes from HEK 293 cells transiently expressing different adenylyl cyclase isoforms were incubated in the presence or absence of purified AKAP79 prior to stimulation with purified $G\alpha_s$ (Efendiev et al., 2010). When incubated with AKAP79, AC2, AC5, and AC6 exhibited a significantly reduced response for acute $G\alpha_s$ - mediated stimulation (Efendiev et al., 2010). Conversely, AC3 showed

no difference in response following treatment with or without AKAP79 (Efendiev et al., 2010). Furthermore, when a peptide corresponding to residues 77-153 of the AKAP79 polybasic B region was titrated into the reaction, it was capable of disrupting the AC5-AKAP79 interaction and restored AC5 activity in a dose-dependent manner (Efendiev et al., 2010). Together these data support that AKAP79 interaction with AC5 is inhibitory, and the polybasic B region of AKAP79 is required for its interaction (Dessauer et al., 2017; Efendiev et al., 2010). These data further highlight the point that protein interactions can directly and specifically influence adenylyl cyclase signaling.

1.2.5.3 Phosphodiesterases

While adenylyl cyclases initiate cAMP signaling, phosphodiesterases (PDEs) are metallohydrolases that catalyze the breakdown of cAMP into the inactive 5'-AMP, thus mediating or terminating the cAMP response (Stangherlin & Zaccolo, 2012). There are 11 families of PDEs that are encoded by 21 different genes which are capable of producing more than 80 variants through multiple promoters and alternative splicing (Stangherlin & Zaccolo, 2012). PDE1, PDE2, PDE3, PDE10, and PDE11 exhibit dual specificity, catalyzing the degradation of both cAMP and cGMP (Stangherlin & Zaccolo, 2012). PDE4, PDE7, and PDE8 specifically degrade cAMP, while PDE5, PDE6, and PDE9 are specific for cGPM (Stangherlin & Zaccolo, 2012). Generally, PDEs contain a highly conserved cyclic nucleotide binding site and a more variable N-terminal domain that can undergo phosphorylation/dephosphorylation or interact with regulatory proteins, and is responsible for conferring the differential regulatory properties to the isoforms (Stangherlin & Zaccolo, 2012).

Curiously, PDEs exhibit not only different tissue distribution, but also unique patterns of intracellular localization (Baillie et al., 2007; Stangherlin & Zaccolo, 2012; Willoughby, Wong, Schaack, Scott, & Cooper, 2006). The specificity of their localization is due in part to their unique N-terminal domain, as well as their ability to form interactions with other proteins that are specifically localized (Stangherlin & Zaccolo, 2012). For example, following agonist stimulation, the β_2-AR rapidly desensitizes upon recruitment of β-arrestin (Goodman et al., 1996). PDE4D5 can be recruited to the receptor in complex with β-arrestin, where it then regulates the PKA-mediated phosphorylation of β_2-AR (Baillie et al., 2007). An alanine-scanning peptide array analysis of the N-terminal domain of PDE4D5 implicated Arg-26 as a residue of significant

importance for the interaction, as well as both Lys-18 or Thr-20, which moderately reduced interaction with β-arrestin upon substitution (Baillie et al., 2007). Similarly, analysis of the β-arrestin 2 C-domain identified Arg-286 and Asp-291, as well as a region defined by Leu-215 through His-220, as important for binding PDE4D5 but not PDE4D3 (Baillie et al., 2007).

Scaffolding proteins such as AKAPs are also able to organize components of cAMP signaling. In HEK 293 cells expressing both PKA and PDE4D both proteins were shown to interact with AKAP12, thereby providing a central organizational scaffold of the cAMP regulatory complex (Stangherlin & Zaccolo, 2012; Willoughby et al., 2006). Specific pharmacological inhibition of PKA or PDE4 prevented the return of subplasmalemmal cAMP to basal levels (Willoughby et al., 2006). Similarly, peptide-mediated disruption of the PKA-AKAP interaction also prevented the return of cAMP to basal levels (Willoughby et al., 2006). siRNA knockdown of AKAP12 prevented co-immunoprecipitation, and further indicates that both PKA and PDE4 are organized through their interaction with AKAP12 (Willoughby et al., 2006).

1.2.5.4 Protein kinases and phosphatases

Protein phosphorylation is a significant regulator of nearly all cellular processes including enzyme activity, protein interactions, and intracellular localization. There are approximately 500 protein kinases encoded by the human genome, and the substantial range of phosphorylatable targets therefore requires a diversity of approximately 200 protein phosphatases to balance their actions and promote homeostasis (Virshup, 2000). This diversity is achieved through the ability to form heteromeric complexes that combine a relatively small number of catalytic subunits with a large number of regulatory and structural subunits (Virshup, 2000). Research has illustrated that post-translational modifications of adenylyl cyclases can directly regulate its catalytic activity, in a isoform and kinase dependent manner (Beazely & Watts, 2006; Sadana & Dessauer, 2009; Watts & Neve, 2005). PKA-mediated phosphorylation of AC5 and AC6 has an inhibitory effect, reducing their activity through a cAMP feedback mechanism (Y. Chen et al., 1997; Iwami et al., 1995). Phosphorylation by PKC affects adenylyl cyclase in an isoform-dependent manner, stimulating AC1, AC2, AC3, AC5, and AC7, while inhibiting AC4, AC6, and AC9 (Defer et al., 2000; Sadana & Dessauer, 2009). Additionally, calmodulin kinase 4 (CaMK IV) exhibits specificity for inhibiting AC1, while calmodulin kinase 2 (CaMK II) inhibits AC3 activity (Wayman et al., 1996; J. Wei et al., 1996). Additional modifications can regulate cyclase-protein or cyclase-lipid

interactions that direct the localization preferences of cyclases (Dessauer et al., 2017). While the role of co/post-translational modifications of cyclases has been previously researched, the presence of cyclase modifications unique to conditions for heterologous sensitization has not been pursued.

Adenylyl cyclase dephosphorylation has also been proposed as a regulatory mechanism, however there has been less research studying this opposing pathway. One such phosphatase is the protein phosphatase 2A, a ubiquitously expressed serine/threonine phosphatase that is involved in many aspects of cellular function (Virshup, 2000; Y. Xu et al., 2006). The foundation of the PP2A enzyme is a 65kDa scaffolding "A subunit ," or PR65 subunit, which further binds the catalytic and regulatory subunits to create a functional enzyme (Y. Xu et al., 2006). The catalytic or "C subunit" has two isoforms that share high sequence homology in mammalian cells (Y. Xu et al., 2006). In contrast, the regulatory "B subunits" have four subfamilies (B, B′, B″, B‴) that contain at least 16 members (Y. Xu et al., 2006). The regulatory subunits have very low sequence homology between subfamilies, and their individual expression levels vary greatly depending on cell and tissue type (Y. Xu et al., 2006). These factors emphasize that the regulatory subunits largely determine substrate specificity and spatiotemporal functions of the complete PP2A enzyme (Virshup, 2000; Y. Xu et al., 2006).

Results have shown that PP2A regulatory subunits can be targeted and phosphorylated by PKA in a cAMP-dependent manner (Usui et al., 1998). Residues Ser-60, Ser-75, and Ser-573 were observed to be phosphorylated in the presence of the PP1/PP2A inhibitor okadaic acid, while Ser-75 and Ser-573 were phosphorylated in the absence of okadaic acid (Usui et al., 1998). Interestingly, the phosphorylation of the regulatory subunit increases PP2A activity and alters its substrate specificity without the dissociation of the regulatory subunit (Usui et al., 1998). A subsequent study found that phosphorylation of Ser-566 of the B56δ subunit was significantly increased following cellular treatment with the cAMP analog dibutyryl cAMP (Ahn et al., 2007). Curiously, the authors found that transfecting DARPP-32 into HEK cells (followed by treatment of forskolin) promoted Thr-34 and Thr-75 DARPP-32 phosphorylation (Ahn et al., 2007). However, co-transfecting the B56δ subunit and DARPP-32 reduced Thr-34 and Thr-75 phosphorylation (Ahn et al., 2007). Although increasing the expression of a PKA target could easily explain the decreased DARPP-32 phosphorylation, the authors present evidence that the B56δ subunit must be phosphorylated at Ser-566 to promote DARPP-32 dephosphorylation, as a potential regulatory mechanism (Ahn et al., 2007).

PP2A is also a component of kinase suppressor of Ras (KSR) complexes (Ory, Zhou, Conrads, Veenstra, & Morrison, 2003). Kinase suppressor of Ras (KSR) is a scaffolding protein that coordinates the assembly of membrane localized, multiprotein MAP kinase signaling complexes, including Raf-1, MEK1/2 and ERK 1/2 (Morrison, 2001; Ory et al., 2003). In resting cells, phosphorylated KSR1 is localized to the cytoplasm, and following stimulation, KSR1 is dephosphorylated and associates with the membrane (Ory et al., 2003; F. D. Smith et al., 2010). KSR complexes have been shown to interact with AKAPs to form an efficient signaling network that transduces signals from RAF to MEK and onto ERK1/2 (F. D. Smith et al., 2010). The cAMP activated protein kinase A (PKA), which localizes to AKAPs, phosphorylates KSR1 on Ser-838 and is subsequently required for cAMP-dependent activation of MAPK1 and/or MAPK3 (F. D. Smith et al., 2010). The role of PP2A in this complex appears to be the dephosphorylation of S392 on KSR1 and S259 on Raf-1, steps required for their localization to the membrane (Ory et al., 2003; F. D. Smith et al., 2010).

More recent evidence has shown that the N-terminus of the Ca^{2+}/calmodulin-stimulated isoform AC8 also interacts directly with the protein phosphatase PP2A (Crossthwaite, Ciruela, Rayner, & Cooper, 2006). Using the N-terminal tail in a bait and prey binding assay, both the PP2A catalytic and scaffolding subunits were validated as interacting partners (Crossthwaite et al., 2006). These results were further supported by an additional study that has identified a Ca^{2+}/calmodulin sensitive interaction between the B56δ subunit and full length AC8 N-terminal tail (Willoughby et al., 2012). The interaction between the AC8 N-terminal fragment and PP2A catalytic subunit was antagonized by Ca^{2+}/calmodulin because of overlapping binding domains (Crossthwaite et al., 2006; Willoughby et al., 2012). While it is generally understood that the combination of structural, catalytic, and regulatory domains dictates substrate recognition, the diversity of the regulatory subunits appears to be the driving force for PP2A substrate specificity.

Together, these data indicate that the phosphorylation and de-phosphorylation of adenylyl cyclase can regulate acute activity in an isoform and site-specific manner. However, the results are disconnected and far from comprehensive. Significant effort needs to be invested to create a more encompassing and consistent study of adenylyl cyclase phosphorylation sites, and what specific kinases and phosphatases are directly responsible. The power of proteomics to perform such a study is presently available, and we neglect to use it.

1.2.6 Post-translational modification

1.2.6.1 Phosphorylation

AC5 and AC6 can both be directly phosphorylated *in vitro* by incubation with PKA catalytic subunits. This results in a decrease of stimulation by both the small molecule forskolin and high concentrations of $G\alpha_s$ subunits (Y. Chen et al., 1997; Iwami et al., 1995), and this inhibition may be reduced or prevented by including an excess of the PKA regulatory subunit in these reactions (Y. Chen et al., 1997; Iwami et al., 1995). Biochemical studies of AC6 have found that serine Ser-674 is the likely site of PKA phosphorylation (Beazely & Watts, 2006; Y. Chen et al., 1997). Mutation of Ser-674 to alanine blocks AC6 phosphorylation and PKA- mediated reduction of $G\alpha_s$ stimulation (Beazely & Watts, 2006; Y. Chen et al., 1997). A peptide that encodes this region of AC6 (residues 660-682) can effectively block $G\alpha_s$ stimulation of AC6 and AC2 when overexpressed, presumably by sequestering PKA as an easy phosphorylation target (Y. Chen et al., 1997). Mutation of Ser-674 to aspartic acid on this peptide removes the ability of the peptide to prevent cyclase stimulation by $G\alpha_s$ (Y. Chen et al., 1997). Taken together, these data suggest that Ser-674 on AC6 is required for stimulation by $G\alpha_s$ and can be disrupted by either phosphorylation or blockade through the addition of a peptide mimetic.

Specific PKA phosphorylation sites on AC5 have yet to be identified; however, phosphopeptide mapping indicates that PKA and PKC target different sites (Beazely & Watts, 2006; Iwami et al., 1995). Because of the high homology between the Group 3 adenylyl cyclases, it is believed that AC5 contains 14 potential phosphorylation sites, including Ser-788 that is proposed to be analogous to the Ser-674 residue in AC6 (Beazely & Watts, 2006). AC5 and AC6 inhibition by PKA phosphorylation illustrates a classical feedback loop necessary to regulate the activity of adenylyl cyclase and to control the production of the second messenger cAMP. The role of such feedback loops in the context of heterologous sensitization remains largely unaddressed.

Protein kinase C is a diverse family of serine/threonine kinases that can be divided into three main groups: 1) conventional (α, βI, βII, and γ), which are dependent on calcium and diacylglycerols (or phorbol esters) for activation, 2) novel (δ, ε, η, θ), which require diacylglycerols (or phorbol esters) but not calcium for their activation, and 3) atypical (ι/λ and ζ), which are independent of either calcium or diacylglycerols (Nishizuka, 1992). Various PKC isoforms have been shown to phosphorylate AC5 and AC6 to modulate their activity. The PKC isozymes PKC_α and PKC_ζ have been demonstrated to phosphorylate recombinant AC5 expressed in insect and

mammalian cells, and to enhance its catalytic activity in a dose-dependent manner (but through different mechanisms and phosphorylation sites) (Ji Kawabe et al., 1996; J. Kawabe et al., 1994). PKC_{α} activates AC5 in a calcium-dependent manner when stimulated with the phorbol ester PMA (J. Kawabe et al., 1994). PKC_{ζ} lacks a calcium-binding domain and is not influenced by the presence of calcium but can be stimulated by arachidonic acid and phosphatidylinositol 3,4,5-triphosphate (Ji Kawabe et al., 1996; J. Kawabe et al., 1994). The stimulation of AC5 activity by PKC isozymes occurs in a dose- and time-dependent manner and can be abolished following treatment with the PKC inhibitor, staurosporine (Ji Kawabe et al., 1996). Incubation of AC5 with both PKC_{α} and PKC_{ζ} increases cAMP accumulation in an additive effect greater than that produce by either isozyme alone (J. Kawabe et al., 1994). Furthermore, trypsin digestion and western blotting of AC5 in following these experiments revealed that PKC_{α} and PKC_{ζ} target different sites of AC5 for phosphorylation (J. Kawabe et al., 1994).

In contrast to AC5, PKC has been implicated in the inhibition of AC6 following prolonged A_{2A} adenosine receptor stimulation (i.e desensitization of cyclase). PC12 cells were treated with the A_{2A} selective agonist CGS21680 for 30 minutes, before cells were lysed and membrane fractions collected (H. L. Lai et al., 1997). Membranes from cells that received the CGS21680 pretreatment exhibited reduced response to forskolin and A_{2A} stimulation (H. L. Lai et al., 1997). Although, traditionally cyclase desensitization is associated with a PKA-mediated feedback inhibition mechanism, the conclusions from Lai et al.'s study demonstrate that while pretreatment with H8, a non-selective inhibitor of PKC and PKA, is capable of preventing A_{2A} mediated AC6 desensitization, the PKA selective inhibitor H89 does not prevent AC6 desensitization under these conditions (H. L. Lai et al., 1997).

In evaluating the potential PKC phosphorylation sites of AC6, Lai et al. identified serines 10, 568, 674 and threonine 931 on AC6, or in consensus peptides expressed in Sf-21 membranes (H. L. Lai et al., 1999). Truncation of residues 1-86 of the N-terminal tail or Ser-10-Ala mutation significantly attenuates the desensitization of AC6, thus highlighting the importance of the N-terminus (H. L. Lai et al., 1999). Interestingly, incubation of AC6-containing membranes with purified protein phosphatase PP2A also reduced the inhibition during A_{2A} desensitization *in vitro*, indicating that PP2A is capable of regulating AC6 activity, likely through interaction with the N-terminal tail (H. L. Lai et al., 1997).

In HEK293 cells stably expressing AC6, PMA incubation produced no effect on basal levels of cAMP; however, PMA was able to significantly potentiate forskolin-stimulated AC6 activity. This effect was not restricted to small molecule stimulation of AC6, as PMA also potentiated isoproterenol-induced $G\alpha_s$-stimulated AC6 activity (Beazely et al., 2005). Pretreatment of cells with the PKC inhibitor bisindolylmaleimide was able to prevent PMA potentiation of FSK-stimulated cAMP accumulation in AC6 expressing cells (Beazely et al., 2005). Ser-674 has previously been identified as an AC6 phosphorylation site involved in the negative regulation of cyclase activity by both PKA and PKC (Y. Chen et al., 1997; T. H. Lin et al., 2002). Cells expressing AC6 containing the Ser-674-Ala mutation demonstrated that chronic treatment with PMA significantly reduced cAMP accumulation in AC6 WT cells when compared with AC6 S674 transfected cells (Beazely et al., 2005).

Regarding heterologous sensitization, some evidence exists for the involvement of the PIP3/PIP3K pathway in this phenomenon. Using FRET-based biosensors to monitor real-time intracellular cAMP accumulation, heterologous sensitization could be blocked through the manipulation of PIP3 concentrations (Reddy et al., 2015). Incubation with the non-specific PI3K inhibitor wortmannin, in both HEK 293 cells and atrial myocytes, ablated the $G\alpha_i$-mediated sensitization response (Reddy et al., 2015). Similarly, overexpression of the PIP3 phosphatase, PTEN, in cells co-transfected with AC5 decreased the heterologous sensitization response (Reddy et al., 2015). Further investigation found that both AKT inhibition with 1mM SH-5 and typical PKC-isoform inhibition with 1mM staurosporine did not affect the $G\alpha_i$-mediated sensitization response (Klippel, Kavanaugh, Pot, & Williams, 1997; Reddy et al., 2015; S. H. Tang & Sharp, 1998). Together, these data indicate that PIP3, rather than downstream kinases, may be required for the development of heterologous sensitization. As such, the biosynthesis of phosphatidyl inositol and the role of its metabolites in signal transduction has quickly become a topic of increased interest, as the metabolic products of phosphoinositides themselves are critical second messengers that function downstream of many GPCR pathways, such as in the regulation of PLC-mediated calcium mobilization and PKC activation (Toker et al., 1994).

1.2.6.2 Nitrosylation

Cysteine residues and their function within proteins can be generally divided into four functional groups: structural, regulatory, catalytic, and metal binding (Gould, Doulias, Tenopoulou, Raju, &

Ischiropoulos, 2013). Modifications of regulatory residues by nitrosylation or acetylation regulate protein function and stability (Gould et al., 2013) while modifications of cysteine residues involved in the coordination of metal binding impact protein activity (Gould et al., 2013). Sodium nitroprusside (SNP) treatment of N18TG2 neuroblastoma cells significantly reduced both secretein and PGE_1-mediated $G\alpha_s$ stimulation of adenylyl cyclase activity, as well as the forskolin-stimulated response through covalent S-nitrosylation (McVey, Hill, Howlett, & Klein, 1999). Analysis of the cyclase kinetics before and after treatment indicated no change in the Km, suggesting that SNP treatment did not affect substrate binding. However, a reduced Vmax indicated that SNP treatment reduced the rate of conversion from substrate to product (McVey et al., 1999). Moreover, catalytic site occupancy afforded some protection against SNP-mediated nitrosylation inhibition. Incubation of membranes with Mg^{2+}/ATP, as well as Mg_{2+}/AMP-PNP, dramatically reduced the inhibitory effects of SNP and maintained forskolin-stimulated activity (McVey et al., 1999). In contrast, when membranes were incubated with forskolin or PGE_1 to stimulate $G\alpha_s$, no protection was observed (McVey et al., 1999). These results suggest that nitrosylation of residues specific to the catalytic site mediate the inhibitory effects, although the specific residues are unknown. Additionally, treatment of membranes with reducing agents are able to reverse SNP mediated inhibition of cyclase activity in a dose-dependent manner (McVey et al., 1999).

Nitrosylation-mediated inhibition of adenylyl cyclase has been shown to occur in an isoform and cell type-dependent manner and may be further regulated by the ability of nitric oxide synthase to localize to lipid rafts and caveolin-rich signaling complexes. (Beazely & Watts, 2006; Goldstein, Silberstein, & Ibarra, 2002; Hill, Howlett, & Klein, 2000; Ostrom, Bundey, & Insel, 2004). The expression of AC1 and AC2 in N18TG2 cells indicated that nitric oxide donors such as SNP or S-nitroso-N-acetyl-D,L-penicillamine (SNAP) do not inhibit forskolin-stimulated activity (Hill et al., 2000). However, in COS-7 cells expressing AC1, near total inhibition was observed (Goldstein et al., 2002). High inhibition of AC6 was also observed, although no effect of SNP was observed with AC2 and AC5 (Goldstein et al., 2002). Curiously, rat striatal membranes exhibit high expression of AC5, and treatment with NO donors attenuates both forskolin and D_1 agonist-stimulated AC activity (Hudson, Corbett, Howlett, & Klein, 2001). Similarly, rat cardiac myocytes - which preferentially express isoforms AC5 and AC6 - exhibited inhibition by nitrosylation (Ostrom et al., 2004).

1.2.6.3 Glycosylation

It has been estimated that half of all expressed cellular proteins undergo glycosylation -the covalent addition of branched sugar chains to specific amino acids (Moremen, Tiemeyer, & Nairn, 2012). Protein glycosylation can regulate protein function, enzymatic activity, intracellular transport, protein-protein interactions, and endocytosis depending on the specific pattern of glycosidic linkage, composition, structure, and length (Kizuka & Taniguchi, 2016; W. Li et al., 2007). Multiple adenylyl cyclases are glycosylated, and glycosylation appears to be a common modification across membrane bound AC isoforms. Furthermore, there is experimental evidence to show that AC2, AC3, AC6, AC8, and AC9 are directly glycosylated (Bol, Hulster, & Pfeuffer, 1997; Cali, Zwaagstra, Mons, Cooper, & Krupinski, 1994; Cumbay & Watts, 2004; W. Li et al., 2007; G. C. Wu, Lai, Lin, Chu, & Chern, 2001).

Glycosyltransferase enzymes modify the common core glycan structure by adding and removing branches to establish specific structures (Kizuka & Taniguchi, 2016). The glycotransferase GNT-3 introduces a bisecting N-acetylglycosamine residue to the N-glycan structure (W. Li et al., 2007). This modification is known to suppress elongation of branches by GNT-4 and GNT-5, thus modifying the downstream signaling effects of the glycan (Kizuka & Taniguchi, 2016; W. Li et al., 2007). Increasing the expression of GNT-3 by stable transfection has been shown to significantly increase forskolin stimulated cAMP production of AC3 in Neuro-2a cells (Kizuka & Taniguchi, 2016; W. Li et al., 2007). This data indicates that N-glycan structure plays a role in the regulation of cyclase activity, and subsequently, the activity downstream effectors.

Evidence supports that the glycosylation of adenylyl cyclase type 6 *in vivo*, and contributes to the regulation of AC6 activity. Mutation of asparagine residues Asn-805 and/or Asn-890 that reside on extracellular loops 5 and 6 (Asn-805-Gln/Asn-890-Gln) substantially reduced the molecular mass of AC6 as assessed though Western blot (G. C. Wu et al., 2001). These data indicate that one or both of these asparagine residues are likely sites of a large post-translational modification consistent with glycosylation (G. C. Wu et al., 2001). Inhibition of N-linked glycosylation through the addition of tunicamycin reduced the molecular weight of AC6 in a manner consistent with mutating asparagine residues Asn-805 and Asn-890 (G. C. Wu et al., 2001). The glycosylation-deficient AC6 mutant exhibited lower forskolin stimulated activity; however, stimulation through the $G\alpha_s$-coupled adenosine A_{2A} receptor using the selective agonist CGS21680 produced no significant difference in response between wild-type and mutant AC6 (G.

C. Wu et al., 2001). The glycosylation of AC6 also appears to influence $G\alpha_{i/o}$-mediated inhibition. Quinpirole stimulation of the D_2 dopamine receptor exhibited reduced efficacy in the Asn-805-Gln/Asn-890-Gln mutant AC6 expressing cells compared with wild-type AC6 (G. C. Wu et al., 2001). Additionally, N805Q/N890Q mutant AC6 expressing cells exhibited no PKC-mediated inhibition of forskolin-stimulated activity compared with wild-type (G. C. Wu et al., 2001). Finally, the inhibition of N-linked glycosylation through addition of tunicamycin did not disrupt the trafficking of AC6 to the plasma membrane (G. C. Wu et al., 2001). Further characterization of the role of cyclase glycosylation in subcellular localization, or localization to various components within the membrane, has yet to be investigated.

1.2.7 Heterologous sensitization

1.2.7.1 History

The acute activation of $G\alpha_{i/o}$-coupled receptors results in the inhibition of adenylyl cyclase through non-competitive inhibition with $G\alpha_s$, thus decreasing the production of cAMP (Watts, 2002; Watts & Neve, 2005). However, prolonged $G\alpha_{i/o}$-mediated inhibition results in a paradoxical enhancement of adenylyl cyclase activity after the inhibitory signal has ended (Watts, 2002; Watts & Neve, 2005). This unusual compensatory mechanism of enhanced activity following prolonged inhibition is known as heterologous sensitization, or cAMP overshoot, and has been studied for nearly 50 years without a clear mechanism resolved (Watts & Neve, 2005).

The significance of G protein-coupled receptors and their effectors can be illustrated by the strong history of research awarded Nobel Prizes. While investigating the enzyme glycogen phosphorylase, Earl Sutherland first recognized that adding epinephrine to a solution of liver homogenates containing cell membranes could activate the cytosolic enzyme glycogen phosphorylase (Berthet, Rall, & Sutherland, 1957). This observation led to the hypothesis that a cytoplasmic messenger must be transmitting the action of the membrane-localized epinephrine receptor into the cytosol where glycogen phosphorylase resides (Berthet et al., 1957). This unknown messenger was eventually identified as cAMP, the first identified second messenger responsible for transmitting the activity of GPCRs intracellularly (Berthet et al., 1957). Dr. Sutherland's highly regarded work in identifying the role of adenylyl cyclase in the production of cAMP led to him being awarded the Nobel Prize in Physiology or Medicine in 1971 (Berthet et al., 1957; H. H. Lin, 2013). Building upon this knowledge, the research of Sir James Black

expanded the field of pharmacology and receptor mediated signaling by identifying and characterizing a series of receptor antagonists. Passionately involved in the development of medications for heart disease and stomach ulcers, Black's discoveries lead to the development of the highly successful medications propranolol and Tagamet, antagonists of β-adrenergic and H_2-histamine receptors, respectively (H. H. Lin, 2013). James Black's contribution to the fields of pharmacology and medicine through the development and characterization of novel pharmaceuticals led to him being awarded a Nobel Prize in 1988 (H. H. Lin, 2013).

The phenomenon of heterologous sensitization was first observed in 1975 while Marshall Nirenberg's laboratory was investigating cellular adaptations in response to opiate receptor stimulation (Sharma, Nirenberg, & Klee, 1975). Their findings demonstrated that acute opiate treatment in NG108 cells resulted in a decrease in adenylyl cyclase activity and reduced cAMP levels, while chronic exposure resulted in an increase in adenylyl cyclase activity (Sharma, Klee, & Nirenberg, 1977). The enhanced compensatory response was observed as a result of adding the opioid receptor antagonist naloxone to arrest the inhibitory signal (Sharma et al., 1977; Sharma, Nirenberg, et al., 1975). While Marshall Nirenburg was jointly awarded the 1968 Nobel Prize in Physiology or Medicine for his work on genetics and protein synthesis, the identification of the heterologous sensitization response perhaps remains a greater mystery.

This enhanced activity following prolonged inhibition observed with heterologous sensitization is a relevant cellular adaptive response and is still investigated as a potential mechanism underlying opiate withdrawal symptoms (Sharma, Nirenberg, et al., 1975; Watts & Neve, 2005). The ability to develop heterologous sensitization is a property shared by numerous $G\alpha_{i/o}$ coupled receptors; however, there is increasing evidence that the underlying mechanism involves the interplay of multiple proteins (Dessauer et al., 2017; Watts & Neve, 2005).

1.2.7.2 Role of G protein subunits

Prolonged $G\alpha_{i/o}$-mediated signaling is a required step in the development of the sensitization response and is believed to be a divergent pathway from acute adenylyl cyclase inhibition (Watts & Neve, 2005; Watts, Taussig, Neve, & Neve, 2001). This requirement of prolonged receptor activation for sensitization expression is robustly supported in the relevant literature and by data showing cells that express the D_2 dopamine receptor exhibit an enhanced cAMP response

following 2-hour pre-treatment with either dopamine or the D_2 agonist quinpirole compared with vehicle treated cells (Watts et al., 2001). This enhanced sensitization response could be blocked by administration of the D_2 antagonist spiperone or by covalently inactivating the $G\alpha_{i/o}$ subunits via pertussis toxin-mediated ADP ribosylation (Watts et al., 2001).

Experiments first examining the effects of pertussis toxin-insensitive Gα subunits on the D_2 mediated sensitization response indicated that $G\alpha_o$, but not $G\alpha_{i1}$, $G\alpha_{i2}$, $G\alpha_{i3}$, were capable of developing heterologous sensitization in NS20Y cells (Watts et al., 1998). A subsequent study supported this conclusion, indicating that $G\alpha_{i1}$, $G\alpha_{i2}$, $G\alpha_{i3}$ subunits could not support the sensitization response following μ-opioid or κ-opioid receptor activation (Tso & Wong, 2001). However, contradictory evidence suggests that $G\alpha_o$, $G\alpha_{i1}$, $G\alpha_{i2}$, and $G\alpha_{i3}$ can all develop μ-opioid receptor-mediated sensitization in C6 glioma and HEK293T cells, although to a lesser degree, and that the sensitization response is dependent upon the relative level of expression of the individual Gα subunit (Clark, Furman, Gilson, & Traynor, 2006; Clark & Traynor, 2006). Together, these data highlight the fact that receptor-mediated $G\alpha_{i/o}$ signaling is a required step for the development of heterologous sensitization, and this process likely involves multiple Gα isoforms for the full effect.

Interestingly, Gβγ subunits have also been shown to play a role in the sensitization response. Data using COS-7 cells expressing the μ-opioid receptor were sensitive to acute inhibition of forskolin-stimulated adenylyl cyclase activity using the μ-opioid agonist DAMGO, while prolonged treatment with DAMGO resulted in an enhanced sensitization response (Avidor-Reiss, Nevo, Levy, Pfeuffer, & Vogel, 1996). The role of Gβγ in this observation was assessed using a common method for evaluating the role of Gβγ subunits in signaling by expressing proteins that bind and sequester free Gβγ subunits (Avidor-Reiss et al., 1996). The overexpression of the C-terminus of GRK2 (βARK-Ct) had no effect on the ability of DAMGO to acutely inhibit forskolin-stimulated adenylyl cyclase activity (Avidor-Reiss et al., 1996). However, βARK-CT expression reduced the sensitization response to near control levels, indicating that Gβγ subunits do contribute to the regulation of the sensitization response (Avidor-Reiss et al., 1996). Several studies support the consensus that sequestration of Gβγ subunits opposes the heterologous sensitization response (Avidor-Reiss et al., 1996; Nguyen & Watts, 2005; Rhee, Nevo, Avidor-Reiss, Levy, & Vogel, 2000; Cumbay & Watts, 2001; Ejendal et al., 2012). However, despite evidence showing that

sequestration of Gβγ subunits can attenuate the sensitization response, it is unlikely that heterologous sensitization results from a direct interaction with the Gβγ heterodimer (Brand et al., 2015; Dessauer et al., 2017). Rather, the role of Gβγ subunits as regulators of diverse cellular functions appears more in line with evidence indicating that downstream effectors of Gβγ play a role in the development and expression of the sensitization response (Brust, Conley, & Watts, 2015; Dessauer et al., 2017).

1.2.7.3 Isoform-dependent characteristics

Because various adenylyl cyclase isoforms are uniquely regulated, the characteristics of the sensitization response are dependent on the individual isoform as well as the signaling pathways present within a particular cell type. The calcium-stimulated isoforms AC1, AC3 and AC8 all exhibit enhanced responses to stimulation by the calcium ionophores A23187 or ionomycin following prolonged $G\alpha_{i/o}$-mediated inhibition (Avidor-Reiss, Nevo, Saya, Bayewitch, & Vogel, 1997; Cumbay & Watts, 2001; Nevo et al., 1998; Watts & Neve, 1996). While AC1 produced a robust response after only 2-hour D_2 mediated inhibition, AC3 exhibited a very slight, although statistically significant, enhancement following 18-hour quinpirole treatment, while AC8 did not show significant sensitizaiton (Watts & Neve, 1996). The Gβγ-activated isoforms AC2, AC4, and AC7 are unusual in that they do not exhibit a sensitized response to $G\alpha_s$-mediated stimulation (Watts & Neve, 2005). Rather, PMA-mediated PKC stimulation of AC2 is robustly sensitized by prolonged D_2-mediated inhibition (Avidor-Reiss et al., 1997; Cumbay & Watts, 2001; Nevo et al., 1998; Watts & Neve, 1996). Curiously, data shows that acute activation of the D_2 dopamine receptor paradoxically enhances AC2 activity, whereas chronic D_2 activity surprisingly decreases AC2 activity in a dose-dependent manner when stimulated by $G\alpha_s$-coupled receptors (Avidor-Reiss et al., 1997; Cumbay & Watts, 2001; Nevo et al., 1998; Watts & Neve, 1996). The calcium-inhibited isoforms, AC5 and AC6, display very strong heterologous sensitization responses to both $G\alpha_s$ and forskolin-mediated stimulation (Avidor-Reiss et al., 1997; Cumbay & Watts, 2001; Nevo et al., 1998; Watts & Neve, 1996). The lone member of group 4, isoform AC9, also exhibits expression of a D_2-mediated sensitization response following $G\alpha_s$ mediated stimulation (Cumbay & Watts, 2001).

1.2.7.4 Changes in protein expression

Long-term activation of GPCR-mediated cell signaling pathways often results in changes in the steady state of cellular mRNA and/or protein expression levels (Ammer & Schulz, 1996; Hadcock & Malbon, 1993). Chronic stimulation of adenylyl cyclase with the small molecule forskolin promotes the desensitization of stimulatory GPCR pathways by decreasing the expression of stimulatory GPCRs at the membrane while simultaneously increasing the expression of inhibitory subunits such as $G\alpha_{i2}$ (Hadcock & Malbon, 1993; Watts & Neve, 1996). Similarly, chronic activation of inhibitory $G\alpha_{i/o}$-coupled receptors results in the desensitization of inhibitory pathways and increased sensitivity of adenylyl cyclase to stimulatory pathways (Hadcock & Malbon, 1993). The increased sensitivity to stimulatory pathways is observed phenotypically as enhanced magnitude and sensitivity to $G\alpha_s$-mediated stimulation, presently referred to as the heterologous sensitization response (Hadcock & Malbon, 1993). Genotypically, the enhanced adenylyl cyclase response is accompanied by increased $G\alpha_s$ subunit and stimulatory receptor expression, as well as the down-regulation of adenylyl cyclase and $G\alpha_i$ translation elements (Ammer & Schulz, 1996; Hadcock & Malbon, 1993; Watts & Neve, 1996).

These early results highlighting the cross-regulation of adenylyl cyclase strongly suggest that changes in the expression and/or receptor-mediated activity of G proteins play a key role in the enhanced adenylyl cyclase activity observed during heterologous sensitization. However, additional data directly contradicts this assertion by clearly indicating that protein expression is not necessary for the development of the sensitization response (Lisinicchia & Watts, 2003; Palmer, Harris, Coote, & Stiles, 1997; Reithmann & Werdan, 1995). The addition of pseudomonas exotoxin A or cycloheximide had no effect on the magnitude or ability of $G\alpha_{i/o}$-coupled receptors to develop the sensitization response (Lisinicchia & Watts, 2003; Palmer et al., 1997; Reithmann & Werdan, 1995).

1.2.8 Modulators of adenylyl cyclase activity

Adenylyl cyclases are essential downstream effectors of GPCR activation and are attractive potential drug targets for a variety of disorders, as adenylyl cyclases and cAMP signaling pathways play a vital role in processing and amplifying G protein-mediated nociceptive stimuli (Pierre, Eschenhagen, Geisslinger, & Scholich, 2009). For example, mediators of inflammation, such as

adenosine and prostaglandins, enhance adenylyl cyclase activity through the stimulation of $G\alpha_s$ coupled receptors that leads to downstream neuronal excitability (Brust et al., 2017; Pierre et al., 2009). Neuronal knockout studies have implicated the Ca^{2+}/calmodulin-stimulated isoforms AC1 and AC8, as well as the Ca^{2+} inhibited isoform AC5, as particularly important targets in the regulation of pain pathways (Brust et al., 2017; Hayes, Soto-Velasquez, Fowler, Watts, & Roman, 2018; Pierre et al., 2009). The non-specific adenylyl cyclase activator forskolin, as well as inhibitors of phosphodiesterases, have been used in animal models to promote the production and accumulation of cAMP to enhance the response to painful stimuli (Brust et al., 2017; Pierre et al., 2009). In contrast, inhibitors of adenylyl cyclase reduce the production of cAMP and dampen the response to painful stimuli (Brust et al., 2017; Pierre et al., 2009). While opioids are the most powerful analgesics known, the development of physiological dependence and addiction limit their use outside of emergency and trauma care. Thus, the development of isoform-specific adenylyl cyclase inhibitors may lead to novel, potentially non-addictive analgesics.

As discussed previously, the adenylyl cyclase isoforms AC5 and AC6 are both highly expressed in cardiac tissues, and transgenic expression of AC5 in cardiac myocytes has been shown to improve basal cardiac functioning but dramatically reduces the ability of the heart to cope with chronic stress (Pierre et al., 2009; D. E. Vatner et al., 2015; S. F. Vatner et al., 2013). Some evidence suggests that the enhanced AC5 activity observed in the transgenic mice results in the repressed expression of superoxide dismutase enzymes in the heart, making them more susceptible to oxidative stress (D. E. Vatner et al., 2015; S. F. Vatner et al., 2013). AC5-specific inhibitors could potentially mitigate this pathway by reducing AC5 activity and restoring the endogenous expression levels of antioxidant enzymes (Pierre et al., 2009; D. E. Vatner et al., 2015; S. F. Vatner et al., 2013). Interestingly, despite the high homology between AC5 and AC6, the two enzymes appear to have distinct functions in the heart. In contrast to AC5, overexpression of AC6 appears to improve cardiac function in models of heart failure (Pierre et al., 2009). These results highlight the need for isoform-specific modulators of adenylyl cyclase to precisely regulate divergent signaling pathways.

Recent studies have implicated the Ca^{2+}/calmodulin-stimulated isoform AC8 as a key regulator of glucose homeostasis (Dou et al., 2015; Raoux et al., 2015; Roger et al., 2011). As blood glucose levels become elevated, the ATP/ADP ratio shift results in the inactivation of K_{ATP} channels which depolarizes the membrane and subsequently promotes Ca^{2+} influx to initiate the

exocytosis of insulin (Dou et al., 2015; Raoux et al., 2015; Roger et al., 2011), and increased cAMP production by AC8 promotes vesicle fusion and insulin release through both PKA-dependent and -independent enhancement of Ca^{2+} flux (Dou et al., 2015; Renstrom, Eliasson, & Rorsman, 1997; Roger et al., 2011). Furthermore, AC8 is also highly expressed in the hypothalamus, a brain region highly involved in maintaining physiological homeostasis (Raoux et al., 2015), further suggesting that isoform-specific small molecule modulators of AC8 have the potential to play a substantial role in the management of diabetes, a disease that affects over 400 million individuals worldwide (Pierre et al., 2009; Raoux et al., 2015). Together, this data highlights the importance of adenylyl cyclases as regulators of diverse physiological pathways and identifies a need for enhanced screening for isoform-specific small molecule modulators.

1.2.8.1 Activators of adenylyl cyclase

The small molecule forskolin is a non-selective activator of all membrane bound adenylyl cyclase isoforms with the exception of AC9 (Pierre et al., 2009). Forskolin binds at a hydrophobic pocket present at the interface of the cytosolic C1 and C2 catalytic domains and also forms hydrogen bonds with Val-506 and Ser-508 of AC5 and Ser-942 of AC2 (Tesmer & Sprang, 1998; Tesmer et al., 1997). Forskolin is believed to elicit a conformational change similar to $G\alpha_s$-mediated activation, although synergistic activation of the 5C1:2C2 construct has been observed with both forskolin and $G\alpha_s$, suggesting potentially different mechanisms (Dessauer et al., 2017; Pierre et al., 2009; Tesmer & Sprang, 1998; Tesmer et al., 1997). However, efforts to identify an endogenous ligand that binds at the forskolin binding site to stimulate adenylyl cyclase activity has so far been unsuccessful (Dessauer et al., 2017).

Research to identify isoform selective activators has been attempted by conducting limited structure-activity relationships with forskolin derivatives and testing these derivatives against recombinant adenylyl cyclase isoforms AC1, AC2, and AC5, representatives of the three major classes. Results indicate that forskolin remains the most potent of all diterpene analogs tested (with 10-fold higher affinity for AC1 than AC2) (Dessauer et al., 2017; Pinto et al., 2008; Soto-Velasquez et al., 2018). Deletion of the C_7-acetyl group or C_9-hydroxyl of forskolin resulted in a decrease in potency and efficacy of diterpenes, likely through the disruption of hydrogen bonding (Pinto et al., 2008). The addition of bulky hydrophilic groups such as a N-methylpiperasiono-γ-butyryloxy group also disrupted potency and efficacy (Pinto et al., 2008). The deletion of the C_1-

hydroxyl group significantly reduced the ability to stimulate adenylyl cyclase activity, thus highlighting the importance of the hydrogen bond formation with Val-506 (Pinto et al., 2008). The bulky BODIPY forskolin construct, initially designed to identify cyclase localization, exhibited reduced efficacy at AC1 and AC5 and acted as an inverse agonist at AC2 (Pinto et al., 2008).

Coleus forskohlii extracts are widely sold as energy or weight loss supplements, however with unreliable and undetermined forskolin content, the potential for harm far outweighs any potential beneficial effects. Clinically, a water-soluble forskolin derivative NKH477 (also known as colforsin daropate HCl) has been used clinically to treat acute heart failure in Japan (Hosono, 1999). The compound's enhanced water solubility was believed to reduce off-target CNS effects and has been shown to effectively improve cardiac function in some heart failure models (Hosono, 1999). Furthermore, colforsin administered in conjunction with the phosphodiesterase III inhibitor olprinone has been shown to be effective in alleviating septic lung inflammation through the activation of AKT pathways independent of CREB (Oishi et al., 2012). These results highlight some of the potential benefits of adenylyl cyclase activators and further emphasize the need for available isoform specific tools to better investigate adenylyl cyclase pathways and roles in physiology.

1.2.8.2 Small molecule inhibitors of adenylyl cyclase

One class of adenylyl cyclase inhibitors are referred to as P-site inhibitors, as they bind the catalytic site and uncompetitively or noncompetitively stabilize the pyrophosphate-bound transition state, thus preventing the formation of cAMP from ATP. A unique feature of P-site inhibitors is that they are activity-dependent - the greater activity of the enzyme, the more transition states are exposed for potential inhibition and a larger degree of inhibition is achieved. While membrane permeability has consistently presented as an obstacle to targeting cyclases, three membrane permeable P-site inhibitors have been well characterized in cell models: NKY80 (2-amino-7-(2-furanyl)-7,8-dihydro-5(6H)-quinazolinone, SQ22,536 (9-(tetrahydro-2-furanyl)-9H-purin-6-amine), and vidarabine (9-β-D arabinofuranosyladenine).

Vidarabine (9-β-D arabinofuranosyladenine) was first synthesized in 1960 as an anti-cancer therapeutic but quickly found use as an FDA approved antiviral medication (Seifert, 2014). As a nucleoside analog, vidarabine works by competing with dATP at the DNA polymerase, leading to incorporation of vidarabine and inhibition of viral DNA synthesis (Seifert, 2014). More

recently, data had initially indicated that vidarabine is a potent and selective P-site inhibitor of AC5 and could be utilized as a heart failure therapeutic (Brand, Hocker, Gorfe, Cavasotto, & Dessauer, 2013; Seifert, 2014). However, only representative adenylyl cyclase isoforms were tested, and upon further evaluation, vidarabine exhibited selectivity for AC5 and AC6 relative to isoforms but no difference in potency between the two class 3 isoforms (Brand et al., 2013; Seifert, 2014). The structural characteristics make this class of inhibitors highly prone to off-target effects, as vidarabine is known to be toxic and therefore has been limited to topical clinical applications in keratitits (Brand et al., 2013; Seifert, 2014). Despite clear evidence that inhibitors such as vidarabine are neither potent nor selective, some labs stubbornly persist to develop isoform selective inhibitors based on this imperfect scaffold to no clear success (Seifert, 2014; J. Zhang et al., 2018).

SQ22,536 and NKY80 share adenine-like structures with vidarabine and have also been shown to exhibit some selectivity between isoforms with greater potency observed at AC5 and AC6 compared with other membrane bound isoforms (Brand et al., 2013; Dessauer et al., 2017). NKY80 was developed as an analog of SQ22,536 with modifications made to the adenine moiety to reduce potential off-target effects observed with vidarabine (Brand et al., 2013; Dessauer et al., 2017). Presently, there is substantial interest in the development of AC5 selective inhibitors, as experiments with AC5 knockout mice, as well as *in vitro* data, suggest that AC5 selective inhibition may be a valuable treatment of heart failure (Brand et al., 2013; Dessauer et al., 2017; Pierre et al., 2009). Furthermore, a recently identified series of AC5 gain-of-function mutations have been linked to an AC5 associated dyskinesia (Brand et al., 2013; D. H. Chen et al., 2015; Dessauer et al., 2017). The use of AC5 selective P-site inhibitors have the potential to be effective therapies for both heart failure, as well as AC5 associated dyskinesia. However, because AC5 is broadly expressed in many different organ systems, the potential for toxic off target effects of inhibitors is high (Brand et al., 2013; Dessauer et al., 2017). AC5 inhibition has been associated with Parkinsonian-like moment deficits, and the high homology between AC5 and AC6 indicates that current AC5 inhibitors cannot discriminate between the isoforms (Dessauer et al., 2017; Iwamoto et al., 2003). Additionally, the adenosine-like structure of P-site inhibitors has been shown to bind adenosine receptors with high affinity (Klotz & Kachler, 2016). It seems possible to overcome a majority of these obstacles by increasing isoform selectivity as well as potency, however restricting a small molecule modulator of AC5 to the periphery or central nervous system

is more difficult and may not be easily resolved by formulating a pro-drug or altering the lipophilicity of the compound.

Another class of small molecule adenylyl cyclase inhibitors are the competitive MANT (N-methylanthraniloyl)-containing nucleotide analogs (Brand et al., 2013; Dessauer et al., 2017). Crystallographic studies have shown that the MANT group binds to a conserved region of hydrophobic residues at the interface of the C1 and C2 catalytic domains and prevents the conformational change necessary for activation (Brand et al., 2013; Dessauer et al., 2017). MANT inhibitors compete for the catalytic site but bind in a reversed orientation compared to ATP (Brand et al., 2013{Dessauer, 2017 #334; Dessauer et al., 2017). Because this class of inhibitors cannot readily cross the cell membrane, any clinically relevant inhibitors would have to be designed as prodrugs (Pierre et al., 2009). In cell free assays, some inhibitors have been identified with strong preference for AC1, AC5, and AC6 (Brand et al., 2013; Dessauer et al., 2017; Pierre et al., 2009). Although molecular modeling studies have suggested that the catalytic site may be flexible to accommodate various inhibitor scaffolds, the very high similarity of the active site across isoforms presents a significant obstacle in the development of isoform selective inhibitors (Dessauer et al., 2017; Pierre et al., 2009).

Indeed, allosteric modulation of adenylyl cyclase offers the best chance to identify and characterize isoform selective small molecules (Seifert & Beste, 2012). However, without a full-length crystal structure of adenylyl cyclase, *in silico* screening and fragment-based drug design approaches are limited to the 5C1:2C2 structure. Presently, high throughput screening (HTS) approaches offer the best chances of identifying isoform selective molecules. HTS offers the benefit of screening vast libraries of dissimilar scaffolds, which may interact with unique areas of the protein, to effect a functional change. Recombinant expression of adenylyl cyclase isoforms in whole cell or membrane preparations offers tremendous flexibility in designing screen/counterscreen functional assays. The greatest limitation to conducting such as screen aside from cost is access to large enough chemical libraries.

Peptide inhibitors have been developed from the AKAP79 interaction interface with AC5. Previous research has shown that AC5 preferentially binds and associates with AKAP79 at the membrane, and that this interaction inhibits AC5 activity (Efendiev et al., 2010). Membranes from HEK cells transfected with various cyclase isoforms were incubated with or without purified AKAP79, then stimulated with $G\alpha_s$ (Efendiev et al., 2010). A significant decrease in activity was

observed with isoforms AC2, AC5, and AC6 (Efendiev et al., 2010). By mapping the interaction interface, a peptide based on the AKAP79 polybasic B region (77-153) was developed and shown to inhibit AC5 and AC6 activity, showing no effect at AC2 (Efendiev et al., 2010). By titrating increasing concentrations of $AKAP79^{77-153}$ into a reaction of purified AKAP79 and AC5 expressing membrane, the peptide was able to disrupt the AKAP79-AC5 interaction and increase AC5 activity in a dose-dependent manner (Efendiev et al., 2010). These findings highlight that manipulating or disrupting the protein interactions that occur in macromolecular complexes can be used to regulate adenylyl cyclase activity. Presently, these peptides are restricted to use as research tools in cell-free assays.

1.3 Bimolecular Fluorescence Complementation

1.3.1 BiFC Development

Many areas of science have been advanced with the use of the *Aequorea* green fluorescent protein (GFP). First isolated from bioluminescent jellyfish, the 238 amino acid protein forms an 11-strand anti-parallel beta barrel that encapsulates an alpha helix (Yang, Moss, & Phillips, 1996). The chromophore itself is formed from three central residues (65-67) of the protein, and through a process of cyclization followed by oxidation, a large delocalized pi-bond system is formed that produces a unique green fluorescent signal (Yang et al., 1996). Though this unusual multi-step process is highly susceptible to changes pH, the GFP protein is able to remain fluorescent despite a variety of structural permutations, mutations, and insertions (Baird, Zacharias, & Tsien, 1999).

An enhanced form of GFP with a single emission peak was first developed with a single Ser-65-Thr mutation that increased the brightness five-fold and decreased the maturation time of the fluorophore (Tsien, 1998). Further site directed mutagenesis (Phe-64-Leu), increased the maturation efficiency at 37°C, and thus first provided scientists an important tool for investigating biological processes in living cells (Tsien, 1998). Mutations to the three central amino acids in the chromophore were found to alter the spectral properties of the fluorescent protein by modifying the extended π-bond network, resulting in a variety of different classes of colored fluorescent proteins that gained improved pH resistance and photostability (Tsien, 1998). Interestingly, one GFP mutation (T203Y) that occurred outside of the central three residues involved in chromophore development produced a shift to longer wavelengths, resulting in the yellow fluorescent protein

(YFP) (Nagai et al., 2002). Compared with GFP, the excitation and emission properties of YFP are right-shifted with maximum excitation and emission at 514nm and 527 respectively (Nagai et al., 2002). An improved form of YFP (also known as Venus) was developed through further mutagenesis (Phe-46-Leu), and exhibits substantially improved maturation speed, improved pH sensitivity, and increased brightness (Nagai et al., 2002).

The circular permutation of YFP further highlights the protein's resilience to maintain fluorescence despite changes in sequence structure. By changing the order of amino acids in the fluorescent protein, the N-terminus was ligated to the C-terminus and splitting the circularized protein in other structural regions created new N/C-termini (Baird et al., 1999). This method altered the sequence of amino acids in the peptide sequence but preserved the overall 3-dimensional structure (Baird et al., 1999; C. D. Hu, Chinenov, & Kerppola, 2002; Kerppola, 2006). By grafting the calcium-modulated protein calmodulin into the newly formed N/C termini of YFP, researchers produced a targeted calcium indicator capable of expression and real time measurement within cellular compartments (C. D. Hu et al., 2002; Kerppola, 2006; Robert et al., 2001). Further dissecting the circularly permutated fluorescent protein into independent C- and N-terminal fragments led to the development of bimolecular fluorescence complementation (BiFC) (C. D. Hu et al., 2002; Kerppola, 2006).

Bimolecular fluorescence complementation is a technique based on the non-covalent reconstitution of a complete fluorescent protein, when two non-fluorescent complementary fragments are brought together as a result of a pair of interacting proteins (Kerppola, 2006; Kodama & Hu, 2012). Once the intact fluorescent protein is formed, it is essentially irreversible and thus allows for the identification of weak or transient interacting partners (Kerppola, 2006; Kodama & Hu, 2012). Therefore, BiFC assays offer both high sensitivity and a high signal-to-noise ratio because the independent fragments are non-fluorescent and produce minimal background signal (Kerppola, 2006). Furthermore, BiFC allows for the direct visualization of protein interactions or macromolecular protein complexes in living mammalian cells with no additional required reagents (Kerppola, 2006). In 2002, Hu and colleagues demonstrated that YFP divided between residues 154 and 155 (YN155 and YC155) exhibited the highest fluorescence and maintained a similar excitation/emission spectra to the parent YFP (C. D. Hu et al., 2002; Kerppola, 2006; Kodama & Hu, 2012). When these fragments were fused to C-terminal ends of the basic leucine zipper (bZIP) domains of Jun and Fos and expressed in COS-1 cells, a high-intensity

fluorescent signal was observed (C. D. Hu et al., 2002; Kodama & Hu, 2012). When expressed individually, or as mutants lacking the bZIP domains, no fluorescent signal was observed (C. D. Hu et al., 2002; Kodama & Hu, 2012). These results indicate that the fluorescent signal observed was not the result of self-assembly of the fluorescent fragments, but was instead driven by the interaction of the two proteins (C. D. Hu et al., 2002; Kodama & Hu, 2012).

Despite these advantages, BiFC assays require strong controls to validate the authenticity of the signal. Perhaps the most apparent issue is that the introduction of a BiFC fragment onto the protein of interest may interfere with its endogenous function or ability to interact naturally (Kodama & Hu, 2012; Miller, Kim, Huh, & Park, 2015). It is essential that the functionality of the fusion protein be confirmed, the final construct may require substantial optimization of both BiFC fragment size and fusion location to produce a functional protein for use in assays (Miller et al., 2015). To ensure a positive interaction is valid, it is necessary to have a known binding partner that can be mutated at the binding interface to disrupt the interaction, thus serving as a negative control (Kodama & Hu, 2012; Miller et al., 2015). This level of structural information is often not available for novel protein targets and can be a substantial obstacle to performing accurate BiFC assays.

1.3.1.1 Protein-protein interaction screening methods

The binding partners of specific proteins can be identified through methods such as immunoprecipitation and tandem affinity purification; however, the processing steps associated with these techniques often disrupts all but the tightest binding partners, thus reducing the overall detection ability for these techniques (Magliery et al., 2005). A classical method for identifying protein interactions for a particular target, such as using a library of potential partners, is yeast two-hybrid analysis (Fields & Song, 1989). This method relies on the activation of a downstream reporter gene through the binding of a transcription factor to an upstream activation sequence (Fields & Song, 1989). In yeast two-hybrid screening, the protein target of interest (bait) is linked to the DNA binding domain fragment of the transcription factor (Fields & Song, 1989). A plasmid library is constructed such that each protein in the library will be expressed conjugated to the activation domain fragment of the transcription factor (prey) (Fields & Song, 1989). If the bait and prey proteins interact, the DNA binding domain and activation domain fragments connect, and the activation domain is brought in proximity to the transcription initiation site, allowing for

transcription of the reporter gene (Magliery et al., 2005). This method is effective, however it must be completed in yeast rather than mammalian cells (Magliery et al., 2005). Additionally, yeast two-hybrid does not require direct interaction and false positives seem to plague the screens, particularly proteins that promote the activation of transcription or interact non-specifically (Magliery et al., 2005).

Bimolecular fluorescence complementation offers similar benefits to the bait and prey library screening methods of yeast two-hybrid, but with the added benefits that screens can be conducted in live mammalian cells, displays excellent sensitivity to detect weak or transient protein interactions, and is more resistant to false positives when conducted with proper controls (Kerppola, 2006; Magliery et al., 2005; Morell, Espargaro, Aviles, & Ventura, 2008). The simplest application of BiFC is to investigate or validate individual protein interactions by examining the fluorescence intensity and intracellular distribution in reference to positive and negative controls under different treatment conditions (Kerppola, 2006; Magliery et al., 2005; Morell et al., 2008). This application can be scaled up exponentially to screen for protein interacting partners by constructing rationally designed BiFC constructs. The bait protein, or target of interest, is optimized to be linked to one fragment of a fluorescent protein (Kerppola, 2006). A cDNA library expressing the complementary BiFC fragment can then be expressed in cells contain the target construct and monitored for positive fluorescent signals indicative of a protein interaction (Kerppola, 2006). Although BiFC reconstitution is driven by the affinity of two interacting proteins, over-expression of a BiFC linked DNA library can promote spontaneous reconstitution of the fluorescent protein, leading to an increased rate of false positives, thus proper controls are essential for analysis. (Kerppola, 2006; Magliery et al., 2005)

1.3.1.2 Large-scale applications of BiFC

Early efforts to better understand cellular protein interaction networks were quick to utilize BiFC as a method for high-throughput screening for interacting partners. One early large-scale study combined a GFP-based BiFC screen with fluorescence activated cell sorting (FACS) to identify AKT interacting proteins in COS-1 mammalian cells (Remy & Michnick, 2004). AKT linked to the C-terminal GFP fragment served as bait to screen a human brain cDNA library, which was linked to the complementary N-terminal BiFC fragment (Remy & Michnick, 2004). The plasmid DNA from GFP-positive cells was extracted and transformed into DH5α bacterial cells, which

were then cultured under selection for plasmid containing cells (Remy & Michnick, 2004). Clones were then picked, and plasmid DNA transfected into COS-1 cells containing the AKT-BiFC construct and subjected to FACS a second time as a validation step (Remy & Michnick, 2004). Cells that passed this validation had their plasmid DNA sequenced to identify the interacting partner (Remy & Michnick, 2004). This screening methodology identified hFt1 as a novel AKT interacting partner, and further analyses have implicated in hFt1's role in the regulation of AKT-mediated apoptotic signaling (Remy & Michnick, 2004).

While multiple large-scale BiFC screens have been conducted in mammalian systems, BiFC assays have been used across species to investigate protein interactions in plants (Berendzen et al., 2012). A genome-wide investigation of *Arabidopsis* sought to identify novel protein interacting partners, and employed a similar BiFC-linked cDNA library screening approach coupled with FACS (Berendzen et al., 2012). The cDNA library was recombined into a split YFP C-terminal fragment expression plasmid (pE-SPYCE) to generate a random YC-linked cDNA library (Berendzen et al., 2012). The library was then screened against YN-linked calcium-dependent protein kinase 3 (CPK3) (Berendzen et al., 2012). BiFC positive cells were sorted using FACS, and interacting partners were validated with BiFC assays as well as fluorescence-lifetime imaging microscopy (Berendzen et al., 2012). This screening strategy successfully identified four novel CPK3 interacting proteins (Berendzen et al., 2012).

Presently, nearly a dozen cell-based BiFC screens have been successfully completed and published in various organisms, including yeast, plants, and mammalian cells (Miller et al., 2015). The development of BiFC for high-throughput screening has uncovered its potential for identifying protein complexes or protein networks in living cells under unique treatment conditions. As biochemical and cellular processes are controlled by specific or condition dependent protein-protein interaction, abnormal protein-protein interactions can contribute to the pathology and etiology of several diseases and therefore represent a large class of potentially druggable interaction targets (Klussmann & Rosenthal, 2008). However, because of the large diversity of protein-protein interactions, targeting these interactions remains a difficult task (Klussmann & Rosenthal, 2008), and BiFC assays have a high potential for not only identifying novel interacting partners, but also for high-throughput screening in drug discovery.

1.3.1.3 Detection and isolation of BiFC signal

Various methods of microscopy can be used to monitor BiFC signals in living cells, from widely available epi-fluorescent and confocal microscopes, to more technically involved 2-photon and high content screening systems such as the Opera Phenix. However, the combination of BiFC with flow cytometry is unmatched in high-speed quantification and analysis of protein interactions in living cells. Fluorescent activated cell sorting (FACS) provides a highly sensitive and technically simple method to identify and segregate cells with a fluorescent signal above a pre-determined threshold (Morell et al., 2008). Using flow cytometry, thousands of cells can be analyzed across multiple fluorescent wavelengths in seconds, thus encouraging the multiplexing of assays or the use of multicolor BiFC to track protein interactions across treatment conditions (Kerppola, 2006; Morell et al., 2008; Vidi, Przybyla, Hu, & Watts, 2010).

1.3.1.4 Next Generation sequencing

DNA sequencing has progressed tremendously in the half-century since its initial development thanks to parallel advancements in biochemistry and biotechnology. While the overall goal of determining the exact order of nucleotides within a specific DNA strand remains consistent, the development of recombinant DNA technology, as well as introduction of computer based rapid DNA sequencing, have greatly stimulated research and discovery in biology and medicine. Early DNA sequencing methods relied on the incorporation of chain-terminating dideoxynucleotides by DNA polymerase during replication (Mardis, 2013; Sanger, Nicklen, & Coulson, 1992; R. Wu, 1972). These nucleotides lack the 3'-hydroxyl group required for phosphodiester bond formation and stop extension of the DNA strand (Mardis, 2013; Sanger et al., 1992), and incubation with P^{32} radiolabeled dATP molecules allowed for the identification of fragment positions when exposed to X-ray film (Mardis, 2013; Sanger et al., 1992). However, early Sanger sequencing was a long and labor-intensive process to sequence, even for short sequences of interest.

The introduction of fluorescence labeling marked a significant change in DNA sequencing technology (Mardis, 2013; Sanger et al., 1992). In 1986, Applied Biosystems Inc. unveiled a commercial fluorescent DNA sequencing instrument that replaced radiolabeled dATP with specific primers that contained a different fluorophore for each nucleotide reaction (Mardis, 2013). Laser scanning excited the fluorescent primers during the process of electrophoresis, further simplifying a complex process (Mardis, 2013). In the early 2000's, Next-Generation sequencing

represented the revolutionary changes in biochemistry and technology that were now available. The Next-Gen sequencing procedure effectively removed an independent cloning step from the procedure by combining nucleotide addition with nucleotide detection to run simultaneously (Mardis, 2013). By introducing adapters that covalently link the DNA library fragments to a solid-state surface, thousands to billions of individual reactions are run simultaneously instead of distinct processes, exponentially increasing the DNA sequencing capacity (Mardis, 2013).

CHAPTER 2. THE IDENTIFICATION OF THE AC5 'INTERACTOME' USING A NOVEL BIFC NEURONAL CDNA LIBRARY SCREEN

2.1 Abstract

Adenylyl cyclase type 5 (AC5) is known to play an important role in mediating striatal dopaminergic signaling. Acute activation of $G\alpha_{i/o}$ coupled G protein-coupled receptors (GPCR) results in the inhibition of adenylyl cyclase activity and reduction of the second messenger cAMP. However, chronic $G\alpha_{i/o}$-mediated inhibition of adenylyl cyclase activity results in a paradoxical enhancement of cAMP production after termination of the inhibitory signal. This unusual phenomenon of enhanced adenylyl cyclase activity is known as heterologous sensitization, and AC5 mediated sensitization is believed to play a role in the dysfunctional signaling associated with several neurological disorders. Evidence suggests that multiple proteins are involved in the development of heterologous sensitization, however it is unknown how prolonged $G\alpha_{i/o}$ coupled receptor stimulation alters the association of proteins with AC5. Here, we present a screening strategy that employs bimolecular fluorescence complementation (BiFC) followed by next generation sequencing (NGS) to capture and identify the AC5 interactome that occurs during chronic $G\alpha_{i/o}$ coupled receptor stimulation in living neuronal cells. Through this unbiased strategy, we have identified genes and proteins that associate with AC5 following D_2 dopamine receptor-mediated heterologous sensitization.

2.2 Introduction

Adenylyl cyclases (AC) are key intersections for the integration of both stimulatory and inhibitory signals that initiate from G protein-coupled receptor (GPCR) activation. Acute activation of $G\alpha_s$ coupled receptors stimulates the enzymatic activity of the nine membrane-bound isoforms of adenylyl cyclase, increasing the production of the intracellular second messenger cAMP (Rasmussen et al., 2011; Watts & Neve, 2005). In contrast, acute activation of $G\alpha_{i/o}$ coupled receptors results in inhibition of adenylyl cyclase, decreasing the intracellular levels of cAMP (Defer et al., 2000; Dessauer et al., 1998; Taussig et al., 1993). However, chronic $G\alpha_{i/o}$-mediated inhibition of adenylyl cyclase activity results in a paradoxical enhancement of cAMP production after termination of the inhibitory signal (Sharma, Klee, & Nirenberg, 1975; Watts & Neve, 2005).

This unusual phenomenon of enhanced adenylyl cyclase activity is known as heterologous sensitization or superactivation, and has been the subject of intense study for nearly half a century.

The development of heterologous sensitization is a property shared by numerous $G\alpha_{i/o}$ coupled receptors, however there is increasing evidence that the underlying mechanism involves multiple proteins (Q. Wang & Traynor, 2011; Watts & Neve, 2005; Xie, Masuho, Brand, Dessauer, & Martemyanov, 2012) in addition to the receptor and the cyclase. Prolonged $G\alpha_{i/o}$ signaling is a required step in the development of the sensitization response and is believed to be a divergent pathway from acute $G\alpha_{i/o}$ coupled-receptor stimulation (Levitt, Purington, & Traynor, 2011; Watts & Neve, 1996). Pretreatment with pertussis toxin results in the covalent inactivation of $G\alpha_{i/o}$ subunits, preventing receptor signaling and thus abolishing the sensitization response (Kapiloff et al., 2009; Watts & Neve, 1996). GPCR stimulation promotes the activation of Gα as well as the release of Gβγ subunits. The dissociation of Gβγ leads to diverse signaling events, including Gβγ mediated modulation of adenylyl cyclase isoform activity. The sequestration of Gβγ heterodimers through the overexpression of the carboxy-terminus of β-adrenergic receptor kinase (βARKct) can also prevent the sensitization response in a receptor specific manner without affecting the ability of $G\alpha_{i/o}$ to acutely inhibit adenylyl cyclase activity (Avidor-Reiss et al., 1996). The role of stimulatory $G\alpha_s$ subunits in adenylyl cyclase sensitization has also been investigated. Enhanced coupling of $G\alpha_s$ with both receptors and adenylyl cyclases has been associated with the development of sensitization (J. Chen & Rasenick, 1995; Watts & Neve, 1996). While $G\alpha_s$ insensitive adenylyl cyclase mutants can still be stimulated by the small molecule forskolin (FSK), uncoupling $G\alpha_s$ from adenylyl cyclases has been shown to reduce the sensitization response in some adenylyl cyclase isoforms (Dessauer & Gilman, 1996; Palmer et al., 1997; Sunahara, Dessauer, Whisnant, Kleuss, & Gilman, 1997). These data suggest both G protein-dependent and independent mechanisms for the development of heterologous sensitization in different isoforms of adenylyl cyclase.

Adenylyl cyclases do not exist in isolation, but rather as a part of a dynamic macromolecular complex of interacting partners. A-Kinase Anchoring Proteins (AKAPs) are central to the formation of adenylyl cyclase macromolecular signaling complexes that include protein kinases, protein phosphatases, phosphodiesterases, regulators of G protein signaling, and cAMP activated guanine nucleotide exchange factors (Dessauer, 2009; Efendiev et al., 2010; Guinzberg et al., 2017). Not only have the protein interactions facilitated by AKAPs been shown

to directly modulate the activity of adenylyl cyclase, they also effectively organize key components of cAMP signaling to discrete locations within the cell (Dessauer, 2009; Guinzberg et al., 2017; Kapiloff et al., 2009). These findings highlight the point that protein interactions and macromolecular networks have modulatory effects on the activity of adenylyl cyclases, as well as the spatiotemporal regulation of cAMP signaling within cellular compartments.

As a result of this complexity, one hypothesis for the mechanism underlying the development of heterologous sensitization is that chronic $G\alpha_{i/o}$ coupled-receptor stimulation alters the network of protein interactions encompassing adenylyl cyclase. Alterations in this protein network may directly prime the adenylyl cyclase for an enhanced response, or result in the rearrangement or trafficking of established complexes to promote amplified signaling. Adenylyl cyclase type 5 (AC5) is known to play an important role mediating striatal dopaminergic signaling and has been implicated in the regulation of dyskinesias associated with neurological disorders (Mons & Cooper, 1994; Park et al., 2014; Rangel-Barajas et al., 2011). Understanding the protein interactions that modulate adenylyl cyclase signaling will lead to a better understanding of the adaptive pathological changes associated with neurological disorders. Here we present a screening strategy utilizing bimolecular fluorescence complementation (BiFC), a technique based on the complementation of fragments from fluorescent proteins, to capture and identify the adenylyl cyclase interactome that occurs during chronic $G\alpha_{i/o}$ coupled receptor stimulation in living neuronal cells (Kodama & Hu, 2012). Through this strategy, we have identified proteins that associate with and regulate AC5 following D_2-mediated heterologous sensitization in an unbiased manner.

2.3 Materials and Methods

2.3.1 Cell culture:

Human embryonic kidney (HEK) 293 cells stably expressing the long isoform of the human D_2 dopamine receptor (D_{2L}) and human adenylyl cyclase type 5 (HEK-AC5/D_{2L}) were cultured in Dulbecco's Modified Eagle Medium (Life Technologies, Grand Island, NY), supplemented with 5% bovine calf serum (Hyclone, Logan, UT), 5% fetal clone I (Hyclone, Logan, UT), 1% Antibiotic-Antimycotic 100x solution (Life Technologies, Grand Island, NY). Stable cell clones were maintained in culture media containing 800µg/ml G418 (Invivogen, San Diego, CA) and 2µg/ml puromycin (Sigma Aldrich, St. Louis, MO). A Cath a. differentiated (CAD) cell line was

constructed to express the long isoform of the human D_2 dopamine receptor (D_{2L}) and human AC5 linked by the N-terminus to the N-terminal BiFC fragment of the Venus fluorescent protein (VN155-AC5) through a short alanine rich, flexible linker CAD VN-AC5/D_{2L} cells). Stable cell clones were cultured in Dulbecco's Modified Eagle Medium (Life Technologies, Grand Island, NY), supplemented with 5% bovine calf serum (Hyclone, Logan, UT), 5% fetal bovine serum (Hyclone, Logan, UT), 1% Antibiotic-Antimycotic 100x solution (Life Technologies, Grand Island, NY). Stable cell clones were maintained in culture media containing 800µg/ml G418 (Invivogen, San Diego, CA) and 2µg/ml puromycin. All cell lines were maintained in a humidified incubator at 37°C and 5% CO_2.

2.3.2 Development and culture of CAD VN-AC5/D_{2L} stable cell line:

The Cath a. differentiated (CAD) cell line was constructed to express the long isoform of the human D_2 dopamine receptor (D_{2L}) and human AC5 linked by the N-terminus to the N-terminal BiFC fragment of the Venus fluorescent protein (VN155-AC5) through a short alanine rich, flexible linker CAD VN-AC5/D_{2L} cells). Briefly, CAD VN-AC5/D_{2L} stable cell clones expressing VN-AC5 were assessed by their response to acute forskolin stimulation. Clones providing a robust FSK response were then transfected with the human D_{2L}, and subsequently selected based upon the development of D_2-mediated heterologous sensitization. Final CAD VN-AC5/D_{2L} clones were selected based upon functional results, as well as their ability to produce a strong BiFC response with complementary interacting partners. Stable cell clones were cultured in Dulbecco's Modified Eagle Medium (Life Technologies, Grand Island, NY), supplemented with 5% bovine calf serum (Hyclone, Logan, UT), 5% fetal bovine serum (Hyclone, Logan, UT), 1% Antibiotic-Antimycotic 100x solution (Life Technologies, Grand Island, NY). Stable cell clones were maintained in culture media containing 800µg/ml G418 (Invivogen, San Diego, CA) and 200µg/ml puromycin. All cell lines were maintained in a humidified incubator at 37°C and 5% CO_2.

2.3.3 BiFC plasmid construction and validation:

The BiFC plasmid vector used for cDNA library screening was synthesized by Genscript (Piscataway, NJ). Briefly, a plasmid was constructed using the pcDNA3.1+ backbone. The complementary VC155 BiFC fragment was separated from an EcoRI restriction site by a 15 amino acid glycine rich flexible linker. To validate the function of the BiFC plasmids, AC5-interacting

partners were cloned into the EcoRI restriction site and the orientation validated by sequencing. CAD VN-AC5/D_{2L} cells were plated in 6-well dish and cultured to 80-90% confluency, culture media was replaced, and cells were transfected with BiFC plasmid controls using Lipofectamine 2000 according to the manufacturer's recommendations. Images were collected 48 hours after transfection using a Nikon A1 confocal microscope system and NIS-Elements software (Nikon Instruments, Mellville, NY), and analyzed using ImageJ software (NIH, Bethesda, MD).

2.3.4 cDNA library transfection and cell treatment:

Express Genomics cloned a unique human fetal brain cDNA library (Express genomics, Frederick, MD), which contained a minimum of $1x10^6$ independent clones into the EcoRI restriction sites of the BiFC vector. The resulting BiFC linked cDNA library was then validated by a cDNA insert sizing analysis. CAD VN-AC5/D_{2L} cells were seeded in four 100mm culture dishes, then incubated at 37°C and 5% CO_2 in selection media until they reached approximately 80% confluency. Selection media was gently aspirated and replaced with CAD culture media lacking any selection agents. 14µg of the cDNA library was transfected using Lipofectamine 2000 following the manufacturer's recommended directions. Twenty-four hours following the cDNA library transfection, the media was gently aspirated, then replaced with culture media containing DMSO (vehicle) or 1µM quinpirole treatment. All plates were returned to the incubator overnight. To remove cells, they were washed gently with warm PBS and dissociated using non-enzymatic cell dissociation buffer (Gibco, Grand Island, NY). Cells were collected in a conical tube and pelleted by centrifugation at 800xg for 5min. The supernatant liquid was aspirated, and the cell pellet was re-suspended in a solution of warm HBSS containing 10mM HEPES and 2% BSA for FACS analysis.

2.3.5 Fluorescence activated cell sorting (FACS):

The fluorescence collection parameters for each FACS sort were first established using a sample of non-transfected cells to determine basal levels of fluorescence and scatter. For each treatment condition, cDNA library transfected cells exhibiting positive fluorescence above basal were collected. Flow cytometry and FACS analyses were performed using a BD FACS Aria II (BD Biosciences, San Jose, CA). Excitation at 488nm using an argon laser, 50LP filter with 525/50 emission was used for FACS sorts. Transfected cells were passed through a 40µm cell strainer

before FACS analyses. FACS analyses were run under 20.0 psi (sample/sheath) using a 100μm nozzle. Sheath fluid was 1x PBS at pH 7.0, cells were sorted directly into a collecting tube containing HBSS with 0.01% HEPES and 1% BSA. BiFC fluorescent positive sorted cells were centrifuged at 800xg for 10 min, supernatant aspirated, and remaining cell pellet stored at -80 °C until use.

2.3.6 Plasmid extraction and PCR:

Cell pellets were removed from -80°C, and freeze fractured in liquid nitrogen to lyse cells. Plasmid DNA extraction and isolation was performed using a Spin Miniprep Kit (Qiagen, Germantown, MD) according to the manufacturers protocol. The cDNA insert region of the extracted plasmid DNA was amplified and prepared for NextGen sequencing using a two-step PCR approach. The 1st stage PCR primers contained a locus specific sequence unique to the cDNA insert region of the BiFC plasmid, and an overhanging adapter sequence for binding the 2nd stage PCR primers. The 2nd stage PCR reaction added the adapters for Illumina sequencing, and a small sequence unique to each FACS sort and treatment to the amplified cDNA sequence. PCR products were cleaned between reactions using a DNA cleanupkit (Qiagen, Germantown, MD), according the manufacturer's protocol. The PCR reactions were carried out using a T100 Thermal Cycler (BioRad) in 50μl volumes. The thermocycler program included a longer extension time to account for the unknown amplicon size, and is outlined below. The final PCR products from each FACS sort were then pooled together for sequencing.

2.3.7 Library preparation Illumina MiSeq sequencing:

Sequencing of the variable cDNA region amplicon library was done on the Illumina MiSeq platform at the Purdue University Genomics Core facility, and 300bp paired-end reads generated. After trimming the adaptor and primer sequences from the Illumina reads, the raw sequences of the cDNA library were compared against the reference human genome GRCh38. A list was compiled of the genes that appeared under each treatment condition, for all three independent FACS events. Genes that appeared in at least two of the three sorts were selected for further evaluation.

2.3.8 Cisbio HTRF cAMP Assay:

Acute cAMP accumulation was measured by adding 10µl/well a mixture of FSK and 3-isobutyl-1-methylxanthine (IBMX) (3µM and 500µM final concentrations, respectively) to the wells, plates were incubated at room temperature for 1 hour before cell lysis and cAMP accumulation measurements. Assay plates using the Cisbio HTRF cAMP dynamic-2 assay kit was excited using 330nm wavelength and analyzed for fluorescent emissions at 620 and 665nm using a Synergy4 (BioTek, Winooski, VT). Ratiometric analyses were performed with GraphPad Prism (GraphPad Software, La Jolla, CA) by dividing the 665nm emission by the 620nm emission to interpolate cAMP concentrations from a cAMP standard curve.

Acute cAMP inhibition experiments were conducted by adding 5µl/well quinpirole (final concentration 3µM), and then the plates were briefly centrifuged to ensure all liquid was collected at the bottom of the well. Plates were incubated at room temperature for 15 minutes, then stimulated by adding 5µl/well forskolin in 3-isobutyl-1-methylxanthine (IBMX) (3µM and 500µM final concentrations, respectively) to the wells, plates were incubated at room temperature for 1 hour before cell lysis and cAMP accumulation measurements.

Sensitization cAMP accumulation was measured by adding 5µl/well of the D_2R ligand quinpirole (3µM final concentration) and incubating the plate at 37°C and 5% CO_2 for 2 hours. 5µl/well forskolin (300nM final concentration) in 2mM 3-isobutyl-1-methylxanthine (IBMX) and 1µM spiperone was added to the wells, then plates were incubated at room temperature for 1 hour before cell lysis and cAMP accumulation measurements.

2.3.9 Reverse siRNA Transfection for qPCR and Western Blotting:

Lyophilized siRNA was re-suspended in 1x siRNA buffer (Dharmacon, Longmont, CO) and diluted to 20µM stocks, then further diluted to 0.5µM in OptiMEM. Lipofectamine RNAiMAX was diluted in OptiMEM (9µl/ml) and 320µl of 0.5µM siRNA was mixed with 1024µl dilute RNAiMax, then added to a 6-well dish to incubate for 30 minutes at room temperature. Cells in culture had the media aspirated, were rinsed briefly with phosphate buffered saline, then dissociated with non-enzymatic cell dissociation buffer. Cell suspensions were centrifuged at 500xg for 5 minutes and cells were re-suspended in OptiMEM containing 7.5% heat inactivated fetal bovine serum (Hyclone, Logan, UT). Cells were diluted, then 2.5mL cell solution added to

the 6-well dish containing siRNA. Cells were incubated in a humidified incubator at 37°C and 5% CO_2 for 72 hours before dissociation for qPCR or western blotting.

2.3.10 Quantitative PCR (qPCR):

Cells were washed in phosphate buffered saline, then removed from plates using non-enzymatic cell dissociation buffer. RNA extraction was performed with the RNeasy mini kit (Qiagen, Germantown, MD). Reverse transcription step was carried out using iScript cDNA synthesis kit (BioRad, Hercules, CA). RT-qPCR was completed using SYBR Green Reagents kit according to manufacturer's protocol (Thermoscientific) in 384 well qPCR plates (Dot Scientific, Burton, MI) using 15µl/well volumes. RT-qPCR was read using a ViiA 7 Real-Time PCR System (Thermoscientific). qPCR primers were purchased from Integrated DNA Technologies (Coralville, IA).

2.3.11 Western Blotting:

Unless otherwise listed, reagents were purchased from Sigma Aldrich (St. Louis, MO) Anti $G\alpha_{s/olf}$ antibody was purchased from Santa Cruz biotechnology (Dallas, TX). Anti-NAPA, anti-HERC1, anti-vinculin, and anti-alpha tubulin antibodies were purchased from Novus biological (Littleton, CO). Anti-huntingtin and anti-PPP2CB antibodies were purchased from Abcam (Cambridge, MA). Anti-IGBP1 antibody was purchased from Bethyl Labs (Montgomery, TX).

Cells were briefly with phosphate buffered saline, before being dissociated from the plate with non-enzymatic cell dissociation buffer and centrifuged at 800xg for 5 minutes. The supernatant was aspirated, and the cell pellet re-suspended by pipetting in RIPA buffer (final concentrations in water, 150mM NaCl, 5mM EDTA, 50mM Tris, 1.0% TritonX, 0.5% sodium deoxycholate, 0.1% sodium dodecylsulfate) containing phenylmethanesulfonyl fluoride (PMSF) and protease inhibitor cocktail before being placed on ice for 30 minutes. The cell samples were centrifuged for 15 minutes at 18,000xg at 4°C, with the soluble fraction being preserved. A BCA protein assay (Biorad, Hercules, CA) was used according to the manufactures directions to determine the protein concentration of each sample. 15ug of each sample were combined with Laemmli buffer (final concentration, 60mM Tris-HCl, pH 6.8, 2% SDS, 10% glycerol, 5% β-mercaptoethanol, 0.01% bromophenol blue) and boiled for 5 minutes. Denatured proteins were separated via SDS-PAGE on a 4-18% polyacrylamide gel (BioRad, Hercules, CA) and transferred

to a PVDF membrane, pore size 0.45μm (Millipore, Billerica, MA). Membranes were blocked in 5% non-fat milk for 1 hour at room temperature, the membrane was probed for the protein of interest with primary antibodies diluted in PBS + 0.5% Tween20 (PBST) with 1% milk, by rocking overnight at 4°C. The membrane was washed with PBST, then incubated with a secondary IRDye 680RD anti-mouse or IRDye 800CW anti-rabbit (LICOR Biotechnology, Lincoln, NE) at 1:10,000 for 1 hour at room temperature. Detection of immunostaining was carried out using LICOR Odessey CLx imager. Bands were quantified using ImageJ Software (NIH, Bethesda, MD).

2.3.12 Immunoprecipitation:

Unless otherwise specified, reagents were purchased from Sigma Aldrich (St. Louis, MO). Immunoprecipitation of adenylyl cyclase activity was conducted as previously described. Briefly, non-transfected HEK AC5/D_{2L} cells were grown to 90% confluency in 10-cm dishes. Cells were washed with 3-5mL ice-cold PBS, removing PBS by aspiration, and lysis buffer added to plate, and left on ice for 5 min (300μL; 50mM HEPES, pH 7.5, 1mM EDTA, 1mM $MgCl_2$, 150mM NaCl, 0.5% $C_{12}E_{10}$, plus protease inhibitor cocktail). Cells were scraped and collected in an Eppendorf tube, a 23-gauge needle and 1mL syringe were used to homogenize cells. Cell lysate was centrifuged at 13,000xg for 10 min at 4°C to remove cellular debris. Supernatant was collected in new Eppendorf tube, and protein concentration determined by BCA assay. Samples were diluted to 500μg/mL, and 500μL aliquoted in Eppendorf for each condition. 1-2μg of antibody was added to appropriate vial, and rotated overnight at 4°C. 30μl of washed anti-protein A agarose beads were added to each vial, then rotated for 1hr at 4°C. After incubation, samples were centrifuged, and supernatant removed. The beads were washed three times with 300μl wash buffer (lysis buffer containing 0.05% $C_{12}E_{10}$). Samples for western blotting were resuspended in 40μl 1x SDS sample buffer and run as western blots described previously. Samples for adenylyl cyclase activity assays were resuspended in 50μl membrane buffer (50mM HEPES, pH 7.5, 1mM EDTA, 1mM $MgCl_2$, 0.05% $C_{12}E_{10}$) and 10μl/well plated in white, flat bottom, tissue culture-treated 384-well plate (PerkinElmer, Shelton, CT). 5μl membrane buffer without $C_{12}E_{10}$ was added to all wells. 5μl 4x stimulation buffer (33mM HEPES, 0.05% $C_{12}E_{10}$, 10mM $MgCl_2$, 1mM ATP, 4μM GTPγS, 2mM IBMX, 200μM forskolin, 200nM purified, $G\alpha_s$-GTPγS) was added to appropriate wells. 5μl stimulation buffer lacking forskolin and purified $G\alpha_s$ were added to basal wells. Plates were

incubated at room temperature for 1 hour before cell lysis and cAMP accumulation measurements as described previously for Cisbio HTRF cAMP assays.

2.3.13 Protein Expression and Purification:

$G\alpha_s$-His protein was expressed using the pQE60 construct and purified as previously described (E. Lee, Linder, & Gilman, 1994). Briefly, protein was first subjected to affinity chromatography using 5 ml His-Pur Ni-NTA resin (Thermo Scientific, Waltham, MA). Elute from Ni-NTA resin was further purified with ion exchange chromatography using 1 ml HiTrap Q Sepharose column (GE Healthcare, Chicago, IL). $G\alpha_s$-His containing fractions were snap frozen in liquid nitrogen and stored at −80°C. Nucleotide exchange was performed as previously described in 50mM HEPES, 2mM DTT, 250μM GTPγS, and 1mM $MgCl_2$ for 20 minutes on ice, followed by 30 minutes at 30°C (Chen-Goodspeed, Lukan, & Dessauer, 2005).

2.4 Results

2.4.1 Development and Validation of BiFC Screening Platform in a Neuronal Cell Model

To take advantage of the bimolecular fluorescence complementation system, we first developed and characterized a novel neuronal cellular model to study drug-induced BiFC of adenylyl cyclase type 5 (AC5) with novel interacting partners (Fig. 2.1). Our BiFC studies used Cath a. differentiated (CAD) cells because they have been effectively used to visualize GPCR interactions in living cells and as a platform for multicolor BiFC analysis of receptor dimerization (Ejendal, Conley, Hu, & Watts, 2013). CAD cells were stably transfected with a human AC5 BiFC fusion (i.e VN-AC5) and the long isoform of the human D_2 dopamine receptor (D_{2L}). The resulting CAD VN-AC5/D_{2L} clones were examined for D_2 agonist-induced heterologous sensitization of adenylyl cyclase activity. The clone selected for the screen CAD VN-AC5/D_{2L} demonstrated a robust 6.5 fold quinpirole-induced sensitization response over vehicle treatment (Fig. 2.2). The quinpirole-induced sensitization was blocked by pretreatment with the D_2 antagonist spiperone or overnight pertussis toxin treatment indicating that the sensitization was both receptor and $G\alpha_{i/o}$-dependent as previously described (Watts & Neve, 1996).

To assess the fluorescence intensity and distribution profile of the CAD VN-AC5 /D_{2L} cell line BiFC response, we developed complementary BiFC constructs using the known AC5 interacting partner AKAP79. Mapping studies have identified a direct interaction of AC5 with

residues 77-108 of AKAP79; deletion of this region ($AKAP79^{77\text{-}108}$) abolishes AC5-AKAP79 interaction in living cell models (Efendiev et al., 2010). To establish positive and negative interactome controls, a BiFC plasmid was constructed in which AKAP79 and $AKAP79^{77\text{-}108}$ were linked to the complementary VC155 BiFC fragment, separated by a 15 amino acid glycine rich flexible linker. Transient transfection of AKAP79-VC into the CAD VN-AC5/D_{2L} cell line resulted in reconstitution of the Venus fluorescent protein and produced a robust, membrane-localized fluorescence response. As expected, expression of $AKAP79^{77\text{-}108}$-VC failed to produce a specific membrane localized fluorescent signal, indicating a lack of interaction with VN-AC5 (Fig. 2.3). As an assessment of the fluorescent signal that resulted from random interaction between the complementary BiFC fragments, the CAD VN-AC5/D_{2L} cells were transfected with a plasmid with VC155 alone. Transfection of the VC155 BiFC fragment produced a detectable fluorescent response, however, the intensity was lower and more dispersed throughout the cell than the signal resulting from a directed interaction. Taken together, these data offer evidence that the established CAD VN-AC5 /D_{2L} cell line is a suitable platform for the study of D_2 mediated heterologous sensitization of AC5, and that co-transfection with VC155-tagged fusions provide appropriate assay controls to for expression and screening a cDNA library for protein interactions using BiFC.

Figure 2.1: Screen workflow for identification of AC5 interaction partners using novel BiFC tagged cDNA library.

A unique human brain cDNA library was cloned into the BiFC plasmid, such that each individual cDNA would be expressed linked to the C-terminal fragment of Venus (i.e cDNA-VC). The BiFC tagged cDNA library was transiently expressed into CAD VN-AC5+D_{2L} and development of heterologous sensitization initiated. Fluorescence activated cell sorting was used to identify and isolate cells that exhibited an AC5-protein interaction, as determined by a BiFC fluorescent signal. Next generation sequencing was used to identify the potential interacting proteins from the complementing cDNAs, followed by siRNA knockdown of identified genes to confirm their role in heterologous sensitization

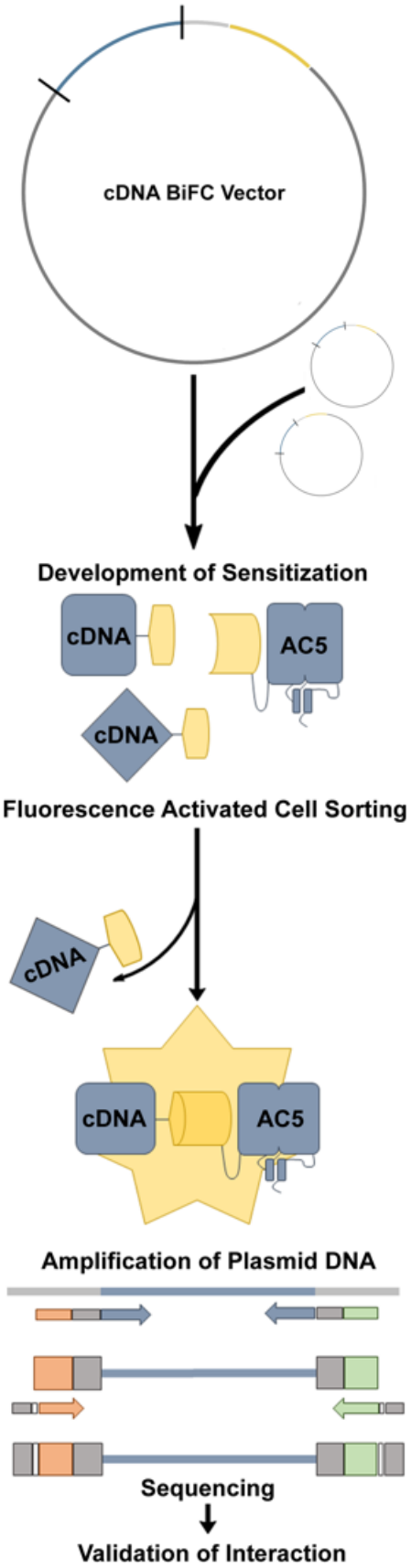
cDNA BiFC Vector
Development of Sensitization
cDNA
AC5
cDNA
Fluorescence Activated Cell Sorting
cDNA
cDNA
AC5
Amplification of Plasmid DNA
Sequencing
Validation of Interaction

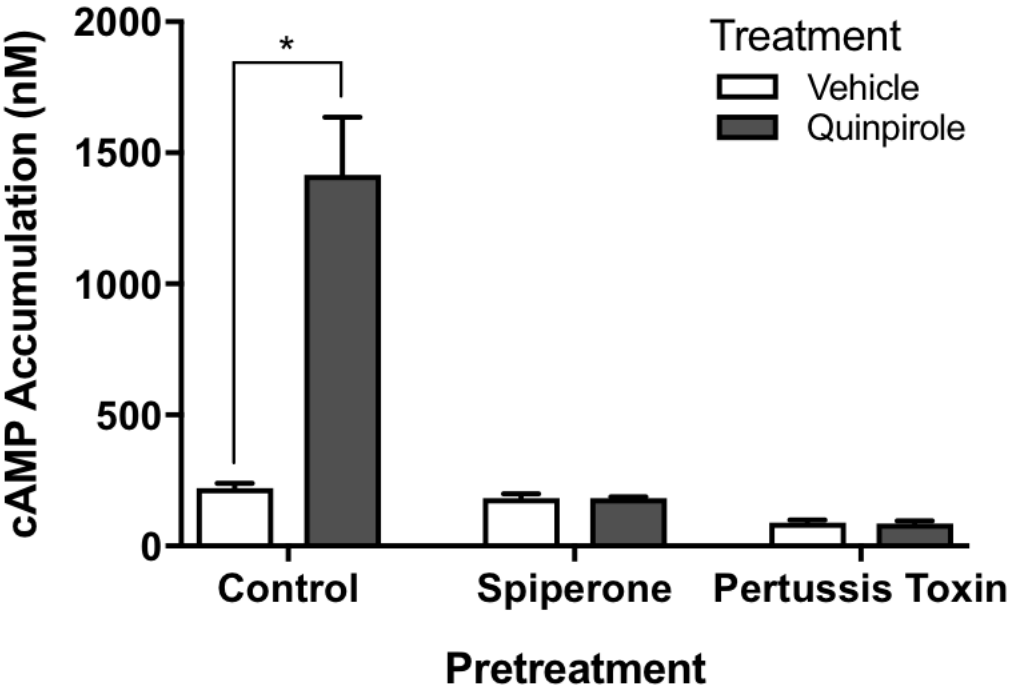

Figure 2.2: The heterologous sensitization profile of CAD VN-AC5+D_{2L} cell line.

A stable cell model co-expressing the D_{2L} dopamine receptor as well as AC5 fused to the N-terminal BiFC fragment of Venus fluorescent protein (VN-AC5) was constructed. Accumulation of cAMP upon treatment with 300nM FSK was monitored in cells pre-treated for 4hrs in the presence of 3μM quinpirole or vehicle. This was repeated in the presence of D_2 antagonist spiperone and pertussis toxin to examine requirement of D_{2L} and $G\alpha_{i/o}$ proteins, respectively. Statistics (t test) for *P < 0.05. Experiments (n = 3) were performed with duplicate wells with SEM shown.

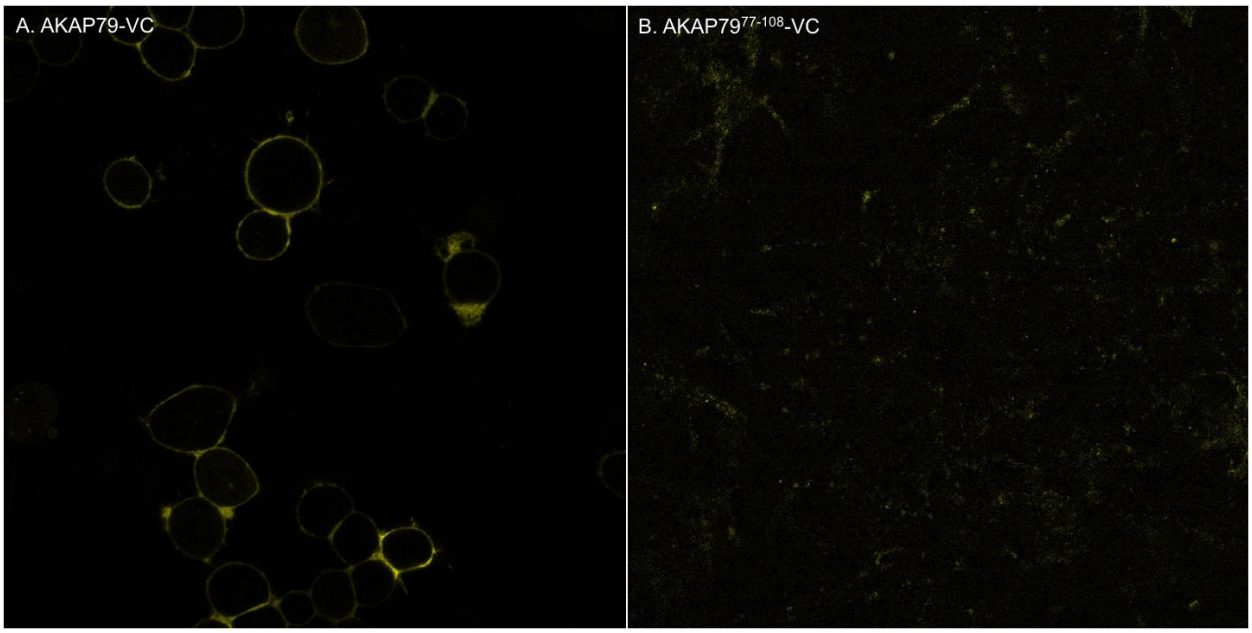

Figure 2.3: Validation of CAD VN-AC5/D_{2L} BiFC response.

Positive and negative BiFC controls were used to validate the specificity and fluorescence intensity of the CAD VN-AC5+D_{2L} cell line. 60x confocal images of CAD VN-AC5+D_{2L} transfected with 1μg of (A) the positive control AKAP79-VC, where Venus fluorescence is clearly observed localized to the cell membrane or (B) the negative control AKAP79$^{77-108}$-VC that exhibits no specific localization.

2.4.2 BiFC Screening of Human Brain cDNA library Identified AC5 Interacting Partners Using Fluorescence Activated Cell Sorting

To identify novel AC5-protein interactions or complexes that occur during the development of heterologous sensitization, we developed a multi-step workflow to transfect a BiFC-tagged cDNA library, assess AC5 interaction by fluorescence, and then isolate these cells for gene identification using next-generation sequencing. The basis of this experimental workflow was in a unique human fetal brain cDNA library that was cloned into a custom BiFC plasmid vector to create the BiFC-tagged cDNA library. The coding sequence of each individual cDNA was cloned into the plasmid to create a collection of cDNA-VC fusion proteins that would emit a fluorescent signal if interactions with the VN-AC5 construct occurred. For each screening trial, CAD VN-AC5/D_{2L} cells were transfected with purified cDNA BiFC plasmid library DNA and incubated for 24 hours, before being treated with either vehicle or 1μM quinpirole overnight to stimulate D_2 mediated heterologous sensitization. After the incubation period, transfected CAD VN-AC5/D_{2L} cells with positive BiFC signals were detected and sorted by fluorescent activated cell sorting (FACS) for each treatment condition. The BiFC positive cells were sorted and collected for plasmid DNA extraction. Using PCR primers that target the insert region of the BiFC plasmid, we amplified the purified cDNA extracted from the BiFC positive cells for both vehicle and quinpirole treatment conditions separately. Two subsequent rounds of PCR prepared the amplified cDNA sequence library for NextGen sequencing by adding adapter regions that adhere the DNA to the solid state, and barcode sequences that allow for differentiation of the treatment group and date of FACS sort. After trimming the primer and adapter sequences from the results, the resulting raw sequences were matched against a human reference genome.

Three independent trials of cDNA library transfection and FACS sorting were completed, and a list of the genes that appeared with each treatment condition was compiled. From all three sorting events, 1387 sequences from vehicle treated cells were matched to the human genome and 1099 sequences matched from the quinpirole treatment group (Supplemental File 1). By narrowing our focus to protein coding genes that appeared in at least 2 of the 3 separate FACS trials, we identified 106 genes exclusive to the vehicle treatment, 48 genes were identified under the quinpirole treatment, and 59 genes showed overlap in both vehicle and quinpirole conditions (Appendix Table 1), for a total of 213 genes. Our BiFC-based protein interaction screen successfully identified some previously known AC5 interacting proteins including AKAP6,

Tspan7 and PKCζ (Crossthwaite et al., 2006; X. Gao et al., 2007; Kapiloff et al., 2009; J. Kawabe et al., 1994).

2.4.3 Validation of Target Genes Identified from Screen using siRNA

From the 213 genes that were identified in at least 2 of the 3 independent FACS trials, 51 genes of interest were selected for further evaluation based on their role in known signaling pathways. We nominated 20 genes from the vehicle treatment group, 21 genes from the sensitization development treatment group, and 10 genes that appeared to interact with AC5 or an AC5 complex regardless of pretreatment conditions. To confirm that these genes were involved in adenylyl cyclase signaling or the development of heterologous sensitization, we performed a 72 hour pooled siRNA transfection to knockdown gene expression, followed by functional assays to test AC5 acute and sensitization signaling, as well as cellular viability assays (Appendix Tables 2, 3). To ensure the targeted genes were endogenously expressed, we chose to use HEK 293 cells that stably expressed human AC5 and the long isoform of the D_2 dopamine receptor for RNA interference experiments.

Of the 51 genes of interest selected, siRNA knockdown reduced the AC5 heterologous sensitization response by 50% or greater for 32 genes (Fig. 2.4), suggesting that these 32 genes play a role in heterologous sensitization. Furthermore, 28 of the 32 genes demonstrated a preferential reduction of the sensitization response, with less than 50% inhibition of the acute adenylyl cyclase response. To validate the knockdown data, for these 28 genes, we tested the effect of the four individual siRNA that made up the pooled sample used for the initial assessment, on the sensitization response of AC5. Importantly, only 17 genes had at least 2 of the 4 individual siRNA reduce AC5 sensitization by greater than 50%. This validation approach was designed to ensure that the functional reduction in the sensitization response was dependent upon gene knockdown, rather than an artifact from the procedure (Table 5).

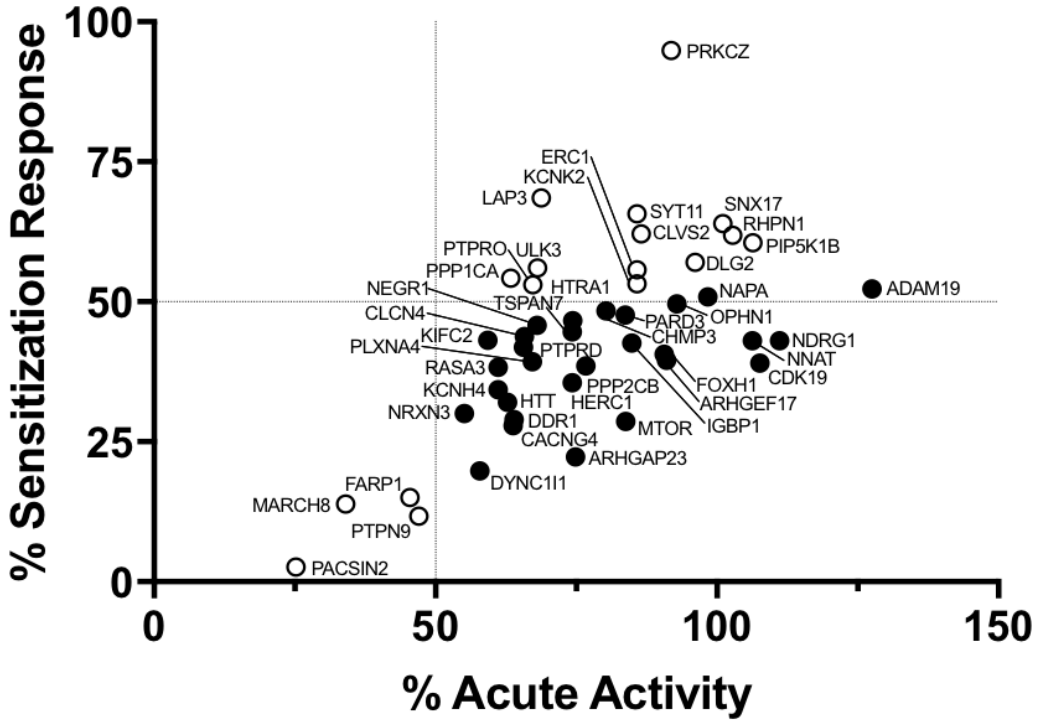

Figure 2.4: Effects of gene knockdown on acute versus heterologous sensitization response.

siRNA screening results of the 51 selected hit genes (46 shown) indicate the effect of gene knockdown on inhibition of AC5 acute activation (X-axis) versus heterologous sensitization response (Y-axis). Gene targets of interest (black circles) exhibited a preferential reduction of the sensitization response over acute activity.

2.4.4 Functional Validation and Characterization of Target Genes

Based on our findings, five validated genes were selected for further genetic and biochemical studies to investigate their role in AC5 signaling and the development of heterologous sensitization. The protein phosphatase 2A (PP2A) catalytic subunit beta (PPP2CB) and its regulatory counterpart immunoglobulin binding protein 1 (IGBP1) both appeared exclusively in the vehicle treatment condition. While the HECT and RLD domain containing E3 ubiquitin ligase 1 (HERC1), huntingtin (HTT), and NSF sensitive attachment protein alpha (NAPA) emerged in the screen only following chronic quinpirole treatment. Using pooled siRNA for each of these five genes, we tested the effect of knockdown of heterologous sensitization of adenylyl cyclase using increasing concentrations of the D_2 receptor agonist quinpirole. $G\alpha_s$ (GNAS) siRNA was used as a positive control of inhibition, due to its known role in the development of the sensitization (Watts, 2002). These results indicate that there is no change in the potency of quinpirole to induce heterologous sensitization, only a reduction in the maximal AC5 response (Fig. 2.5A). The siRNA knockdown of NAPA expression resulted a nearly 90% reduction of the sensitization response, followed in effect by HERC1, IGBP1, PPP2CB, and finally HTT. Furthermore, acute adenylyl cyclase inhibition assays demonstrate that $G\alpha_{i/o}$ signaling remains intact and capable of acutely inhibiting AC5 (Fig. 2.5B). These results suggest that the reduced sensitization response caused by gene knockdown were not the result of disrupted $G\alpha_{i/o}$ signaling.

Initial measurements of gene knockdown following siRNA treatment were assessed by qPCR, and showed range of decreases in mRNA following gene knockdown (Fig 2.6A). Because changes in mRNA are not equal with regard to translation into proteins, analysis by Western blot confirmed that siRNA knockdown significantly reduced ($P \leq 0.0001$) the protein expression for the genes HTT, PPP2CB, IGBP1 and NAPA (Fig. 2.6 B-E) (Schwanhausser et al., 2011). Unfortunately, no adequate antibodies were available to determine changes in the protein levels of the 532kDa HERC1 protein upon siRNA-mediated knockdown. Together these findings suggest that the reduction in maximal sensitization response is correlated to a reduction in protein levels via siRNA knockdown, but that these molecular mechanisms are not the result of disrupted $G\alpha_{i/o}$ signaling.

Of the validated genes, two were selected to further substantiate their interaction with AC5 or AC5 complex by co-immunoprecipitation activity assays. The protein phosphatase 2A

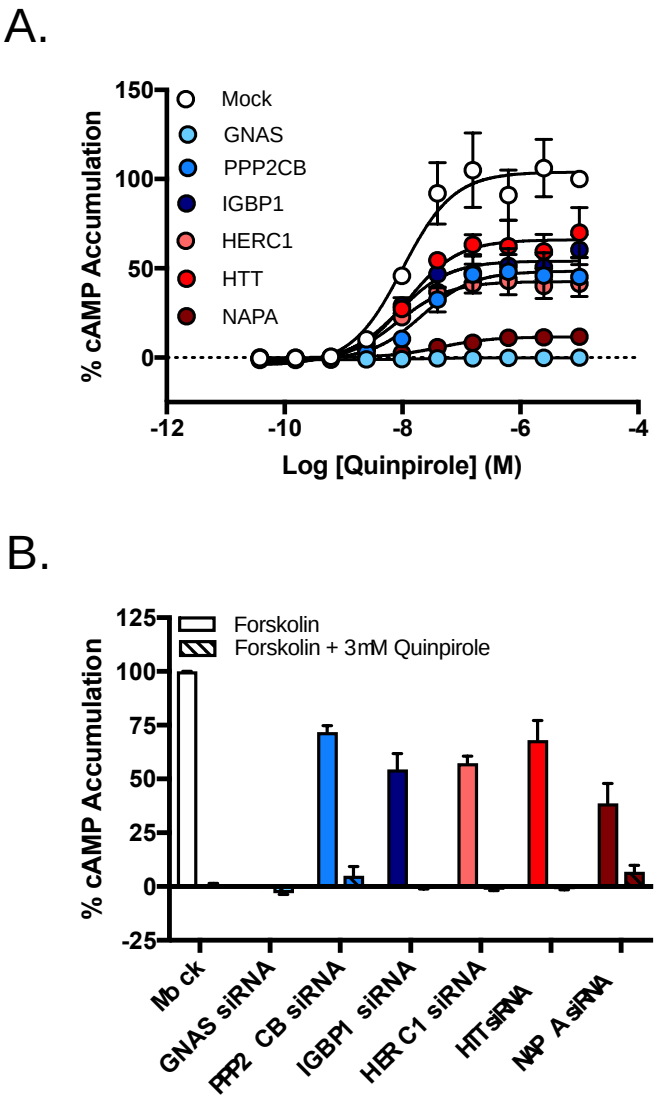

Figure 2.5: Gene knockdown decreases maximum efficacy of AC5 heterologous sensitization response.

siRNA knockdown of target genes reduced the maximal efficacy of the AC5 sensitization response without affecting the potency of quinpirole to promote sensitization development (A). The ability of the $G\alpha_{i/o}$-coupled D_2 receptor to inhibit AC5 remained intact following gene knockdown (B). 3μM quinpirole decreased the maximal AC5 response to acute treatment with 3μM forskolin. Experiments (n = 3) were performed in duplicate with SEM shown

(PP2A) catalytic subunit beta (PPP2CB) was observed as an AC5 BiFC interacting partner under vehicle treatment conditions. Endogenous PPP2CB was immunoprecipitated from HEK AC5/D_{2L} cell lysates using anti-PPP2CB antibody and protein A conjugated agarose beads. The PPP2CB immunoprecipitates were stimulated with activated $G\alpha_s$ and FSK and exhibited significantly increased adenylyl cyclase activity versus control (Fig 2.7A). The NSF sensitive attachment protein alpha (NAPA) was an interacting partner observed in the AC5 BiFC screen exclusively following chronic quinpirole treatment. Stimulation of endogenous NAPA immunoprecipitates following vehicle treatment showed no significant difference in adenylyl cyclase activity compared to the control (Fig 2.7B). In contrast, overnight treatment of cells with quinpirole resulted in a significant increase in the adenylyl cyclase activity observed in endogenous NAPA immunoprecipitates compared with the vehicle treated group (Fig 2.7C).

2.5 Discussion

Heterologous sensitization of adenylyl cyclase is a cellular adaptive response that results from chronic $G\alpha_{i/o}$-mediated inhibition, and has been implicated in major neurological disorders such as Parkinson's disease, dyskinesias, the development of addiction, and chronic pain models (Brust et al., 2017; Y. Z. Chen et al., 2014; Park et al., 2014; Watts, 2002). In this study we developed a screening strategy that used a unique BiFC linked cDNA library to identify novel AC5-protein interacting partners during the development of heterologous sensitization. Through fluorescent activated cell sorting (FACS) followed by next generation sequencing (NGS), we collected and identified proteins and genes associated with the development of D_2-mediated heterologous sensitization in an unbiased manner. The role of these interacting partners was validated through siRNA knockdown, where we observed that the expression of the identified protein interaction networks were necessary for the full development and expression of AC5 mediated heterologous sensitization.

Rapid progress has been made in the identification and characterization of compartmental signaling pathways, and research has highlighted that adenylyl cyclases do not exist in an isolated environment, but rather as a part of dynamic complexes of interacting partners that govern spatiotemporal cAMP signaling within the cell (Dessauer et al., 2017; Efendiev et al., 2010). To better understand the composition and function of these signaling complexes, novel strategies have been developed to characterize the totality of large sets of interacting proteins. It

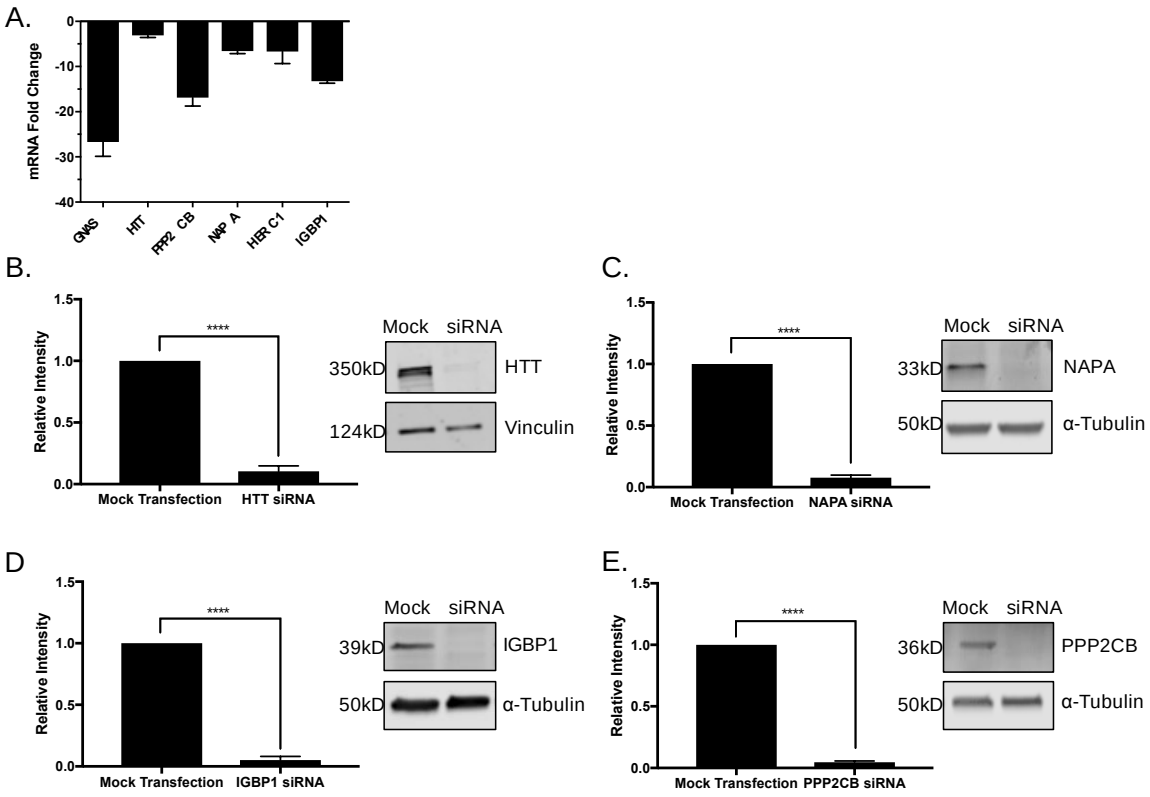

Figure 2.6: siRNA knockdown significantly reduces protein expression of target gene.

Biochemical validation of siRNA knockdown was carried out by qPCR (A) and Western blotting (B-E). Cell fractions from mock or siRNA treated cells were subjected to Western blot analysis using target antibodies for (B) HTT, (C) NAPA, (D) IGBP1, (E) PPP2CB as well as listed loading controls. Data standardized to mock transfection (left) and representative immunoblots (right). Statistics (t test) for ****P < 0.0001. Experiments (n = 3)

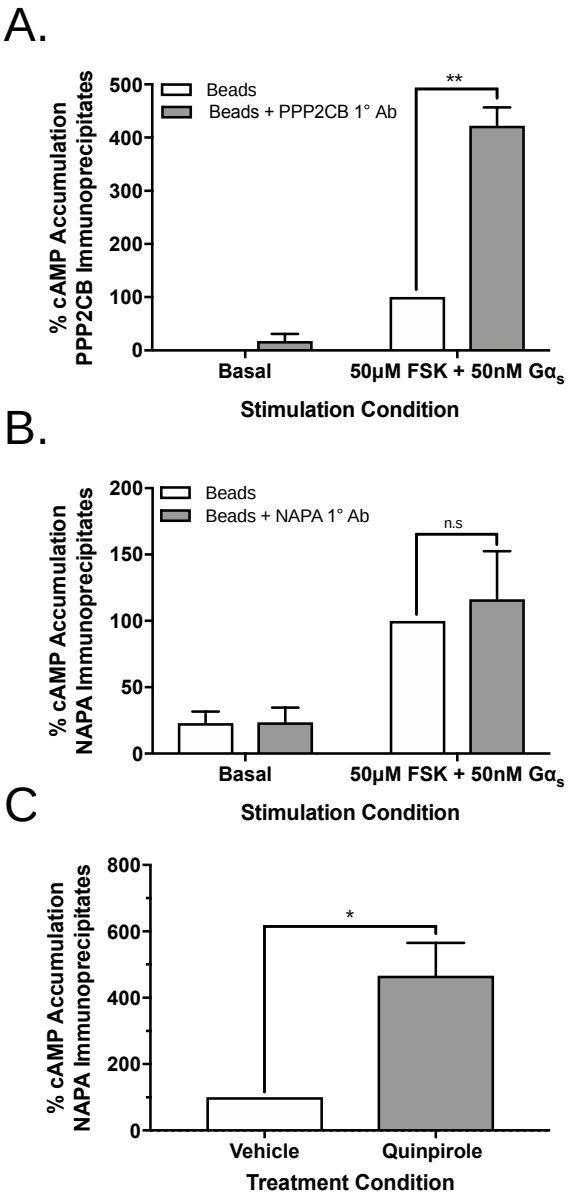

Figure 2.7: AC activity is elevated in immunoprecipitates of interacting partners.

Immunoprecipitation of interacting partners PPP2CB and NAPA resulted in enhanced adenylyl cyclase activity in the pulldown product in a treatment dependent manner. The PPP2CB immunoprecipitate exhibited 4-fold enhancement of adenylyl cyclase activity under vehicle treatment conditions (A). The NAPA immunoprecipitate exhibited no significant difference in adenylyl cyclase activity under vehicle treatment conditions (B). Quinpirole pretreatment resulted in a significant 4.5-fold enhancement of adenylyl cyclase activity from NAPA immunoprecipitates compared to the vehicle treated group (C). Statistics (t test) for *$P < 0.05$. Experiments ($n = 3$) were performed in duplicate with SEM shown.

has been well established that BiFC can specifically identify weak or transient interacting partners under a variety of physiologic conditions (Kodama & Hu, 2012). These properties have made BiFC screening an attractive alternative to yeast two-hybrid methods for conducting large-scale protein interaction screening studies. Indeed, several groups have successfully utilized the powerful combination of BiFC with FACS to screen cDNA libraries to identify interacting partners or effector proteins (Berendzen et al., 2012; Zheng & Chang, 2014). We have expanded upon their successes by creating a new screening strategy that utilized a unique BiFC tagged cDNA library created from human fetal brain cDNA, and conducted the screen for novel AC5 interacting partners in a neuronal cellular model under sensitized and non-sensitized conditions. The subsequent amplification of the cDNA inserts with PCR and next generation sequencing allowed for the identification of protein interaction networks under each treatment condition. Interestingly, our screen successfully captured several previously established AC5 interacting partners, and subsequent siRNA validation identified new components of the AC5 signaling complex.

2.5.1 HTT, PPP2CB, IGBP1

Of these interacting partners, one interesting protein identified was Huntingtin (HTT), whose role and interactions are under intense investigation for the research of Huntington's disease (HD). HD is a progressive neurodegenerative disease that is outwardly characterized by abnormal movements, dementia, and cognitive dysfunction (Ross et al., 2014; Watts, 2002). Pathologically, HD may be identified by profound atrophy and cellular degeneration of striatal medium spiny neurons caused by the protein aggregation of mutant huntingtin (mHTT) containing a polyglutamine repeat expansion (Langfelder et al., 2016). The huntingtin protein contains a conserved AKT phosphorylation site at serine 421 (S421). Previous findings have shown that the dephosphorylation of this residue promotes retrograde transport of mHTT and results in increased aggregation and cytotoxicity, while phosphorylation of S421 restores its function in axonal transport (Colin et al., 2008; Kratter et al., 2016; Zala et al., 2008).

Research has shown that chronic D_2 receptor stimulation promotes the dephosphorylation of S421 and may contribute to the development of mHTT aggregates as well as HD symptoms (Beaulieu et al., 2005; Cyr, Sotnikova, Gainetdinov, & Caron, 2006; Kratter et al., 2016; Metzler et al., 2010). Sustained D_2 stimulation has also been shown to increase the activity of the protein phosphatase PP2A, a known interacting partner of AC8, which can dephosphorylate and inhibit AKT (Beaulieu

et al., 2005; Crossthwaite et al., 2006). Furthermore, recent evidence suggests that PP2A may dephosphorylate HTT directly, thereby promoting the deleterious effects of mHTT through two parallel mechanisms (Metzler et al., 2010). When PP2A forms a complex with Immunoglobin Binding Protein 1 (IGBP1), the phosphatase is protected from polyubiquitination and degradation, enhancing the enzyme's catalytic lifetime (LeNoue-Newton et al., 2011).

Our data demonstrate that AC5 is part of an interacting protein network with HTT, PP2A, and IGBP1. Further characterization of this relationship has indicated that decreasing the expression of these three enzymes through RNA interference reduces the development of heterologous sensitization, but not the ability of the D_2 receptor to acutely inhibit AC5 activity. These results suggest that alterations in the protein network that occur during the development of HD may dampen a key compensatory mechanism in cAMP signaling which may result in dysfunctional neuronal signaling. In fact, AC5 as well as the phosphodiesterase PDE10A have been identified as important players in the development of a broad range of dyskinesias, highlighting the role of cAMP signaling in neuronal circuits involved with movement (Mencacci & Carecchio, 2016).

2.5.2 HERC1, NAPA

Although adenylyl cyclases are widely expressed throughout the various tissues in the body, their function and regulatory abilities are highly compartmentalized (Dessauer, 2009; Guinzberg et al., 2017; Ostrom et al., 2012). The specificity of signaling is critically dependent upon the isoform-specific signaling complexes that direct spatiotemporal cAMP regulation (Agarwal, Miyashiro, Latt, Ostrom, & Harvey, 2017; Piggott et al., 2008). Much like GPCRs, adenylyl cyclases are believed to organize within membrane microdomains (Insel et al., 2005; Ostrom et al., 2012). The construction and maintenance of these microdomains relies substantially on the cellular trafficking machinery. We have observed two genes of particular interest in our BiFC screen of the AC5 "interactome" which have known roles in intracellular trafficking, and may influence the compartmentalization and thus signaling of AC5.

HERC1 is a member of HERC family of ubiquitin ligases and has been shown to stimulate guanine nucleotide exchange on ARF and Rab GTPases (Chong-Kopera et al., 2006; Rosa, Casaroli-Marano, Buckler, Vilaro, & Barbacid, 1996). Predominately localized to the Golgi apparatus and the cytosol, the ability of HERC1 to complex with clathrin and to act as a GTPase

activating protein (GAP) suggest it may play a role in intracellular trafficking rather than vesicular exocytosis (Chong-Kopera et al., 2006; Rosa & Barbacid, 1997; Sanchez-Tena, Cubillos-Rojas, Schneider, & Rosa, 2016). In addition to its function as a guanine nucleotide exchange factor, HERC1 is also believed to act as an E3 ubiquitin ligase (Chong-Kopera et al., 2006; Utine et al., 2017). Curiously, previous research has identified that prolonged $G\alpha_{i/o}$ coupled-receptor stimulation promoted the ubiquitin-mediated proteosomal degradation of RGS proteins (Q. Wang & Traynor, 2011). The association of AC5 with an E3 ligase supports the possibility that the removal of an interacting partner, rather than the initiation of a novel interaction, may promote the development of heterologous sensitization.

Another protein identified in our BiFC screen was the NSF attachment protein alpha (NAPA). NAPA is a member of the SNAP family of proteins that, along with their SNARE binding counterparts, are critically involved the trafficking and transport of proteins within the cell, as well as vesicle release. Previous research has shown that NAPA phosphorylation by the cAMP dependent protein kinase (PKA) reduces the ability of NAPA to bind the SNARE complex, leading to a disassembly of the fusion complex (Hanson, Otto, Barton, & Jahn, 1995; Hirling & Scheller, 1996). Inhibition of NAPA results in impaired intra-Golgi transport, a process not only involved in the movement of cargo within the cell, but also in the development of protein complexes and signaling cascades (Mayinger, 2011). These data suggest that chronic D_2 mediated inhibition of cAMP would reduce PKA activity, potentially increasing NAPA dependent trafficking mechanisms that may play a role in enhancing adenylyl cyclase signaling.

Evidence supports that heterologous sensitization is the result of changes in multiple proteins or protein complexes which alter adenylyl cyclase signaling. Though we have successfully identified several novel proteins in the "sensitization interactome", we anticipate further validation of existing hits, as well as additional characterization to establish isoform selective effects. Furthermore, we are actively studying the effects of the ubiquitin-protease system on the development and expression of heterologous sensitization. Continued research to understand the molecular mechanisms underlying heterologous sensitization will further our scientific understanding of adaptive pathological changes in cellular signaling associated with neurological disorders

CHAPTER 3. FUNCTIONAL CHARACTERIZATION OF AC5 GAIN-OF-FUNCTION MUTATIONS LINKED TO FAMILIAL DYSKINESIA AND FACIAL MYOKYMIA

3.1 Abstract

Adenylyl cyclases are key points for the integration of stimulatory and inhibitory G protein-coupled receptor (GPCR) signals. Adenylyl cyclase type 5 (AC5) is highly expressed in striatal medium spiny neurons (MSNs), and is known to play an important role in mediating striatal dopaminergic signaling. Dopaminergic signaling from the D_1 expressing MSNs of the direct pathway, as well as the D_2 expressing MSNs of the indirect pathway both function through the regulation of AC5 activity, controlling the production of the 2^{nd} messenger cAMP, and subsequently the downstream effectors. Here, we have used a newly developed cell line that used Crispr-Cas9 to eliminate the predominate adenylyl cyclase isoforms to more accurately characterize a series of AC5 gain-of-function mutations which have been identified in familial dyskinesis and facial myokymia (FDFM). Our results demonstrate that the AC5 mutants exhibit enhanced activity to $G\alpha_s$-mediated stimulation in both cell-based and purified protein assays. We further show that the increased cAMP response at the membrane effectively translates into increased downstream gene transcription in a neuronal model. Subsequent analysis of inhibitory pathways we show that the AC5 mutants exhibit significantly reduced to D_2 dopamine receptor-mediated inhibition. These observations support a model by which enhanced direct pathway activity and blunted effects of the indirect pathway result in an imbalance of cAMP signaling that contributes to the etiology of FDFM. Finally, we demonstrate that a class of adenylyl cyclase transition state inhibitors may be an effective future therapeutic by preferentially inhibiting the overactive AC5 gain-of-function mutants.

3.2 Introduction

In the central nervous system, neuromodulators elicit their effects predominately through binding and activating G protein-coupled receptors (GPCRs) expressed on the cell surface. Receptor activation transduces the extracellular signal across the plasma membrane and regulates intracellular effector pathways through the activation of heterotrimeric G proteins. Membrane

bound adenylyl cyclases (ACs) are one of the best-characterized G protein effectors, which catalyze production of the second messenger cAMP from ATP (Dessauer et al., 2017). ACs serve as key intersections for the integration of both stimulatory and inhibitory signals that initiate from GPCR activation.

Adenylyl cyclase signaling is a critical regulator of the diverse cortical and thalamic inputs that converge on striatal medium spiny neurons (MSNs), the principal neuron type of the striatum (Tepper & Bolam, 2004). Adenylyl cyclase type 5 (AC5) has been identified as the primary AC isoform expressed in MSNs, accounting for an estimated 80% of cAMP generated (K. W. Lee et al., 2002; Pieroni, Miller, Premont, & Iyengar, 1993). AC5 integrates signals from key receptors in striatal MSNs, such as the stimulatory D_1 dopamine (D_1R) and A_{2A} adenosine ($A_{2A}R$) receptors (Corvol et al., 2001; Herve, 2011). Conversely, AC5 is also specifically regulated by the inhibitory D_2 dopamine (D_2R) and M_4 muscarinic (M_4R) receptors which reduce cAMP production in striatal MSNs (K. W. Lee et al., 2002; Nair, Gutierrez-Arenas, Eriksson, Vincent, & Hellgren Kotaleski, 2015; G. Sanchez et al., 2009).

The initiation and control of movement by the striatum is dependent upon a complex system of neural circuitry and requires delicately balanced GPCR and adenylyl cyclase signaling. D_1R expressing MSNs of the direct pathway project to and inhibit the substantia nigra pars reticulata (SNr) to promote movement, whereas activation of the D_2R MSNs of the indirect striatopallidal pathway results in the suppression of movement. The importance of maintaining this balance is highlighted by recent whole genome sequencing results which have identified novel gain-of-function mutations in the gene coding for AC5 in patients with familial dyskinesia and facial myokymia (FDFM) (D. H. Chen et al., 2015; Y. Z. Chen et al., 2014; Y. Z. Chen et al., 2012; Fernandez et al., 2001). This rare hyperkinetic movement disorder is characterized by early-onset paroxysmal dyskinesia, dystonia, chorea, and myoclonus, involving the limbs and/or trunk (D. H. Chen et al., 2015; Dy et al., 2016). Initial *in vitro* functional studies have shown that the AC5 gain-of-function mutations cause a significant enhancement of cAMP production in response to β-adrenergic stimulation compared to wildtype (Y. Z. Chen et al., 2014). While over a dozen unique AC5 mutations have been identified in FDFM patients, the molecular mechanisms by which AC5 gain-of-function mutations translates to hyperkinetic movement disorders remains unknown, increasing the difficulty to effectively treat patients to manage their symptoms (Carecchio et al., 2017; Dy et al., 2016). Current pharmacological therapies vary widely, ranging from

benzodiazapines and barbituates to carbidopa-levodopa with limited effectiveness (Dy et al., 2016). Here, we took advantage of a newly developed HEK cell line that used Crispr-Cas9 to eliminate AC3 and AC6, the two most abundant endogenous ACs in HEK cells to reduce the background AC activity and cAMP signal (Soto-Velasquez, Hayes, Alpsoy, Dykhuizen, & Watts, 2018). Using this novel cell line, we examined the functional characteristics of five highly prevalent AC5 mutations that have been identified in patients with FDFM, and further explore AC5 as a potential therapeutic target for this unique disorder.

3.3 Materials and Methods

3.3.1 Cell culture:

Both human embryonic kidney (HEK) 293 cells and stable CRISPR/Cas9 AC3 and AC6 knockout human embryonic kidney cells (HEK-ACΔ3/6) were cultured in Dulbecco's Modified Eagle Medium (Life Technologies, Grand Island, NY), supplemented with 5% bovine calf serum (Hyclone, Logan, UT), 5% fetal clone I (Hyclone, Logan, UT), and 1% Antibiotic-Antimycotic 100x solution (Life Technologies, Grand Island, NY) as described previously (Soto-Velasquez et al., 2018). Cath a. differentiated (CAD) cells were cultured in Dulbecco's Modified Eagle Medium, supplemented with 5% bovine calf serum, 5% fetal bovine serum (Hyclone, Logan, UT), and 1% Antibiotic-Antimycotic 100x solution.

AC5 wildtype, R418W, R418Q, A726T, M1029K, and K694_M696del (Δ9bp) constructs were cloned into the c_eGFP vector as described previously (Y. Z. Chen et al., 2014). For transient transfections, cells were seeded in 6-well culture dishes containing culture media, then incubated at 37°C and 5% CO_2 overnight to a confluency of 80%. 1.5 μg of the AC isoform plasmid DNA was transfected per well using Lipofectamine 2000 following the manufacturer's protocol. 1 μg D_{2L} dopamine receptor plasmid DNA or 1 μg CRE-pGL3 luciferase reporter plasmid DNA was additionally co-transfected for select experiments. Twenty-four hours following the transfection, media was aspirated and replaced with culture media, before being returned to the incubator overnight. Forty-eight hours following transfection, cells were washed gently with warm phosphate buffered saline (PBS) and dissociated using non-enzymatic cell dissociation buffer (Gibco, Grand Island, NY). Cells were collected in a conical tube and pelleted by centrifugation

at 500 xg for 5 minutes. The supernatant liquid was aspirated, and the cell pellet was re-suspended in warm OptiMEM (Gibco, Grand Island, NY) for assay.

3.3.2 Membrane Fraction Preparation and Assay:

HEK-ACΔ3/6 cells were grown and transiently transfected as described above. Culture media was aspirated and replaced with ice-cold lysis buffer (1mM HEPES, 2mM EDTA, pH 7.4) and incubated on ice for 15 minutes. Cells were scraped from the plate using sterile scrapers, collected, suspended in lysis buffer, and triturated by pipetting. Cells were centrifuged at 30,000 xg for 20 minutes at 4 °C. The supernatant was discarded, and the remaining pellet resuspended in receptor binding buffer (4 mM $MgCl_2$, 50 mM Tris, pH 7.4). The cell membrane resuspension was homogenized using a Kinematica homogenizer (Kinematica, Switzerland) and aliquotted in 1 ml fractions. The aliquots were centrifuged at 12,000 xg for 10 minutes at 4 °C, the supernatant removed by aspiration, and the remaining membrane pellet was frozen at -80 °C until use.

Briefly, adenylyl cyclase membrane aliquots were thawed on ice and resuspended in membrane buffer (33 mM HEPES, pH 7.4, 0.5 mM EGTA, 0.1% Tween20). A BCA assay was used to determine the protein concentration for each sample, which were diluted to 25 μg/ml. Diluted membranes were plated into a white, flat bottom, tissue culture-treated 384 well plate (PerkinElmer, Shelton, CT) at 10 μl/well, and briefly centrifuged. An additional 5 μl/well of membrane buffer or activated $G\alpha_{i1}$ was added to the appropriate wells. Activated $G\alpha_s$ was diluted in stimulation buffer (33 mM HEPES, pH 7.4, 10 mM $MgCl_2$, 1 mM ATP, 4 μM GTPγS, 0.1% Tween20, 2 mM IBMX), and 5 μl/well added to appropriate wells. The plate was briefly centrifuged and incubated at room temperature for 1 hour before addition of Cisbio HTRF cAMP detection reagents and cAMP measurement as described further below.

3.3.3 CRE-Luciferase Assay:

Cath a. Differentiated (CAD) cells were transiently transfected as described above. Twenty-four hours following transfection, cell culture media was aspirated, and cells were dissociated using non-enzymatic cell dissociation buffer and centrifuged at 500 xg for 5 minutes. The supernatant was discarded, and cell pellet resuspended and diluted in OptiMEM buffer. 20 μl/well of the diluted cell suspension was plated into a white, flat bottom, tissue culture-treated 384 well plate (PerkinElmer, Shelton, CT), then briefly centrifuged, before being stored in a humidified incubator

at 37°C and 5% CO_2 for 24 hours. To stimulate the endogenously expressed $G\alpha_s$-coupled adenosine A_{2A} receptors on CAD cells, 10 μl/well of the A_{2A} receptor agonist CGS 21680 was added (1 μM final concentration), briefly centrifuged, then the plate incubated at 37 °C and 5% CO_2 for 3 hours. Steadylite plus (PerkinElmer, Shelton, CT) luciferase reagent was added according to manufacturer's instructions, and luminescence measured using a Synergy Neo2 (BioTek, Winooski, VT).

3.3.4 Cisbio HTRF cAMP Assay:

cAMP accumulation was measured using the Cisbio HTRF cAMP dynamic-2 assay kit according to the manufacturer's instructions. Transfected cells had their culture media aspirated, then gently washed with warm PBS, then dissociated with non-enzymatic cell dissociation buffer. Cell suspensions were centrifuged at 500xg for 5 minutes, supernatant aspirated, and cell pellets resuspended in warm OptiMEM buffer. Cells were diluted as indicated, and 10 μl/well plated into a white, flat bottom, tissue culture-treated 384-well plate (PerkinElmer, Shelton, CT). Assay plates containing live cells were briefly centrifuged at 100 xg for 30 seconds and incubated in a humidified incubator at 37 °C and 5% CO_2 for 1 hour before receiving further treatment.

Acute cAMP accumulation was measured by adding 10 μl/well isoproterenol or prostaglandin E2 (PGE2) to stimulate endogenously expressed $G\alpha_s$ coupled GPCRs, or 5 μl/well forskolin (FSK) to stimulate the adenylyl cyclase directly, in OptiMEM containing 3-isobutyl-1-methylxanthine (IBMX) 500 μM final concentration. Plates were briefly centrifuged, then incubated at room temperature for 1 hour before cell lysis and measurement of cAMP accumulation. Assay plates were excited using 330 nm wavelength, and fluorescent emission at 620 nm and 665 nm analyzed using a Synergy Neo2 (BioTek, Winooski, VT). Ratiometric analyses were performed with GraphPad Prism (GraphPad Software, La Jolla, CA) by dividing the 665nm emission by the 620nm emission to interpolate cAMP concentrations from a cAMP standard curve.

Acute cAMP inhibition experiments were conducted by adding 5 μl/well of either inhibitor or the D_2 agonist quinpirole, as specified. Plates were briefly centrifuged, then incubated for 15 minutes at room temperature, then stimulated by adding 5 μl/well isoproterenol (1 μM final concentration) in IBMX to the wells. Plates were incubated for 1 hour at room temperature before cell lysis and cAMP measurement as described above. Sensitization cAMP accumulation was

measured by adding 5 µl/well of quinpirole (3 µM final concentration) and incubating the plate in a humidified incubator at 37 °C and 5% CO_2 for 2 hours. 5 µl/well isoproterenol in IBMX was then added to the appropriate wells, plates were incubated for 1 hour at room temperature, followed by cell lysis and cAMP measurement as described above.

3.3.5 Protein Expression and Purification:

The $G\alpha_s$-His protein was expressed using the pQE60 construct and purified as described previously (E. Lee et al., 1994). Briefly, the protein was subjected to affinity chromatography using 5 ml His-Pur Ni-NTA resin (Thermo Scientific, Waltham, MA). The Elute from Ni-NTA resin was further purified using ion exchange chromatography using a 1ml HiTrap Q Sepharose column (GE Healthcare, Chicago, IL). $G\alpha_s$-His containing fractions were snap frozen in liquid nitrogen and stored at -80°C until use. Nucleotide exchange was performed in 50 mM HEPES, 2 mM DTT, 250 µM $GTP\gamma S$, and 1 mM $MgCl_2$ for 20 minutes on ice, followed by 30 minutes at 30°C as described previously (Chen-Goodspeed et al., 2005). The purified activated myristoylated $G\alpha_{i1}$ protein was a kind gift from Dr. Carmen Dessauer.

3.3.6 Western Blotting:

Unless otherwise listed, regents were purchased from Thermo Fisher (Thermo Scientific, Waltham, MA). Anti-GFP antibody was purchased from Takara Bio (Kusatsu, Japan) and used at 1:1,000, anti-α tubulin antibody was purchased from Novus biological (Littleton, CO) and used at 1:5,000. Briefly, transfected cells were washed with ice cold PBS before being dissociated from the cell culture dish with non-enzymatic cell dissociation buffer and centrifuged at 800 xg for 5 minutes. The cell pellet or membrane fraction was re-suspended in lysis buffer containing 50 mM HEPES, pH 7.4, 150 mM NaCl, 1mM EDTA, 1 mM $MgCl_2$, 0.5% $C_{12}E_{10}$, 1 mM DTT, and protease inhibitor cocktail and incubated on ice for 30 minutes before being centrifuged at 18,000 xg at 4 °C for 10 minutes to separate the insoluble fraction. Supernatant was transferred to a new Eppendorf tube, and protein concentration determined by BCA assay. Protein samples were separated on 4-16% gradient gels and transferred to PVDF membrane. Membranes were blocked in 5% non-fat milk for 1 hour at room temperature, the membrane was probed for the protein of interest with primary antibodies diluted in TBST with 1% milk, by rocking overnight at 4°C. The membrane was washed with TBST, then incubated with a secondary IRDye 680RD anti-mouse or

IRDye 800CW anti-rabbit at 1:10,000 for 1 hour at room temperature (LICOR Biotechnology, Lincoln, NE). Band intensities were quantified using ImageJ software (NIH, Bethesda, MD).

3.4 Results

3.4.1 AC5 mutants exhibit enhanced activity to $G\alpha_s$-mediated stimulation in cell-based assays

Recent studies have reported on two AC5 gain-of-function mutations, R418W and A726T, which significantly enhanced AC activity compared to wildtype in response to single point stimulation of 10 μM isoproterenol (Y. Z. Chen et al., 2014). The work presented here expands on these previous results by examining the specific signaling characteristics for five of the most prevalent AC5 gain-of-function mutations associated with FDFM in recently developed adenylyl cyclase knockout HEK293 cell line (Y. Z. Chen et al., 2014; Douglas et al., 2017). HEK-ACΔ3/6 cells, lacking the predominant adenylyl cyclase isoforms AC3 and AC6 exhibit a 95% reduction in Fsk-stimulated cAMP accumulation, with similar reductions observed for stimulation by $G\alpha_s$-coupled receptors (Soto-Velasquez et al., 2018). This cell line allows for the specific examination of the unique signaling characteristics of AC5 mutants, in the absence of cAMP accumulation caused by the most abundant endogenous AC isoforms.

To assess the activity of each AC5 mutant, HEK-ACΔ3/6 cells were transiently transfected with the respective AC5-eGFP tagged construct, and stimulation by two endogenous GPCRs and the small molecule allosteric activator FSK was assessed. Activation of the prostaglandin receptor (PGER) with PGE_2 revealed all five AC5 mutants exhibited significantly enhanced cAMP production compared to wildtype AC5 (Fig. 3.1A). At 10 μM PGE_2, the Δ9bp mutant showed 528±20% cAMP accumulation compared to wildtype. The next highest increase in AC activity

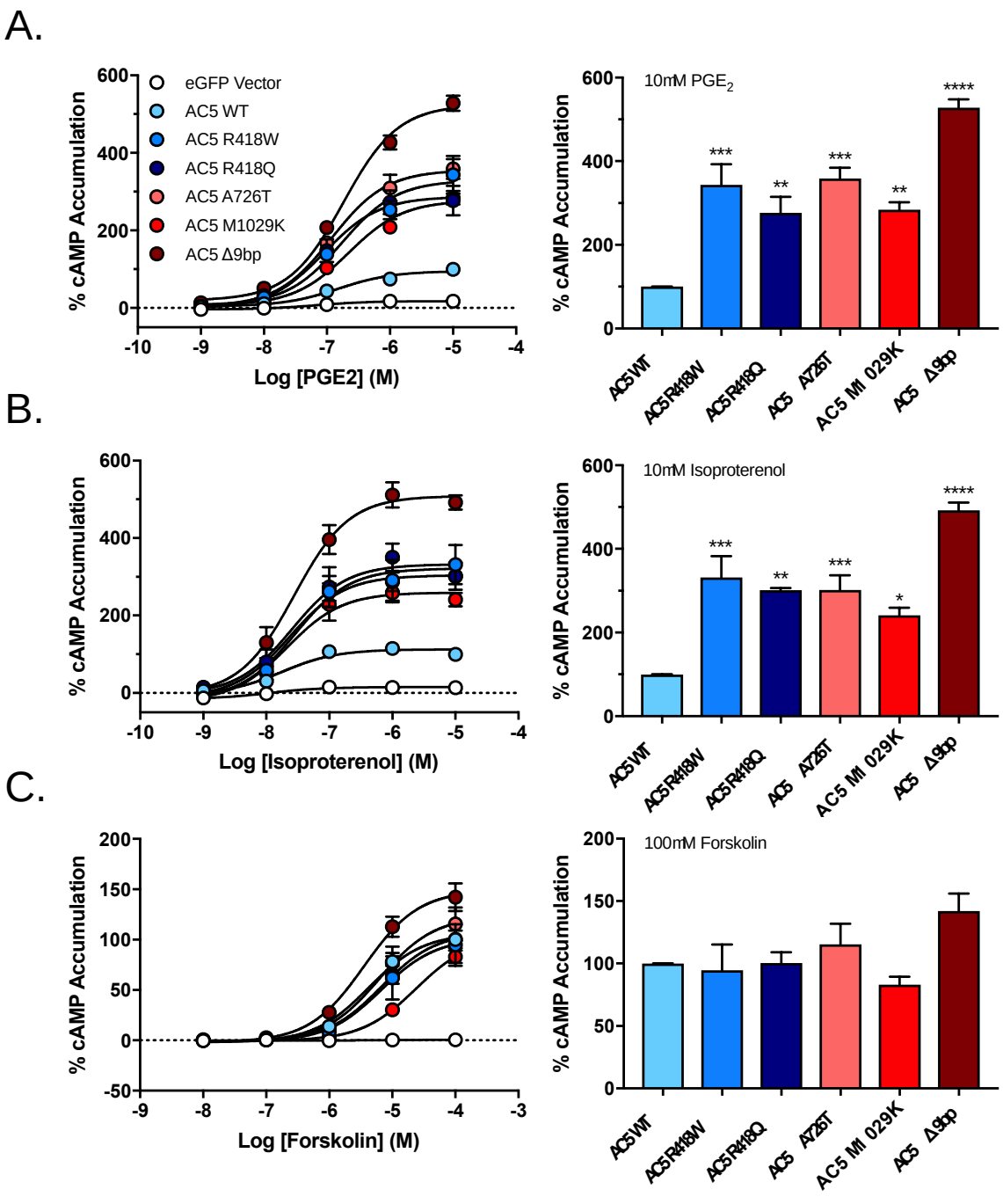

Figure 3.1: Gα_s-coupled receptor and forskolin-mediated cAMP formation by AC5 and mutants.

Activity of indicated AC5-eGFP fusions expressed in HEK AC3/AC6Δ cells was measured using CisBio HTRF assay in response to stimulation with PGE_2/PGER (A), Isoproterenol/β_2AR (B), or FSK (C). Bar graphs represent response observed at highest concentration stimulant tested (10 μM PGE_2, 10 μM Isoproterenol, 100 μM FSK). Data were normalized to wildtype AC5, where basal activity is 0% and maximal observed activity is 100%. Data represent mean ± SEM from three individual experiments, each performed with duplicate wells. **** $P \leq 0.0001$, as determined using one-way ANOVA

was observed with R418W and A726T, which showed 344±49% and 359±25% of wildtype activity, respectively. The R418Q mutant exhibited a 277±38% increase in cAMP production compared to wildtype AC5, and M1029K exhibited 284±17%. Though each mutant showed changes in the efficacy of PGE_2, no significant differences in potency were observed (Table 3.1). These results were corroborated through use of another endogenously expressed $G\alpha_s$ coupled receptor, the β-adrenergic receptor (βAR), which was activated with isoproterenol. Similarly, all five AC5 mutants exhibited significantly enhanced cAMP production in response to isoproterenol-mediated stimulation (Fig. 3.1B). At 10 μM isoproterenol the Δ9bp mutant was the most active with 492±19% of wildtype AC5 activity. R418W exhibited a 332±51% activity, followed by A726T (302±35%), R418Q (301±5%), and finally M1029K (241±18%). Similar to PGE_2, no significant differences in potency to isoproterenol were observed (Table 3.1). In contrast, stimulation by FSK did not produce any significant difference in activity at 100 μM between the wildtype AC5 and the five mutants tested (Fig. 3.1C). Though not statistically significant, the most active mutant Δ9bp exhibited 142±14% activity, compared to wildtype AC5. Western blotting was used to assess AC5 construct expression, and no significant differences were observed (Fig. 3.2)

Table 3.1: Effects of receptor-mediated stimulation and inhibition of AC5 and mutants.

Biochemical characterization of AC5 and mutants in response to receptor and small molecule-mediated stimulation in intact HEK-ACΔ3/6 cells using Cisbio HTRF cAMP assay. Data represent the mean maximal efficacy (Max%) with SEM from *n* = 3 independent experiments, each with duplicate wells. EC50 and IC50 data are listed with 95% CI in parentheses.

Cyclase	PGE2		Isoproterenol		Forskolin		Quinpirole	
	Max %	EC50 (nM)	Max %	EC50 (nM)	Max %	EC50 (μM)	Max %	IC50 (nM)
AC5 WT	100	151 (88-282)	100	18 (7-42)	100	4 (3-7)	96±4	1 (1-2)
AC5 R418W	343±49	173 (63-595)	332±51	29 (9-98)	95±21	7 (1-30)	50±3	6 (2-23)
AC5 R418Q	277±38	91 (35-226)	301±5	25 (9-74)	100±9	7 (4-12)	64±2	12 (6-26)
AC5 A726T	359±25	118 (65-221)	302±35	24 (11-54)	115±17	6 (2-15)	59±2	12 (5-26)
AC5 M1029K	284±17	220 (117-445)	241±18	22 (9-57)	83±6	24 (15-41)	52±4	5 (2-10)
AC5 Δ9bp	528±20	182 (129-262)	492±19	28 (14-55)	142±14	4 (2-6)	54±5	6 (2-23)

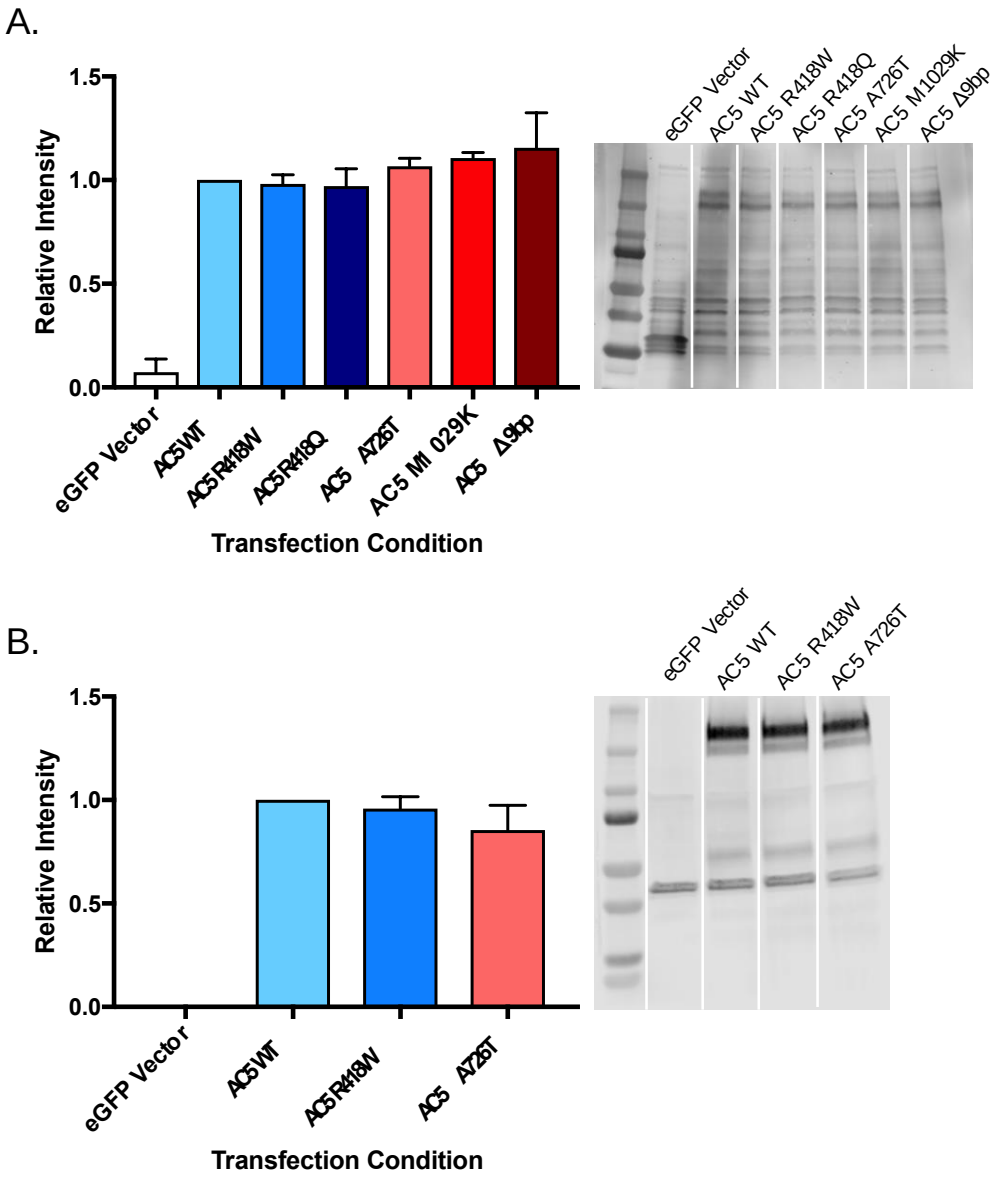

Figure 3.2: Western blot expression of AC5 constructs.

Biochemical validation of construct expression was carried out by Western blotting. Whole cell fractions (A) or isolated membranes (B) from HEK-ACΔ3/6 cells expressing listed eGFP-AC5 construct were subject to western blot analysis using target antibodies for eGFP. Data were normalized to wildtype AC5 expression. Bar graph (left) represents relative band intensity with representative immunoblots (right). Data represent mean ± SEM from three individual experiments, significance determined using two-way ANOVA.

3.4.2 Purified $G\alpha_s$ reproduces exaggerated cAMP response observed with AC5 mutants in cell-free assay

The protein-protein interactions that make up macromolecular AC signaling complexes have been demonstrated to directly modulate acute AC5 activity (Dessauer et al., 2017; Efendiev et al., 2010). To ensure that the enhanced activity associated with the gain-of-function AC5 mutations was the result of heightened enzymatic activity, rather than changes in intracellular signaling pathways, we examined two representative mutants in a cell-free assay. Membrane preparations of HEK-ACΔ3/6 cells transiently transfected with either 418W or 726T were stimulated with increasing concentrations of purified $G\alpha_s$ protein. Membranes containing R418W or A726T AC5 mutants exhibited robust and significantly enhanced cAMP production compared to membranes containing wildtype AC5 (Fig. 3.3) The R418W mutant increased cAMP production to 166±5% of wildtype AC5, while the A726T mutant exhibited 178±4%. As observed in living cells treated with PGE_2 or isoproterenol, no difference in the potency of purified $G\alpha_s$ was observed between wildtype AC5 and R418W or A726T. Western blotting confirmed that no significant differences in membrane expression were observed between any transfected constructs (Fig. 3.2B).

3.4.3 Increased cAMP response translates into increased downstream gene transcription in neuronal cell model

In order to determine whether the enhanced activity of the AC5 mutants translated into downstream changes in gene transcription, we evaluated the ability of two representative AC5 mutants to activate transcription of a cAMP response element (CRE) luciferase reporter in a neuronal cell model. Cath a. Differentiated (CAD) cells transiently expressing the respective AC5 construct and the CRE-Luc reporter were treated with 1 μM CGS21680 to selectively activate endogenous A_{2A} adenosine receptors ($A_{2A}R$). Consistent with the previous functional data, the R418W and A726T mutants significantly increased downstream CRE-mediated transcription compared to wildtype AC5 (Fig. 3.4). $A_{2A}R$ stimulation increased relative luminescence of R418W and A726T expressing CAD cells by 164±3% and 147±2%, respectively, over cells expressing AC5 wildtype.

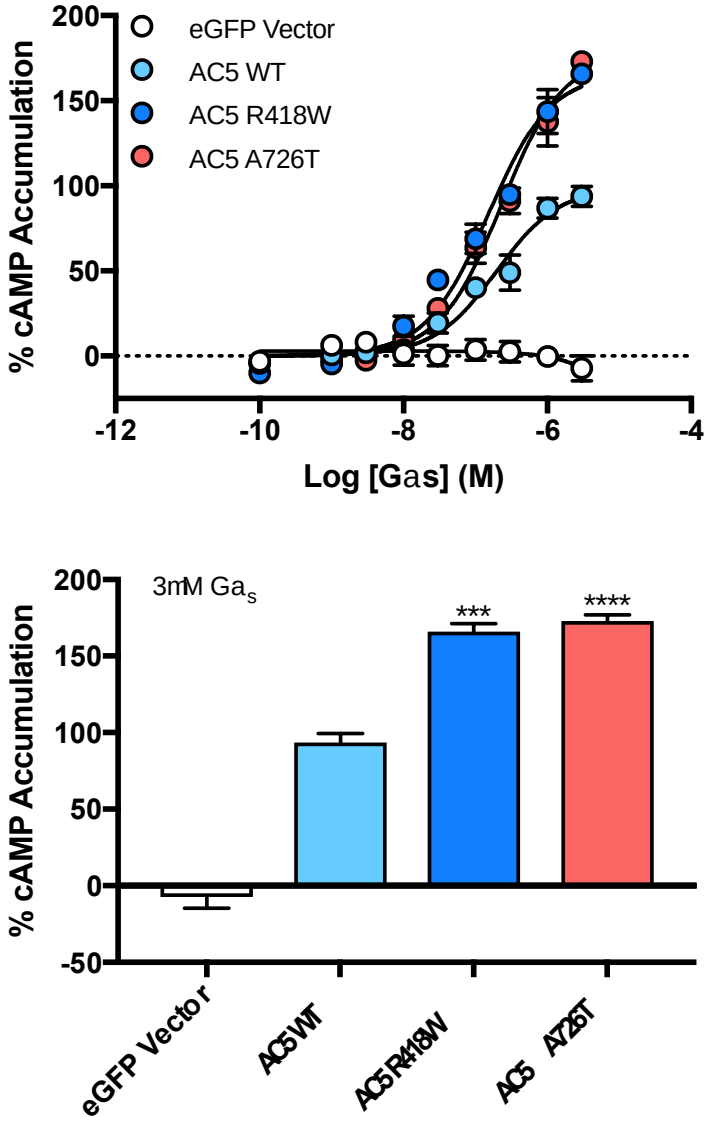

Figure 3.3: Stimulation of AC5 mutants by recombinant $G\alpha_s$-GTPγS.

Membranes preparations of HEK AC3/AC6Δ cells expressing indicated AC5 construct at 250 ng/well were stimulated using purified $G\alpha_s$-GTPγS and cAMP measured using CisBio HTRF. Data were normalized to wildtype AC5, where basal activity is 0% and maximal observed activity is 100%. Data represent mean ± SEM from three individual experiments, each performed with duplicate wells. *** $P \leq 0.001$,**** $P \leq 0.0001$, as determined using one-way ANOVA.

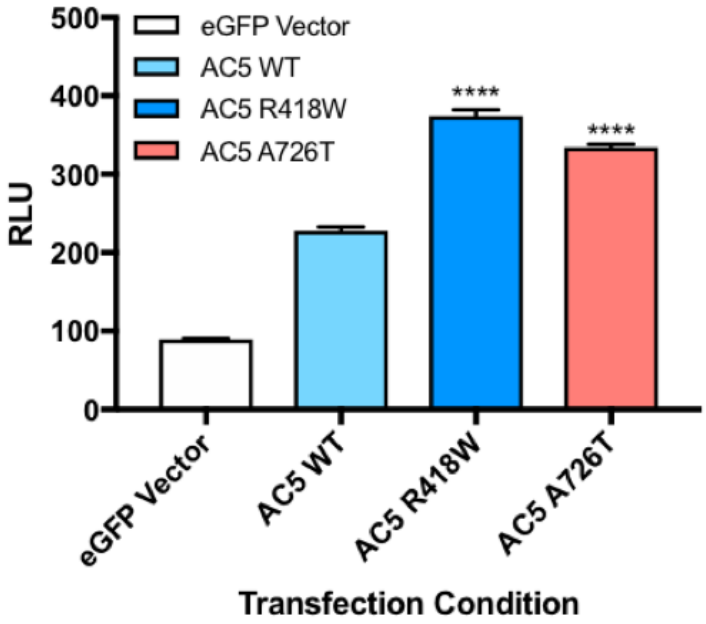

Figure 3.4: Evaluation of downstream cAMP signaling of AC5 mutants in neuronal cell line.

CRE-driven luciferase activity was measured in CAD cells transfected with indicated AC5 construct in response to stimulation with 1 μM CGS 21680 ($A_{2A}R$ receptor agonist). Data presented as relative luminescence units (RLU). Data represent mean ± SEM from three individual experiments, each performed with duplicate wells. **** $P \leq 0.0001$, as determined using one-way ANOVA.

3.4.4 AC5 mutants exhibit significantly reduced inhibition to D_2 dopamine receptor-mediated inhibition

Additionally, AC5 shows robust inhibition by $G\alpha_{i/o}$-coupled receptor activation. We therefore tested whether the AC5 mutations associated with gain-of-function activity affected $G\alpha_{i/o}$-mediated inhibition. HEK-ACΔ3/6 cells expressing the D_2 dopamine receptor (D_2R) and respective AC5 constructs were treated with the D_2R selective agonist quinpirole, and then stimulated with 1 μM isoproterenol. Wildtype AC5 exhibited a robust inhibition of 96±4% in response to D_2R activation. Interestingly, D_2-mediated inhibition of all five AC5 mutants was significantly blunted (Fig. 3.5). Isoproterenol stimulated activity of the R418W mutant was reduced by 50±3% at 10 μM quinpirole; followed by M1029K at 52±4%, Δ9bp at 54±5%, A726T at 59±2%, and R418Q at 64±2%. No significant change in quinpirole potency was observed (Table 3.1).

3.4.5 P-site inhibitors preferentially inhibit overactive AC5 mutants

P-site inhibitors are a class of AC inhibitors that bind the transition state of the enzyme, preventing the formation of cAMP. This class of inhibitors are activity dependent, as the enzyme activity increases, more transition states are available for inhibition (Dessauer, 2002). We therefore assessed the ability of SQ 22,536 to inhibit isoproterenol stimulated AC5 activity. SQ 22,536 inhibited the five AC5 mutants to a significantly greater degree compared to wildtype (Fig. 3.6). Similar results were obtained with each mutant, with inhibition ranging from 88±1% for the Δ9bp mutant (highest inhibition) to 84±1% for A726T (lowest inhibition), compared to 53±6% inhibition of wildtype AC5. No significant differences in potency were observed between the mutants and wildtype AC5 (Table 3.1).

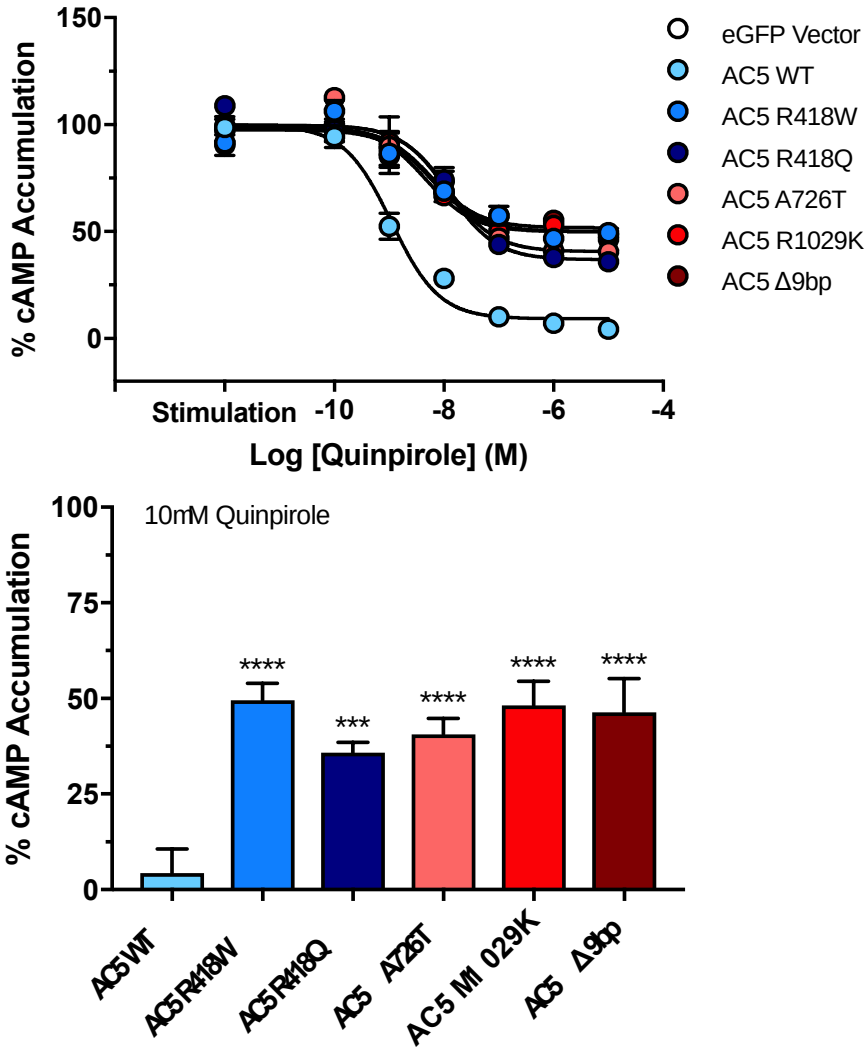

Figure 3.5: $G\alpha_{i/o}$-mediated inhibition of AC5 mutants.

HEK-ACΔ3/6 cells expressing $D_{2L}R$ and indicated AC5 mutant were treated with increasing concentrations of D_2R agonist quinpirole, followed by stimulation with 1 μM isoproterenol. Data were normalized to wildtype AC5, where basal activity is 0% and maximal observed activity in the absence of quinpirole is 100%. Bar graph represents stimulation observed following treatment with 10 μM quinpirole. Data represent mean ± SEM from three individual experiments, each performed with duplicate wells. *** $P \leq 0.001$, **** $P \leq 0.0001$, as determined using one-way ANOVA.

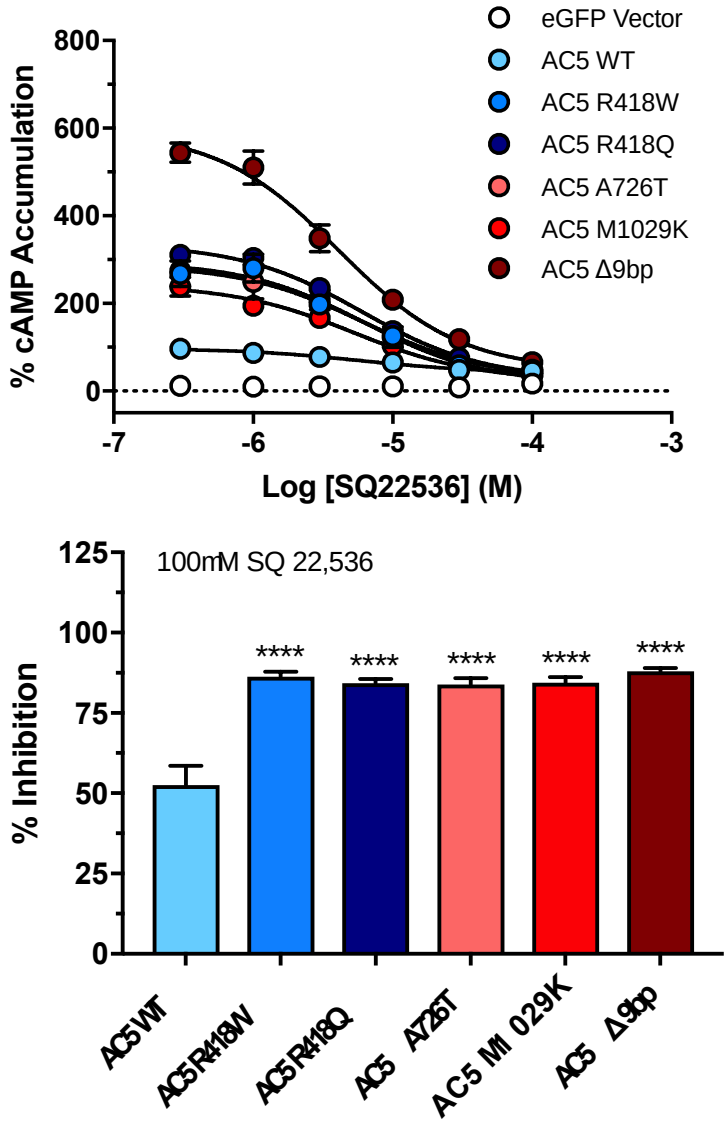

Figure 3.6: Inhibition of AC5 mutant activity by P-site inhibitor SQ 22,536.

HEK-ACΔ3/6 cells expressing indicated AC5 mutant were treated with increasing concentrations of P-site inhibitor SQ 22,536, followed by stimulation with 1 μM isoproterenol. Data were normalized to wildtype AC5, where basal activity is 0% and maximal observed activity in the absence of inhibitor is 100%. Bar graph represents % inhibition of stimulation following treatment with 100 μM SQ 22,536. Data represent mean ± SEM from three individual experiments, each performed with duplicate wells. **** $P \leq 0.0001$, as determined using one-way ANOVA.

3.5 Discussion

Considerable progress in medical genetics has greatly influenced our scientific understanding of the molecular etiology for rare and neglected diseases. Whole exome sequencing of patients with a previously unspecified dyskinesia resulted in the identification of a series of unique mutations in the gene for AC5. The identification of these mutations provided a foundation by which to expand our scientific knowledge of G protein-coupled receptor (GPCR) signal transduction, with the goal of improving medical treatment for a small and very unique population of patients. In this study, we further expand on existing research by functionally characterizing five of the most prevalent AC5 gain-of-function mutations that have been observed in patients exhibiting symptoms of familial dyskinesia and facial myokymia (FDFM). To assist in the specific characterization of these AC5 mutations, we utilized a recently developed HEK cell line that lacks the predominant AC isoforms, thus allowing for focused analysis of the unique signaling characteristics of each AC5 mutant without non-specific background noise caused by endogenously expressed ACs (Soto-Velasquez et al., 2018).

To investigate how different populations of endogenously expressed stimulatory GPCRs affect adenylyl cyclase activity, we examined whether lipid raft localized receptors exhibited differences in signaling efficiency with the AC5 gain-of-function mutants. Areas of the lipid bilayer have been demonstrated to form specialized microdomains, known as lipid rafts, which promote the assembly of signaling complexes and facilitate the formation of efficient GPCR signaling complexes (Dessauer et al., 2017; Villar, Cuevas, Zheng, & Jose, 2016). We compared the ability of prostaglandin receptors (PGERs), which typically do not associate in lipid rafts, with the lipid raft localized β-adrenergic receptors to stimulate AC5 activity (Dessauer et al., 2017). The results indicate that stimulation by both receptor subtypes elicited a significantly enhanced cAMP response from the five AC5 mutants compared to wildtype, suggesting that lipid raft localization of $G\alpha_s$-coupled receptors does not play a substantial role in the enhanced stimulatory signaling observed with the five gain-of-function mutants. Through the use of isolated cell membranes and purified $G\alpha_s$ protein, we demonstrate that two representative AC5 mutants, R418W and A726T, displayed significantly increased cAMP production compared to wildtype AC5 in response to $G\alpha_s$-mediated stimulation. Together these observations suggest that the enhanced cAMP production associated with the AC5 gain-of-function mutations in cell-based assays is the result of increased $G\alpha_s$ stimulated enzymatic activity.

To further understand how enhanced cAMP production at the cell membrane influences downstream effectors, we examined the effect of two representative AC5 gain-of-function mutants on cAMP response element (CRE)-mediated gene transcription in a neuronal cell model. CRE activation is the final step in a signal transduction cascade, which is initiated by adenylyl cyclase stimulation. The subsequent increase in cAMP production promotes the dissociation and activation of protein kinase A catalytic subunits, which translocate into the nucleus and phosphorylate a number of proteins, including the cAMP response element binding protein (CREB) to stimulate transcription. Cath. a differentiated (CAD) cells endogenously express multiple adenylyl cyclase isoforms, as indicated by the increase of luminescence from control vector expressing cells in response to A_{2A} adenosine receptor-mediated stimulation. Despite the elevated background, CAD cells expressing the R418W or A726T AC5 mutation displayed significantly higher CRE-mediated gene transcription compared to wildtype AC5 expressing cells. Gene transcription in neuronal cells is a tightly regulated event. These results therefore indicate that the enhanced cAMP production observed with the AC5 gain-of-function mutations is not limited to membrane localized effects, but rather their activity can permeate downstream effector pathways to elicit global effects.

Presently, our knowledge regarding the structure and functional regulation of the catalytic domains of mammalian adenylyl cyclases is largely based upon X-ray structural analysis of recombinant catalytic domains. This structure indicates that none of the five mutations studied here occur in the catalytic domains or at the interface with $G\alpha_s$. Furthermore, the mutated residues are not directly involved in the coordination of substrate, product, metal ions, or the allosteric activator forskolin within the catalytic site. Rather, modeling places these mutations at the juxtamembrane junction between membrane spanning helices and the cytosolic regions responsible for catalysis. Bacterial adenylyl cyclase crystal structures suggest that these regions are likely helical and may function to regulate C1 and C2 catalytic domain interactions. $G\alpha_s$ stimulation of adenylyl cyclase promotes the stabilization of the C1 and C2 domains to form catalytically active pseudo-heterodimers, as well as the loops and structural features that support catalysis. Therefore, it seems likely that the AC5 gain-of-function mutations facilitate the interaction of the C1 and C2 catalytic domains in response to binding of $G\alpha_s$, which promotes enhanced cAMP production.

AC5 is characteristically sensitive to $G\alpha_{i/o}$-mediated inhibition; we therefore examined how the activation of the D_2 dopamine receptor (D_2R) effected $G\alpha_s$-mediated stimulation. Our

results indicate that selective activation of D_2R robustly inhibits wildtype AC5, however the maximal inhibition of all five AC5 gain-of-function mutants was significantly blunted. These results indicate that not only do the mutant cyclases respond more robustly to $G\alpha_s$-mediated stimulation, they are also more weakly inhibited by $G\alpha_{i/o}$-coupled receptors, further shifting the delicate balance of intracellular cAMP signaling within the neural circuitry of the striatum. As previously described, the striatum is a principal input structure of the basal ganglia and receives neurological input from the motor cortex; which is dynamically controlled with the support of the direct and indirect striatal output pathways to provide opposing influence on the initiation and maintenance of movement. Our results suggest that patients expressing AC5 gain-of-function mutations may have enhanced direct pathway activity, in combination with reduced disinhibition from the D_2R-mediated indirect pathway. This loss of cooperative activity in both direct and indirect pathways likely results in an unsynchronized enhancement of movement initiation (Fig. 3.7).

The increasing awareness of AC5 related movement disorders is compounded by the limited clinical treatments available to treat affected patients, further increasing the difficulty of effectively managing patient symptoms to increase quality of life. While barbiturates and benzodiazepines appear to be medications commonly trialed in patients with AC5 related movement disorders, dopamine receptor agonists in the form of carbidopa-levodopa have also been used with limited success (Dy et al., 2016). The mechanism for the enhanced activity of the AC5 mutants may suggest a more targeted therapeutic. Specifically, we observed that P-site inhibitors have a significantly enhanced effect at the AC5 gain-of-function mutants compared to wildtype. Because P-site inhibitors bind to the catalytic pocket and mimic a cAMP-bound transition state, increased enzyme activity results in a more inaccessible conformation, essentially selectively targeting the most active enzymes. Unfortunately, the only FDA approved P-site inhibitor Vidarabine lacks AC5 selectivity and presumably has significant side effects. A genetic loss of AC5 is associated with a number of beneficial effects, including longevity further highlighting the impetus for the development of selective AC5 inhibitors that could be applied to ADCY5 dyskinesias and other clinically relevant condition.

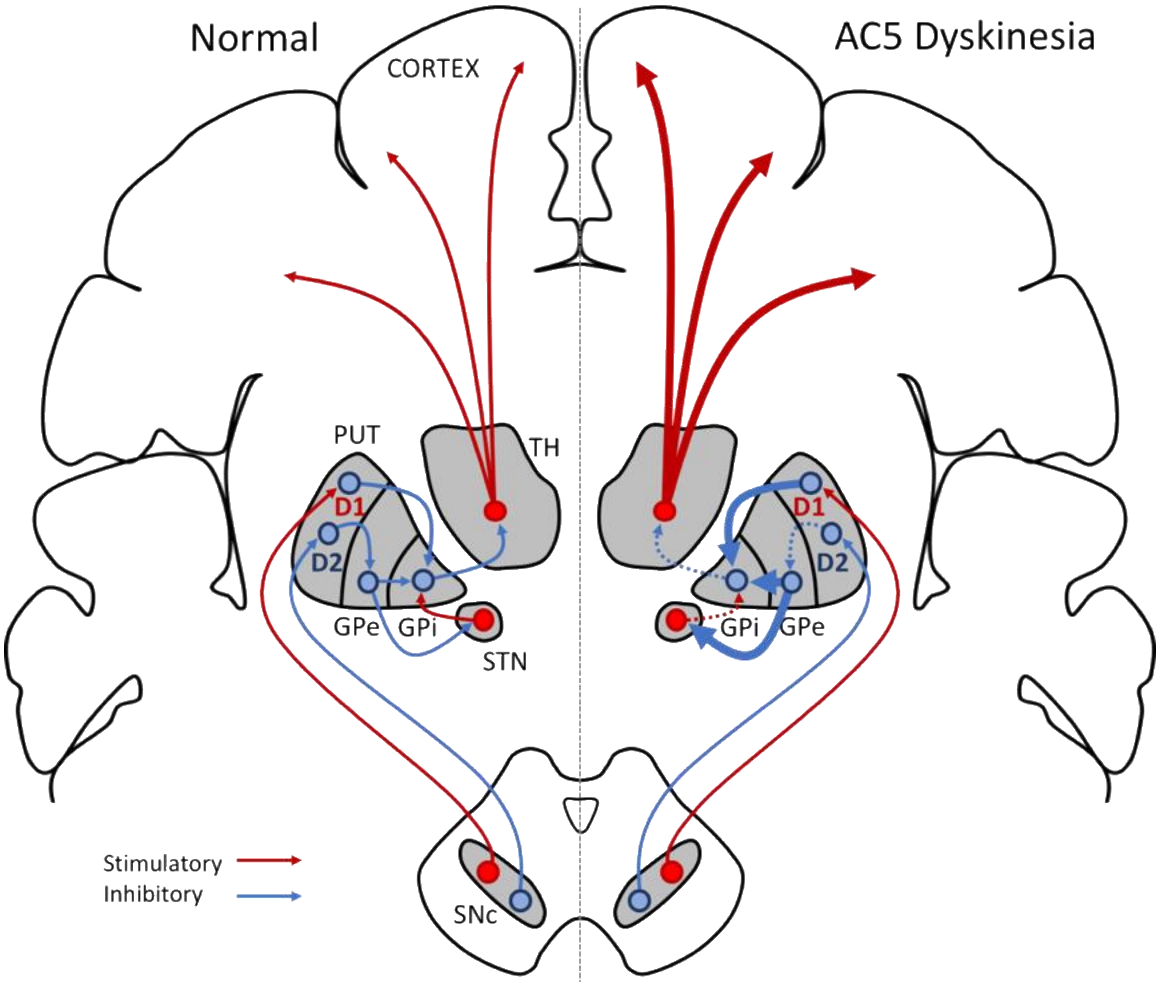

Figure 3.7: Pathway model of AC5 mutant effects.

A schematic model of normal basal ganglia signaling (left) versus that possibly observed in AC5-associated dyskinesia (right). As previously described, AC5 is the principal adenylyl cyclase isoform expressed in the striatum, and preferentially couples to both D_1 and D_2 dopamine receptors. Our results suggest that the enhanced activity observed following $G\alpha_s$-mediated stimulation of AC5 gain-of-function mutations may lead to increased direct pathway activity. Furthermore, the observation that AC5 gain-of-function mutants are weakly inhibited by D_2 receptor activation suggest that decreased activity of the indirect pathway may be observed. Together, this loss of cooperative activity in both direct and indirect pathways may possibly result in the unsynchronized enhancement of movement initiation observed in AC5-associated dyskinesia.

CHAPTER 4. IDENTIFICATION OF ISOFORM SELECTIVE SMALL MOLECULE MODULATORS OF ADENYLYL CYCLASE TYPE 8

4.1 Abstract

Adenylyl cyclase (AC) isoforms are critical regulators of diverse physiological processes. Recent genetic studies have implicated adenylyl cyclase type 8 (AC8) as a common factor in signaling pathways that mediate long-term anxiety and ethanol consumption. Because these disorders are often co-occuring, the identification of a common player offers a novel method of studying and potentially treating these disorders. However further advancements in characterizing AC8 specific signaling pathways has been stalled by a lack of potent and isoform-selective small molecule modulators. Though structurally diverse AC inhibitors have been developed, their practical use is limited by poor membrane permeability and isoform selectivity. Thus, the development and functional characterization of an AC8 selective small molecule inhibitor would accelerate the study of isoform specific neuronal signaling pathways, and have therapeutic potential in the treatment of comorbid excessive alcohol consumption and stress-induced anxiety. The present report describes the development and implementation of a high-throughput screen and validation paradigm of small molecules for the discovery of AC8 selective inhibitors. Multiple collections central nervous system targeted small molecules were screened for inhibitors of AC8 activity using Ca^{2+} stimulated cAMP as a functional assessment. Active compounds were subsequently counter-screened against the closely related isoform AC1 to remove non-selective molecules. Compounds were subsequently validated in intact cell functional assays, and mechanism of inhibition probed using enriched membrane fractions and purified protein. The screening effort identified two lead compounds that demonstrate enhanced efficacy and selectivity over AC1 compared to currently available adenylyl cyclase inhibitors.

4.2 Introduction

Anxiety is a part of life for most people, helping us to adapt and overcome acutely stressful situations. However, for some anxiety is characterized by intense bursts or prolonged periods of enhanced stress that dramatically impact their daily life. Increasingly, the use of alcohol to decrease anxiety is a strategy employed to self-medicate, as evident by the growing comorbidity of anxiety

and alcohol abuse disorders (Gimeno et al., 2017; J. P. Smith & Book, 2010; J. P. Smith & Randall, 2012). Research has demonstrated that excessive alcohol consumption promotes changes in neuronal NMDA receptor-mediated Ca^{2+} signaling, which result in significantly increased susceptibility to anxiety (Holmes et al., 2012; H. Wang et al., 2003). Furthermore, multiple neurobiological and genetic studies have identified the Ca^{2+}-stimulated adenylyl cyclase type 8 (AC8) as a critical regulator of both prolonged anxiety and neuronal ethanol sensitivity (Bernabucci & Zhuo, 2016; Maas et al., 2005). Despite the strong evidence implicating AC8 in these pathways, a scarcity of isoform-selective small-molecule modulators has hampered the study of adenylyl cyclase (AC) isoforms as biological and therapeutic targets (Brand et al., 2013; Dessauer et al., 2017; Seifert & Beste, 2012).

Adenylyl cyclases are key intersections for the integration of diverse signaling events. Stimulation of ACs increases the production of the second messenger cyclic AMP (cAMP), subsequently promoting the activation of downstream targets such as PKA, CREB, and EPAC (Dessauer et al., 2017). The spatiotemporal signaling of each AC isoform can be uniquely regulated by heterotrimeric G proteins, Ca^{2+}, protein kinases, and post-translational modifications (Dessauer et al., 2017; Ostrom et al., 2002; Sadana & Dessauer, 2009). Group 1 ACs, represented by AC1, AC3, and AC8, are unique and characteristically stimulated by calmodulin (CaM) in a Ca^{2+}-dependent manner. Importantly, increased AC3 activity is only observed during co-stimulation by $G\alpha_{s,}$ whereas AC1 and AC8 can be stimulated by Ca^{2+}/CaM even in the absence of $G\alpha_s$ activity (Defer et al., 2000; Dessauer et al., 2017; Willoughby & Cooper, 2007). Both AC1 and AC8 are highly expressed in the central nervous system, with overlapping expression patterns observed within the hippocampus (Conti et al., 2007; Sanabra & Mengod, 2011). Importantly, these two AC isoforms have been implicated in both Ca^{2+} dependent and independent mechanisms of long-term potentiation (LTP) and long-term memory (LTM) (Villacres, Wong, Chavkin, & Storm, 1998; H. Wang et al., 2003; H. Wang & Zhang, 2012).

The development of mice genetically deficient in AC1 ($AC1^{-/-}$), AC8 ($AC8^{-/-}$), or double knockout (DKO) allowed for the identification and characterization and behaviors unique to each isoform (Ferguson & Storm, 2004; Krishnan et al., 2008; H. Wang et al., 2003). AC1 and AC8 were both shown to be essential for hippocampus-dependent LTP and LTM (Ferguson & Storm, 2004; H. Wang et al., 2003). However genetic deletion of AC8, but not AC1, eliminated the long-lasting anxiety induced by repeated elevated plus maze exposure (Bernabucci & Zhuo, 2016).

These results suggest that Ca^{2+}/CaM stimulated AC8 may specifically modulate pathways required for prolonged anxiety. Interestingly $AC8^{-/-}$ mice, but not $AC1^{-/-}$ animals, exhibit significant decreases in voluntary ethanol consumption compared to wild-type mice (Maas et al., 2005). This separation of voluntary ethanol consumption between genotypes suggests that AC8 may be important in determining the rewarding effects of ethanol or drinking behaviors. Together, these observations indicate that the regulation of AC8 activity may be a common factor in both alcohol consumption and stress-induced anxiety, further emphasizing the role of common signaling pathways in comorbid disorders.

Research has demonstrated that the distinct expression patterns and regulatory properties of individual AC isoforms likely underlie specific physiological and pathophysiological conditions. As such, there has been strong interest in identification of isoform selective, small molecule AC modulators. These compounds could be used to further investigate ACs as biological and therapeutic targets, as there are currently no AC inhibitors in use clinically. While structurally diverse AC inhibitors have been developed, a lack of isoform selectivity and membrane permeability obstruct their further use as chemical probes. Thus, the development and functional characterization of an AC8 selective small molecule inhibitor would accelerate the study of isoform specific neuronal signaling pathways and have therapeutic potential in the treatment of comorbid excessive alcohol consumption and stress-induced anxiety. While Ca^{2+}/CaM robustly stimulates both AC1 and AC8, structural analyses have identified non-conserved regions of the cytosolic domains. Both the C1 and C2 domains share 46% identity between isoforms, highlighting the fact that unique structural features between isoforms offer possible targets to elicit isoform specificity. In this study we describe a unique high-throughput screening methodology used to identify the first isoform selective AC8 small molecule inhibitor.

4.3 Materials and Methods

4.3.1 General Materials:

The TimTec, OTAVA, Enamine, and Chemdiv CNS collections were provided by the Purdue Institute for Drug Discovery. A23187, 3-isobutyl-1-methylxanthine (IBMX), G418, Puromycin were purchased from Sigma-Aldrich (St. Louis, MO). SQ 22,536 was purchased from Tocris

Bioscience (Ellisville, MO). Dulbecco's modified Eagle's medium (DMEM), Lipofectamine 2000, and OptiMEM were purchased from Life Technologies (Grand Island, NY).

4.3.2 Stable Cell Line Generation and Cell Culture:

Human embryonic kidney (HEK) 293 cells and HEK AC3/AC6Δ cells were cultured in Dulbecco's modified Eagle's medium (DMEM) supplemented with 5% bovine calf serum, 5% fetal clone I, and 1% 100x antibiotic-antimycotic solution (Hyclone (Logan, UT). Cells were maintained in a humidified incubator at 37°C and 5% CO_2. HEK293 clonal stable cell lines were created by transfecting cells with pcDNA3.1(+) encoding human AC1, AC2, AC5, or pReceiver encoding human AC8, using lipofectamine 2000 according to the manufacturer's protocol. Stable cell clones were selected in media containing 600μg/ml G418 (AC1, AC2, AC8) or 4μg/ml puromycin (AC8). Stable plasmid expression was validated functionally by measuring cAMP accumulation in response to pharmacological stimulation by A23187 (AC1, AC8), phorbol 12-myristate 13-acetate (PMA), or forskolin (AC5). Pooled HEK AC3/AC6Δ cell lines were developed as described previously (Soto-Velasquez et al., 2018).

4.3.3 Adenylyl Cyclase Membrane Preparation:

HEK AC3/AC6Δ pooled cell lines were grown in selection media as described above. Media was aspirated from plates, then cells briefly washed with ice-cold phosphate buffered saline before adding ice-cold lysis buffer (1mM HEPES, 2mM EDTA, pH 7.4) and incubated on ice for 15 minutes. Cells were scraped from plates using sterile scrapers, collected, and triturated by pipetting. Cells were centrifuged at 30,000xg for 20 minutes at 4°C. The supernatant was discarded, and the remaining pellet re-suspended in receptor binding buffer (4mM $MgCl_2$, 50mM Tris, pH 7.4). The cell membrane suspension was homogenized using a Kinematica homogenizer (Kinematica, Switzerland) and aliquotted into 1mL fractions. The aliquots were centrifuged at 12,000xg for 10 minutes at 4°C, the supernatant aspirated, and the remaining membrane pellet frozen at -80°C until use.

4.3.4 Adenylyl Cyclase Membrane Assay:

Briefly, adenylyl cyclase membrane aliquots were thawed on ice before re-suspending in membrane buffer (33mM HEPES, 0.5mM EGTA, 0.1% Tween20, pH 7.4). Protein concentration was determined by BCA assay, before diluting each sample to appropriate concentration. Diluted

membranes were plated into white, flat bottom, tissue culture-treated 384-well plate (PerkinElmer, Shelton, CT) at 10µl/well and briefly centrifuged to settle liquid. Compound dilutions were made in membrane buffer, then 5µl/well added to appropriate wells. Compounds were pre-incubated for 30 minutes before adding 5µl/well of forskolin diluted in stimulation buffer (33mM HEPES, pH 7.4, 10mM $MgCl_2$, 1mM ATP, 4µM GTPγS, 0.1% Tween20, 2mM IBMX). The plate was then briefly centrifuged and incubated at room temperature for 1 hour before the addition of Cisbio HTRF cAMP detection reagents and cAMP measurement as described further below.

4.3.5 Cisbio HTRF cAMP Assay:

Cellular and membrane cAMP levels were measured using the Cisbio HTRF cAMP dynamic 2 assay kit according to the manufacturer's instructions. Cells in culture had their media aspirated, then washed with warm PBS, before being dissociated with non-enzymatic cell dissociation buffer (Gibco, Grand Island, NY). Cell suspensions were centrifuged at 500xg for 5 minutes, supernatant aspirated, and cell pellets re-suspended in warm OptiMEM buffer. Cells were diluted as indicated, and 10µl/well plated into a white, flat bottom, tissue culture-treated 384 well plate (PerkinElmer, Shelton, CT). Assay plates containing live cells were briefly centrifuged at 100xg for 30 seconds and incubated in a humidified incubator at 37 °C and 5% CO_2 for 1 hour before receiving further treatment. Cells were then treated with indicated ligand diluted in OptiMEM for 30 minutes at room temperature. Cells were stimulated with 5µl/well of either forskolin or A23187 diluted in OptiMEM containing 2mM IBMX for 1 hour at room temperature. The stimulation was terminated by sequential addition of 10µl/well cAMP-d2 and 10µl/well anti-cAMP cryptate conjugate. Time-resolved fluorescence energy transfer (TR-FRET) was measured with an integration time of 300µs and lag time of 100µs using a Synergy Neo 2 (BioTek, Winooski, VT) fluorescence plate reader. Assay plates were excited at 330nm wavelength, and fluorescent emission at 620nm and 665nm collected. Ratiometric analyses were performed with GraphPad Prism (GraphPad Software, La Jolla, CA) by dividing the 665nm emission by 620nm emission to interpolate cAMP concentrations from a standard curve.

4.3.6 Screening Conditions:

Cryopreserved HEK-hAC1 or HEK-hAC8 cells were seeded into 384-well plate at 15µl/well using a Multidrop (ThermoFisher, Waltham, MA) reagent dispenser. After 1 hour incubation at room temperature, 80nl of test compounds were added to the cells with an Echo liquid handling system (Lancyte, San Jose, CA) and allowed to incubate at room temperature for at least 30 minutes. Cells were then stimulated with 5µl A23187 diluted in warm OptiMEM containing 2mM IBMX, followed by incubation at room temperature for 1 hour. The stimulation was terminated by sequential addition of 10µl/well cAMP-d2 and 10µl/well anti-cAMP cryptate conjugate using a MultiFlo (BioTek, Winooski, VT) bulk reagent dispenser. Analyses was conducted as described above.

4.3.7 Computational Profiling of Hit Molecules:

Chemical structures were managed and analyzed using Canvas (Version 2.8.014, Schödinger, LLC). Structures were given hashed fingerprints using MOLPRINT2D fingerprinting method and clustered hierarchically using the Tanimoto similarity metric to determine the similarity/distance matrix. Clusters were then linked using the average distance between all inter-cluster pairs. Molecules containing known PAINs moieties were identified and filtered using the FAF-Drugs4 online service (Lagorce, Sperandio, Baell, Miteva, & Villoutreix, 2015).

4.3.8 Adenylyl Cyclase Catalytic Domain Purification and Assay:

Catalytic domains of human AC8 were expressed as N-terminal TEV-cleavable 6xHis-MBP fusion proteins in pET His6 MBP TEV LIC vector (Addgene #29656), which as a kind gift from Scott Gradia. C1a domain construct contained residues L375 to S593, and C2 construct contained residues Q917 to N1215. Rosetta2 (DE3) *E. coli* were transformed and single colonies picked and grown at 37 °C in TB until OD_{600} reached 1.0-1.5. At this time temperature was lowered to 18 °C and protein expression was induced using 200 µM IPTG for 16 hours. Cultures were pelleted and resuspended in 25 mM HEPES pH 8.0, 500 mM NaCl, 2 mM $MgCl_2$, 2 mM β-ME, 10 mM imidazole supplemented with protease inhibitors and frozen in liquid nitrogen. Cells were enzymatically lysed with lysozyme and DnaseI and supernatant from centrifugation at 30,000 *g* for 1 hr at 4 °C was collected. Supernatant was subjected to immobilized metal and amylose affinity chromatography to obtain pure fusion protein. 6xHis-MBP tag was cleaved using TEV

protease, and untagged catalytic domain was further purified using anion exchange chromatography. To asses inhibition by screen hits, 14 nM AC8-C2 domain was incubated with approximately five-fold molar excess AC8-C1 in 20 mM HEPES pH 8, 10 mM $MgCl_2$ in the presence of 50 μM FSK and indicated concentration of compound at room temperature for 30 min in a volume to 15 μL in white 384-well plate. Catalytic activity was then stimulated by addition of 5 μL ATP to reach a final concentration of 1 mM and reaction allowed to proceed at room temperature for 45 min, after which, Cisbio reagents were used to quench reaction and cAMP quantified as described above.

4.3.9 Peptide Inhibition Assay:

CaM/AC peptide fluorescence polarization assays were performed as described previously (Hayes et al., 2018). Briefly, 20 microliters per well of 300 nM Cy5 labelled AC8 or AC1 peptides (100 nM final) in assay buffer (20 mM HEPES, pH 7.4, 100 mM KCl, 50 μM $CaCl_2$) was added to 384-well, black polystyrene, nonbinding plates (Corning) with 20 microliters per well of indicated compound at 3X concentration and incubated for 0.5 hr at room temperature in the dark. Finally 20 microliters of 3× concentrated GST-CaM was added to each well and incubated for 2 hr in the dark, after which time, FP was read using a BioTek Synergy 2 (Winooski, VT) with 620/40 nm and 680/30 nm filters for excitation and emission, respectively, and a 660 nm dichroic mirror with polarizers. Polarization (in mP) was calculated as follows: $P = 1000 \times (I_{\text{parallel}} - I_{\text{perpendicular}}) / (I_{\text{parallel}} + I_{\text{perpendicular}})$ where P represents polarization and I represent fluorescence intensity in indicated polarity.

4.4 Results

The lack of AC8 isoform selective, small molecule inhibitors has effectively delayed further study of the intracellular signaling pathways that may mediate long-term anxiety and ethanol consumption. Multiple published reports on $AC8^{-/-}$ and $AC1^{-/-}$ mice have suggested that AC8 specific signaling events are important to the etiology of these two co-morbid disorders. Therefore, the goal for this study was the development of a high-throughput screening methodology to identify and validate novel inhibitors of AC8 activity in living cells. To accomplish this goal, we developed and optimized assay parameters to screen and counter-screen small molecule libraries for the inhibition of Ca^{2+}-stimulated AC8 activity in a 384-well format.

4.4.1 Development and Optimization of Screening Conditions

Because HEK293 cells endogenously express several AC isoforms, it is essential to identify conditions that selective stimulate the heterologously expressed isoform of interest, AC8. Both AC1 and AC8 are unique in that they are robustly stimulated by Ca^{2+} bound calmodulin, with AC1 being slightly more sensitive to Ca^{2+} than AC8 (Villacres et al., 1995). Therefore, to study the activity of these two isoforms, HEK293 cells stably expressing human AC8 or AC1 were developed and assessed for cAMP accumulation in response to Ca^{2+}-mediated stimulation. For this screen, the Ca^{2+} specific ionophore A23187 was used for the stimulation of AC8 and AC1. A23187 treatment provided a concentration dependent increase in cAMP accumulation (Fig. 4.1A). AC8 was half-maximally stimulated at 2.7 ± 0.2 μM. We selected 3μM A23187 to stimulate AC8 and AC1 for the screen and counter-screen conditions, respectively. This concentration provided a signal window of 25-fold above basal for AC8, and 50-fold for AC1. As positive control for the inhibition of AC8 activity, we used the AC1/AC8 non-selective inhibitor JK211, which was previously discovered in a screening campaign against A23187-stimulated AC1 activity. Treatment with JK211 inhibited A23187-stimulated activity of both AC8 (IC_{50} of 2.0 ± 0.6 μM) and AC1 (IC_{50} of 2.2 ± 0.8 μM) in a dose dependent manner (Fig. 4.1B). These results indicate that 30 μM JK211 is sufficient to completely inhibit activity of AC8 at 3μM A23187.

The robustness of our screening platform was assessed by Z' analysis, using 3μM A23187 as the maximal response and 3μM A23187 + 30μM JK211 as the minimum response. In an effort to continuously monitor the signal window, both maximum and minimum conditions were included as controls in each assay plate. Analysis of Z' for each of the assay plates demonstrated a rigorous standard, with an average Z' factor across all screened plates of 0.744 ± 0.005 (n=55) (Fig. 4.2A). These results confirm that our screening platform was above standards for compound library screening (J. H. Zhang, Chung, & Oldenburg, 1999). The compound library consisted of 17,280 diverse chemical structures from central nervous system targeted and focused libraries. The compounds which make up this library are targeted toward neuromodulator receptor groups and have been assessed for chemical features such as low polar surface area and low degree of possible hydrogen bond formation, consistent with being blood-brain barrier penetrant. Screening these collections at a final concentration of 20 μM against AC8 identified 144 compounds (0.8% of total compounds) that exhibited or greater than 80% inhibition. These 144 hit compounds were the

counter-screened against inhibition of AC1 activity. Of the initial 144 hits, 28 compounds inhibited less than 40% of 3μM A23187 stimulated AC1 activity. As outlined above (Fig. 4.2B), using ZINC the public access database and tool set, we filtered hit compounds for the removal of pan-assay interfering compounds (PAINS). Of the 28 AC8 selective hits identified, two were flagged and as having physiochemical features highly consistent with known assay interfering compounds and were not pursued in subsequent experiments. Similarly, the Aggregator Advisor tool created by the Shoichet group was employed to remove all known aggregating compounds (Irwin et al., 2015). The remaining 26 compounds were clustered by their structural features into nine groups.

4.4.2 Concentration Response of Screen Hits

In order to confirm hits and assess their potency, one representative compound from each of the nine structural groups was selected for validation. Concentration-response curves were generated for all nine compounds (Data not shown). Dose dependent inhibition of 3μM A23187-stimulated AC8 and AC1 activity was tested using each compound (Table 4.1). Interestingly, of the nine compounds tested only two demonstrated selectivity for AC8. Compound 1 inhibited AC8 with an IC_{50} of 5 μM (1-34.7, 95%CI) at AC8 and 439 μM (95%CI NC) at AC1 (Fig. 3A). Alternatively, Compound 2 inhibited AC8 with an IC_{50} of 9.2 μM (3.6-23.8, 95%CI) and 121 μM (95%CI NC) respectively (Fig. 3B).

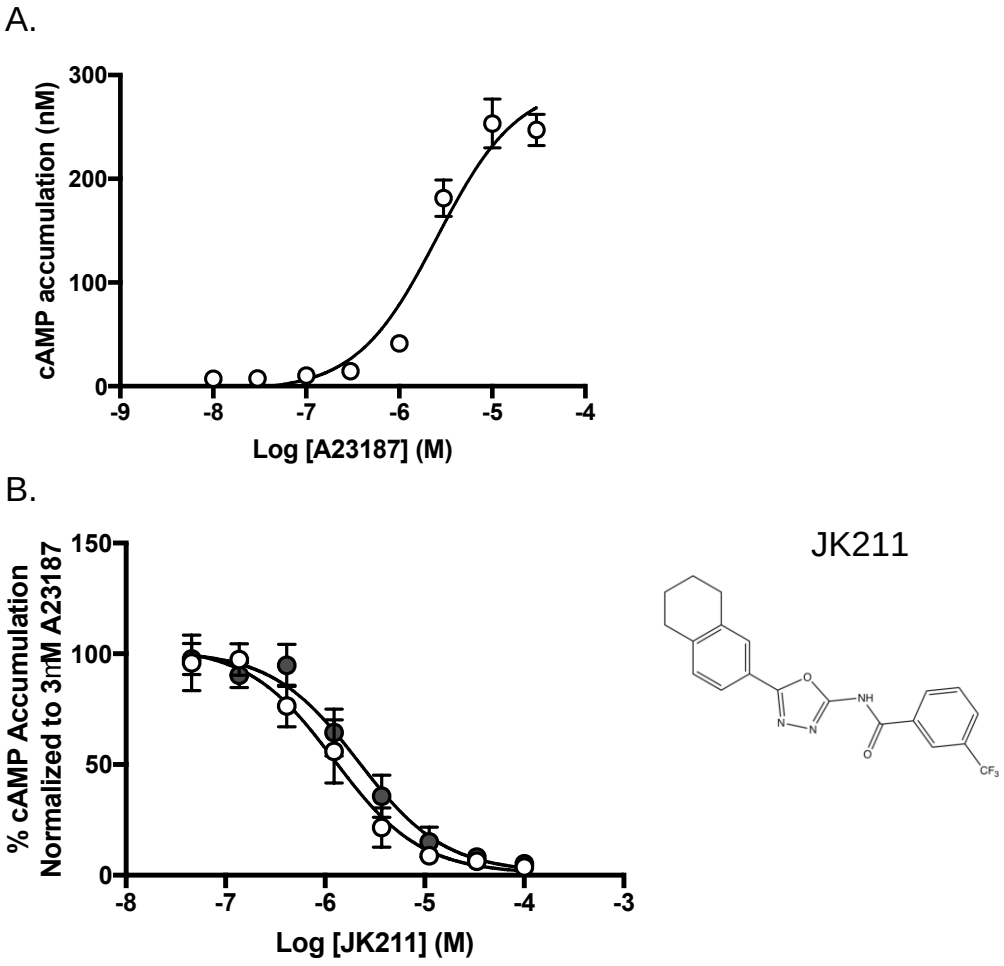

Figure 4.1: Development and optimization of screening controls.

Optimization of conditions for intact-cell high-throughput screening assay for the small molecule inhibitors of AC8. A concentration response curve of the Ca^{2+}ionophore A23187 to stimulate AC8 activity in HEK AC8 cells (A). The non AC1/AC8 selective inhibitor JK211 was used as a positive control for inhibition of 3μM A23187 stimulated activity (B). Data represent the mean ± SEM of three independent experiments.

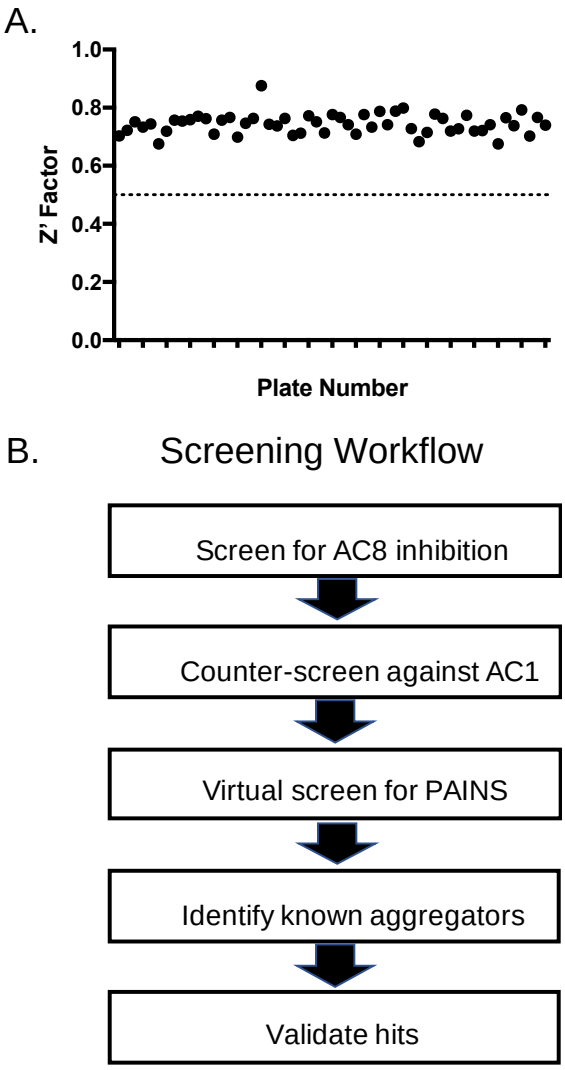

Figure 4.2: Evaluation of screening robustness and workflow.

Each screening plate included controls for A23187 stimulation and JK211 inhibition, which were used to track Z' analysis variability throughout the screening process (A). The AC8 screen was followed by counter-screening at AC1 further validation steps (B).

4.4.3 Activity at Representative AC Isoforms

Compounds **1** and **2** exhibited modest selectivity for AC8 over AC1 and were selected for further testing against representative isoforms of Group 2 and 3 cyclases, AC2 and AC5, respectively. The previously identified AC2 inhibitor 30 μM SKF83566 inhibited 60% of PMA stimulated AC2 activity (Fig. 4.4A) (Conley et al., 2013). Previously inhibitors of AC1 or AC1/AC8 such as ST034307 or JK211 have revealed potentiation of AC2 activity as an unwelcomed side effect of small molecule inhibitors (Fig 4.4A). Compounds **1** and **2** exhibited no significant inhibition or enhancement of AC2 activity (Fig. 4.4B). 100 μM SQ22536, which has known activity against AC5, inhibited 80% of forskolin stimulated AC5 activity (Fig. 4.4B). Again, **1** and **2** showed no significant inhibition (or enhancement) of AC5 activity (Fig. 4.4B). Additional experiments aimed at the

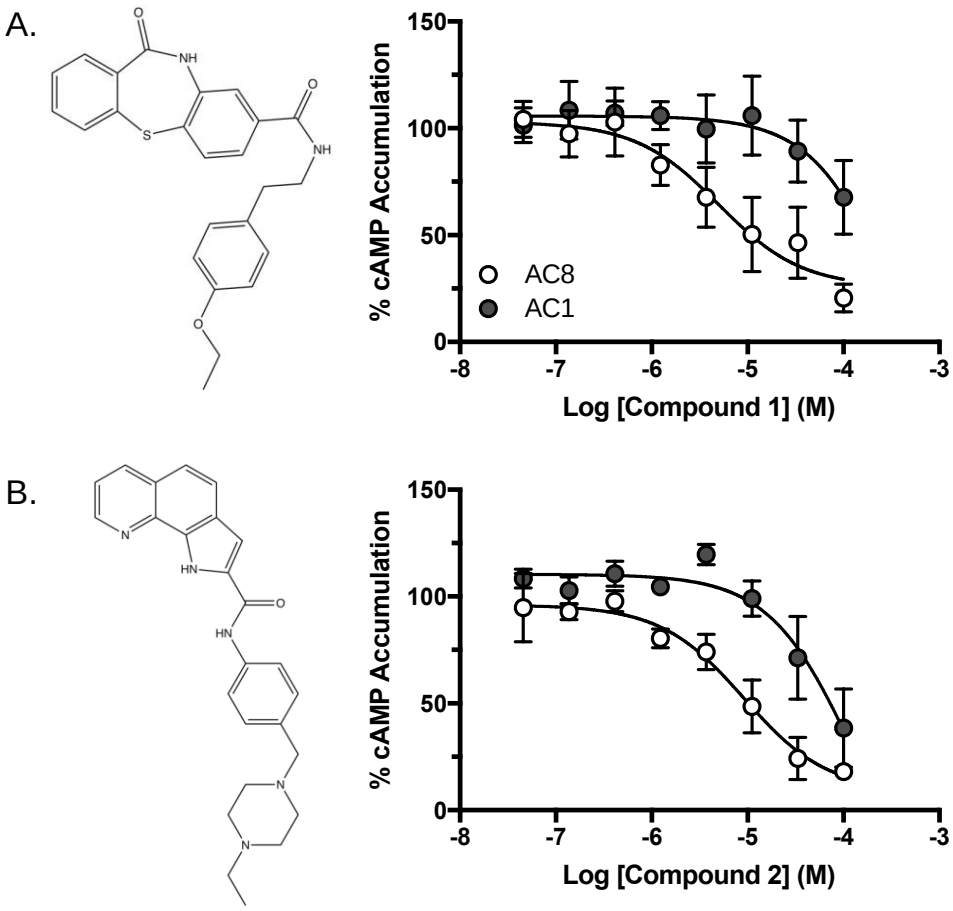

Figure 4.3: Concentration response analysis of hit compounds.

Dose response curves of Compound 1 (A), and Compound 2 (B), for inhibition of 3 μM A23187-mediated stimulation in intact HEK AC8 cells. Data represent the mean ± SEM of three independent experiments.

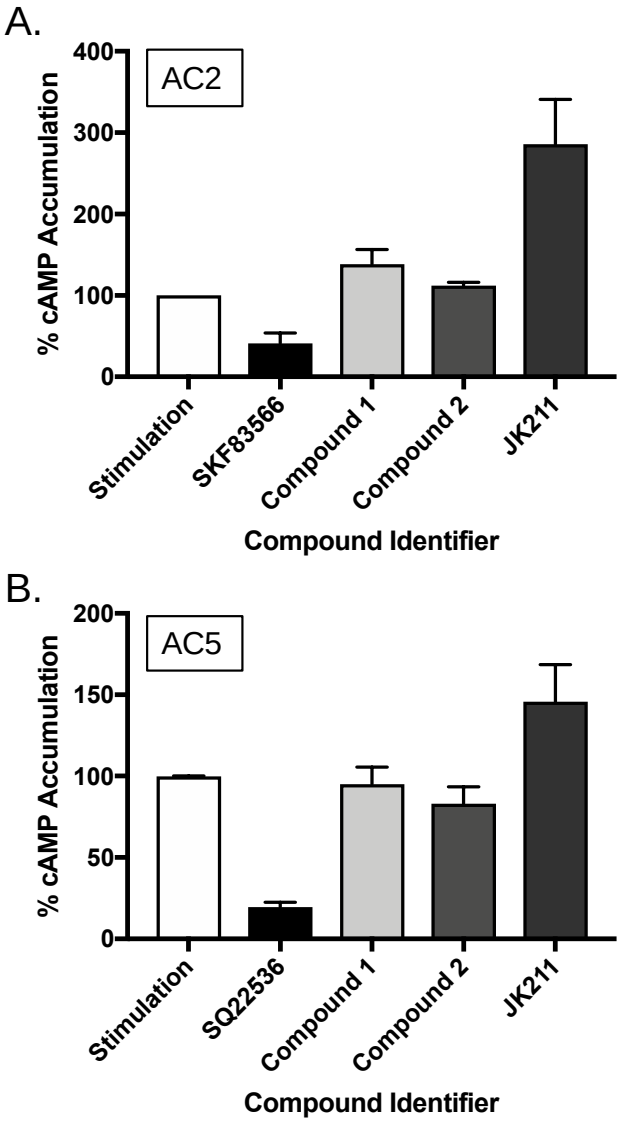

Figure 4.4: Hit compound activity at representative AC isoforms.

Compounds 1 and 2 were tested at 30 μM for inhibition of PMA stimulated cAMP in HEK AC2 cells (A). The existing AC2 inhibitor SKF83566 was used as a positive control for inhibition, and JK211 used as a positive control for potentiation of activity. Compounds 1 and 2 were tested at 30 μM for inhibition of FSK stimulated cAMP in HEK AC5 cells (B). The existing AC5 inhibitor SQ 22,536 was used as a positive control for inhibition, and JK211 used as a positive control for potentiation of activity. Data represent the mean ± SEM of three independent experiments.

assessment of cell toxicity revealed that pretreatment with **1** and **2** did not significantly increase cell death (Data not shown).

4.4.4 Compounds Do Not Disrupt CaM Interaction with AC-derived Peptides

Our screening strategy used A23187 to stimulate AC8 via Ca^{2+}-dependent CaM activation. Therefore, it is possible that the compounds identified may exert their cAMP-attenuating effects through the inhibition of CaM interaction with AC8. In an effort to determine the mechanism of action of compounds **1** and **2**, a previously described fluorescence polarization assay utilizing Cy5-labeled peptides derived from the N-terminus and C2b regions of AC8, as well as the C1b region of AC1 was used (Hayes et al., 2018). Peptides from these regions were selected as previous work demonstrated their involvement in mediating AC/CaM interactions. As expected, increasing concentrations of the CaM antagonist calmidazolium (CDZ) produced dose-dependent decreases in fluorescence polarization for each AC region, with IC_{50} values of 2.8 ± 0.1 μM, 5.6 ± 0.6 μM, 15 ± 3.5 μM for AC8 N-terminus, AC8 C2b, and AC1 C1b, respectively (Fig. 4.5 A-C). At 30 μM, the highest concentration tested, compounds **1** and **2** demonstrated no disruption of the CaM interaction with the AC8 N-terminus, AC8 C2b, or AC1 C1b peptides. This data implies that compounds **1** and **2** do not inhibit Ca^{2+}-stimulated AC8 activity by inhibiting CaM interaction with either the N-terminus or C2b regions.

4.4.5 Regulation of FSK-Stimulated cAMP Accumulation

The lack of inhibition of AC peptide/CaM interaction by **1** and **2** may suggest their AC8 inhibitory activity occurs via a Ca^{2+}/CaM-independent mechanism. Therefore, we examined the possibility of direct inhibition of AC8 activity by these compounds. In addition to Ca^{2+}/CaM-mediated activation, AC8 can be stimulated by the small molecule AC activator forskolin (FSK), which promotes the interaction of the C1a domain with the C2a domain enhancing AC8 activity (Dessauer et al., 1998; Tesmer & Sprang, 1998). To study the effects of FSK-mediated stimulation of AC8, we took advantage of a newly developed HEK cell line that used CRISPR-Cas9 to eliminate AC3 and AC6, resulting in a cell line with 95% reduced cAMP formation by endogenous ACs in response to FSK (Brand et al., 2013). Following overexpression of AC1 or AC8 in these cells, membrane fractions were prepared, and FSK-mediated stimulation was measured in the

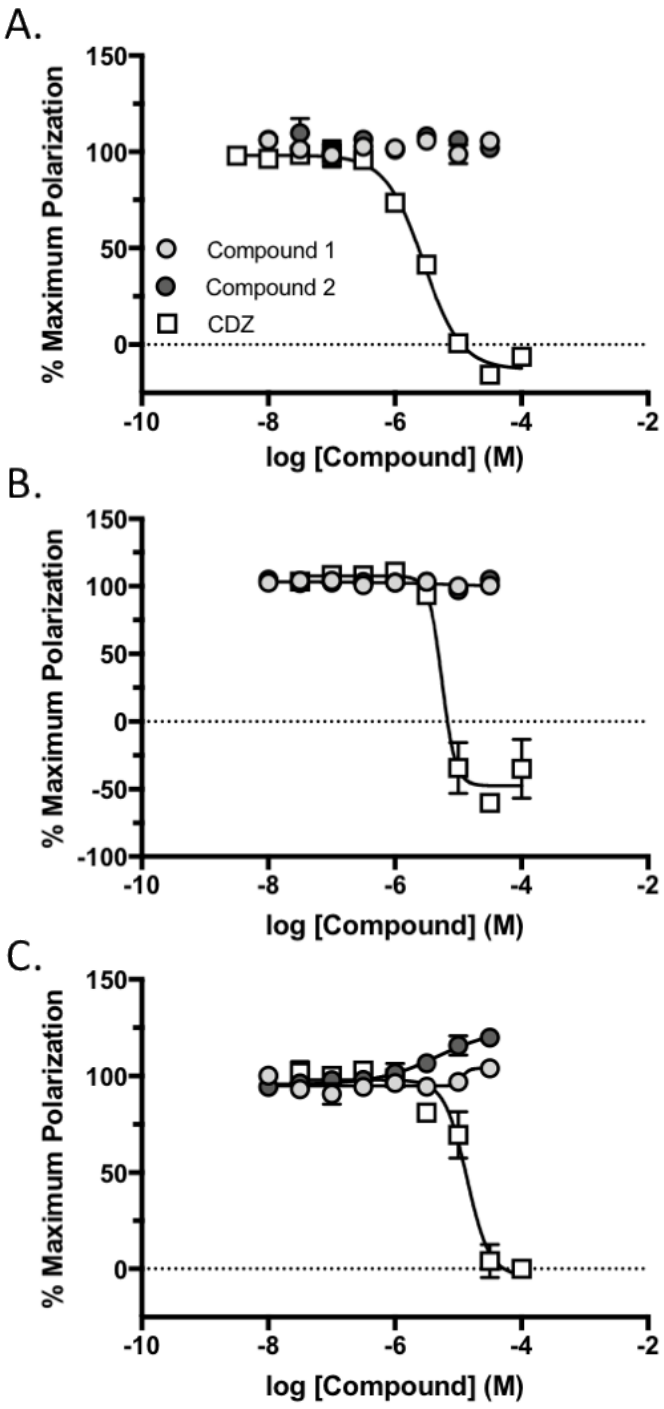

Figure 4.5: Hit Compounds do not disrupt CaM Interaction with AC-derived Peptides.

Compounds 1 and 2 were tested for inhibition of purified CaM with peptides derived from the N-terminus of AC8 (A), the C2b cytosolic region of AC8 (B), and the C1b cytosolic region of AC1 (C). Calmidazolium (CDZ) served as positive control for inhibition of CaM binding. Data represent mean ± SEM from three independent experiments.

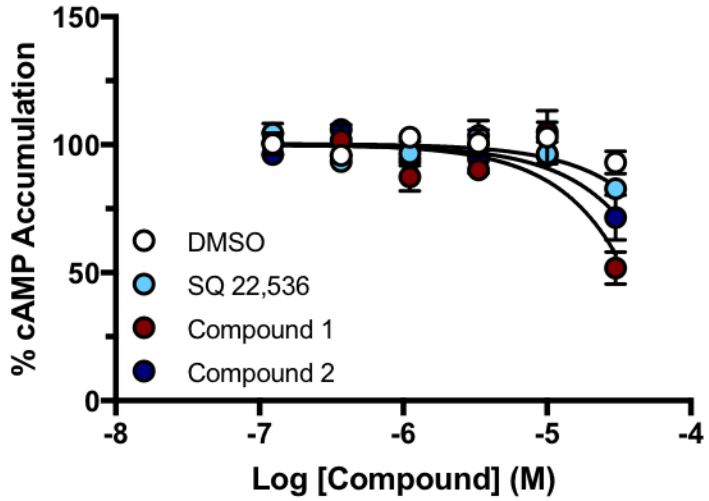

Figure 4.6: Compound concentration response inhibition of forskolin-mediated stimulation.

Concentration response curves from membranes preparations of HEK AC3/AC6Δ cells expressing AC8 at 250 μg/ml were stimulated using 10 μM FSK and cAMP measured using CisBio HTRF. Data were normalized to 10 μM FSK activity where basal activity is 0% and maximal observed activity is 100%. Data represent mean ± SEM from three individual experiments, each performed with duplicate wells.

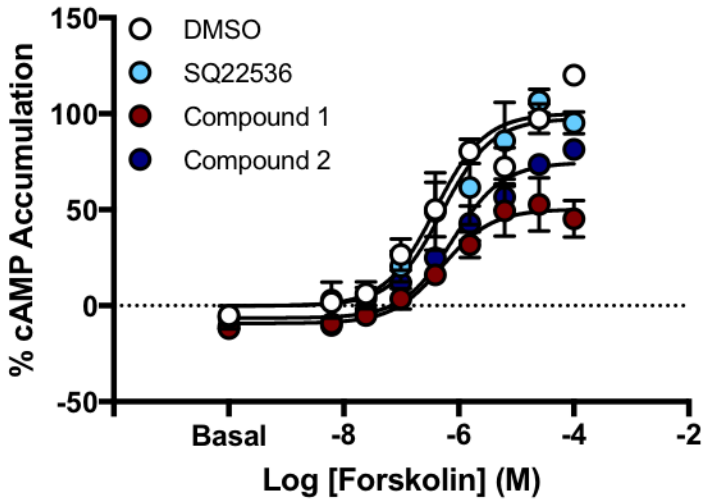

Figure 4.7: Forskolin dose response in the presence inhibitor.

Forskolin concentration response curves in the presence of 30 μM indicated compound from membranes preparations of HEK AC3/AC6Δ cells expressing AC8 at 250 μg/ml and cAMP measured using CisBio HTRF. Data were normalized to 100 μM FSK activity for DMSO where basal activity is 0% and maximal observed activity is 100%. Data represent mean ± SEM from three individual experiments, each performed with duplicate wells.

presence of compounds **1** and **2**. Surprisingly, compounds **1** and **2** showed limited inhibition that was failed to significantly inhibit AC8 or AC1 activity stimulated in response to10 μM FSK (Fig. 4.6). This result led us to believe that neither compound 1 nor 2, exert their inhibitory activity through binding to the conserved FSK binding site.

Another site on ACs that can be occupied by small molecule inhibitors is known as the P-site which is also the ATP-binding site. P-site inhibitors are a class of uncompetitive AC inhibitor that bind the transition state of the enzyme, preventing the further synthesis of cAMP (Dessauer et al., 2017). This class of inhibitors are dependent upon activity, as the enzyme activity increases, more transition state sites are available for inhibition. We therefore assessed the ability of compounds **1** and **2** to inhibit FSK stimulated AC8 activity in an activity-dependent manner (Fig. 4.7). Unfortunately, the available P-site inhibitors have little activity at AC8 (Brand et al., 2013). We confirmed this result using a representative P-site inhibitor, SQ 22,536 revealing less than 10% inhibition at 100 μM FSK. Compound 2 also appeared more efficacious than SQ22,536, inhibiting 25% activity at 100 μM FSK. Compound 1 demonstrated more significant inhibition of AC8, reducing activity to 50% at 100 μM FSK.

4.5 Discussion

While several studies have implicated AC8 in physiological models of long-term anxiety and ethanol consumption, there have been a lack of tools available to specifically study AC8 signaling pathways. The present study developed and implemented a high-throughput screen for AC8 selective small molecule inhibitors and identified two promising lead compounds. These exciting findings suggest that Compounds 1 and 2 are more efficacious and isoform selective than existing AC8 small molecule inhibitors, do not potentiate or inhibit representative AC isoforms or promote cell death. The use of purified CaM and AC peptides provided evidence which support Compounds 1 and 2 do not interfere with Ca2+/CaM binding of AC8 or AC1. The ability of Compounds 1 and 2 to inhibit FSK stimulated AC8 activity in an activity-dependent manner is consistent with the actions of known P-site inhibitors, and supports their action at the substrate binding site. We are confident that further SAR and focused compound development will enhance the isoform selective properties and further characterize the exact mechanism of action of these inhibitors.

Table 4.1: Summary of hit compounds validated in intact cells.

Concentration response curves of the nine hit compounds were tested up to 100 μM for inhibition of 3μM A23187-mediated AC8 and AC1 stimulation. Data are reported as Mean and 95% CI from at least three independent experiments.
*NC = not calculated.

Compound	AC8		AC1	
	IC_{50} (μM)	95% CI	IC_{50} (μM)	95% CI
1	5.0	1.0-34.7	> 100	NC
2	9.2	3.6-23.8	> 100	NC
3	> 100	NC	> 100	NC
4	3.8	0.6-32.1	41.4	NC
5	5.2	0.7-83	12.6	1.7-127.5
6	1.6	0.8-3.4	6.9	2.8-18.8
7	13.4	1.9-119.3	6.8	0.9-67.8
8	90.9	35.3-850	> 100	NC
9	6.7	3.8-12	43.3	21.8-103.5
JK211	1.2	0.6-2.4	2.2	1.2-3.9

CHAPTER 5. CONCLUSIONS AND FUTURE DIRECTIONS

The research presented in this dissertation addressed multiple aspects of adenylyl cyclase signaling from three main aims; First, to develop and implement a high-throughput screening methodology of a novel BiFC-tagged cDNA library to investigate changes in AC5-protein interactions that occur following prolonged $G\alpha_{i/o}$-mediated inhibition. Secondly, to characterize a subset of AC5 gain-of-function mutations that have been recently identified in patients exhibiting symptoms of familial dyskinesia with facial myokymia (FDFM). Finally, to develop and conduct a high-throughput screening paradigm for the discovery of isoform-selective small molecule inhibitors of AC8. The conclusions and avenues for future research are discussed below.

The unusual compensatory phenomenon of heterologous sensitization was first identified in the late 1970's at the National Institutes of Health (NIH). There, Dr. Marshall Nirenberg's laboratory was studying the neuronal effects of opiates and identified that a neuroblastoma-glioma hybrid cell line (NG108-15) abundantly expressed opiate receptors (Xia et al., 2011). They noted that while acute morphine treatment reduced adenylyl cyclase activity, chronic exposure to morphine resulted in a paradoxical enhancement of adenylyl cyclase activity and cAMP production (Xia et al., 2011). This phenomenon of enhanced activity following prolonged $G\alpha_{i/o}$-mediated inhibition is known as heterologous sensitization, and it has been implicated in numerous pathophysiological conditions including drug-induced withdrawal symptoms, epilepsy, and levodopa-induced dyskinesia in Parkinson's patients (Watts, 2002; Watts & Neve, 1996, 2005). Despite efforts to further understand the root cause of the sensitization response, the underlying mechanisms remain poorly understood nearly 50 years after its discovery (Brust et al., 2015). Previous research examining heterologous sensitization has predominately focused on the roles of heterotrimeric G proteins (e.g, $G\alpha_s$, $G\alpha_{i/o}$, $G\beta\gamma$ subunits), activators and regulators of G protein signaling (AGS and RGS proteins), as well as protein kinases downstream of $G\alpha_{i/o}$-coupled receptor activation (Avidor-Reiss et al., 1996; Brust et al., 2015; Cumbay & Watts, 2001; Iwami et al., 1995; Watts, 2002; Watts & Neve, 1996). However, it has become increasingly evident that the localization of adenylyl cyclases within macromolecular signaling complexes exposes them to diverse and condition-dependent protein interactions (Brust et al., 2015; Dessauer et al., 2017). Furthermore, research has explicitly shown that protein-cyclase interactions can directly modulate adenylyl cyclase activity (Dessauer et al., 2017; Efendiev et al., 2010). We therefore developed an

unbiased screening approach to investigate the role of protein-cyclase interactions in the development and expression of D_2-mediated heterologous sensitization.

Through the implementation of a novel screening methodology presented in Chapter 2, we successfully screened a unique BiFC-tagged cDNA library for interaction with an AC5 BiFC construct (i.e VN-AC5) under vehicle and chronic quinpirole pretreatment conditions. Prolonged $G\alpha_{i/o}$-mediated inhibition is a required step in the development of heterologous sensitization, and extended activation of the D_2 dopamine receptor with quinpirole has been previously shown to robustly sensitize AC5 (Watts & Neve, 1996, 2005; Watts et al., 2001). Of the 213 genes that had been identified by Next Generation sequencing in at least two of the three independent FACS events, 106 were unique to vehicle treatment, 48 exclusive to quinpirole pretreatment, and 59 showed overlap between the two conditions. The successful identification of previously characterized AC5 interacting partners such as PKCζ, TSPAN7, and AKAP6 provides further evidence in support of the validity of this novel screening methodology (Beazely & Watts, 2006; Dessauer, 2009; X. Gao et al., 2007; Ji Kawabe et al., 1996; J. Kawabe et al., 1994). While multiple genes were found to play a role in acute and sensitization cAMP signaling through siRNA knockdown and validation, the more thorough characterization and validation of two unique AC5 interacting partners have subsequently opened up new avenues of study. The catalytic subunit of phosphatase PP2A (PPP2CB) appeared as an AC5 interacting partner exclusively under the vehicle treatment condition. Immunoprecipitation of PPP2CB following vehicle treatment resulted in a significant increase of adenylyl cyclase activity in the pull-down product. These results further emphasize a potential role for post-translational modifications, particularly regulation of the phosphorylation state, in adenylyl cyclase signaling. In contrast, the SNAP protein NSF-sensitive attachment factor alpha (NAPA) demonstrated association with AC5 only following prolonged D_2-mediated inhibition. While immunoprecipitation of NAPA under vehicle treatment conditions resulted in no significant enhancement of adenylyl cyclase activity in the pull-down product, an extended quinpirole pretreatment dramatically increased cAMP production in the pull-down product. These results suggest that cyclase trafficking or vesicular transport may influence cAMP signaling following chronic $G\alpha_{i/o}$-mediated inhibition. While we have presented evidence to strongly support the interaction of both PPP2CB and NAPA with AC5, or and AC5 associated protein complex under different treatment conditions, we still have no information on their specific

binding sites. Future studies should be devoted to further characterizing the specific regions involved in mediating AC5 interaction with both PPP2CB and NAPA.

AC5 has an unusually long α-helical N-terminal tail compared to other isoforms, increasing its ability to interact with other proteins (Brand et al., 2015; Dessauer et al., 2017). Indeed, several studies have previously demonstrated protein interaction with AC5 through the N-terminal region. Specifically, the N-terminal region of AC5 has been shown to mediate interaction with AKAP79, mAKAP, as well as Gβγ subunits (Brand et al., 2015; Dessauer, 2009; Efendiev et al., 2010). The likelihood of the N-terminus mediating interaction with PPP2CB and NAPA is further bolstered by the fact that the VN155 fragment was conjugated to the N-terminus for BiFC interaction screening. While multiple avenues could be explored to establish interaction, the most direct method would likely be to assess the immunoprecipitation of an affinity-tagged, purified AC5 N-terminal helix with both PPP2CB and NAPA. The initial use of purified protein excludes the possibility that any resulting interaction will be the result of a protein complex (i.e AKAPs). If interaction is confirmed in this method, subsequent alanine scanning, charge reversal, and phosphorylation site mutation could be employed to further identify specific patches or residues necessary for interaction. Once identified, mutations could be made to the full length AC5 and further characterized in cellular models following both vehicle and prolonged $G\alpha_{i/o}$-mediated inhibition. If the N-terminal tail fails to validate as an interacting partner, a similar workflow could be followed using the purification of C1a and C2a catalytic domains, as well as the C2b regulatory domain. Unfortunately, the catalytic domains are resistant to mutation, and demonstrate poor conservation of activity if critical residues are disrupted. Rather, isotopically labeled C1a and C2a catalytic domains could be used for biomolecular NMR to identify residues involved with mediating protein-protein interactions. While previous studies have shown that the N-terminal tail of AC8 scaffolds PP2A, further supporting that this region is necessary for the interaction between AC5 and PPP2CB, the catalytic subunit of PP2A (Crossthwaite et al., 2006). However, no phosphorylation sites have been identified within the N-terminal region (Beazely & Watts, 2006; Dessauer et al., 2017). Rather, phosphorylation by PKA and PKC appear to be in regions flanking the catalytic domains (Beazely & Watts, 2006). These results raise the question, is the interaction between PPP2CB and the N-terminal tail of AC5 physiologically relevant? To answer this larger question, future efforts must demonstrate that PP2A can oppose AC5 phosphorylation, and that this change in phosphorylation state effects AC5 activity or translocation. Unfortunately, only

limited efforts have been devoted to understanding the range and effects of post-translational modifications on adenylyl cyclase signaling.

Interestingly, multiple studies have demonstrated that post-translational modifications of adenylyl cyclases can directly regulate acute catalytic activity. Molecular studies have shown that PKA phosphorylation of AC5 is inhibitory, reducing forskolin and $G\alpha_s$-mediated stimulation (Beazely & Watts, 2006; Y. Chen et al., 1997). In contrast, phosphorylation by both typical and atypical isoforms of PKC enhances basal AC5 activity, as well as the forskolin and $G\alpha_s$-mediated response, in a PKC isoform dependent manner (Beazely & Watts, 2006; Ji Kawabe et al., 1996; J. Kawabe et al., 1994). However, the exact phosphorylation sites of human AC5 have not yet been confirmed, instead relying on AC6 consensus sequences, sequence analysis, or similarity to animal models to determine the likely targeted residues (Beazely & Watts, 2006; Y. Chen et al., 1997; Huttlin et al., 2010). Adding further complexity, both nitrosylation and acetylation have been shown to effect adenylyl cyclase catalytic activity, however the exact residues targeted for modification remain unknown (Beazely & Watts, 2006; Huttlin et al., 2010; McVey et al., 1999). Additional modifications have been shown to modulate cyclase-protein, or cyclase-lipid interactions, which direct the localization of cAMP signaling to discrete areas within the cell, but also remain uncharacterized (Kizuka & Taniguchi, 2016; W. Li et al., 2007; Morgan et al., 2004; Reddy et al., 2015). Taken together, these studies highlight the gaps in the collective understanding of the molecular mechanisms that regulate post-translational modifications of adenylyl cyclase isoforms.

Presently, the results of our BiFC-tagged cDNA screen for AC5 interacting partners presented in Chapter 2 has identified association with acetyltransferases, kinases, phosphatases, peptidases, E2 and E3 ubiquitin ligases, as well as multiple proteins involved with the biosynthesis of N-linked glycans for glycosylation. These initial results provide a strong foundation for the characterization of adenylyl cyclase post-translational modifications that occur under varying conditions. While the role of post-translational modifications on acute adenylyl cyclase activity has been lightly researched, the presence of modifications unique to the enhanced signaling observed during heterologous sensitization has not been pursued. Modern advancements in peptide and proteomic databases, separation techniques, and protein chemistry have converged to allow mass spectrometry to become a substantial tool to probe protein modifications that occur to a fully processed protein in the native environment. However, the greatest obstacle to characterizing

modifications to a full-length adenylyl cyclase is the difficulty in isolating and enriching large, membrane-localized proteins from mammalian cells. I strongly believe that devoting future studies to improving and optimizing the enrichment of affinity tagged adenylyl cyclase from live cells for proteomic analysis would be a very productive area of research. Assessing the changes in modifications that occur under basal versus acute stimulation or prolonged $G\alpha_{i/o}$-mediated inhibition would allow for a more directed approach in uncovering the molecular mechanisms underlying heterologous sensitization, as well as cAMP signaling as a whole.

To gain a better understanding of endogenous cAMP signaling, it is important to transition research from immortalized cell lines and into primary cells that are more physiologically relevant. Immortalized cell lines are cells that have been genetically modified to promote indefinite growth and division under set conditions (M. S. Carter, J., 2015). Such cell lines are often used as a platform to study biological and cell signaling processes, and have played an essential role in the development and screening of the BiFC-tagged cDNA library discussed in Chapter 2. There are many advantages to using such immortalized cells lines, since there are standard cell lines widely available from repositories across the world, immortalized cell lines are very well characterized. They are meant to be genetically homogenous, thus able to provide consistent and reproducible results (M. S. Carter, J., 2015; Kleinjans, 2014). Additionally, because they have been selected based upon cell culture characteristics, in addition to their genetic makeup, immortalized cell lines are typically easier to grow and propagate in culture compared to primary cells (M. S. Carter, J., 2015; Montano, 2015). Furthermore, these cells are often more receptive to the introduction of plasmid DNA for the overexpression and study of specific proteins or protein complexes (M. S. Carter, J., 2015; Montano, 2015). However, a major disadvantage of immortalized cell lines is that research often fails to progress into primary cells. Primary cells are taken directly from living tissue and then cultured *in vitro* (M. S. Carter, J., 2015; Montano, 2015). Because primary cells are not a homogenous population, research that has been clearly defined in immortalized cell lines often fails to replicate in primary cells. As a result, the substantial obstacle of proving or disproving years of work by translating into primary cell lines often goes unaddressed or fails quietly without being published. The subsequent dependence on overexpression systems to characterize signaling pathways often results in conflicting results and ambiguous conclusions. A significant shortcoming of the BiFC screen outlined in Chapter 2 is the failure to further characterize the AC5 interacting partners PPP2CB and NAPA in primary cells or tissues. Future endeavors should make translation

of research into primary cell lines a priority. This can be greatly assisted through the use of newly developed fluorescent biosensors and super-resolution microscopy. Fluorescent biosensors are rapidly evolving, with dramatic improvements of signal to noise ratio and fluorescent intensity. When used in conjunction with super-resolution microscopy techniques such as stochastic optical reconstruction microscopy (STORM) and single-molecule localization microscopy (SMLM), fluorescent biosensors offer the ability to characterize endogenous cellular signaling pathways within primary cells in real time. Future studies which promote the translation of research away from immortalized cell lines and into primary cells will have a variety of novel technology and techniques to assist in studying physiologically relevant systems, rather than artifacts of overexpression systems.

In Chapter 3 we highlighted the recent advances in genetic sequencing that have linked a series of AC5 gain-of-function mutations to a movement disorder known as familial dyskinesia and facial myokymia (Y. Z. Chen et al., 2014). In the striatum, neurotransmitter signaling through G-protein coupled receptors (GPCRs) is essential for the initiation and maintenance of movement (Herve, 2011). Central to this signaling pathway is the membrane localized adenylyl cyclase type 5 (AC5), which integrates GPCR signaling to control the production of the second messenger cAMP (Dessauer et al., 2017). Studies have indicated that AC5 is the predominant cyclase isoform expressed in striatal medium spiny neurons (MSNs), and account for approximately 80% of cAMP generated in these cells (K. W. Lee et al., 2002; Pieroni et al., 1993; Tepper & Bolam, 2004). Additionally, AC5 has been shown to preferentially couple to both stimulatory D_1 and inhibitory D_2 dopamine receptors (Corvol et al., 2001; Herve, 2011; K. W. Lee et al., 2002; Nair et al., 2015). The unique expression patterns and signaling preferences of AC5 highlight its significant role in information processing within the striatum. The striatum is a principal input structure of the basal ganglia, receiving neurological signals from the motor cortex (Haber, 2014). This information is further processes and modified before these signals are transferred back to the motor cortex via the thalamus for the initiation and maintenance of both conscious and unconscious movements (Haber, 2014). The control of movement by the striatum is dependent upon a complex system of neural circuitry. D_1R expressing MSNs are the predominate striatal output of the direct pathway, which projects to and inhibits the substantia nigra pars reticulata (SNr) to promote movement (Bordia & Perez, 2018; Haber, 2014). In contrast, activation of the D_2R MSNs of the indirect striatopallidal

pathway results in the suppression of movement (Bordia & Perez, 2018; Haber, 2014). The control and execution of movement requires delicately balanced GPCR and adenylyl cyclase signaling within striatal MSNs. Dysfunction of striatal cAMP signaling has been profoundly implicated in a variety of movement disorders (Carecchio et al., 2017; Kumar et al., 2014; Lanska, 2010).

To further expand upon the preliminary research examining enhanced signaling of these AC5 gain-of-function mutations, we studied the five most prevalent mutations identified in patients with FDFM to further characterize and explore AC5 as a potential therapeutic target. Our research demonstrated that the AC5 mutants exhibited enhanced activity in response to stimulation by lipid raft localize β-adrenergic receptors, as well as the non-lipid raft localized prostaglandin receptors. Through the use of purified $G\alpha_s$ and AC5 membranes, we presented further evidence to support that the enhanced response observed from the AC5 mutants was the result of enhanced enzymatic activity. Interestingly, D_2-mediated inhibition of the gain-of-function mutants was blunted compared to wildtype AC5. Together, these results indicate that the enhanced activity observed following $G\alpha_s$-mediated stimulation of AC5 gain-of-function mutations might lead to increased direct pathway activity. Moreover, the observation that AC5 gain-of-function mutants are weakly inhibited by D_2 receptor activation suggests that decreased activity of the indirect pathway may be observed. Together, this loss of cooperative activity in both direct and indirect pathways may possibly result in the unsynchronized enhancement of movement initiation observed in AC5-associated dyskinesia. We finally propose that AC5 isoform selective P-site inhibitors may be an effective therapeutic for this very unique type of disorder.

To identify how enhanced cAMP signaling is being translated into increased neuronal excitability, future studies should employ electrophysiology to characterize the changes in current and ion channel activity in response to adenylyl cyclase activity. While cAMP signaling is usually compartmentalized, the enhanced activity observed with the AC5 gain-of-function mutations likely overwhelms phosphodiesterase-mediated degradation, inadvertently promoting activation of downstream effectors. A fundamental property of ion channels is their ability to be modulated by second messenger systems, either by interaction with the messenger or through covalent modification by an effector. One possible effector is the cAMP activated protein kinase A (PKA), which has been demonstrated to phosphorylate a variety of ion channels. Voltage sensitive Na^+ channels have shown variable response to PKA phosphorylation, increasing sodium current in some models, while decreasing in others (Emerick, Shenkel, & Agnew, 1993; Gershon, Weigl,

Lotan, Schreibmayer, & Dascal, 1992; M. Li, West, Lai, Scheuer, & Catterall, 1992; R. D. Smith & Goldin, 1992). P and L-type calcium channels demonstrate increased Ca^{2+} current, as well as a shift in the voltage necessary for activation, following PKA phosphorylation (Fournier, Bourinet, Nargeot, & Charnet, 1993; Josephson & Sperelakis, 1991; Sculptoreanu, Figourov, & De Groat, 1995). Calcium-activated potassium channels respond to PKA phosphorylation by increasing K^+ current, while N-type potassium channels exhibit a decrease in K^+ current (Payet & Dupuis, 1992; Rehm et al., 1989). It is clear that PKA phosphorylation can widely influence ion channel characteristics; determining whether PKA function correlates with channel phosphorylation and subsequent changes in channel properties to promote neuronal firing is an important step in further characterizing the AC5 mutants and their role in FDFM. Cyclic nucleotide-gated (CNG) ion channels are a class of nonselective cation channels that function in response to binding cyclic nucleotides such as cAMP (Zhao et al., 2016). While CNG channel signal transduction has been predominantly studied in retinal photoreceoptors and olfactory receptors, recent studies have reported hyperpolarization-activated CNG channel expression in striatal neurons (Zhao et al., 2016). Moreover, dopamine-mediated stimulation of the D_2 receptor can modulate neuronal firing rates by reducing adenylyl cyclase activity, subsequently inhibiting hyperpolarization-activated CNG channels (Deng, Zhang, & Xu, 2007; Zhao et al., 2016). While CNG channels have not been studied to the degree of PKA regulation of ion channel properties, they do represent a possible avenue by which cAMP may be modulating neuronal firing rates. Further electrophysiological characterization will be necessary to accurately define and characterize the pathways responsible for the enhanced activity that results in FDFM.

In Chapter 4 we briefly discussed the characterization of unique behaviors observed in mice genetically deficient in AC1 or AC8. Both AC1 and AC8 are highly expressed in the CNS, particularly the hippocampus, and genetic ablation of either isoform significantly disrupted hippocampus-dependent LTP and LTM. Curiously, however, AC8 knockout animals demonstrated reduced long-term anxiety induced by repeated elevated plus maze exposure, whereas AC1 knockout did not have the same effect. Characterization of ethanol drinking behaviors in these animals indicated that AC8 knockout mice exhibited reduced voluntary ethanol consumption compared to wildtype mice, whereas AC1 knockout mice did not show the same reduction compared to wildtype. Together, this data suggests that AC8 may participate in signaling

pathways involved with the regulation of long-term anxiety and ethanol consumption. Because anxiety and alcohol abuse disorders are often comorbid in humans, there is some data to further support that shared pathways may link these two disorders. Unfortunately, a majority of the data in support of this hypothesis are the results of genetic knockout animal studies. Despite strong interest in developing isoform selective small molecule modulators of adenylyl cyclase, there were currently no inhibitors that can distinguish between AC8 and the closely related AC1.

To address this lack of isoform selective small molecules, we performed a screen of approximately 17,000 compounds from four libraries of neurologically active compounds against inhibition of calcium stimulated AC8 activity. Of the initial pool, 144 compounds displayed substantial inhibition and were counter-screened against inhibition of calcium stimulated AC1 activity. From the hits that demonstrated AC8 selective inhibition, an assessment was conducted to remove suspected pan-assay interfering compounds and potential aggregators. The remaining compounds were clustered by their structural features, and nine representative compounds were selected for further validation. Of the nine selected, only two demonstrated 10-fold or greater selectivity between AC8 and AC1. We performed a very limited SAR-by-catalog, selecting only a limited number of available compounds with non-logical structural features. As expected, this Hail-Mary of second round of analogs produced no increases in potency or efficacy. This project has identified two structures which demonstrate selectivity for AC8 over AC1, which could be developed into very useful research probes to further validate the cellular signaling pathways which underlie physiological behaviors observed in the genetic knockout animals. However, the project is still in its infancy and requires a concerted effort to develop chemical analogs based upon logical SAR. In addition to the development of analogs, care should be taken to validate the functional results through an orthogonal assay to ensure potency and efficacy are fully established with no false positives. Successful completion of these steps should lead to further analysis of aqueous solubility and the propensity to form aggregates. Dynamic light scattering is a simple and cost-effective method to detect and quantify aggregation of hit compounds that could be easily completed with the Purdue core facilities. Further assessment of the pharmacokinetic properties could be completed with the assistance of the Purdue School of Veterinary Medicine before moving forward with analysis in animal models. Collaboration with a lab well versed in the assessment of long-term anxiety and ethanol consumption behaviors will be absolutely essential in correctly validating the efficacy of any lead compounds, and to avoid the pitfalls associated with

poor animal models. In summary, this screen has produced intriguing hit compounds for AC8 selective inhibitors, but significant effort must be invested to further improve and validate their efficacy.

APPENDIX A. CHAPTER 2 SUPPLEMENTAL DATA

Appendix Table 1: Gene identification by treatment condition

Genes Appearing in Vehicle Treatment Gene Name	**Genes Appearing in Quinpirole Treatment** Gene Name	**Genes Appearing in Both Groups** Gene Name
ACOT7	ANKRD13D	AGAP1
ADAM19	AP1M1	ALKBH5
ADAMTS6	ARHGAP23	ATP5B
ADSL	CCNI	BACE2
AEBP2	DDR1	CACNG4
AKAP6	DDX41	CDK19
ARHGEF17	ERC1	CHIT1
BLCAP	FAM168A	CHPT1
CDC37	FOXH1	COL6A1
CDIPT	HERC1	CTNNA2
CEP131	HKR1	CTSA
CHMP3	HTT	CTSB
CHPF	KIFC2	DAP3
CLCN4	LAP3P2	DCAF11
CLDND1	MALRD1	DDAH2
CLVS2	MARCH8	DDB1
CMSS1	MFAP1	DNAJB12
CPOX	MVK	DPYSL5
CYSLTR2	MYL6	DYNC1I1
DAP3P2	MYLK	EDRF1
DAZAP2	NAPA	FAM219B
DHRSX	NCAPD3	HSD11B1L
DHX35	NDRG1	HTRA1
DIO3OS	NEGR1	ILF3
DLG2	OPHN1	KCNH4
EFHC2	PARN	LAP3
EIF2AK1	PCDH11Y	MACROD2
EIF2B5	PGAP3	MADD
EME2	PGK1	MLLT4
ENO2	PLXNA4	MLLT6
FARP1	PTPN9	MPI
FBXL13	RASA3	MSL1
FILIP1L	RBFOX3	MYO18B

Genes Appearing in Vehicle Treatment	Genes Appearing in Quinpirole Treatment	Genes Appearing in Both Groups
Gene Name	Gene Name	Gene Name
GAS6	RHPN1	NAT1
GCK	RPL8	NUDT16L1
GEN1	SERPINF1	OLAH
GFRA2	SNX17	PACSIN2
GPIHBP1	SPTAN1	PAPPA
GRIN2A	SUGP2	PDYN
H6PD	SYT11	PITPNA
HBG2	TARBP1	PLTP
HEPH	TENM2	PTPRO
HS6ST1	TM4SF2	R3HCC1
IGBP1	TMEM132C	RNH1
IGBP1P1	TNFRSF11A	RPL36
IGF2BP1	TNRC18	RTN4IP1
IGHG1	TSPAN7	RUVBL2
IGSF8	WSCD1	SCRT2
IL1RAP		SH2D4B
INHBA		SLC25A22
ITIH5		SLC8A1
JAZF1		TMEM163
KAZN		TRO
KCNIP1		UBE2H
KCNK2		ULK3
KIF1A		UPF1
LMAN2L		VPS39
LRRC37A16P		WDR5
MAFG		ZFPM2
MAN2B1		
MGAT4B		
MIIP		
MTOR		
NAT10		
NELFCD		
NIPAL4		
NKAIN2		
NNAT		
NR2C2		
NRXN3		
OFCC1		

Genes Appearing in Vehicle Treatment	Genes Appearing in Quinpirole Treatment	Genes Appearing in Both Groups
Gene Name	Gene Name	Gene Name
PAAF1		
PANK4		
PARD3		
PIP5K1B		
PPP1CA		
PPP1R42		
PPP2CB		
PRKCZ		
PTPN5		
PTPRD		
RAD9A		
RBM5		
ROBO2		
RPLP0		
SBNO2		
SEC13		
SERINC3		
SETD3		
SH3GL1P3		
SIRT7		
SMC6		
SMOC1		
SPATA20		
SPSB3		
SUPT5H		
SYN1		
TMEM229B		
TMX2		
TRIB2		
TTC12		
TTYH3		
UIMC1		
VPS26B		
ZER1		
ZNF275		

Appendix Table 2: Effect of gene knockdown on AC5 acute and sensitization response.

AC5 Sensitization (% Mock)			**AC5 Acute (% Mock)**		
Gene	Mean	SEM	Gene	Mean	SEM
ADAM19	52	3	ADAM19	128	10
AGAP1	118	15	AGAP1	594	43
AKAP6	132	33	AKAP6	361	83
AP1M1	141	16	AP1M1	211	33
ARHGAP23	22	3	ARHGAP23	75	13
ARHGEF17	39	2	ARHGEF17	91	11
CACNG4	28	0	CACNG4	64	10
CDC37	97	10	CDC37	316	32
CDK19	39	1	CDK19	108	4
CLCN4	44	7	CLCN4	66	7
CLVS2	62	15	CLVS2	86	9
CHMP3	47	6	CHMP3	74	7
DDR1	29	6	DDR1	64	7
DLG2	57	3	DLG2	96	10
DYNC1I1	20	3	DYNC1I1	58	8
ERC1	56	7	ERC1	86	5
FARP1	15	9	FARP1	45	10
FOXH1	41	7	FOXH1	91	9
HERC1	36	5	HERC1	74	13
HTRA1	48	2	HTRA1	80	17
HTT	32	4	HTT	63	13
IGBP1	43	7	IGBP1	85	3
KCNH4	34	4	KCNH4	61	12
KCNK2	53	6	KCNK2	86	7
KIFC2	43	2	KIFC2	59	12
LAP3	69	7	LAP3	69	11
MARCH8	14	3	MARCH8	34	8
MTOR	29	3	MTOR	84	20
NAPA	37	5	NAPA	91	10
NAT1	147	8	NAT1	197	19
NDRG1	43	7	NDRG1	111	12
NEGR1	46	6	NEGR1	68	13
NNAT	43	8	NNAT	106	13
NRXN3	30	4	NRXN3	55	9
OPHN1	50	6	OPHN1	93	15
PACSIN2	3	1	PACSIN2	25	8
PARD3	48	7	PARD3	84	7
PIP5K1B	61	8	PIP5K1B	106	9

Gene	Mean	SEM	Gene	Mean	SEM
PLXNA4	39	2	PLXNA4	67	10
PPP1CA	54	5	PPP1CA	63	14
PPP2CB	39	6	PPP2CB	77	13
PRKCZ	95	9	PRKCZ	92	28
PTPN9	12	2	PTPN9	47	14
PTPRD	42	5	PTPRD	66	9
PTPRO	53	6	PTPRO	67	6
RASA3	38	5	RASA3	61	13
RHPN1	62	12	RHPN1	103	16
SNX17	64	13	SNX17	101	10
SYT11	66	8	SYT11	86	8
TSPAN7	45	9	TSPAN7	74	5
ULK3	56	2	ULK3	68	11
GNAS	0	0	GNAS	0	0
MOCK	100	0	MOCK	100	0

Appendix Table 3: Effect of siRNA knockdown on cellular viability.

Gene	% Viability	Gene	% Viability
ADAM19	69	NAPA	58
AGAP1	37	NAT1	105
AKAP6	80	NEGR1	92
AP1M1	94	NDRG1	64
ARHGAP23	54	NNAT	70
ARHGEF17	50	NRXN3	69
CACNG4	72	OPHN1	87
CDC37	79	PACSIN2	32
CDK19	69	PARD3	71
CLCN4	97	PIP5K1B	72
CLVS2	95	PLXNA4	87
CHMP3	95	PPP1CA	81
DDR1	74	PPP2CB	76
DLG2	83	PRKCZ	70
DYNC1I1	38	PTPN9	41
ERC1	68	PTPRD	77
FARP1	62	PTPRO	92
FOXH1	58	RASA3	68
HERC1	96	RHPN1	68
HTRA1	82	SNX17	72
HTT	81	SYT11	81
IGBP1	84	TSPAN7	76
KCNH4	48	ULK3	55
KCNK2	48		
KIFC2	82	GNAS	82
LAP3	48	MOCK	100
MARCH8	81	Lysis Buffer	0
MTOR	65		

Appendix Table 4: siRNA Validation

AC5 Sensitization (% Mock)		
Gene	Sensitization	SEM
ARHGAP23 #1	55	12
ARHGAP23 #2	46	10
ARHGAP23 #3	32	6
ARHGAP23 #4	12	3
CHMP3 #1	54	4
CHMP3 #2	23	4
CHMP3 #3	32	7
CHMP3 #4	12	4
FOXH1 #1	52	7
FOXH1 #2	26	6
FOXH1 #3	60	10
FOXH1 #4	19	4
HERC1 #1	24	5
HERC1 #2	24	5
HERC1 #3	33	9
HERC1 #4	42	6
HTRA1 #1	85	15
HTRA1 #2	44	7
HTRA1 #3	44	10
HTRA1 #4	36	5
HTT #1	42	7
HTT #2	41	5
HTT #3	56	13
HTT #4	40	5
IGBP1 #1	33	6
IGBP1 #2	57	6
IGBP1 #3	43	8
IGBP1 #4	33	5

Gene	Sensitization	SEM
MTOR #1	21	6
MTOR #2	23	5
MTOR #3	24	6
MTOR #4	141	27
NAPA #1	18	5
NAPA #2	53	8
NAPA #3	48	11
NAPA #4	21	3
NDRG1 #1	33	7
NDRG1 #2	79	11
NDRG1 #3	31	3
NDRG1 #4	22	4
NEGR1 #1	55	9
NEGR1 #2	48	4
NEGR1 #3	29	4
NEGR1 #4	74	2
NNAT #1	10	4
NNAT #2	22	4
NNAT #3	52	8
NNAT #4	94	13
NRXN3 #1	45	9
NRXN3 #2	39	7
NRXN3 #3	48	1
NRXN3 #4	46	4
OPHN1 #1	29	8
OPHN1 #2	40	7
OPHN1 #3	38	8
OPHN1 #4	99	23
PARD3 #1	40	8
PARD3 #2	61	7
PARD3 #3	19	3
PARD3 #4	53	8

Gene	Sensitization	SEM
PPP2CB #1	36	6
PPP2CB #2	32	7
PPP2CB #3	42	9
PPP2CB #4	69	20
SNX17 #1	66	12
SNX17 #2	46	6
SNX17 #3	33	9
SNX17 #4	55	10

APPENDIX B. CHAPTER 2 SUPPLEMENTAL METHODS

CHAPTER 2 SUPPLEMENTAL INFORMATION

PCR Conditions and primers for amplification of cDNA insert:

Thermocycler Program:

Initial Denaturation	95°C	30sec
40 Cycles	95°C	30sec
	60°C	60sec
	72°C	5min
Final Extension	72°C	10min
Hold	4°C	

Primers:

PCR primers were purchased from Integrated DNA Technologies (Coralville, IA)

Forward - 1st PCR

5'-ACACTCTTTCCCTACACgACgCTCTTCCgATCTggAgACCCAAgCTggCTAgCg-3'

Reverse - 1st PCR

5'-gTgACTggAgTTCAgACgTgTgCTCTTCCgATCTgTCggATCCACCTgATCCgCC-3'

Forward Vehicle -2nd PCR Forward Vehicle – FACS#1

5'-AATGATACGGCGACCACCGAGATCTACACTGAACCTTACACTCTTTCCCTACACGAC-3'

Reverse Vehicle -2nd PCR Reverse Vehicle – FACS#1

5'-CAAGCAGAAGACGGCATACGAGATATCACGACGTGACTGGAGTTCAGACGTG-3'

Forward Quinpirole- 2nd PCR Forward Treatment – FACS#1

5'-AATGATACGGCGACCACCGAGATCTACACTGCTAAGTACACTCTTTCCCTACACGAC-3'

Reverse Treatment - 2nd PCR Reverse Treatment – FACS#1

5'-CAAGCAGAAGACGGCATACGAGATACAGTGGTGTGACTGGAGTTCAGACGTG-3'

Forward Vehicle – 2nd PCR Forward Vehicle – FACS#2

5’-AATGATACGGCGACCACCGAGATCTACACTGTTCTCTACACTCTTTCCCTACACGAC-3’

Reverse Vehicle - 2nd PCR Reverse Vehicle – FACS#2

5’-CAAGCAGAAGACGGCATACGAGATCAGATCCAGTGACTGGAGTTCAGACGTG-3’

Forward Quinpirole - 2nd PCR Forward Treatment – FACS#2

5’-AATGATACGGCGACCACCGAGATCTACACTAAGACACACACTCTTTCCCTACACGAC-3’

Reverse Treatment - 2nd PCR Reverse Treatment – FACS#2

5’-CAAGCAGAAGACGGCATACGAGATACAAACGGGTGACTGGAGTTCAGACGTG-3

Forward Vehicle – 2nd PCR Forward Vehicle – FACS#3

5’-AATGATACGGCGACCACCGAGATCTACACCTAATCGAACACTCTTTCCCTACACGAC-3’

Reverse Vehicle - 2nd PCR Reverse Vehicle – FACS#3

5’-CAAGCAGAAGACGGCATACGAGATACCCAGCAGTGACTGGAGTTCAGACGTG-3’

Forward Quinpirole - 2nd PCR Forward Treatment – FACS#3

5’-AATGATACGGCGACCACCGAGATCTACACCTAGAACAACACTCTTTCCCTACACGAC-3’

Reverse Treatment - 2nd PCR Reverse Treatment – FACS#3

5’-CAAGCAGAAGACGGCATACGAGATAACCCCTCGTGACTGGAGTTCAGACGTG-3’

qPCR Primers:

GAPDH

Forward: 5’-GTCGGAGTCAACGGATTTG-3’

Reverse: 5’-GACGGTGCCATGGAATTT-3’

GNAS

Forward: 5’-TGAACGTGCCTGACTTTG-3’

Reverse: 5’-TCGATCTTGTCCAGGAAGTA-3’

AC5

Forward: 5’-AGATGAACCGCCAGAGAA-3’

Reverse: 5’-CTCAGACCGAAGCCTATCA-3’

HTT

Forward: 5’-CTTCGGAGTGACAAGGAAAGA-3’

Reverse: 5’-GGTCTTGGTGCTGTGTATGA-3’

PPP2CB

Forward: 5’-GTGGAGACTGTGACTCTTCTTG-3’

Reverse: 5’-CTTGGGTAATTTGTCGGCTTTC-3’

NAPA

Forward primer: 5’-CTGTTTGATGCGAGCAATCG-3’

Reverse primer: 5’-GTCCACCAACTCTGTCTCATAG-3’

HERC1

Forward primer: 5’-GTGTCAGCTGGATACAGACATAG-3’

Reverse primer: 5’-TGCTGTCACCATGACCTAATC-3’

IGBP1

Forward primer: 5’-TCCTCCATGGCTTATCCTAGT-3’

Reverse primer: 5’-CCTATGCTCCAACTCCTTCTTC-3’

REFERENCES

Agarwal, S. R., Clancy, C. E., & Harvey, R. D. (2016). Mechanisms Restricting Diffusion of Intracellular cAMP. *Sci Rep, 6*, 19577. doi:10.1038/srep19577

Agarwal, S. R., Miyashiro, K., Latt, H., Ostrom, R. S., & Harvey, R. D. (2017). Compartmentalized cAMP Responses to Prostaglandin EP2 Receptor Activation in Human Airway Smooth Muscle Cells. *Br J Pharmacol*. doi:10.1111/bph.13904

Ahn, J. H., McAvoy, T., Rakhilin, S. V., Nishi, A., Greengard, P., & Nairn, A. C. (2007). Protein kinase A activates protein phosphatase 2A by phosphorylation of the B56delta subunit. *Proc Natl Acad Sci U S A, 104*(8), 2979-2984. doi:10.1073/pnas.0611532104

Ajit, S. K., Ramineni, S., Edris, W., Hunt, R. A., Hum, W. T., Hepler, J. R., & Young, K. H. (2007). RGSZ1 interacts with protein kinase C interacting protein PKCI-1 and modulates mu opioid receptor signaling. *Cell Signal, 19*(4), 723-730. doi:10.1016/j.cellsig.2006.09.008

Alewijnse, A. E., Timmerman, H., Jacobs, E. H., Smit, M. J., Roovers, E., Cotecchia, S., & Leurs, R. (2000). The effect of mutations in the DRY motif on the constitutive activity and structural instability of the histamine H(2) receptor. *Mol Pharmacol, 57*(5), 890-898.

Alexander, S. P., Christopoulos, A., Davenport, A. P., Kelly, E., Marrion, N. V., Peters, J. A., . . . Collaborators, C. (2017). THE CONCISE GUIDE TO PHARMACOLOGY 2017/18: G protein-coupled receptors. *Br J Pharmacol, 174 Suppl 1*, S17-S129. doi:10.1111/bph.13878

Ammer, H., & Schulz, R. (1996). Morphine dependence in human neuroblastoma SH-SY5Y cells is associated with adaptive changes in both the quantity and functional interaction of PGE1 receptors and stimulatory G proteins. *Brain Res, 707*(2), 235-244.

Antoni, F. A., Wiegand, U. K., Black, J., & Simpson, J. (2006). Cellular localisation of adenylyl cyclase: a post-genome perspective. *Neurochem Res, 31*(2), 287-295. doi:10.1007/s11064-005-9019-1

Attwood, T. K., & Findlay, J. B. (1994). Fingerprinting G-protein-coupled receptors. *Protein Eng, 7*(2), 195-203.

Avidor-Reiss, T., Nevo, I., Levy, R., Pfeuffer, T., & Vogel, Z. (1996). Chronic opioid treatment induces adenylyl cyclase V superactivation. Involvement of Gbetagamma. *J Biol Chem, 271*(35), 21309-21315.

Avidor-Reiss, T., Nevo, I., Saya, D., Bayewitch, M., & Vogel, Z. (1997). Opiate-induced adenylyl cyclase superactivation is isozyme-specific. *J Biol Chem, 272*(8), 5040-5047.

Baillie, G. S., Adams, D. R., Bhari, N., Houslay, T. M., Vadrevu, S., Meng, D., . . . Houslay, M. D. (2007). Mapping binding sites for the PDE4D5 cAMP-specific phosphodiesterase to the N- and C-domains of beta-arrestin using spot-immobilized peptide arrays. *Biochem J, 404*(1), 71-80. doi:10.1042/BJ20070005

Baird, G. S., Zacharias, D. A., & Tsien, R. Y. (1999). Circular permutation and receptor insertion within green fluorescent proteins. *Proc Natl Acad Sci U S A, 96*(20), 11241-11246.

Bauman, A. L., Soughayer, J., Nguyen, B. T., Willoughby, D., Carnegie, G. K., Wong, W., . . . Scott, J. D. (2006). Dynamic regulation of cAMP synthesis through anchored PKA-adenylyl cyclase V/VI complexes. *Mol Cell, 23*(6), 925-931. doi:10.1016/j.molcel.2006.07.025

Bavencoffe, A., Li, Y., Wu, Z., Yang, Q., Herrera, J., Kennedy, E. J., . . . Dessauer, C. W. (2016). Persistent Electrical Activity in Primary Nociceptors after Spinal Cord Injury Is Maintained by Scaffolded Adenylyl Cyclase and Protein Kinase A and Is Associated with Altered Adenylyl Cyclase Regulation. *J Neurosci, 36*(5), 1660-1668. doi:10.1523/JNEUROSCI.0895-15.2016

Bayewitch, M. L., Avidor-Reiss, T., Levy, R., Pfeuffer, T., Nevo, I., Simonds, W. F., & Vogel, Z. (1998). Differential modulation of adenylyl cyclases I and II by various G beta subunits. *J Biol Chem, 273*(4), 2273-2276.

Beaulieu, J. M., Sotnikova, T. D., Marion, S., Lefkowitz, R. J., Gainetdinov, R. R., & Caron, M. G. (2005). An Akt/beta-arrestin 2/PP2A signaling complex mediates dopaminergic neurotransmission and behavior. *Cell, 122*(2), 261-273. doi:10.1016/j.cell.2005.05.012

Beazely, M. A., Alan, J. K., & Watts, V. J. (2005). Protein kinase C and epidermal growth factor stimulation of Raf1 potentiates adenylyl cyclase type 6 activation in intact cells. *Mol Pharmacol, 67*(1), 250-259. doi:10.1124/mol.104.001370

Beazely, M. A., & Watts, V. J. (2006). Regulatory properties of adenylate cyclases type 5 and 6: A progress report. *Eur J Pharmacol, 535*(1-3), 1-12. doi:10.1016/j.ejphar.2006.01.054

Berendzen, K. W., Bohmer, M., Wallmeroth, N., Peter, S., Vesic, M., Zhou, Y., . . . Harter, K. (2012). Screening for in planta protein-protein interactions combining bimolecular fluorescence complementation with flow cytometry. *Plant Methods, 8*(1), 25. doi:10.1186/1746-4811-8-25

Bernabucci, M., & Zhuo, M. (2016). Calcium activated adenylyl cyclase AC8 but not AC1 is required for prolonged behavioral anxiety. *Mol Brain, 9*(1), 60. doi:10.1186/s13041-016-0239-x

Berthet, J., Rall, T. W., & Sutherland, E. W. (1957). The relationship of epinephrine and glucagon to liver phosphorylase. IV. Effect of epinephrine and glucagon on the reactivation of phosphorylase in liver homogenates. *J Biol Chem, 224*(1), 463-475.

Birnbaumer, L. (2007). The discovery of signal transduction by G proteins: a personal account and an overview of the initial findings and contributions that led to our present understanding. *Biochim Biophys Acta, 1768*(4), 756-771. doi:10.1016/j.bbamem.2006.09.027

Birnbaumer, L. (2010). Signal Transduction by G Proteins: Basic Principles, Molecular Diversity, and Structural Basis of Their Actions. In E. D. Ralph Bradshaw (Ed.), *Handbook of Cell Signaling* (2 ed., pp. 1597-1614): Academic Press.

Blumer, J. B., & Lanier, S. M. (2014). Activators of G protein signaling exhibit broad functionality and define a distinct core signaling triad. *Mol Pharmacol, 85*(3), 388-396. doi:10.1124/mol.113.090068

Blumer, J. B., Oner, S. S., & Lanier, S. M. (2012). Group II activators of G-protein signalling and proteins containing a G-protein regulatory motif. *Acta Physiol (Oxf), 204*(2), 202-218. doi:10.1111/j.1748-1716.2011.02327.x

Blumer, J. B., Smrcka, A. V., & Lanier, S. M. (2007). Mechanistic pathways and biological roles for receptor-independent activators of G-protein signaling. *Pharmacol Ther, 113*(3), 488-506. doi:10.1016/j.pharmthera.2006.11.001

Bol, G. F., Hulster, A., & Pfeuffer, T. (1997). Adenylyl cyclase type II is stimulated by PKC via C-terminal phosphorylation. *Biochim Biophys Acta, 1358*(3), 307-313.

Boran, A. D., Chen, Y., & Iyengar, R. (2011). Identification of new Gbetagamma interaction sites in adenylyl cyclase 2. *Cell Signal, 23*(9), 1489-1495. doi:10.1016/j.cellsig.2011.05.002

Bordia, T., & Perez, X. A. (2018). Cholinergic control of striatal neurons to modulate L-dopa-induced dyskinesias. *Eur J Neurosci*. doi:10.1111/ejn.14048

Brand, C. S., Hocker, H. J., Gorfe, A. A., Cavasotto, C. N., & Dessauer, C. W. (2013). Isoform selectivity of adenylyl cyclase inhibitors: characterization of known and novel compounds. *J Pharmacol Exp Ther, 347*(2), 265-275. doi:10.1124/jpet.113.208157

Brand, C. S., Sadana, R., Malik, S., Smrcka, A. V., & Dessauer, C. W. (2015). Adenylyl Cyclase 5 Regulation by Gbetagamma Involves Isoform-Specific Use of Multiple Interaction Sites. *Mol Pharmacol, 88*(4), 758-767. doi:10.1124/mol.115.099556

Brust, T. F., Alongkronrusmee, D., Soto-Velasquez, M., Baldwin, T. A., Ye, Z., Dai, M., . . . Watts, V. J. (2017). Identification of a selective small-molecule inhibitor of type 1 adenylyl cyclase activity with analgesic properties. *Sci Signal, 10*(467). doi:10.1126/scisignal.aah5381

Brust, T. F., Conley, J. M., & Watts, V. J. (2015). Galpha(i/o)-coupled receptor-mediated sensitization of adenylyl cyclase: 40 years later. *Eur J Pharmacol, 763*(Pt B), 223-232. doi:10.1016/j.ejphar.2015.05.014

Buhl, A. M., Johnson, N. L., Dhanasekaran, N., & Johnson, G. L. (1995). G alpha 12 and G alpha 13 stimulate Rho-dependent stress fiber formation and focal adhesion assembly. *J Biol Chem, 270*(42), 24631-24634.

Bunney, T. D., & Katan, M. (2011). PLC regulation: emerging pictures for molecular mechanisms. *Trends Biochem Sci, 36*(2), 88-96. doi:10.1016/j.tibs.2010.08.003

Cali, J. J., Zwaagstra, J. C., Mons, N., Cooper, D. M., & Krupinski, J. (1994). Type VIII adenylyl cyclase. A Ca2+/calmodulin-stimulated enzyme expressed in discrete regions of rat brain. *J Biol Chem, 269*(16), 12190-12195.

Carecchio, M., Mencacci, N. E., Iodice, A., Pons, R., Panteghini, C., Zorzi, G., . . . Nardocci, N. (2017). ADCY5-related movement disorders: Frequency, disease course and phenotypic variability in a cohort of paediatric patients. *Parkinsonism Relat Disord, 41*, 37-43. doi:10.1016/j.parkreldis.2017.05.004

Carter, B. D., & Medzihradsky, F. (1993). Go mediates the coupling of the mu opioid receptor to adenylyl cyclase in cloned neural cells and brain. *Proc Natl Acad Sci U S A, 90*(9), 4062-4066.

Carter, M. S., J. (2015). *Guide to Research Techniques in Neuroscience*: Elsevier Science Direct.

Casey, P. J. (1995). Protein lipidation in cell signaling. *Science, 268*(5208), 221-225.

Celver, J., Vishnivetskiy, S. A., Chavkin, C., & Gurevich, V. V. (2002). Conservation of the phosphate-sensitive elements in the arrestin family of proteins. *J Biol Chem, 277*(11), 9043-9048. doi:10.1074/jbc.M107400200

Chen, D. H., Meneret, A., Friedman, J. R., Korvatska, O., Gad, A., Bonkowski, E. S., . . . Raskind, W. H. (2015). ADCY5-related dyskinesia: Broader spectrum and genotype-phenotype correlations. *Neurology, 85*(23), 2026-2035. doi:10.1212/WNL.0000000000002058

Chen, J., DeVivo, M., Dingus, J., Harry, A., Li, J., Sui, J., . . . et al. (1995). A region of adenylyl cyclase 2 critical for regulation by G protein beta gamma subunits. *Science, 268*(5214), 1166-1169.

Chen, J., & Rasenick, M. M. (1995). Chronic treatment of C6 glioma cells with antidepressant drugs increases functional coupling between a G protein (Gs) and adenylyl cyclase. *J Neurochem, 64*(2), 724-732.

Chen, Y., Harry, A., Li, J., Smit, M. J., Bai, X., Magnusson, R., . . . Iyengar, R. (1997). Adenylyl cyclase 6 is selectively regulated by protein kinase A phosphorylation in a region involved in Galphas stimulation. *Proc Natl Acad Sci U S A, 94*(25), 14100-14104.

Chen, Y. Z., Friedman, J. R., Chen, D. H., Chan, G. C., Bloss, C. S., Hisama, F. M., . . . Torkamani, A. (2014). Gain-of-function ADCY5 mutations in familial dyskinesia with facial myokymia. *Ann Neurol, 75*(4), 542-549. doi:10.1002/ana.24119

Chen, Y. Z., Matsushita, M. M., Robertson, P., Rieder, M., Girirajan, S., Antonacci, F., . . . Raskind, W. H. (2012). Autosomal dominant familial dyskinesia and facial myokymia: single exome sequencing identifies a mutation in adenylyl cyclase 5. *Arch Neurol, 69*(5), 630-635. doi:10.1001/archneurol.2012.54

Chen-Goodspeed, M., Lukan, A. N., & Dessauer, C. W. (2005). Modeling of Galpha(s) and Galpha(i) regulation of human type V and VI adenylyl cyclase. *J Biol Chem, 280*(3), 1808-1816. doi:10.1074/jbc.M409172200

Cherezov, V., Rosenbaum, D. M., Hanson, M. A., Rasmussen, S. G., Thian, F. S., Kobilka, T. S., . . . Stevens, R. C. (2007). High-resolution crystal structure of an engineered human beta2-adrenergic G protein-coupled receptor. *Science, 318*(5854), 1258-1265. doi:10.1126/science.1150577

Choi, E. J., Xia, Z., & Storm, D. R. (1992). Stimulation of the type III olfactory adenylyl cyclase by calcium and calmodulin. *Biochemistry, 31*(28), 6492-6498.

Chong-Kopera, H., Inoki, K., Li, Y., Zhu, T., Garcia-Gonzalo, F. R., Rosa, J. L., & Guan, K. L. (2006). TSC1 stabilizes TSC2 by inhibiting the interaction between TSC2 and the HERC1 ubiquitin ligase. *J Biol Chem, 281*(13), 8313-8316. doi:10.1074/jbc.C500451200

Chung, K. Y., Rasmussen, S. G., Liu, T., Li, S., DeVree, B. T., Chae, P. S., . . . Sunahara, R. K. (2011). Conformational changes in the G protein Gs induced by the beta2 adrenergic receptor. *Nature, 477*(7366), 611-615. doi:10.1038/nature10488

Clark, M. J., Furman, C. A., Gilson, T. D., & Traynor, J. R. (2006). Comparison of the relative efficacy and potency of mu-opioid agonists to activate Galpha(i/o) proteins containing a pertussis toxin-insensitive mutation. *J Pharmacol Exp Ther, 317*(2), 858-864. doi:10.1124/jpet.105.096818

Clark, M. J., Harrison, C., Zhong, H., Neubig, R. R., & Traynor, J. R. (2003). Endogenous RGS protein action modulates mu-opioid signaling through Galphao. Effects on adenylyl cyclase, extracellular signal-regulated kinases, and intracellular calcium pathways. *J Biol Chem, 278*(11), 9418-9425. doi:10.1074/jbc.M208885200

Clark, M. J., & Traynor, J. R. (2006). Mediation of adenylyl cyclase sensitization by PTX-insensitive GalphaoA, Galphai1, Galphai2 or Galphai3. *J Neurochem, 99*(6), 1494-1504.

Clement, N., Glorian, M., Raymondjean, M., Andreani, M., & Limon, I. (2006). PGE2 amplifies the effects of IL-1beta on vascular smooth muscle cell de-differentiation: a consequence of the versatility of PGE2 receptors 3 due to the emerging expression of adenylyl cyclase 8. *J Cell Physiol, 208*(3), 495-505. doi:10.1002/jcp.20673

Colin, E., Zala, D., Liot, G., Rangone, H., Borrell-Pages, M., Li, X. J., . . . Humbert, S. (2008). Huntingtin phosphorylation acts as a molecular switch for anterograde/retrograde transport in neurons. *EMBO J, 27*(15), 2124-2134. doi:10.1038/emboj.2008.133

Conley, J. M., Brand, C. S., Bogard, A. S., Pratt, E. P., Xu, R., Hockerman, G. H., . . . Watts, V. J. (2013). Development of a high-throughput screening paradigm for the discovery of small-molecule modulators of adenylyl cyclase: identification of an adenylyl cyclase 2 inhibitor. *J Pharmacol Exp Ther, 347*(2), 276-287. doi:10.1124/jpet.113.207449

Conti, A. C., Maas, J. W., Jr., Muglia, L. M., Dave, B. A., Vogt, S. K., Tran, T. T., . . . Muglia, L. J. (2007). Distinct regional and subcellular localization of adenylyl cyclases type 1 and 8 in mouse brain. *Neuroscience, 146*(2), 713-729. doi:10.1016/j.neuroscience.2007.01.045

Cooper, D. M. (2003). Molecular and cellular requirements for the regulation of adenylate cyclases by calcium. *Biochem Soc Trans, 31*(Pt 5), 912-915. doi:10.1042/

Cooper, D. M., & Tabbasum, V. G. (2014). Adenylate cyclase-centred microdomains. *Biochem J, 462*(2), 199-213. doi:10.1042/BJ20140560

Corvol, J. C., Studler, J. M., Schonn, J. S., Girault, J. A., & Herve, D. (2001). Galpha(olf) is necessary for coupling D1 and A2a receptors to adenylyl cyclase in the striatum. *J Neurochem, 76*(5), 1585-1588.

Costanzi, S., Siegel, J., Tikhonova, I. G., & Jacobson, K. A. (2009). Rhodopsin and the others: a historical perspective on structural studies of G protein-coupled receptors. *Curr Pharm Des, 15*(35), 3994-4002.

Crossthwaite, A. J., Ciruela, A., Rayner, T. F., & Cooper, D. M. (2006). A direct interaction between the N terminus of adenylyl cyclase AC8 and the catalytic subunit of protein phosphatase 2A. *Mol Pharmacol, 69*(2), 608-617. doi:10.1124/mol.105.018275

Cumbay, M. G., & Watts, V. J. (2001). Heterologous sensitization of recombinant adenylate cyclases by activation of D(2) dopamine receptors. *J Pharmacol Exp Ther, 297*(3), 1201-1209.

Cumbay, M. G., & Watts, V. J. (2004). Novel regulatory properties of human type 9 adenylate cyclase. *J Pharmacol Exp Ther, 310*(1), 108-115. doi:10.1124/jpet.104.065748

Cumbay, M. G., & Watts, V. J. (2005). Galphaq potentiation of adenylate cyclase type 9 activity through a Ca2+/calmodulin-dependent pathway. *Biochem Pharmacol, 69*(8), 1247-1256. doi:10.1016/j.bcp.2005.02.001

Cyr, M., Sotnikova, T. D., Gainetdinov, R. R., & Caron, M. G. (2006). Dopamine enhances motor and neuropathological consequences of polyglutamine expanded huntingtin. *FASEB J, 20*(14), 2541-2543. doi:10.1096/fj.06-6533fje

De Lean, A., Stadel, J. M., & Lefkowitz, R. J. (1980). A ternary complex model explains the agonist-specific binding properties of the adenylate cyclase-coupled beta-adrenergic receptor. *J Biol Chem, 255*(15), 7108-7117.

De Vries, L., Fischer, T., Tronchere, H., Brothers, G. M., Strockbine, B., Siderovski, D. P., & Farquhar, M. G. (2000). Activator of G protein signaling 3 is a guanine dissociation inhibitor for Galpha i subunits. *Proc Natl Acad Sci U S A, 97*(26), 14364-14369. doi:10.1073/pnas.97.26.14364

Defer, N., Best-Belpomme, M., & Hanoune, J. (2000). Tissue specificity and physiological relevance of various isoforms of adenylyl cyclase. *Am J Physiol Renal Physiol, 279*(3), F400-416.

Delint-Ramirez, I., Willoughby, D., Hammond, G. R., Ayling, L. J., & Cooper, D. M. (2011). Palmitoylation targets AKAP79 protein to lipid rafts and promotes its regulation of calcium-sensitive adenylyl cyclase type 8. *J Biol Chem, 286*(38), 32962-32975. doi:10.1074/jbc.M111.243899

Deng, P., Zhang, Y., & Xu, Z. C. (2007). Involvement of I(h) in dopamine modulation of tonic firing in striatal cholinergic interneurons. *J Neurosci, 27*(12), 3148-3156. doi:10.1523/JNEUROSCI.5535-06.2007

Dessauer, C. W. (2002). Kinetic analysis of the action of P-site analogs. *Methods Enzymol, 345*, 112-126.

Dessauer, C. W. (2009). Adenylyl cyclase--A-kinase anchoring protein complexes: the next dimension in cAMP signaling. *Mol Pharmacol, 76*(5), 935-941. doi:10.1124/mol.109.059345

Dessauer, C. W., & Gilman, A. G. (1996). Purification and characterization of a soluble form of mammalian adenylyl cyclase. *J Biol Chem, 271*(28), 16967-16974.

Dessauer, C. W., Tesmer, J. J., Sprang, S. R., & Gilman, A. G. (1998). Identification of a Gialpha binding site on type V adenylyl cyclase. *J Biol Chem, 273*(40), 25831-25839.

Dessauer, C. W., Watts, V. J., Ostrom, R. S., Conti, M., Dove, S., & Seifert, R. (2017). International Union of Basic and Clinical Pharmacology. CI. Structures and Small Molecule Modulators of Mammalian Adenylyl Cyclases. *Pharmacol Rev, 69*(2), 93-139. doi:10.1124/pr.116.013078

Diel, S., Beyermann, M., Llorens, J. M., Wittig, B., & Kleuss, C. (2008). Two interaction sites on mammalian adenylyl cyclase type I and II: modulation by calmodulin and G(betagamma). *Biochem J, 411*(2), 449-456. doi:10.1042/BJ20071204

Dixon, R. A., Kobilka, B. K., Strader, D. J., Benovic, J. L., Dohlman, H. G., Frielle, T., . . . Strader, C. D. (1986). Cloning of the gene and cDNA for mammalian beta-adrenergic receptor and homology with rhodopsin. *Nature, 321*(6065), 75-79. doi:10.1038/321075a0

Dou, H., Wang, C., Wu, X., Yao, L., Zhang, X., Teng, S., . . . Zhou, Z. (2015). Calcium influx activates adenylyl cyclase 8 for sustained insulin secretion in rat pancreatic beta cells. *Diabetologia, 58*(2), 324-333. doi:10.1007/s00125-014-3437-z

Douglas, A. G., Andreoletti, G., Talbot, K., Hammans, S. R., Singh, J., Whitney, A., . . . Foulds, N. C. (2017). ADCY5-related dyskinesia presenting as familial myoclonus-dystonia. *Neurogenetics, 18*(2), 111-117. doi:10.1007/s10048-017-0510-z

Duc, N. M., Kim, H. R., & Chung, K. Y. (2015). Structural mechanism of G protein activation by G protein-coupled receptor. *Eur J Pharmacol, 763*(Pt B), 214-222. doi:10.1016/j.ejphar.2015.05.016

Dy, M. E., Chang, F. C., Jesus, S. D., Anselm, I., Mahant, N., Zeilman, P., . . . Waugh, J. L. (2016). Treatment of ADCY5-Associated Dystonia, Chorea, and Hyperkinetic Disorders With Deep Brain Stimulation: A Multicenter Case Series. *J Child Neurol, 31*(8), 1027-1035. doi:10.1177/0883073816635749

Eckstein, F., Romaniuk, P. J., Heideman, W., & Storm, D. R. (1981). Stereochemistry of the mammalian adenylate cyclase reaction. *J Biol Chem, 256*(17), 9118-9120.

Efendiev, R., Samelson, B. K., Nguyen, B. T., Phatarpekar, P. V., Baameur, F., Scott, J. D., & Dessauer, C. W. (2010). AKAP79 interacts with multiple adenylyl cyclase (AC) isoforms and scaffolds AC5 and -6 to alpha-amino-3-hydroxyl-5-methyl-4-isoxazole-propionate (AMPA) receptors. *J Biol Chem, 285*(19), 14450-14458. doi:10.1074/jbc.M110.109769

Ejendal, K. F., Conley, J. M., Hu, C. D., & Watts, V. J. (2013). Bimolecular fluorescence complementation analysis of G protein-coupled receptor dimerization in living cells. *Methods Enzymol, 521*, 259-279. doi:10.1016/B978-0-12-391862-8.00014-4

Emerick, M. C., Shenkel, S., & Agnew, W. S. (1993). Regulation of the eel electroplax Na channel and phosphorylation of residues on amino- and carboxyl-terminal domains by cAMP-dependent protein kinase. *Biochemistry, 32*(36), 9435-9444.

Esposito, G., Perrino, C., Ozaki, T., Takaoka, H., Defer, N., Petretta, M. P., . . . Chiariello, M. (2008). Increased myocardial contractility and enhanced exercise function in transgenic mice overexpressing either adenylyl cyclase 5 or 8. *Basic Res Cardiol, 103*(1), 22-30. doi:10.1007/s00395-007-0688-6

Evans, R. M., & Zamponi, G. W. (2006). Presynaptic Ca2+ channels--integration centers for neuronal signaling pathways. *Trends Neurosci, 29*(11), 617-624. doi:10.1016/j.tins.2006.08.006

Ferguson, G. D., & Storm, D. R. (2004). Why calcium-stimulated adenylyl cyclases? *Physiology (Bethesda), 19*, 271-276. doi:10.1152/physiol.00010.2004

Fernandez, M., Raskind, W., Wolff, J., Matsushita, M., Yuen, E., Graf, W., . . . Bird, T. (2001). Familial dyskinesia and facial myokymia (FDFM): a novel movement disorder. *Ann Neurol, 49*(4), 486-492.

Fields, S., & Song, O. (1989). A novel genetic system to detect protein-protein interactions. *Nature, 340*(6230), 245-246. doi:10.1038/340245a0

Flanagan, C. A. (2005). A GPCR that is not "DRY". *Mol Pharmacol, 68*(1), 1-3. doi:10.1124/mol.105.014183

Fournier, F., Bourinet, E., Nargeot, J., & Charnet, P. (1993). Cyclic AMP-dependent regulation of P-type calcium channels expressed in Xenopus oocytes. *Pflugers Arch, 423*(3-4), 173-180.

Fredriksson, R., Lagerstrom, M. C., Lundin, L. G., & Schioth, H. B. (2003). The G-protein-coupled receptors in the human genome form five main families. Phylogenetic analysis, paralogon groups, and fingerprints. *Mol Pharmacol, 63*(6), 1256-1272. doi:10.1124/mol.63.6.1256

Gao, B. N., & Gilman, A. G. (1991). Cloning and expression of a widely distributed (type IV) adenylyl cyclase. *Proc Natl Acad Sci U S A, 88*(22), 10178-10182.

Gao, X., Sadana, R., Dessauer, C. W., & Patel, T. B. (2007). Conditional stimulation of type V and VI adenylyl cyclases by G protein betagamma subunits. *J Biol Chem, 282*(1), 294-302. doi:10.1074/jbc.M607522200

Gershon, E., Weigl, L., Lotan, I., Schreibmayer, W., & Dascal, N. (1992). Protein kinase A reduces voltage-dependent Na+ current in Xenopus oocytes. *J Neurosci, 12*(10), 3743-3752.

Gilman, A. G. (1987). G proteins: transducers of receptor-generated signals. *Annu Rev Biochem, 56*, 615-649. doi:10.1146/annurev.bi.56.070187.003151

Gimeno, C., Dorado, M. L., Roncero, C., Szerman, N., Vega, P., Balanza-Martinez, V., & Alvarez, F. J. (2017). Treatment of Comorbid Alcohol Dependence and Anxiety Disorder: Review of the Scientific Evidence and Recommendations for Treatment. *Front Psychiatry, 8*, 173. doi:10.3389/fpsyt.2017.00173

Glatt, C. E., & Snyder, S. H. (1993). Cloning and expression of an adenylyl cyclase localized to the corpus striatum. *Nature, 361*(6412), 536-538. doi:10.1038/361536a0

Goldstein, J., Silberstein, C., & Ibarra, C. (2002). Adenylyl cyclase types I and VI but not II and V are selectively inhibited by nitric oxide. *Braz J Med Biol Res, 35*(2), 145-151.

Goodman, O. B., Jr., Krupnick, J. G., Santini, F., Gurevich, V. V., Penn, R. B., Gagnon, A. W., . . . Benovic, J. L. (1996). Beta-arrestin acts as a clathrin adaptor in endocytosis of the beta2-adrenergic receptor. *Nature, 383*(6599), 447-450. doi:10.1038/383447a0

Gottle, M., Geduhn, J., Konig, B., Gille, A., Hocherl, K., & Seifert, R. (2009). Characterization of mouse heart adenylyl cyclase. *J Pharmacol Exp Ther, 329*(3), 1156-1165. doi:10.1124/jpet.109.150953

Gould, N., Doulias, P. T., Tenopoulou, M., Raju, K., & Ischiropoulos, H. (2013). Regulation of protein function and signaling by reversible cysteine S-nitrosylation. *J Biol Chem, 288*(37), 26473-26479. doi:10.1074/jbc.R113.460261

Grace, C. R., Perrin, M. H., DiGruccio, M. R., Miller, C. L., Rivier, J. E., Vale, W. W., & Riek, R. (2004). NMR structure and peptide hormone binding site of the first extracellular domain of a type B1 G protein-coupled receptor. *Proc Natl Acad Sci U S A, 101*(35), 12836-12841. doi:10.1073/pnas.0404702101

Grauschopf, U., Lilie, H., Honold, K., Wozny, M., Reusch, D., Esswein, A., . . . Rudolph, R. (2000). The N-terminal fragment of human parathyroid hormone receptor 1 constitutes a hormone binding domain and reveals a distinct disulfide pattern. *Biochemistry, 39*(30), 8878-8887.

Grundmann, M., Merten, N., Malfacini, D., Inoue, A., Preis, P., Simon, K., . . . Kostenis, E. (2018). Lack of beta-arrestin signaling in the absence of active G proteins. *Nat Commun, 9*(1), 341. doi:10.1038/s41467-017-02661-3

Gu, C., & Cooper, D. M. (1999). Calmodulin-binding sites on adenylyl cyclase type VIII. *J Biol Chem, 274*(12), 8012-8021.

Gueguen, M., Keuylian, Z., Mateo, V., Mougenot, N., Lompre, A. M., Michel, J. B., . . . Limon, I. (2010). Implication of adenylyl cyclase 8 in pathological smooth muscle cell migration occurring in rat and human vascular remodelling. *J Pathol, 221*(3), 331-342. doi:10.1002/path.2716

Guellich, A., Mehel, H., & Fischmeister, R. (2014). Cyclic AMP synthesis and hydrolysis in the normal and failing heart. *Pflugers Arch, 466*(6), 1163-1175. doi:10.1007/s00424-014-1515-1

Guinzberg, R., Diaz-Cruz, A., Acosta-Trujillo, C., Vilchis-Landeros, M. M., Vazquez-Meza, H., Lozano-Flores, C., . . . Pina, E. (2017). Newly synthesized cAMP is integrated at a membrane protein complex signalosome to ensure receptor response specificity. *FEBS J, 284*(2), 258-276. doi:10.1111/febs.13969

Haber, S. N. (2014). The place of dopamine in the cortico-basal ganglia circuit. *Neuroscience, 282*, 248-257. doi:10.1016/j.neuroscience.2014.10.008

Hacker, B. M., Tomlinson, J. E., Wayman, G. A., Sultana, R., Chan, G., Villacres, E., . . . Storm, D. R. (1998). Cloning, chromosomal mapping, and regulatory properties of the human type 9 adenylyl cyclase (ADCY9). *Genomics, 50*(1), 97-104. doi:10.1006/geno.1998.5293

Hadcock, J. R., & Malbon, C. C. (1993). Agonist regulation of gene expression of adrenergic receptors and G proteins. *J Neurochem, 60*(1), 1-9.

Hanson, P. I., Otto, H., Barton, N., & Jahn, R. (1995). The N-ethylmaleimide-sensitive fusion protein and alpha-SNAP induce a conformational change in syntaxin. *J Biol Chem, 270*(28), 16955-16961.

Hargrave, P. A., McDowell, J. H., Curtis, D. R., Wang, J. K., Juszczak, E., Fong, S. L., . . . Argos, P. (1983). The structure of bovine rhodopsin. *Biophys Struct Mech, 9*(4), 235-244.

Hauser, A. S., Chavali, S., Masuho, I., Jahn, L. J., Martemyanov, K. A., Gloriam, D. E., & Babu, M. M. (2018). Pharmacogenomics of GPCR Drug Targets. *Cell, 172*(1-2), 41-54 e19. doi:10.1016/j.cell.2017.11.033

Hayes, M. P., Soto-Velasquez, M., Fowler, C. A., Watts, V. J., & Roman, D. L. (2018). Identification of FDA-Approved Small Molecules Capable of Disrupting the Calmodulin-Adenylyl Cyclase 8 Interaction through Direct Binding to Calmodulin. *ACS Chem Neurosci, 9*(2), 346-357. doi:10.1021/acschemneuro.7b00349

Herve, D. (2011). Identification of a specific assembly of the g protein golf as a critical and regulated module of dopamine and adenosine-activated cAMP pathways in the striatum. *Front Neuroanat, 5*, 48. doi:10.3389/fnana.2011.00048

Higgins, J. B., & Casey, P. J. (1994). In vitro processing of recombinant G protein gamma subunits. Requirements for assembly of an active beta gamma complex. *J Biol Chem, 269*(12), 9067-9073.

Hill, J., Howlett, A., & Klein, C. (2000). Nitric oxide selectively inhibits adenylyl cyclase isoforms 5 and 6. *Cell Signal, 12*(4), 233-237.

Hirling, H., & Scheller, R. H. (1996). Phosphorylation of synaptic vesicle proteins: modulation of the alpha SNAP interaction with the core complex. *Proc Natl Acad Sci U S A, 93*(21), 11945-11949.

Holmes, A., Fitzgerald, P. J., MacPherson, K. P., DeBrouse, L., Colacicco, G., Flynn, S. M., . . . Camp, M. (2012). Chronic alcohol remodels prefrontal neurons and disrupts NMDAR-mediated fear extinction encoding. *Nat Neurosci, 15*(10), 1359-1361. doi:10.1038/nn.3204

Hooks, S. B., Waldo, G. L., Corbitt, J., Bodor, E. T., Krumins, A. M., & Harden, T. K. (2003). RGS6, RGS7, RGS9, and RGS11 stimulate GTPase activity of Gi family G-proteins with differential selectivity and maximal activity. *J Biol Chem, 278*(12), 10087-10093. doi:10.1074/jbc.M211382200

Hosono, M. (1999). [Cardiovascular effects of colforsin daropate hydrochloride, a novel drug for the treatment of acute heart failure]. *Nihon Yakurigaku Zasshi, 114*(2), 83-88.

Hu, B., Nakata, H., Gu, C., De Beer, T., & Cooper, D. M. (2002). A critical interplay between Ca2+ inhibition and activation by Mg2+ of AC5 revealed by mutants and chimeric constructs. *J Biol Chem, 277*(36), 33139-33147. doi:10.1074/jbc.M112373200

Hu, C. D., Chinenov, Y., & Kerppola, T. K. (2002). Visualization of interactions among bZIP and Rel family proteins in living cells using bimolecular fluorescence complementation. *Mol Cell, 9*(4), 789-798.

Hudson, T. Y., Corbett, J. A., Howlett, A. C., & Klein, C. (2001). Nitric oxide regulates adenylyl cyclase activity in rat striatal membranes. *J Neurochem, 77*(5), 1279-1284.

Hurley, J. H. (1999). Structure, mechanism, and regulation of mammalian adenylyl cyclase. *J Biol Chem, 274*(12), 7599-7602.

Huttlin, E. L., Jedrychowski, M. P., Elias, J. E., Goswami, T., Rad, R., Beausoleil, S. A., . . . Gygi, S. P. (2010). A tissue-specific atlas of mouse protein phosphorylation and expression. *Cell, 143*(7), 1174-1189. doi:10.1016/j.cell.2010.12.001

Insel, P. A., Head, B. P., Patel, H. H., Roth, D. M., Bundey, R. A., & Swaney, J. S. (2005). Compartmentation of G-protein-coupled receptors and their signalling components in lipid rafts and caveolae. *Biochem Soc Trans, 33*(Pt 5), 1131-1134. doi:10.1042/BST20051131

Irwin, J. J., Duan, D., Torosyan, H., Doak, A. K., Ziebart, K. T., Sterling, T., . . . Shoichet, B. K. (2015). An Aggregation Advisor for Ligand Discovery. *J Med Chem, 58*(17), 7076-7087. doi:10.1021/acs.jmedchem.5b01105

Iwami, G., Kawabe, J., Ebina, T., Cannon, P. J., Homcy, C. J., & Ishikawa, Y. (1995). Regulation of adenylyl cyclase by protein kinase A. *J Biol Chem, 270*(21), 12481-12484.

Iwamoto, T., Okumura, S., Iwatsubo, K., Kawabe, J., Ohtsu, K., Sakai, I., . . . Ishikawa, Y. (2003). Motor dysfunction in type 5 adenylyl cyclase-null mice. *J Biol Chem, 278*(19), 16936-16940. doi:10.1074/jbc.C300075200

Jacobowitz, O., Chen, J., Premont, R. T., & Iyengar, R. (1993). Stimulation of specific types of Gs-stimulated adenylyl cyclases by phorbol ester treatment. *J Biol Chem, 268*(6), 3829-3832.

Jacobowitz, O., & Iyengar, R. (1994). Phorbol ester-induced stimulation and phosphorylation of adenylyl cyclase 2. *Proc Natl Acad Sci U S A, 91*(22), 10630-10634.

Johnstone, T. B., Agarwal, S. R., Harvey, R. D., & Ostrom, R. S. (2018). cAMP Signaling Compartmentation: Adenylyl Cyclases as Anchors of Dynamic Signaling Complexes. *Mol Pharmacol, 93*(4), 270-276. doi:10.1124/mol.117.110825

Josephson, I. R., & Sperelakis, N. (1991). Phosphorylation shifts the time-dependence of cardiac Ca++ channel gating currents. *Biophys J, 60*(2), 491-497. doi:10.1016/S0006-3495(91)82075-6

Jourdan, K. B., Mason, N. A., Long, L., Philips, P. G., Wilkins, M. R., & Morrell, N. W. (2001). Characterization of adenylyl cyclase isoforms in rat peripheral pulmonary arteries. *Am J Physiol Lung Cell Mol Physiol, 280*(6), L1359-1369. doi:10.1152/ajplung.2001.280.6.L1359

Kamato, D., Mitra, P., Davis, F., Osman, N., Chaplin, R., Cabot, P. J., . . . Little, P. J. (2017). Gaq proteins: molecular pharmacology and therapeutic potential. *Cell Mol Life Sci, 74*(8), 1379-1390. doi:10.1007/s00018-016-2405-9

Kang, D. S., Tian, X., & Benovic, J. L. (2013). beta-Arrestins and G protein-coupled receptor trafficking. *Methods Enzymol, 521*, 91-108. doi:10.1016/B978-0-12-391862-8.00005-3

Kapiloff, M. S., & Chandrasekhar, K. D. (2011). A-kinase anchoring proteins: temporal and spatial regulation of intracellular signal transduction in the cardiovascular system. *J Cardiovasc Pharmacol, 58*(4), 337-338. doi:10.1097/FJC.0B013E31822D5C08

Kapiloff, M. S., Piggott, L. A., Sadana, R., Li, J., Heredia, L. A., Henson, E., . . . Dessauer, C. W. (2009). An adenylyl cyclase-mAKAPbeta signaling complex regulates cAMP levels in cardiac myocytes. *J Biol Chem, 284*(35), 23540-23546. doi:10.1074/jbc.M109.030072

Kawabe, J., Ebina, T., Toya, Y., Oka, N., Schwencke, C., Duzic, E., & Ishikawa, Y. (1996). Regulation of type V adenylyl cyclase by PMA-sensitive and -insensitive protein kinase C isoenzymes in intact cells. *FEBS Lett, 384*(3), 273-276.

Kawabe, J., Iwami, G., Ebina, T., Ohno, S., Katada, T., Ueda, Y., . . . Ishikawa, Y. (1994). Differential activation of adenylyl cyclase by protein kinase C isoenzymes. *J Biol Chem, 269*(24), 16554-16558.

Kelly, P., Moeller, B. J., Juneja, J., Booden, M. A., Der, C. J., Daaka, Y., . . . Casey, P. J. (2006). The G12 family of heterotrimeric G proteins promotes breast cancer invasion and metastasis. *Proc Natl Acad Sci U S A, 103*(21), 8173-8178. doi:10.1073/pnas.0510254103

Kerppola, T. K. (2006). Design and implementation of bimolecular fluorescence complementation (BiFC) assays for the visualization of protein interactions in living cells. *Nat Protoc, 1*(3), 1278-1286. doi:10.1038/nprot.2006.201

Khan, S. M., Sleno, R., Gora, S., Zylbergold, P., Laverdure, J. P., Labbe, J. C., . . . Hebert, T. E. (2013). The expanding roles of Gbetagamma subunits in G protein-coupled receptor signaling and drug action. *Pharmacol Rev, 65*(2), 545-577. doi:10.1124/pr.111.005603

Khan, S. M., Sung, J. Y., & Hebert, T. E. (2016). Gbetagamma subunits-Different spaces, different faces. *Pharmacol Res, 111*, 434-441. doi:10.1016/j.phrs.2016.06.026

Kim, K. S., Kim, J., Back, S. K., Im, J. Y., Na, H. S., & Han, P. L. (2007). Markedly attenuated acute and chronic pain responses in mice lacking adenylyl cyclase-5. *Genes Brain Behav, 6*(2), 120-127.

Kim, K. S., Lee, K. W., Lee, K. W., Im, J. Y., Yoo, J. Y., Kim, S. W., . . . Han, P. L. (2006). Adenylyl cyclase type 5 (AC5) is an essential mediator of morphine action. *Proc Natl Acad Sci U S A, 103*(10), 3908-3913. doi:10.1073/pnas.0508812103

Kizuka, Y., & Taniguchi, N. (2016). Enzymes for N-Glycan Branching and Their Genetic and Nongenetic Regulation in Cancer. *Biomolecules, 6*(2). doi:10.3390/biom6020025

Kleinjans, J. (2014). *Toxigenomics-Based Cellular Models*: Elsevier.

Klippel, A., Kavanaugh, W. M., Pot, D., & Williams, L. T. (1997). A specific product of phosphatidylinositol 3-kinase directly activates the protein kinase Akt through its pleckstrin homology domain. *Mol Cell Biol, 17*(1), 338-344.

Klotz, K. N., & Kachler, S. (2016). Inhibitors of membranous adenylyl cyclases with affinity for adenosine receptors. *Naunyn Schmiedebergs Arch Pharmacol, 389*(3), 349-352. doi:10.1007/s00210-015-1197-z

Klussmann, E., & Rosenthal, W. (2008). Protein-protein interactions as new drug targets. Preface. *Handb Exp Pharmacol*(186), v-vi.

Kodama, Y., & Hu, C. D. (2012). Bimolecular fluorescence complementation (BiFC): a 5-year update and future perspectives. *Biotechniques, 53*(5), 285-298. doi:10.2144/000113943

Kolakowski, L. F., Jr. (1994). GCRDb: a G-protein-coupled receptor database. *Receptors Channels, 2*(1), 1-7.

Koval, A., & Katanaev, V. L. (2012). Platforms for high-throughput screening of Wnt/Frizzled antagonists. *Drug Discov Today, 17*(23-24), 1316-1322. doi:10.1016/j.drudis.2012.07.007

Kramer, I. M. (2016). *Signal Transduction* (Third edition ed.). Netherlands: Amsterdam : Elsevier/Academic Press.

Kratter, I. H., Zahed, H., Lau, A., Tsvetkov, A. S., Daub, A. C., Weiberth, K. F., . . . Finkbeiner, S. (2016). Serine 421 regulates mutant huntingtin toxicity and clearance in mice. *J Clin Invest, 126*(9), 3585-3597. doi:10.1172/JCI80339

Krishnan, V., Graham, A., Mazei-Robison, M. S., Lagace, D. C., Kim, K. S., Birnbaum, S., . . . Nestler, E. J. (2008). Calcium-sensitive adenylyl cyclases in depression and anxiety: behavioral and biochemical consequences of isoform targeting. *Biol Psychiatry, 64*(4), 336-343. doi:10.1016/j.biopsych.2008.03.026

Kumar, K. R., Lohmann, K., Masuho, I., Miyamoto, R., Ferbert, A., Lohnau, T., . . . Schmidt, A. (2014). Mutations in GNAL: a novel cause of craniocervical dystonia. *JAMA Neurol, 71*(4), 490-494. doi:10.1001/jamaneurol.2013.4677

Kunishima, N., Shimada, Y., Tsuji, Y., Sato, T., Yamamoto, M., Kumasaka, T., . . . Morikawa, K. (2000). Structural basis of glutamate recognition by a dimeric metabotropic glutamate receptor. *Nature, 407*(6807), 971-977. doi:10.1038/35039564

Lagerstrom, M. C., & Schioth, H. B. (2008). Structural diversity of G protein-coupled receptors and significance for drug discovery. *Nat Rev Drug Discov, 7*(4), 339-357. doi:10.1038/nrd2518

Lagorce, D., Sperandio, O., Baell, J. B., Miteva, M. A., & Villoutreix, B. O. (2015). FAF-Drugs3: a web server for compound property calculation and chemical library design. *Nucleic Acids Res, 43*(W1), W200-207. doi:10.1093/nar/gkv353

Lai, H. L., Lin, T. H., Kao, Y. Y., Lin, W. J., Hwang, M. J., & Chern, Y. (1999). The N terminus domain of type VI adenylyl cyclase mediates its inhibition by protein kinase C. *Mol Pharmacol, 56*(3), 644-650.

Lai, H. L., Yang, T. H., Messing, R. O., Ching, Y. H., Lin, S. C., & Chern, Y. (1997). Protein kinase C inhibits adenylyl cyclase type VI activity during desensitization of the A2a-adenosine receptor-mediated cAMP response. *J Biol Chem, 272*(8), 4970-4977.

Lai, L., Yan, L., Gao, S., Hu, C. L., Ge, H., Davidow, A., . . . Vatner, D. E. (2013). Type 5 adenylyl cyclase increases oxidative stress by transcriptional regulation of manganese superoxide dismutase via the SIRT1/FoxO3a pathway. *Circulation, 127*(16), 1692-1701. doi:10.1161/CIRCULATIONAHA.112.001212

Lambright, D. G., Noel, J. P., Hamm, H. E., & Sigler, P. B. (1994). Structural determinants for activation of the alpha-subunit of a heterotrimeric G protein. *Nature, 369*(6482), 621-628. doi:10.1038/369621a0

Lambright, D. G., Sondek, J., Bohm, A., Skiba, N. P., Hamm, H. E., & Sigler, P. B. (1996). The 2.0 A crystal structure of a heterotrimeric G protein. *Nature, 379*(6563), 311-319. doi:10.1038/379311a0

Langfelder, P., Cantle, J. P., Chatzopoulou, D., Wang, N., Gao, F., Al-Ramahi, I., . . . Yang, X. W. (2016). Integrated genomics and proteomics define huntingtin CAG length-dependent networks in mice. *Nat Neurosci, 19*(4), 623-633. doi:10.1038/nn.4256

Lanska, D. J. (2010). Chapter 33: the history of movement disorders. *Handb Clin Neurol, 95*, 501-546. doi:10.1016/S0072-9752(08)02133-7

Lee, E., Linder, M. E., & Gilman, A. G. (1994). Expression of G-protein alpha subunits in Escherichia coli. *Methods Enzymol, 237*, 146-164.

Lee, K. W., Hong, J. H., Choi, I. Y., Che, Y., Lee, J. K., Yang, S. D., . . . Han, P. L. (2002). Impaired D2 dopamine receptor function in mice lacking type 5 adenylyl cyclase. *J Neurosci, 22*(18), 7931-7940.

Lefkowitz, R. J. (2004). Historical review: a brief history and personal retrospective of seven-transmembrane receptors. *Trends Pharmacol Sci, 25*(8), 413-422. doi:10.1016/j.tips.2004.06.006

LeNoue-Newton, M., Watkins, G. R., Zou, P., Germane, K. L., McCorvey, L. R., Wadzinski, B. E., & Spiller, B. W. (2011). The E3 ubiquitin ligase- and protein phosphatase 2A (PP2A)-binding domains of the Alpha4 protein are both required for Alpha4 to inhibit PP2A degradation. *J Biol Chem, 286*(20), 17665-17671. doi:10.1074/jbc.M111.222414

Levitt, E. S., Purington, L. C., & Traynor, J. R. (2011). Gi/o-coupled receptors compete for signaling to adenylyl cyclase in SH-SY5Y cells and reduce opioid-mediated cAMP overshoot. *Mol Pharmacol, 79*(3), 461-471. doi:10.1124/mol.110.064816

Li, M., West, J. W., Lai, Y., Scheuer, T., & Catterall, W. A. (1992). Functional modulation of brain sodium channels by cAMP-dependent phosphorylation. *Neuron, 8*(6), 1151-1159.

Li, W., Takahashi, M., Shibukawa, Y., Yokoe, S., Gu, J., Miyoshi, E., . . . Taniguchi, N. (2007). Introduction of bisecting GlcNAc in N-glycans of adenylyl cyclase III enhances its activity. *Glycobiology, 17*(6), 655-662. doi:10.1093/glycob/cwm022

Li, Y. Q., Shrestha, Y., Pandey, M., Chen, M., Kablan, A., Gavrilova, O., . . . Weinstein, L. S. (2016). G(q/11)alpha and G(s)alpha mediate distinct physiological responses to central melanocortins. *J Clin Invest, 126*(1), 40-49. doi:10.1172/JCI76348

Lin, H. H. (2013). G-protein-coupled receptors and their (Bio) chemical significance win 2012 Nobel Prize in Chemistry. *Biomed J, 36*(3), 118-124. doi:10.4103/2319-4170.113233

Lin, T. H., Lai, H. L., Kao, Y. Y., Sun, C. N., Hwang, M. J., & Chern, Y. (2002). Protein kinase C inhibits type VI adenylyl cyclase by phosphorylating the regulatory N domain and two catalytic C1 and C2 domains. *J Biol Chem, 277*(18), 15721-15728. doi:10.1074/jbc.M111537200

Lisinicchia, J. G., & Watts, V. J. (2003). Sensitization of adenylate cyclase by short-term activation of 5-HT1A receptors. *Cell Signal, 15*(12), 1111-1117.

Logothetis, D. E., Kurachi, Y., Galper, J., Neer, E. J., & Clapham, D. E. (1987). The beta gamma subunits of GTP-binding proteins activate the muscarinic K+ channel in heart. *Nature, 325*(6102), 321-326. doi:10.1038/325321a0

Maas, J. W., Jr., Vogt, S. K., Chan, G. C., Pineda, V. V., Storm, D. R., & Muglia, L. J. (2005). Calcium-stimulated adenylyl cyclases are critical modulators of neuronal ethanol sensitivity. *J Neurosci, 25*(16), 4118-4126. doi:10.1523/JNEUROSCI.4273-04.2005

Magliery, T. J., Wilson, C. G., Pan, W., Mishler, D., Ghosh, I., Hamilton, A. D., & Regan, L. (2005). Detecting protein-protein interactions with a green fluorescent protein fragment reassembly trap: scope and mechanism. *J Am Chem Soc, 127*(1), 146-157. doi:10.1021/ja046699g

Mangmool, S., & Kurose, H. (2011). G(i/o) protein-dependent and -independent actions of Pertussis Toxin (PTX). *Toxins (Basel), 3*(7), 884-899. doi:10.3390/toxins3070884

Mardis, E. R. (2013). Next-generation sequencing platforms. *Annu Rev Anal Chem (Palo Alto Calif), 6*, 287-303. doi:10.1146/annurev-anchem-062012-092628

Mariman, E. C., Vink, R. G., Roumans, N. J., Bouwman, F. G., Stumpel, C. T., Aller, E. E., . . . Wang, P. (2016). The cilium: a cellular antenna with an influence on obesity risk. *Br J Nutr, 116*(4), 576-592. doi:10.1017/S0007114516002282

Masada, N., Ciruela, A., Macdougall, D. A., & Cooper, D. M. (2009). Distinct mechanisms of regulation by Ca2+/calmodulin of type 1 and 8 adenylyl cyclases support their different physiological roles. *J Biol Chem, 284*(7), 4451-4463. doi:10.1074/jbc.M807359200

Masada, N., Schaks, S., Jackson, S. E., Sinz, A., & Cooper, D. M. (2012). Distinct mechanisms of calmodulin binding and regulation of adenylyl cyclases 1 and 8. *Biochemistry, 51*(40), 7917-7929. doi:10.1021/bi300646y

Mayinger, P. (2011). Signaling at the Golgi. *Cold Spring Harb Perspect Biol, 3*(5). doi:10.1101/cshperspect.a005314

McVey, M., Hill, J., Howlett, A., & Klein, C. (1999). Adenylyl cyclase, a coincidence detector for nitric oxide. *J Biol Chem, 274*(27), 18887-18892.

Mencacci, N. E., & Carecchio, M. (2016). Recent advances in genetics of chorea. *Curr Opin Neurol, 29*(4), 486-495. doi:10.1097/WCO.0000000000000352

Metzler, M., Gan, L., Mazarei, G., Graham, R. K., Liu, L., Bissada, N., . . . Hayden, M. R. (2010). Phosphorylation of huntingtin at Ser421 in YAC128 neurons is associated with protection of YAC128 neurons from NMDA-mediated excitotoxicity and is modulated by PP1 and PP2A. *J Neurosci, 30*(43), 14318-14329. doi:10.1523/JNEUROSCI.1589-10.2010

Miller, K. E., Kim, Y., Huh, W. K., & Park, H. O. (2015). Bimolecular Fluorescence Complementation (BiFC) Analysis: Advances and Recent Applications for Genome-Wide Interaction Studies. *J Mol Biol, 427*(11), 2039-2055. doi:10.1016/j.jmb.2015.03.005

Mombaerts, P. (2004). Genes and ligands for odorant, vomeronasal and taste receptors. *Nat Rev Neurosci, 5*(4), 263-278. doi:10.1038/nrn1365

Mons, N., & Cooper, D. M. (1994). Adenylyl cyclase mRNA expression does not reflect the predominant Ca2+/calmodulin-stimulated activity in the hypothalamus. *J Neuroendocrinol, 6*(6), 665-671.

Montano, M. (2015). *Translational Biology in Meidicne*: Elsevier.

Moore, C. A., Milano, S. K., & Benovic, J. L. (2007). Regulation of receptor trafficking by GRKs and arrestins. *Annu Rev Physiol, 69*, 451-482. doi:10.1146/annurev.physiol.69.022405.154712

Moreira, I. S. (2014). Structural features of the G-protein/GPCR interactions. *Biochim Biophys Acta, 1840*(1), 16-33. doi:10.1016/j.bbagen.2013.08.027

Morell, M., Espargaro, A., Aviles, F. X., & Ventura, S. (2008). Study and selection of in vivo protein interactions by coupling bimolecular fluorescence complementation and flow cytometry. *Nat Protoc, 3*(1), 22-33. doi:10.1038/nprot.2007.496

Moremen, K. W., Tiemeyer, M., & Nairn, A. V. (2012). Vertebrate protein glycosylation: diversity, synthesis and function. *Nat Rev Mol Cell Biol, 13*(7), 448-462. doi:10.1038/nrm3383

Morgan, C. P., Skippen, A., Segui, B., Ball, A., Allen-Baume, V., Larijani, B., . . . Cockcroft, S. (2004). Phosphorylation of a distinct structural form of phosphatidylinositol transfer protein alpha at Ser166 by protein kinase C disrupts receptor-mediated phospholipase C signaling by inhibiting delivery of phosphatidylinositol to membranes. *J Biol Chem, 279*(45), 47159-47171. doi:10.1074/jbc.M405827200

Morrison, D. K. (2001). KSR: a MAPK scaffold of the Ras pathway? *J Cell Sci, 114*(Pt 9), 1609-1612.

Mou, T. C., Masada, N., Cooper, D. M., & Sprang, S. R. (2009). Structural basis for inhibition of mammalian adenylyl cyclase by calcium. *Biochemistry, 48*(15), 3387-3397. doi:10.1021/bi802122k

Murzin, A. G. (1992). Structural principles for the propeller assembly of beta-sheets: the preference for seven-fold symmetry. *Proteins, 14*(2), 191-201. doi:10.1002/prot.340140206

Nagai, T., Ibata, K., Park, E. S., Kubota, M., Mikoshiba, K., & Miyawaki, A. (2002). A variant of yellow fluorescent protein with fast and efficient maturation for cell-biological applications. *Nat Biotechnol, 20*(1), 87-90. doi:10.1038/nbt0102-87

Nair, A. G., Gutierrez-Arenas, O., Eriksson, O., Vincent, P., & Hellgren Kotaleski, J. (2015). Sensing Positive versus Negative Reward Signals through Adenylyl Cyclase-Coupled GPCRs in Direct and Indirect Pathway Striatal Medium Spiny Neurons. *J Neurosci, 35*(41), 14017-14030. doi:10.1523/JNEUROSCI.0730-15.2015

Nathans, J., & Hogness, D. S. (1984). Isolation and nucleotide sequence of the gene encoding human rhodopsin. *Proc Natl Acad Sci U S A, 81*(15), 4851-4855.

Nevo, I., Avidor-Reiss, T., Levy, R., Bayewitch, M., Heldman, E., & Vogel, Z. (1998). Regulation of adenylyl cyclase isozymes on acute and chronic activation of inhibitory receptors. *Mol Pharmacol, 54*(2), 419-426.

Nguyen, C. H., & Watts, V. J. (2005). Dexras1 blocks receptor-mediated heterologous sensitization of adenylyl cyclase 1. *Biochem Biophys Res Commun, 332*(3), 913-920. doi:10.1016/j.bbrc.2005.05.041

Nicol, X., Muzerelle, A., Bachy, I., Ravary, A., & Gaspar, P. (2005). Spatiotemporal localization of the calcium-stimulated adenylate cyclases, AC1 and AC8, during mouse brain development. *J Comp Neurol, 486*(3), 281-294. doi:10.1002/cne.20528

Nielsen, M. D., Chan, G. C., Poser, S. W., & Storm, D. R. (1996). Differential regulation of type I and type VIII Ca2+-stimulated adenylyl cyclases by Gi-coupled receptors in vivo. *J Biol Chem, 271*(52), 33308-33316.

Nishizuka, Y. (1992). Intracellular signaling by hydrolysis of phospholipids and activation of protein kinase C. *Science, 258*(5082), 607-614.

Oishi, H., Takano, K., Tomita, K., Takebe, M., Yokoo, H., Yamazaki, M., & Hattori, Y. (2012). Olprinone and colforsin daropate alleviate septic lung inflammation and apoptosis through CREB-independent activation of the Akt pathway. *Am J Physiol Lung Cell Mol Physiol, 303*(2), L130-140. doi:10.1152/ajplung.00363.2011

Okajima, D., Kudo, G., & Yokota, H. (2010). Brain-specific angiogenesis inhibitor 2 (BAI2) may be activated by proteolytic processing. *J Recept Signal Transduct Res, 30*(3), 143-153. doi:10.3109/10799891003671139

Okumura, S., Kawabe, J., Yatani, A., Takagi, G., Lee, M. C., Hong, C., . . . Ishikawa, Y. (2003). Type 5 adenylyl cyclase disruption alters not only sympathetic but also parasympathetic and calcium-mediated cardiac regulation. *Circ Res, 93*(4), 364-371. doi:10.1161/01.RES.0000086986.35568.63

Ory, S., Zhou, M., Conrads, T. P., Veenstra, T. D., & Morrison, D. K. (2003). Protein phosphatase 2A positively regulates Ras signaling by dephosphorylating KSR1 and Raf-1 on critical 14-3-3 binding sites. *Curr Biol, 13*(16), 1356-1364.

Ostrom, R. S., Bogard, A. S., Gros, R., & Feldman, R. D. (2012). Choreographing the adenylyl cyclase signalosome: sorting out the partners and the steps. *Naunyn Schmiedebergs Arch Pharmacol, 385*(1), 5-12. doi:10.1007/s00210-011-0696-9

Ostrom, R. S., Bundey, R. A., & Insel, P. A. (2004). Nitric oxide inhibition of adenylyl cyclase type 6 activity is dependent upon lipid rafts and caveolin signaling complexes. *J Biol Chem, 279*(19), 19846-19853. doi:10.1074/jbc.M313440200

Ostrom, R. S., & Insel, P. A. (2004). The evolving role of lipid rafts and caveolae in G protein-coupled receptor signaling: implications for molecular pharmacology. *Br J Pharmacol, 143*(2), 235-245. doi:10.1038/sj.bjp.0705930

Ostrom, R. S., Liu, X., Head, B. P., Gregorian, C., Seasholtz, T. M., & Insel, P. A. (2002). Localization of adenylyl cyclase isoforms and G protein-coupled receptors in vascular smooth muscle cells: expression in caveolin-rich and noncaveolin domains. *Mol Pharmacol, 62*(5), 983-992.

Ostrom, R. S., Naugle, J. E., Hase, M., Gregorian, C., Swaney, J. S., Insel, P. A., . . . Meszaros, J. G. (2003). Angiotensin II enhances adenylyl cyclase signaling via Ca2+/calmodulin. Gq-Gs cross-talk regulates collagen production in cardiac fibroblasts. *J Biol Chem, 278*(27), 24461-24468. doi:10.1074/jbc.M212659200

Paavola, K. J., & Hall, R. A. (2012). Adhesion G protein-coupled receptors: signaling, pharmacology, and mechanisms of activation. *Mol Pharmacol, 82*(5), 777-783. doi:10.1124/mol.112.080309

Palczewski, K., Kumasaka, T., Hori, T., Behnke, C. A., Motoshima, H., Fox, B. A., . . . Miyano, M. (2000). Crystal structure of rhodopsin: A G protein-coupled receptor. *Science, 289*(5480), 739-745.

Palmer, T. M., Harris, C. A., Coote, J., & Stiles, G. L. (1997). Induction of multiple effects on adenylyl cyclase regulation by chronic activation of the human A3 adenosine receptor. *Mol Pharmacol, 52*(4), 632-640.

Park, H. Y., Kang, Y. M., Kang, Y., Park, T. S., Ryu, Y. K., Hwang, J. H., . . . Kim, K. S. (2014). Inhibition of adenylyl cyclase type 5 prevents L-DOPA-induced dyskinesia in an animal model of Parkinson's disease. *J Neurosci, 34*(35), 11744-11753. doi:10.1523/JNEUROSCI.0864-14.2014

Paterson, J. M., Smith, S. M., Harmar, A. J., & Antoni, F. A. (1995). Control of a novel adenylyl cyclase by calcineurin. *Biochem Biophys Res Commun, 214*(3), 1000-1008. doi:10.1006/bbrc.1995.2385

Payet, M. D., & Dupuis, G. (1992). Dual regulation of the n type K+ channel in Jurkat T lymphocytes by protein kinases A and C. *J Biol Chem, 267*(26), 18270-18273.

Penny, W. F., Henry, T. D., Watkins, M. W., Patel, A. N., & Hammond, H. K. (2018). Design of a Phase 3 trial of intracoronary administration of human adenovirus 5 encoding human adenylyl cyclase type 6 (RT-100) gene transfer in patients with heart failure with reduced left ventricular ejection fraction: The FLOURISH Clinical Trial. *Am Heart J, 201*, 111-116. doi:10.1016/j.ahj.2018.04.005

Picconi, B., Centonze, D., Hakansson, K., Bernardi, G., Greengard, P., Fisone, G., . . . Calabresi, P. (2003). Loss of bidirectional striatal synaptic plasticity in L-DOPA-induced dyskinesia. *Nat Neurosci, 6*(5), 501-506. doi:10.1038/nn1040

Pieroni, J. P., Miller, D., Premont, R. T., & Iyengar, R. (1993). Type 5 adenylyl cyclase distribution. *Nature, 363*(6431), 679-680. doi:10.1038/363679a0

Pierre, S., Eschenhagen, T., Geisslinger, G., & Scholich, K. (2009). Capturing adenylyl cyclases as potential drug targets. *Nat Rev Drug Discov, 8*(4), 321-335. doi:10.1038/nrd2827

Piggott, L. A., Bauman, A. L., Scott, J. D., & Dessauer, C. W. (2008). The A-kinase anchoring protein Yotiao binds and regulates adenylyl cyclase in brain. *Proc Natl Acad Sci U S A, 105*(37), 13835-13840. doi:10.1073/pnas.0712100105

Pinto, C., Papa, D., Hubner, M., Mou, T. C., Lushington, G. H., & Seifert, R. (2008). Activation and inhibition of adenylyl cyclase isoforms by forskolin analogs. *J Pharmacol Exp Ther, 325*(1), 27-36. doi:10.1124/jpet.107.131904

Pitman, J. L., Wheeler, M. C., Lloyd, D. J., Walker, J. R., Glynne, R. J., & Gekakis, N. (2014). A gain-of-function mutation in adenylate cyclase 3 protects mice from diet-induced obesity. *PLoS One, 9*(10), e110226. doi:10.1371/journal.pone.0110226

Premont, R. T., Matsuoka, I., Mattei, M. G., Pouille, Y., Defer, N., & Hanoune, J. (1996). Identification and characterization of a widely expressed form of adenylyl cyclase. *J Biol Chem, 271*(23), 13900-13907.

Qi, M., Zhuo, M., Skalhegg, B. S., Brandon, E. P., Kandel, E. R., McKnight, G. S., & Idzerda, R. L. (1996). Impaired hippocampal plasticity in mice lacking the Cbeta1 catalytic subunit of cAMP-dependent protein kinase. *Proc Natl Acad Sci U S A, 93*(4), 1571-1576.

Rangel-Barajas, C., Silva, I., Lopez-Santiago, L. M., Aceves, J., Erlij, D., & Floran, B. (2011). L-DOPA-induced dyskinesia in hemiparkinsonian rats is associated with up-regulation of adenylyl cyclase type V/VI and increased GABA release in the substantia nigra reticulata. *Neurobiol Dis, 41*(1), 51-61. doi:10.1016/j.nbd.2010.08.018

Raoux, M., Vacher, P., Papin, J., Picard, A., Kostrzewa, E., Devin, A., . . . Lang, J. (2015). Multilevel control of glucose homeostasis by adenylyl cyclase 8. *Diabetologia, 58*(4), 749-757. doi:10.1007/s00125-014-3445-z

Rasmussen, S. G., DeVree, B. T., Zou, Y., Kruse, A. C., Chung, K. Y., Kobilka, T. S., . . . Kobilka, B. K. (2011). Crystal structure of the beta2 adrenergic receptor-Gs protein complex. *Nature, 477*(7366), 549-555. doi:10.1038/nature10361

Reddy, G. R., Subramanian, H., Birk, A., Milde, M., Nikolaev, V. O., & Bunemann, M. (2015). Adenylyl cyclases 5 and 6 underlie PIP3-dependent regulation. *FASEB J, 29*(8), 3458-3471. doi:10.1096/fj.14-268466

Rehm, H., Pelzer, S., Cochet, C., Chambaz, E., Tempel, B. L., Trautwein, W., . . . Lazdunski, M. (1989). Dendrotoxin-binding brain membrane protein displays a K+ channel activity that is stimulated by both cAMP-dependent and endogenous phosphorylations. *Biochemistry, 28*(15), 6455-6460.

Reithmann, C., & Werdan, K. (1995). Chronic muscarinic cholinoceptor stimulation increases adenylyl cyclase responsiveness in rat cardiomyocytes by a decrease in the level of inhibitory G-protein alpha-subunits. *Naunyn Schmiedebergs Arch Pharmacol, 351*(1), 27-34.

Remy, I., & Michnick, S. W. (2004). A cDNA library functional screening strategy based on fluorescent protein complementation assays to identify novel components of signaling pathways. *Methods, 32*(4), 381-388. doi:10.1016/j.ymeth.2003.10.011

Renstrom, E., Eliasson, L., & Rorsman, P. (1997). Protein kinase A-dependent and -independent stimulation of exocytosis by cAMP in mouse pancreatic B-cells. *J Physiol, 502 (Pt 1)*, 105-118.

Rhee, M. H., Nevo, I., Avidor-Reiss, T., Levy, R., & Vogel, Z. (2000). Differential superactivation of adenylyl cyclase isozymes after chronic activation of the CB(1) cannabinoid receptor. *Mol Pharmacol, 57*(4), 746-752.

Richards, M., Lomas, O., Jalink, K., Ford, K. L., Vaughan-Jones, R. D., Lefkimmiatis, K., & Swietach, P. (2016). Intracellular tortuosity underlies slow cAMP diffusion in adult ventricular myocytes. *Cardiovasc Res, 110*(3), 395-407. doi:10.1093/cvr/cvw080

Robert, V., Gurlini, P., Tosello, V., Nagai, T., Miyawaki, A., Di Lisa, F., & Pozzan, T. (2001). Beat-to-beat oscillations of mitochondrial [Ca2+] in cardiac cells. *EMBO J, 20*(17), 4998-5007. doi:10.1093/emboj/20.17.4998

Roger, B., Papin, J., Vacher, P., Raoux, M., Mulot, A., Dubois, M., . . . Lang, J. (2011). Adenylyl cyclase 8 is central to glucagon-like peptide 1 signalling and effects of chronically elevated glucose in rat and human pancreatic beta cells. *Diabetologia, 54*(2), 390-402. doi:10.1007/s00125-010-1955-x

Rosa, J. L., & Barbacid, M. (1997). A giant protein that stimulates guanine nucleotide exchange on ARF1 and Rab proteins forms a cytosolic ternary complex with clathrin and Hsp70. *Oncogene, 15*(1), 1-6. doi:10.1038/sj.onc.1201170

Rosa, J. L., Casaroli-Marano, R. P., Buckler, A. J., Vilaro, S., & Barbacid, M. (1996). p619, a giant protein related to the chromosome condensation regulator RCC1, stimulates guanine nucleotide exchange on ARF1 and Rab proteins. *EMBO J, 15*(16), 4262-4273.

Rosenbaum, D. M., Rasmussen, S. G., & Kobilka, B. K. (2009). The structure and function of G-protein-coupled receptors. *Nature, 459*(7245), 356-363. doi:10.1038/nature08144

Ross, C. A., Aylward, E. H., Wild, E. J., Langbehn, D. R., Long, J. D., Warner, J. H., . . . Tabrizi, S. J. (2014). Huntington disease: natural history, biomarkers and prospects for therapeutics. *Nat Rev Neurol, 10*(4), 204-216. doi:10.1038/nrneurol.2014.24

Sadana, R., Dascal, N., & Dessauer, C. W. (2009). N terminus of type 5 adenylyl cyclase scaffolds Gs heterotrimer. *Mol Pharmacol, 76*(6), 1256-1264. doi:10.1124/mol.109.058370

Sadana, R., & Dessauer, C. W. (2009). Physiological roles for G protein-regulated adenylyl cyclase isoforms: insights from knockout and overexpression studies. *Neurosignals, 17*(1), 5-22. doi:10.1159/000166277

Samama, P., Cotecchia, S., Costa, T., & Lefkowitz, R. J. (1993). A mutation-induced activated state of the beta 2-adrenergic receptor. Extending the ternary complex model. *J Biol Chem, 268*(7), 4625-4636.

Sanabra, C., & Mengod, G. (2011). Neuroanatomical distribution and neurochemical characterization of cells expressing adenylyl cyclase isoforms in mouse and rat brain. *J Chem Neuroanat, 41*(1), 43-54. doi:10.1016/j.jchemneu.2010.11.001

Sanchez, G., Colettis, N., Vazquez, P., Cervenansky, C., Aguirre, A., Quillfeldt, J. A., . . . Kornisiuk, E. (2009). Muscarinic inhibition of hippocampal and striatal adenylyl cyclase is mainly due to the M(4) receptor. *Neurochem Res, 34*(8), 1363-1371. doi:10.1007/s11064-009-9916-9

Sanchez, J., & Holmgren, J. (2011). Cholera toxin - a foe & a friend. *Indian J Med Res, 133*, 153-163.

Sanchez-Tena, S., Cubillos-Rojas, M., Schneider, T., & Rosa, J. L. (2016). Functional and pathological relevance of HERC family proteins: a decade later. *Cell Mol Life Sci, 73*(10), 1955-1968. doi:10.1007/s00018-016-2139-8

Sanger, F., Nicklen, S., & Coulson, A. R. (1992). DNA sequencing with chain-terminating inhibitors. 1977. *Biotechnology, 24*, 104-108.

Schaefer, M. L., Wong, S. T., Wozniak, D. F., Muglia, L. M., Liauw, J. A., Zhuo, M., . . . Muglia, L. J. (2000). Altered stress-induced anxiety in adenylyl cyclase type VIII-deficient mice. *J Neurosci, 20*(13), 4809-4820.

Scheerer, P., Park, J. H., Hildebrand, P. W., Kim, Y. J., Krauss, N., Choe, H. W., . . . Ernst, O. P. (2008). Crystal structure of opsin in its G-protein-interacting conformation. *Nature, 455*(7212), 497-502. doi:10.1038/nature07330

Schwanhausser, B., Busse, D., Li, N., Dittmar, G., Schuchhardt, J., Wolf, J., . . . Selbach, M. (2011). Global quantification of mammalian gene expression control. *Nature, 473*(7347), 337-342. doi:10.1038/nature10098

Sculptoreanu, A., Figourov, A., & De Groat, W. C. (1995). Voltage-dependent potentiation of neuronal L-type calcium channels due to state-dependent phosphorylation. *Am J Physiol, 269*(3 Pt 1), C725-732. doi:10.1152/ajpcell.1995.269.3.C725

Seifert, R. (2014). Vidarabine is neither a potent nor a selective AC5 inhibitor. *Biochem Pharmacol, 87*(4), 543-546. doi:10.1016/j.bcp.2013.12.025

Seifert, R., & Beste, K. Y. (2012). Allosteric regulation of nucleotidyl cyclases: an emerging pharmacological target. *Sci Signal, 5*(240), pe37. doi:10.1126/scisignal.2003466

Sharma, S. K., Klee, W. A., & Nirenberg, M. (1975). Dual regulation of adenylate cyclase accounts for narcotic dependence and tolerance. *Proc Natl Acad Sci U S A, 72*(8), 3092-3096.

Sharma, S. K., Klee, W. A., & Nirenberg, M. (1977). Opiate-dependent modulation of adenylate cyclase. *Proc Natl Acad Sci U S A, 74*(8), 3365-3369.

Sharma, S. K., Nirenberg, M., & Klee, W. A. (1975). Morphine receptors as regulators of adenylate cyclase activity. *Proc Natl Acad Sci U S A, 72*(2), 590-594.

Shen, J. X., & Cooper, D. M. (2013). AKAP79, PKC, PKA and PDE4 participate in a Gq-linked muscarinic receptor and adenylate cyclase 2 cAMP signalling complex. *Biochem J, 455*(1), 47-56. doi:10.1042/BJ20130359

Shen, J. X., Wachten, S., Halls, M. L., Everett, K. L., & Cooper, D. M. (2012). Muscarinic receptors stimulate AC2 by novel phosphorylation sites, whereas Gbetagamma subunits exert opposing effects depending on the G-protein source. *Biochem J, 447*(3), 393-405. doi:10.1042/BJ20120279

Shenoy, S. K., & Lefkowitz, R. J. (2011). beta-Arrestin-mediated receptor trafficking and signal transduction. *Trends Pharmacol Sci, 32*(9), 521-533. doi:10.1016/j.tips.2011.05.002

Siderovski, D. P., & Willard, F. S. (2005). The GAPs, GEFs, and GDIs of heterotrimeric G-protein alpha subunits. *Int J Biol Sci, 1*(2), 51-66.

Sjogren, B., Blazer, L. L., & Neubig, R. R. (2010). Regulators of G protein signaling proteins as targets for drug discovery. *Prog Mol Biol Transl Sci, 91*, 81-119. doi:10.1016/S1877-1173(10)91004-1

Smith, F. D., Langeberg, L. K., Cellurale, C., Pawson, T., Morrison, D. K., Davis, R. J., & Scott, J. D. (2010). AKAP-Lbc enhances cyclic AMP control of the ERK1/2 cascade. *Nat Cell Biol, 12*(12), 1242-1249. doi:10.1038/ncb2130

Smith, J. P., & Book, S. W. (2010). Comorbidity of generalized anxiety disorder and alcohol use disorders among individuals seeking outpatient substance abuse treatment. *Addict Behav, 35*(1), 42-45. doi:10.1016/j.addbeh.2009.07.002

Smith, J. P., & Randall, C. L. (2012). Anxiety and alcohol use disorders: comorbidity and treatment considerations. *Alcohol Res, 34*(4), 414-431.

Smith, J. S., & Rajagopal, S. (2016). The beta-Arrestins: Multifunctional Regulators of G Protein-coupled Receptors. *J Biol Chem, 291*(17), 8969-8977. doi:10.1074/jbc.R115.713313

Smith, R. D., & Goldin, A. L. (1992). Protein kinase A phosphorylation enhances sodium channel currents in Xenopus oocytes. *Am J Physiol, 263*(3 Pt 1), C660-666. doi:10.1152/ajpcell.1992.263.3.C660

Sondek, J., Bohm, A., Lambright, D. G., Hamm, H. E., & Sigler, P. B. (1996). Crystal structure of a G-protein beta gamma dimer at 2.1A resolution. *Nature, 379*(6563), 369-374. doi:10.1038/379369a0

Soto-Velasquez, M., Hayes, M. P., Alpsoy, A., Dykhuizen, E. C., & Watts, V. J. (2018). A Novel CRISPR/Cas9-Based Cellular Model to Explore Adenylyl Cyclase and cAMP Signaling. *Mol Pharmacol, 94*(3), 963-972. doi:10.1124/mol.118.111849

Souders, C. A., Bowers, S. L., & Baudino, T. A. (2009). Cardiac fibroblast: the renaissance cell. *Circ Res, 105*(12), 1164-1176. doi:10.1161/CIRCRESAHA.109.209809

Stangherlin, A., & Zaccolo, M. (2012). Phosphodiesterases and subcellular compartmentalized cAMP signaling in the cardiovascular system. *Am J Physiol Heart Circ Physiol, 302*(2), H379-390. doi:10.1152/ajpheart.00766.2011

Steiner, D., Saya, D., Schallmach, E., Simonds, W. F., & Vogel, Z. (2006). Adenylyl cyclase type-VIII activity is regulated by G(betagamma) subunits. *Cell Signal, 18*(1), 62-68. doi:10.1016/j.cellsig.2005.03.014

Stergiakouli, E., Gaillard, R., Tavare, J. M., Balthasar, N., Loos, R. J., Taal, H. R., . . . Timpson, N. J. (2014). Genome-wide association study of height-adjusted BMI in childhood identifies functional variant in ADCY3. *Obesity (Silver Spring), 22*(10), 2252-2259. doi:10.1002/oby.20840

Sunahara, R. K., Beuve, A., Tesmer, J. J., Sprang, S. R., Garbers, D. L., & Gilman, A. G. (1998). Exchange of substrate and inhibitor specificities between adenylyl and guanylyl cyclases. *J Biol Chem, 273*(26), 16332-16338.

Sunahara, R. K., Dessauer, C. W., Whisnant, R. E., Kleuss, C., & Gilman, A. G. (1997). Interaction of Gsalpha with the cytosolic domains of mammalian adenylyl cyclase. *J Biol Chem, 272*(35), 22265-22271.

Tang, S. H., & Sharp, G. W. (1998). Atypical protein kinase C isozyme zeta mediates carbachol-stimulated insulin secretion in RINm5F cells. *Diabetes, 47*(6), 905-912.

Tang, T., Lai, N. C., Roth, D. M., Drumm, J., Guo, T., Lee, K. W., . . . Gao, M. H. (2006). Adenylyl cyclase type V deletion increases basal left ventricular function and reduces left ventricular contractile responsiveness to beta-adrenergic stimulation. *Basic Res Cardiol, 101*(2), 117-126. doi:10.1007/s00395-005-0559-y

Tang, W. J., & Gilman, A. G. (1991). Type-specific regulation of adenylyl cyclase by G protein beta gamma subunits. *Science, 254*(5037), 1500-1503.

Tang, X. L., Wang, Y., Li, D. L., Luo, J., & Liu, M. Y. (2012). Orphan G protein-coupled receptors (GPCRs): biological functions and potential drug targets. *Acta Pharmacol Sin, 33*(3), 363-371. doi:10.1038/aps.2011.210

Taussig, R., Iniguez-Lluhi, J. A., & Gilman, A. G. (1993). Inhibition of adenylyl cyclase by Gi alpha. *Science, 261*(5118), 218-221.

Taussig, R., Tang, W. J., Hepler, J. R., & Gilman, A. G. (1994). Distinct patterns of bidirectional regulation of mammalian adenylyl cyclases. *J Biol Chem, 269*(8), 6093-6100.

Tepe, N. M., Lorenz, J. N., Yatani, A., Dash, R., Kranias, E. G., Dorn, G. W., 2nd, & Liggett, S. B. (1999). Altering the receptor-effector ratio by transgenic overexpression of type V adenylyl cyclase: enhanced basal catalytic activity and function without increased cardiomyocyte beta-adrenergic signalling. *Biochemistry, 38*(50), 16706-16713.

Tepper, J. M., & Bolam, J. P. (2004). Functional diversity and specificity of neostriatal interneurons. *Curr Opin Neurobiol, 14*(6), 685-692. doi:10.1016/j.conb.2004.10.003

Tesmer, J. J. (2009). Structure and function of regulator of G protein signaling homology domains. *Prog Mol Biol Transl Sci, 86*, 75-113. doi:10.1016/S1877-1173(09)86004-3

Tesmer, J. J., & Sprang, S. R. (1998). The structure, catalytic mechanism and regulation of adenylyl cyclase. *Curr Opin Struct Biol, 8*(6), 713-719.

Tesmer, J. J., Sunahara, R. K., Gilman, A. G., & Sprang, S. R. (1997). Crystal structure of the catalytic domains of adenylyl cyclase in a complex with Gsalpha.GTPgammaS. *Science, 278*(5345), 1907-1916.

Tian, X., Kang, D. S., & Benovic, J. L. (2014). beta-arrestins and G protein-coupled receptor trafficking. *Handb Exp Pharmacol, 219*, 173-186. doi:10.1007/978-3-642-41199-1_9

Timofeyev, V., Myers, R. E., Kim, H. J., Woltz, R. L., Sirish, P., Heiserman, J. P., . . . Chiamvimonvat, N. (2013). Adenylyl cyclase subtype-specific compartmentalization: differential regulation of L-type Ca2+ current in ventricular myocytes. *Circ Res, 112*(12), 1567-1576. doi:10.1161/CIRCRESAHA.112.300370

Tobin, A. B. (2008). G-protein-coupled receptor phosphorylation: where, when and by whom. *Br J Pharmacol, 153 Suppl 1*, S167-176. doi:10.1038/sj.bjp.0707662

Toker, A., Meyer, M., Reddy, K. K., Falck, J. R., Aneja, R., Aneja, S., . . . Cantley, L. C. (1994). Activation of protein kinase C family members by the novel polyphosphoinositides PtdIns-3,4-P2 and PtdIns-3,4,5-P3. *J Biol Chem, 269*(51), 32358-32367.

Tsien, R. Y. (1998). The green fluorescent protein. *Annu Rev Biochem, 67*, 509-544. doi:10.1146/annurev.biochem.67.1.509

Tso, P. H., & Wong, Y. H. (2001). Opioid-induced adenylyl cyclase supersensitization in human embryonic kidney 293 cells requires pertussis toxin-sensitive G proteins other than G(i1) and G(i3). *Neurosci Lett, 299*(1-2), 25-28.

Usui, H., Inoue, R., Tanabe, O., Nishito, Y., Shimizu, M., Hayashi, H., . . . Takeda, M. (1998). Activation of protein phosphatase 2A by cAMP-dependent protein kinase-catalyzed phosphorylation of the 74-kDa B" (delta) regulatory subunit in vitro and identification of the phosphorylation sites. *FEBS Lett, 430*(3), 312-316.

Utine, G. E., Taskiran, E. Z., Kosukcu, C., Karaosmanoglu, B., Guleray, N., Dogan, O. A., . . . Alikasifoglu, M. (2017). HERC1 mutations in idiopathic intellectual disability. *Eur J Med Genet, 60*(5), 279-283. doi:10.1016/j.ejmg.2017.03.007

Vallon, M., & Essler, M. (2006). Proteolytically processed soluble tumor endothelial marker (TEM) 5 mediates endothelial cell survival during angiogenesis by linking integrin alpha(v)beta3 to glycosaminoglycans. *J Biol Chem, 281*(45), 34179-34188. doi:10.1074/jbc.M605291200

Vatner, D. E., Yan, L., Lai, L., Yuan, C., Mouchiroud, L., Pachon, R. E., . . . Vatner, S. F. (2015). Type 5 adenylyl cyclase disruption leads to enhanced exercise performance. *Aging Cell, 14*(6), 1075-1084. doi:10.1111/acel.12401

Vatner, S. F., Park, M., Yan, L., Lee, G. J., Lai, L., Iwatsubo, K., . . . Vatner, D. E. (2013). Adenylyl cyclase type 5 in cardiac disease, metabolism, and aging. *Am J Physiol Heart Circ Physiol, 305*(1), H1-8. doi:10.1152/ajpheart.00080.2013

Vidi, P. A., Przybyla, J. A., Hu, C. D., & Watts, V. J. (2010). Visualization of G protein-coupled receptor (GPCR) interactions in living cells using bimolecular fluorescence complementation (BiFC). *Curr Protoc Neurosci, Chapter 5*, Unit 5 29. doi:10.1002/0471142301.ns0529s51

Villacres, E. C., Wong, S. T., Chavkin, C., & Storm, D. R. (1998). Type I adenylyl cyclase mutant mice have impaired mossy fiber long-term potentiation. *J Neurosci, 18*(9), 3186-3194.

Villacres, E. C., Wu, Z., Hua, W., Nielsen, M. D., Watters, J. J., Yan, C., . . . Storm, D. R. (1995). Developmentally expressed Ca(2+)-sensitive adenylyl cyclase activity is disrupted in the brains of type I adenylyl cyclase mutant mice. *J Biol Chem, 270*(24), 14352-14357.

Villar, V. A., Cuevas, S., Zheng, X., & Jose, P. A. (2016). Localization and signaling of GPCRs in lipid rafts. *Methods Cell Biol, 132*, 3-23. doi:10.1016/bs.mcb.2015.11.008

Virshup, D. M. (2000). Protein phosphatase 2A: a panoply of enzymes. *Curr Opin Cell Biol, 12*(2), 180-185.

Waalkens, A. J. E., Vansenne, F., van der Hout, A. H., Zutt, R., Mourmans, J., Tolosa, E., . . . Tijssen, M. A. J. (2018). Expanding the ADCY5 phenotype toward spastic paraparesis: A mutation in the M2 domain. *Neurol Genet, 4*(1), e214. doi:10.1212/NXG.0000000000000214

Wang, H., Pineda, V. V., Chan, G. C., Wong, S. T., Muglia, L. J., & Storm, D. R. (2003). Type 8 adenylyl cyclase is targeted to excitatory synapses and required for mossy fiber long-term potentiation. *J Neurosci, 23*(30), 9710-9718.

Wang, H., & Storm, D. R. (2003). Calmodulin-regulated adenylyl cyclases: cross-talk and plasticity in the central nervous system. *Mol Pharmacol, 63*(3), 463-468.

Wang, H., & Zhang, M. (2012). The role of Ca(2)(+)-stimulated adenylyl cyclases in bidirectional synaptic plasticity and brain function. *Rev Neurosci, 23*(1), 67-78. doi:10.1515/revneuro-2011-0063

Wang, Q., & Traynor, J. R. (2011). Opioid-induced down-regulation of RGS4: role of ubiquitination and implications for receptor cross-talk. *J Biol Chem, 286*(10), 7854-7864. doi:10.1074/jbc.M110.160911

Wang, T., & Brown, M. J. (2004). Differential expression of adenylyl cyclase subtypes in human cardiovascular system. *Mol Cell Endocrinol, 223*(1-2), 55-62. doi:10.1016/j.mce.2004.05.012

Warrington, N. M., Howe, L. D., Paternoster, L., Kaakinen, M., Herrala, S., Huikari, V., . . . Palmer, L. J. (2015). A genome-wide association study of body mass index across early life and childhood. *Int J Epidemiol, 44*(2), 700-712. doi:10.1093/ije/dyv077

Watson, N., Linder, M. E., Druey, K. M., Kehrl, J. H., & Blumer, K. J. (1996). RGS family members: GTPase-activating proteins for heterotrimeric G-protein alpha-subunits. *Nature, 383*(6596), 172-175. doi:10.1038/383172a0

Watson, P. A., Krupinski, J., Kempinski, A. M., & Frankenfield, C. D. (1994). Molecular cloning and characterization of the type VII isoform of mammalian adenylyl cyclase expressed widely in mouse tissues and in S49 mouse lymphoma cells. *J Biol Chem, 269*(46), 28893-28898.

Watts, V. J. (2002). Molecular mechanisms for heterologous sensitization of adenylate cyclase. *J Pharmacol Exp Ther, 302*(1), 1-7.

Watts, V. J., & Neve, K. A. (1996). Sensitization of endogenous and recombinant adenylate cyclase by activation of D2 dopamine receptors. *Mol Pharmacol, 50*(4), 966-976.

Watts, V. J., & Neve, K. A. (2005). Sensitization of adenylate cyclase by Galpha i/o-coupled receptors. *Pharmacol Ther, 106*(3), 405-421. doi:10.1016/j.pharmthera.2004.12.005

Watts, V. J., Taussig, R., Neve, R. L., & Neve, K. A. (2001). Dopamine D2 receptor-induced heterologous sensitization of adenylyl cyclase requires Galphas: characterization of Galphas-insensitive mutants of adenylyl cyclase V. *Mol Pharmacol, 60*(6), 1168-1172.

Watts, V. J., Wiens, B. L., Cumbay, M. G., Vu, M. N., Neve, R. L., & Neve, K. A. (1998). Selective activation of Galphao by D2L dopamine receptors in NS20Y neuroblastoma cells. *J Neurosci, 18*(21), 8692-8699.

Wayman, G. A., Wei, J., Wong, S., & Storm, D. R. (1996). Regulation of type I adenylyl cyclase by calmodulin kinase IV in vivo. *Mol Cell Biol, 16*(11), 6075-6082.

Wei, H., Ahn, S., Shenoy, S. K., Karnik, S. S., Hunyady, L., Luttrell, L. M., & Lefkowitz, R. J. (2003). Independent beta-arrestin 2 and G protein-mediated pathways for angiotensin II activation of extracellular signal-regulated kinases 1 and 2. *Proc Natl Acad Sci U S A, 100*(19), 10782-10787. doi:10.1073/pnas.1834556100

Wei, J., Wayman, G., & Storm, D. R. (1996). Phosphorylation and inhibition of type III adenylyl cyclase by calmodulin-dependent protein kinase II in vivo. *J Biol Chem, 271*(39), 24231-24235.

Weitmann, S., Schultz, G., & Kleuss, C. (2001). Adenylyl cyclase type II domains involved in Gbetagamma stimulation. *Biochemistry, 40*(36), 10853-10858.

Wess, J. (1998). Molecular basis of receptor/G-protein-coupling selectivity. *Pharmacol Ther, 80*(3), 231-264.

Whisnant, R. E., Gilman, A. G., & Dessauer, C. W. (1996). Interaction of the two cytosolic domains of mammalian adenylyl cyclase. *Proc Natl Acad Sci U S A, 93*(13), 6621-6625.

Willoughby, D., & Cooper, D. M. (2007). Organization and Ca2+ regulation of adenylyl cyclases in cAMP microdomains. *Physiol Rev, 87*(3), 965-1010. doi:10.1152/physrev.00049.2006

Willoughby, D., Halls, M. L., Everett, K. L., Ciruela, A., Skroblin, P., Klussmann, E., & Cooper, D. M. (2012). A key phosphorylation site in AC8 mediates regulation of Ca(2+)-dependent cAMP dynamics by an AC8-AKAP79-PKA signalling complex. *J Cell Sci, 125*(Pt 23), 5850-5859. doi:10.1242/jcs.111427

Willoughby, D., Wong, W., Schaack, J., Scott, J. D., & Cooper, D. M. (2006). An anchored PKA and PDE4 complex regulates subplasmalemmal cAMP dynamics. *EMBO J, 25*(10), 2051-2061. doi:10.1038/sj.emboj.7601113

Worzfeld, T., Wettschureck, N., & Offermanns, S. (2008). G(12)/G(13)-mediated signalling in mammalian physiology and disease. *Trends Pharmacol Sci, 29*(11), 582-589. doi:10.1016/j.tips.2008.08.002

Wu, G. C., Lai, H. L., Lin, Y. W., Chu, Y. T., & Chern, Y. (2001). N-glycosylation and residues Asn805 and Asn890 are involved in the functional properties of type VI adenylyl cyclase. *J Biol Chem, 276*(38), 35450-35457. doi:10.1074/jbc.M009704200

Wu, H., Zhang, X. Y., Hu, Z., Hou, Q., Zhang, H., Li, Y., . . . Wu, S. (2017). Evolution and heterogeneity of non-hereditary colorectal cancer revealed by single-cell exome sequencing. *Oncogene, 36*(20), 2857-2867. doi:10.1038/onc.2016.438

Wu, R. (1972). Nucleotide sequence analysis of DNA. *Nat New Biol, 236*(68), 198-200.

Wu, Z., Wong, S. T., & Storms, D. R. (1993). Modification of the calcium and calmodulin sensitivity of the type I adenylyl cyclase by mutagenesis of its calmodulin binding domain. *J Biol Chem, 268*(32), 23766-23768.

Xia, M., Guo, V., Huang, R., Shahane, S. A., Austin, C. P., Nirenberg, M., & Sharma, S. K. (2011). Inhibition of morphine-induced cAMP overshoot: a cell-based assay model in a high-throughput format. *Cell Mol Neurobiol, 31*(6), 901-907. doi:10.1007/s10571-011-9689-y

Xie, K., Masuho, I., Brand, C., Dessauer, C. W., & Martemyanov, K. A. (2012). The complex of G protein regulator RGS9-2 and Gbeta(5) controls sensitization and signaling kinetics of type 5 adenylyl cyclase in the striatum. *Sci Signal, 5*(239), ra63. doi:10.1126/scisignal.2002922

Xu, D., Isaacs, C., Hall, I. P., & Emala, C. W. (2001). Human airway smooth muscle expresses 7 isoforms of adenylyl cyclase: a dominant role for isoform V. *Am J Physiol Lung Cell Mol Physiol, 281*(4), L832-843. doi:10.1152/ajplung.2001.281.4.L832

Xu, Y., Xing, Y., Chen, Y., Chao, Y., Lin, Z., Fan, E., . . . Shi, Y. (2006). Structure of the protein phosphatase 2A holoenzyme. *Cell, 127*(6), 1239-1251. doi:10.1016/j.cell.2006.11.033

Yan, S. Z., Huang, Z. H., Andrews, R. K., & Tang, W. J. (1998). Conversion of forskolin-insensitive to forskolin-sensitive (mouse-type IX) adenylyl cyclase. *Mol Pharmacol, 53*(2), 182-187.

Yang, F., Moss, L. G., & Phillips, G. N., Jr. (1996). The molecular structure of green fluorescent protein. *Nat Biotechnol, 14*(10), 1246-1251. doi:10.1038/nbt1096-1246

Yuan, C., Sato, M., Lanier, S. M., & Smrcka, A. V. (2007). Signaling by a non-dissociated complex of G protein betagamma and alpha subunits stimulated by a receptor-independent activator of G protein signaling, AGS8. *J Biol Chem, 282*(27), 19938-19947. doi:10.1074/jbc.M700396200

Zala, D., Colin, E., Rangone, H., Liot, G., Humbert, S., & Saudou, F. (2008). Phosphorylation of mutant huntingtin at S421 restores anterograde and retrograde transport in neurons. *Hum Mol Genet, 17*(24), 3837-3846. doi:10.1093/hmg/ddn281

Zhan, X., Gimenez, L. E., Gurevich, V. V., & Spiller, B. W. (2011). Crystal structure of arrestin-3 reveals the basis of the difference in receptor binding between two non-visual subtypes. *J Mol Biol, 406*(3), 467-478. doi:10.1016/j.jmb.2010.12.034

Zhang, J., Levy, D., Oydanich, M., Bravo, C. A., Yoon, S., Vatner, D. E., & Vatner, S. F. (2018). A novel adenylyl cyclase type 5 inhibitor that reduces myocardial infarct size even when administered after coronary artery reperfusion. *J Mol Cell Cardiol, 121*, 13-15. doi:10.1016/j.yjmcc.2018.05.014

Zhang, J. H., Chung, T. D., & Oldenburg, K. R. (1999). A Simple Statistical Parameter for Use in Evaluation and Validation of High Throughput Screening Assays. *J Biomol Screen, 4*(2), 67-73. doi:10.1177/108705719900400206

Zhang, M., Moon, C., Chan, G. C., Yang, L., Zheng, F., Conti, A. C., . . . Wang, H. (2008). Ca-stimulated type 8 adenylyl cyclase is required for rapid acquisition of novel spatial information and for working/episodic-like memory. *J Neurosci, 28*(18), 4736-4744. doi:10.1523/JNEUROSCI.1177-08.2008

Zhao, Z., Zhang, K., Liu, X., Yan, H., Ma, X., Zhang, S., . . . Wei, X. (2016). Involvement of HCN Channel in Muscarinic Inhibitory Action on Tonic Firing of Dorsolateral Striatal Cholinergic Interneurons. *Front Cell Neurosci, 10*, 71. doi:10.3389/fncel.2016.00071

Zheng, Z. Y., & Chang, E. C. (2014). A bimolecular fluorescent complementation screen reveals complex roles of endosomes in Ras-mediated signaling. *Methods Enzymol, 535*, 25-38. doi:10.1016/B978-0-12-397925-4.00002-X

Zhou, X. E., Melcher, K., & Xu, H. E. (2012). Structure and activation of rhodopsin. *Acta Pharmacol Sin, 33*(3), 291-299. doi:10.1038/aps.2011.171

Zimmermann, G., & Taussig, R. (1996). Protein kinase C alters the responsiveness of adenylyl cyclases to G protein alpha and betagamma subunits. *J Biol Chem, 271*(43), 27161-27166. doi:10.1074/jbc.271.43.27161